Flame retardant solutions for foams: study and characterization

Séverine Bellayer

Habilitation à Diriger des Recherches

École Doctorale Sciences de la matière, du rayonnement et de l'environnement

Flame retardant solutions for foams: study and characterization

« Solution d'ignifugation de mousses à matrices polymères : étude et caractérisation »

Séverine BELLAYER

Discipline : Chimie des matériaux

Unité de Recherche : UMET, UMR 8207

Établissement de soutenance : Université de Lille

Présentée le : 27 Février 2026

Devant le jury composé de :

Président :	Directeur de Recherche Sylvain Caillol, Institut Charles Gerhardt, France
Rapporteur :	Professeure Baljinder Kandola, University of Manchester, UK
Rapporteur :	Professeur Rodolphe Sonnier, IMT Mines d'Alès, France
Rapporteur :	Professeure Marianne Cochez, Université de Lorraine, France
Garant :	Professeure Maude Jimenez, Université de Lille, France

Acknowledgements:

My first thanks go to Prof. Serge Bourbigot and Prof. Michel Traisnel for having think of me for a post doc position, which turned out to be the starting point of my carrier at ENSCL and welcoming me in the team called LSPES at the time. My sincere thanks go to Prof. Sophie Duquesne and Prof. Maude Jimenez, who gave me the opportunity to take part to many very interesting projects and provided me with the best scientific and moral support I could ever hope for. I am very grateful to them for their trust and guidance during all these years. I also thank DR JM. Lefebvre, Prof. A. Legris, Prof. P. Woisel and DR G. Delaplace for having me welcomed in the UMET laboratory in the ISP team and then PReF team, J. Grimblot, B. Fontaine and RN. Vannier for having me welcomed at ENSCL and E. Duflos and T. Maurer at Centrale Lille.

I really would like to thank Prof. Maude Jimenez for reading this HDR manuscript and having participate to the jury.

I am also grateful to Prof. Baljinder Kandola, Prof. Marianne Cochez and Prof. Rodolphe Sonnier for agreeing to take the time to evaluate my work as reviewers and for their expertise. I am deeply grateful to DR. Sylvain Caillol for being part of this jury and for contributing to the evaluation of this work.

To my office mate from the beginning, Maude, for her scientific and moral support during all these years, to my colleagues Sophie, Fabienne, Mathilde, Charaf, Pierre and Johan, thank you for your support, good mood and good words during all these years.

I would like to acknowledge all the students I currently supervise and the ones I have supervised for all the work they have done, for their enthusiasm, their perseverance, their excellent results and their kindness. Without their work, this manuscript would not have been written. I also thank all of the current and former members of the laboratory for their help and friendship over these years.

Particular thanks are addressed to the different members of the different characterization facilities of Institut Chevreul (NMR, electronic microscopy, XPS, Tof-SIMS…) for their expertise and numerous explanations.

I also thank all the industrial and academic partners I have met during the different projects I have been part of.

To finish with, I thank my family and friends for their patience, affection and moral support.

Content

Abbreviation index

ADT	Assistant technician
APP	Ammonium PolyPhosphate
APTES	3-amino propyl triethoxysilane
ASI	Assistant engineer
ATR	Attenuated Total Reflection
BE	Binding Energy
Bp	Boiling point
Char	Carbonaceous residue
CO	Carbon monoxide
CO_2	Carbon dioxide
CP-MAS	Cross Polarisation with Magic Angle Spinning
DBTA	dibutyltindiacetate
DEP	diethyl phosphite
DEPonate	Diethyl ethyl phosphonate
DEPPonate	Diethyl phenyl phosphonate
DMMP	Dimethyl methyl phosphonate
DPTES	Diethylphosphatoethyltriethoxysilane
DSC	Differential Scanning Calorimetry
EPMA	Electron Probe Micro Analyser
EPP	Expanded PolyPropylene
FR	Flame Retardant
FPUF	Flexible PolyUrethane Foam
Fs	Flame Spread
FTIR	Fourier Transform Infrared Spectroscopy
GSH	Globally Harmonized System
GWP	Global Warming Potential
HBr	Hydrogen bromine
HCl	Hydrogen chloride
HPDEC	High Power DECoupling
HRR	Heat Release Rate
HRS4R	Human resources strategy for researchers
ICP-AES	Inductively Coupled Plasma combined with an Atom Emission Spectrometer
IFR	Intumescent flame retardant
IGE	Engineer
Max exp.	Maximum expansion
MDI	Methylene diphenyl DiIsocyanate
MLC	Mass Loss Cone
Mp	Melting point
MTES	Methyltriethoxysilicate
NMR	Nuclear Magnetic Resonance
PAHs	Polycyclic Aromatic Hydrocarbons
PF	Phenolic Foam
P-FR	Phosphorus flame retardants
pHRR	Peak of Heat Release Rate

PIR	Rigid PolyIsocyanurate
ppm	Parts-Per-Million
PUR	Rigid PolyUrethane
QVCT	Quality and conditions of working life
Red. Weight	Residual weight
SEM	Scanning Electron Microscope
std. dev.	Standard Deviation
TECH	Technician
t flaming	Flaming time
t ignition	Ignition time
t pHRR	Time of the Peak of Heat Release Rate
TBPine	Tributyl phosphine oxide
TBrPh	Di-(2-ethylhexyl) tetrabromo phthalate
TCPP	Tris(1-chloro-2-propyl) phosphate
TDI	Toluene DiIsocyanate
TDIPA	Titanium diisopropoxydebis(acetylacetonate)
TEM	Transmission electronic microscopy
TEOS	Tetraethoxysilicate
TEP	Triethyl phosphate
TEPate	Triethyl phosphate
TEPite	Triethyl phosphite
t_f	The time of sustained flaming of the specimen
TGA	ThermoGravimetric Analysis
THE	Tin II 2 ethylhexanoate
THR	Total Heat Release
TPPate	Triphenyl phosphate
TPPine	Triphenyl phoshine oxide
TPPite	Triphenyl phosphite
UMET	Materials and processing unit
WDS	Wavelength Dispersive Spectrometer
wt%	Weight percentage
XRD	X-ray diffraction

Part A:

Summary of the administrative and scientific activities

1. Curriculum Vitae

PERSONAL INFORMATION

Dr Séverine BELLAYER
Research engineer
Nationality: French

Date of birth: May 24th 1978, Le Mans, France

[redacted]

UMET-PReF UMR 8207
Centrale Lille
Cité Scientifique, Bât C7

59652

Villeneuve d'Ascq cedex

Phone: 03.74.95.13.16
Email: severine.bellayer@centralelille.fr

EDUCATION

2002-2005: **PhD, collaboration between NIST, Gaithersburg, USA and** GEMTEX-ENSAIT laboratory, Roubaix, France, defended the 27th of October, 2005 at Lille University, Villeneuve d'Ascq, France
Title: Development of new qualitative and quantitative characterization technics for polymer nanocomposites.

2000-2001: Master in organic and macromolecular chemistry, Univ. Lille, Villeneuve d'Ascq.
Internship: at GEMTEX/ENSAIT, physico-chemical behavior of EVA latex

1998-2001: **Master in textile (French « engineer diplomat »),** ENSAIT, Roubaix, France
Field: Chemistry

CAREER

2008-…: Research engineer "Hors-Classe" at Ecole Nationale Supérieure de Chimie de Lille (ENSCL), and then Centrale Lille, since 2020.

- **Technical manager of the fire test facility (FireResist) of Centrale Lille**
- **Technical manager of the chemical and thermal analysis facility (PACTE) of Centrale Lille**
- **Co-supervision of 4 PhD students (defense in 2021, 2023, 2025 and 2026)**
- **Manager of the electron probe microanalyser (EPMA) of Institut Chevreul**
- **Technical expert for** electronic microscopy characterizations (TEM, SEM et EDS) for the PReF team at UMET
- **Research field: flame retardancy of polymer foam**
- **88 publications (11 as first author), h_{index}: 34**

2006-2008: Post-doctoral research at ENSCL

- **Installation of a new EPMA at ENSCL and its integration into the Lille University characterization facilities** (FEDER project: 700 000 €).
- **Study and characterization of intumescent LLDPE formulations**

2005-2006: CNRS post-doctoral position, 12 months at the Université of Montpellier, Charles Gerhart Institute (under the supervision of Prof. A. Vioux and Prof. J. Le Bideau)

- Study and characterization of silica ionogels

2002-2005: 3 years of PhD research at NIST (National Institute of Standards and Technology)

- **Development of new qualitative and quantitative characterization technics for polymer nanocomposites** (supervisor: Prof. S. Bourbigot, co-supervisor: Dr X. Flambard, examinator 1: Prof. JF. Feller and examinator 2: Prof. J. Devaux).

2. Administrative and management activities

Since my arrival at UMET, formerly called LSPES (Appendix 1), in 2006, I had the opportunity to co-supervised 4 PhD student and supervised 3 master students for various projects. Since 2020, I also supervise 8 people from Centrale Lille permanent staff, for whom, I conduct annual professional interviews and write reports for internal evolution. More details can be found in the following list:

- **Supervision:**

PhD students:

Nov 2023-…: Helena Arellano-Ramirez, "Flame retardant bio-based foams: from the impact of the formulation to the application", co-funding ADEME/Région Hauts de France, supervision rate 50%

Dec 2022-…: Soufyane Laidioui, "Inherently flame-retardant polymer foams", private funding from BASF, supervision rate 50%

Nov 2020-Dec 2023: Melvin Dilger, "Flame retardant expanded polypropylene for applications in electric vehicles: design and mechanism of action", co-funding ISIT/Univ Lille/JSP international company, supervision rate: 50%

Nov 2018-Nov 2021: Alexandre Gossiaux, "Systematic study of FR PU and PIR foams", private funding from BASF, supervision rate 50%

Master students:

2019: Jingyu Zhu, « Development of transparent intumescent fire-resistant sol-gel coatings for glass" private funding from SaintGobain Recherche, supervision rate: 50%

2018: Fengdi Li, « Development of transparent intumescent fire-resistant sol-gel coatings for glass" private funding from SaintGobain Recherche, supervision rate: 50%

2010: Sandor Dippel, « Formulation of sol-gel silicate coatings for titanium substrates »

Engineers and technicians:

Since 2020: As assistant director of the "Technological service" of Centrale Lille, I am the administrative supervisor of: 1 joint technician (ADT), 2 technicians (TECH), 2 assistant engineers (ASI) and 3 engineers (IGE).

The work consists in:

- conduct annual professional interviews
- write the report for internal evolution (success: 1 from IGE "Classe Normale" to IGE "Hors Classe", 1 from ADT to TECH, 1 from TECH to ASI and 1 from ASI to IGE),
- review the position description,
- conduct recruiting interviews,

which necessitates **communication skills, problem-solving skills, conflict management skills and decision-making skills**.

- **Jury member:**

My knowledge and skills in flame retardancy and characterization of materials allowed me to participate a PhD defense and various academic staff recruiting exams:

PhD defense:

2014: Invited member of G. Alogaili PhD defense, "Development of super hydrophobic coatings on stainless steel by atmospheric plasma treatment to limit dairy fouling – fundamental interactions between surface and fouling", supervised by Prof. M. Traisnel and Prof. M. Jimenez.

Jury member of staff recruiting exams: chemistry and material sciences field (BAP B):

2025: Engineer: admission (as **exterior member)**
2024: Technician exam: admissibility et admission (as substitute)
2023: Engineer exam: admission (as **exterior member**)
2020: Technician exam: admissibility (as **president)**
2019: Research engineer exam: admissibility (as **expert member**)
2018: Technician exam: admissibility et admission (as **expert member**)
2017: Technician exam**:** admissibility et admission (as **president)**
2016: Research engineer exam: admission (as **expert member)**
2012: Engineer exam: admissibility (as **expert member)**

- **Teaching and action of training:**

Since 2019: CNRS trainer: 3 days on « microanalysis of solid by EPMA » each year (1700 € per person).
Since 2022: MASTER 2, Integrated Research for Advanced Chemistry and Materials (IRACM), 1h class on « flame retardant sol-gel coatings », every year.
Since 2015: MASTER 2, Dispositifs Médicaux et Biomatériaux (DMB): 1,5h class on surface modification by sol-gel and surface characterization technics, each year.
Since 2010: Practical work, « discovery of the electron probe microanalyser » for the third years students of ENSCL: 12h (2h, 6 groups, 3 or 4 students per group), each year.

- **Responsibilities in the Chevreul Institute facilities**

Since the arrival of the electron probe microanalysis (EPMA) at ENSCL in 2007, I manage the EPMA facility, it is now part of the Advance Characterization Platform (PCA) of Chevreul Institute. Due to my expertise in flame retardancy of materials, I also became technical adviser of the novel "Resistance and reaction to fire" facility (Fire-Resist) created in 2020. In 2022, I also became technical adviser of a new "Elaboration and characterization facility" (PACTE), which I set up with all the practical work teaching devices at ENSCL. Fire-Resist and PACTE are part of the "Plateforme technique d'ingénierie de la chimie des matériaux" (PTICM) of Chevreul Institute. Thus, I share my work time between the three facilities.

Since 2022: PACTE facility (https://pacte.univ-lille.fr/)
PACTE is a facility dedicated to the development and analysis of materials (polymers, paints, glass, ceramics or cements). PACTE offers chemical, physico-chemical and thermal analysis capabilities, thanks to its extensive range of equipment (MPAES, GC, HPLC, FTIR, DVS, UV, Ion Chromatography, Rheometer, Viscosimeter, Granulometer, Tensiometer, two ATG and two DSC). It also has its own equipment for the production of materials (polymer, paint, glass), with two twin-screw extruders and two thermoforming presses, paint dispersers and its own glass-blowing workshop for the custom production of specific glassware and chemical synthesis assemblies.
Equipments are almost entirely part of ENSCL, for the practical work/projects of students, but they are also widely open to the academic and industrial scientific community for collaborative or contract projects (10 000 € budget every year). PACTE's scientific uniqueness lies in the diversity, complementarity and proximity of the various tools.

As technical adviser (10% work time), I organize the technical comities, write the quotations, elaborate the annual financial statements and access conditions. PACTE has the Centrale Lille label, which allows us to get recurrent allocations.

Since 2020: FIRE-RESIST facility (https://fire-resist.univ-lille.fr/)

The main purpose of Fire-Resist is to evaluate the fire behavior of materials based on specific tests simulating particular fire or combustion situations. Due to the complexity of fire-related phenomena, these tests are often carried out on a large scale to ensure a realistic representation of material behavior. However, large-scale testing is expensive and time-consuming, with costs increasing in proportion to the scale used. It was therefore essential to develop methods that enable us to work on a laboratory scale. Within the Fire-Resist platform, an approach combining dimensional and experimental analysis is adopted to establish dimensionless correlations between large-scale and small-scale assessments. This approach is based on strict similarity between the "large-scale" model and its experimental conditions, as well as on the reduced-scale test designed and built in the laboratory. The advanced instrumentation of these test benches enables a better understanding of the physical and chemical phenomena involved. Unlike standardized tests, which are limited to validating or invalidating a concept without providing an in-depth understanding of the phenomena involved, this experimental approach contributes not only to increase fundamental knowledge, but also to optimize systems to meet current standards and validate concepts.

As technical adviser (10% work time), I organize technical comities, write the quotations, the annual financial statements and the access conditions, I also had to write the public contracts to buy 5 new devices for a budget of 300 000 € in 2022. Fire-Resist (30 000 € budget every year) has the Centrale Lille and University of Lille label, which allow us to get recurrent allocations.

Since 2007: EPMA facility

An electron probe microanalyzer (EPMA) is an analytical tool used to determine the chemical composition of a small volume of a solid material. It is the only one north of Paris. It is a 600 000 € analytical equipment, which works similarly to a scanning electron microscope: the sample is bombarded with an electron beam, emitting x-rays at wavelengths characteristic to the elements being analyzed. It enables the quantification and the mapping of elements present within a small volume of sample (typically 1-3 μm^3), using conventional accelerating voltage of 15-20 kV. The concentrations of elements from beryllium to uranium can be measured at levels as low as 100 parts per million (ppm). It is open for academic and industrial projects and represents a budget of 40 000 € each year. In that frame, I regularly collaborate with different research labs (UCCS-UMR 8181-Lille University, PhLAM-UMR 8523-Lille University, LGCGE-Lille University, CEA-Marcoule).

As the manager (60% work time) of the electron probe microanalyser (EPMA) CAMECA SX100, I write quotations, run the experiments and write reports. I also manage the access, as well as all the maintenances of the equipment in collaboration with the supplier.

The common aspect of these three facilities is that they provide access to innovative tools for both academic and industrial research projects, enabling a deeper understanding of the transformations and phenomena occurring in materials under different stimuli.

- **Event organizations:**

2025: Organization of the "Ecole thématique des Sciences des Incendies et Applications » (ESIA 2025), April 6th to 11th, 2025 at Stella Plage, France. One week formation for academics and industrials on the theme of fire science and applications (28 participants and 14 invited speakers for a budget of 25000 €).
2024: Organization of « Fresques du climat et du numérique » workshops for UMET research support staff
2019-2024: Organization of the annual day of the research support staff of UMET
2019-2025: Organization of a CNRS three-day training on "microanalysis by electron probe microanalyser" every year (2 to 5 participants, 2 invited speakers)
2012: Participation to the organization of a summer school in « electronic microscopy and microanalysis »
2009: Participation to the Gatan training on « tomography by transmission electronic microscopy »
2008: Organization of the inauguration day of the EPMA

- **Other collective activities:**

Since 2006:
- **Representative of the quality and conditions of working life at UMET** since 2024.
- **Established the "carbon footprint" of UMET with Labo 1.5 application, in 2024 (presentation of the UMET carbon footprint during the annual general meeting of UMET in January 2005).**
- **Leader of the working group of the transition strategy of UMET.**
- **Human resources strategy for researchers (HRS4S) comity member at** Centrale Lille in 2023.
- Member of the « commission paritaire d'établissement » (**CPE),** since 2009

2003-2005:
- PhD at NIST, USA, **International volunteering at the French Ambassy in** Washington D.C., USA.

3. Summary of research activities

3.1. Doctoral research

This section sums up the work carried out during my PhD thesis, on the subject of "qualitative and quantitative characterizations of polymer nanocomposites for textile applications".

This work was a collaboration between the National Institute of Standards and Technology (NIST), Gaithersburg, MD, USA, and the GEnie des Matériaux TEXtile Laboratory (GEMTEX) of the Ecole Nationale Supérieure des Arts et Industries Textiles (ENSAIT), Roubaix, France. I spent the first 6 months in in the GEMTEX Lab and the last 2.5 years at NIST.

At that time, carbon nanotubes (CNTs) and clay polymer nanocomposites had already demonstrated their potential for enhancing mechanical properties of polymeric materials and even enabled significant advances in different fields, such as automotive and packaging. Since, textile industry was, and still is, in urgent need of renewal, we wanted to adapt polymer nanocomposites to the field of fibers and fabrics, which would benefit from the particular properties of polymer nanocomposites: high mechanical strength and low flammability.
Although fibers had already been produced, no polymer/CNTs nanocomposite fabric had yet been produced. The aim of my doctoral research was to analyze the causes of the difficulties encountered

during knitting and determine ways to overcome them. In the literature, some promising results had been obtained at a laboratory scale, and nanocomposite fibers with improved mechanical or FR properties had been produced. However, manufacturing processes were often unsuitable to industrial textile production. For this reason, my work only focused on melt processing used in industry and the problems involved in adapting it to the production of nanocomposite fibers at an industrial scale.

In both cases, polymer/CNTs and polymer/clay nanocomposites, the melt spinning and drawing method involved pre-mixing the various components in the molten state, using a twin-screw extruder. The resulting yarn is then used to form a knitted textile fabric. In the case of CNTs, a multifilament was obtained and characterized by DSC, TEM, TGA and tensile testing. This multifilament was knitted on an automatic machine, and the first PP/NTC textile fabric was formed and tested on a cone calorimeter. The cone calorimeter tests demonstrated good fire behavior of the nanocomposite structure, leading to the production of a Patent with Nanocyl company, Belgium.

The major problems encountered in the implementation of textile materials concerned polymer/clay nanocomposites, as the surfactants in commercial clays are unsuitable for high temperatures. To overcome this drawback, there was a need to synthesize and characterize a large number of nanocomposites. However, the characterization techniques (TEM, XRD, etc.) used to verify the synthesis of nanocomposites severely limits the quantity that can be analyzed. Therefore, a new characterization technique was developed to be more capable of rapidly and quantitatively characterize a large number of nanocomposites. This original method for characterizing nanocomposites was based on the use of a fluorescent dye and confocal microscopy. The fluorochrome was exchanged inside the clay, and a laser induces fluorescence of the fluorescent dye (Nile Blue A) in the polymer/clay nanocomposite. Self-extinction of the fluorescent dye due to over-concentration dominates until the clay sheets are physically separated by the intercalation of polymer chains. Further separation of the clay sheets then leaded to an exfoliated structure and a sharp increase in fluorescence intensity. Fluorescence was observed by confocal microscopy. Relatively thick samples were observed by acquiring a series of sections along the optical axis of the microscope. Quantitative dispersion data based on the homogeneity and intensity of fluorescence in the images were then obtained.

This new method was validated by full characterization of reference nanocomposite samples using conventional methods, and applied effectively and rapidly in the synthesis of polymer/clay nanocomposites containing a novel surfactant. New surfactants were synthesized to be more thermally stable than those exchanged in commercial clays. A surfactant resulting from the grafting of an imidazolium salt and a polyhedral oligomeric silsesquioxane molecule (DMIPOSS), already known to form thermally stable nanocomposites, gave good results.

The final part of my research aimed at finding a solution to improve the dispersion of carbon nanotubes in polymer matrices. This was achieved by functionalizing CNTs with a dimethyl hexadecyl imidazolium tetrafluoroborate (DMHDIm-TFB) ionic liquid. After melt-mixing the imidazolium-modified CNTs in polystyrene, TEM and confocal analyses revealed an exfoliated CNT structure through the polymer matrix. A computer image processing method was even used to quantify the dispersion enhancement at a nanometer scale. This CNT dispersion appeared to be close to an optimal random dispersion.

The mechanism of dispersion enhancement was investigated and the interactions between the CNTs and the imidazolium were highlighted by XRD and Infra-red analysis. I was able to show that there are "cations - π" type interactions, the cationic imidazolium head remains on the CNTs surface, while the long carbon chain is oriented outwards, enhancing affinity with the polymer. The dispersion of the

CNTs throughout the polymer matrix significantly enhanced the thermal properties of the new material.
In this study, melt spinning was evaluated to enable the formation of polymer/clay and polymer/CNTs nanocomposite textile fibers. A knitted fabric with polymer/CNTs flame-retardant properties was produced for the first time and new methods for qualitative and quantitative characterization enabling the synthesis and rapid evaluation of new materials were developed.

This work led to nine articles, two as first author[1,2,3,4,5,6,7,8,9], and one patent.[10]

3.2. Post doctoral research

- 2005 – 2006 : CNRS, Charles Gerhardt Institute, Montpellier, France

After my doctoral work in the USA, I came back to France to work as a one-year post-doctoral researcher at CNRS, at the Charles Gerhardt Institute. The subject was the design of new materials by immobilizing imidazolium ionic liquids in silica gels.

The design of new materials by the immobilization of ionic liquids in silica gels had already been the subject of a three-year thesis. The system studied was a 1-butyl-3-methylimidazolium bis(trifluoromethylsulfonyl)amidide ([BMI][TFSI]) ionic liquid confined, by sol-gel route, in a tetramethoxysilane (TMOS) silica matrix. This system results in the formation of an ionogel, which ionic conductivity remains comparable to that of the free ionic liquid. The aim of my study was to gain a better understanding of the effect of the organization and confinement of the ionic liquid on its conductivity, but also to broaden the field of application of ionogels.
The conductivity of [BMI][TFSI] ionogels increases with temperature and the amount of confined ionic liquid, and rapidly reaches a maximum; the one of unconfined [BMI][TFSI] ionic liquid. The ionic conductivity of ionogels follows an Arrhenius law, but this law must be adapted to two temperature ranges. Indeed, a break in the slope appears at 60°C. DSC studies have shown a disappearance of the phase transition of the ionic liquid with confinement. No phase transition justifies the slope break observed in conductimetry. The state of the ionic liquid inside the matrix pores was studied. The dynamics of confined ionic liquid was studied using solid state NMR. It appeared that the confined ionic liquid was still in an anisotropic liquid state.
Using NMR relaxometry experiments, an effect of the confinement on the ionic liquid was demonstrated. The relaxation time of each type of proton in the ionic liquid relaxes differently with temperature, whereas in the case of confined ionic liquid, all protons relax simultaneously, even at high temperatures. This phenomenon occurs regardless of the amount of ionic liquid confined in the ionogel. NMR and DSC revealed the liquid state of confined [BMI][TFSI], but could not point the reason for the break of the conductivity slope at 60°C. Therefore, conductivity experiments were carried out on imidazoliums with long carbon chains (hexadecyl-methyl imidazoilium PF6), capable of forming mesophases to try to better understand the behavior of confined ionic liquids. DSC studies carried out on these long chain imidazolium molecules have shown a direct correlation between DSC phase transition and change in activation energy in conductivity. A change in conductivity slope is observed at each phase transition of the ionic liquid (solid/liquid crystal and liquid crystal/isotropic liquid). This result led to specific heat measurement experiments on ionogels [BMI][TFSI]. The results showed a change in specific heat at 50°C. Therefore, there is an order/disorder phase transition at this temperature, which favors the conductivity of the confined ionic liquid.

During this study, ionogels with luminescent properties were also developed, extending the use of ionogels to spectrometry. Indeed, ionic liquid were doped with europium complexes to form monolithic UV-luminescent ionogels. The properties of luminescence of ionogels remained unchanged compared with the pre-doped ionic liquid solutions. A very fine emission peak is obtained, as well as very low photodegradation compared with traditional solvents (acetonitrile, dichloromethane).

This work led to five articles, one as first author.[11,12,13,14,15]

- 2006 – 2008 : UMET UMR8207, ENSCL, Villeneuve d'Ascq,

My second post-doctoral position was an 18 months post-doctoral position at UMET to set up and use an electronprobe microanalyser (EPMA) at Ecole Nationale Supérieure de Chimie de Lille (ENSCL). It was part of the FEDER project « Caractérisation de Matériaux Emergents »: 764 396 € (TTC).

The EPMA instrument was and still is an additional structuring element to complete the electron microscopy facility of the Chevreul Institute for the analysis of traces and light elements in emerging materials. Thanks to its resolution, a few eV for the WDS, and its sensitivity, the electron microprobe is a complementary tool to regional scanning electron microscopes. Whatever the type of material, it provides precise knowledge of the composition and, above all, the distribution of the elements that give the desired functionalities to the materials.
The first step of the project was made possible by the prior setting of a room capable of accommodating an electron microprobe. An air-conditioning and water-cooling system, a nitrogen and argon/methane gas distribution system, and a secure electrical system limiting power cuts or voltage drops were installed to ensure the electron probe's smooth operation. During the 18 months of the post-doctoral position, the second step of the project was to integrate the EPMA into the research network of the university and local industries. Numerous seminars were performed to present the performances of the device and allow its integration into research projects. After 18 years, the EPMA is still in use at ENSCL.

In parallel to the installation of the EPMA, I was fully integrated in the UMET laboratory (called LSPES at the time), and worked on a project founded by a private company, Nexans, France, on the flame retardancy of polyethylene (PE). Polyethylene (PE) is commonly used in the plastic industry and especially for cable covering due to its abrasion resistance, flexibility, excellent electric insulation properties, low toxicity and easy processing. However, PE is highly flammable and drips when burning, hence flame retardant (FR) systems have to be incorporated into the polymer to reduce fire hazards and meet the required standard. The most common fire retardants are halogen-based FR, heat sink FR or intumescent systems. However, due to environmental problems and concerns about smoke production, industries avoid using halogenated FR. FR have to be ecologically friendly, be nontoxic and not produce corrosive and opaque smoke during combustion. The progressive shift away from halogenated FR has led to an interest in mineral fillers. The most effective halogen-free fire-retardant formulations for this kind of application are based on metal hydroxides, such as alumina trihydroxide or magnesium dihydroxide. Such mineral fillers act as fire retardants mainly through their endothermic dehydration, evolving water and the formation of a protective ceramic-like layer at the surfaces of the material. Even if the surface of carbonates and talc does not contain hydroxyl groups or active ions, the addition of mineral fillers into a polymer can contribute to its fire-retardant properties. In this project, I studied the behaviour of common and low-cost mineral fillers into a polyethylene matrix

when exposed to mass loss calorimeter conditions. The different systems are made of linear low-density polyethylene (LLDPE), with 50 wt% of calcium carbonate ($CaCO_3$), magnesium carbonate or talc treated with stearic acid or nontreated. These systems were exposed to an external heat flux of 50 kW/m^2 and their burning behaviors were compared. Significant decrease of heat release rate peaks (pHRR) was obtained with all these mineral fillers; however, even better results were obtained when particles were treated with stearic acid. Indeed, the system with $CaCO_3$-treated stearic acid leads to a surprising intumescent behavior. A rheological study showed no impact of stearic acid on the viscosity of the system and did not explain the appearance of the intumescent phenomenon. However, scanning electron microscopy (SEM) shows that stearic acid enhances the dispersion of particles into the polymer and acts as a dispersive agent. The results also show that the aspect ratio of the particles, the cation nature of the carbonates and the polarity of the polymer matrix have an effect on the appearance or not of the intumescent phenomenon.

In this work, I have also investigated the mechanism of action of the intumescent behavior. The system was fully characterized by FTIR, XRD, TGA and SEM. The carbonation/decarbonation temperatures, the swelling phenomenon and the effect of the thermal stress on the swelling have been examined. The residue is composed of a smooth surface made of chalk and CaO and a bulk of only chalk. Stearic acid allows a good dispersion of chalk particles into the LLDPE matrix, and contributes to form a cohesive network during burning when the thermal stress is high enough. A governing parameter of the intumescent effect is the particle size, which permits the formation of an insulating and cohesive mineral network during burning.

This post-doc position led to two articles as first author.[16,17]

3.3. Current research topic: Flame retardant foams

After 2008, I was fully integrated into the UMET laboratory (Appendix 1), in the team « Ingénierie des Systèmes Polymères » (ISP) until 2023 and then in the team « Procédés de recyclage et de fonctionalisation » (PReF).
My skills in electronic microscopy gained during my PhD and post-doctoral works enabled me to become the expert in electron microscopy for the team and guide researchers towards the analyses best suited for their needs. In the ISP team and then in the PReF team, when needed, I perform optical microscopy, SEM, TEM or EPMA analysis, as well as image processing technics. The knowledge in managing devices and analysis, allowed me to become the technical adviser of a chemical analysis facility (PACTE, 2022) at Centrale Lille.
In parallel to this expertise in electron microscopy and chemical analysis, I also developed an expertise in flame retardancy of materials and more particularly in polymer foams. I contribute to the team's activities by taking part in, writing or running projects (list of projects in section A.4) and developed my own research topic. I became technical adviser of the Fire-Resist facility (2020) of the Chevreul Institute, which studies the reaction and resistance of materials to fire. Since my PhD work and through the years, I have acquired recognized expertise, which now enables me to manage projects in the field of flame retardancy of polymer foams.

During my research work, I used three different approaches to flame retard foams:

- A bulk approach:

Bulk flame retardant foams undergo modifications of the foam to acquire flame-resistant properties. This approach includes the introduction of FR additives, or the use of reactive agents to diminish the material combustibility. The additives or reactive agents act by limiting the combustion reaction or releasing gases that suppress the flame. This way is the most commonly used in the production of items like upholstered foams for furniture, mattresses, or fire-resistant flooring, however, lots of flame retardants already exist in literature. So, the goal of this work was not to synthesize or find new FR but mainly to stimulate the emergence of new FR by studying the influence of different parameters of the FR on the fire behavior of the foams.
This work was carried out in the frame of the PhD work of A. Gossiaux, funded by BASF, Germany. In this work, a scientific approach allowing a quicker and more efficient development of new formulations is proposed. A systematic study was coupled with a multi-scale study of the fire behavior of the foams, and a laboratory-scale fire test was developed (Mini-Single Burning Item), which allowed a quick and efficient examination of the formulations. The FR studied in this work are phosphorus organic FR, which are currently promoted to replace some halogenated FR that could be dangerous for the environment and health. The mechanisms of degradation of virgin and flame retarded foams were elucidated using various analytical tools. In the case of phosphorus FR, we were able to demonstrate that their mode of action varied according to the phosphorus oxidation degree as well as according to their point of decomposition. Moreover, the efficiency of the FR also varies according to the foam used (polyurethane or polyisocyanurate). All these results can thus advantageously be exploited to propose future efficient flame retardants for specific systems to reduce the combustion intensity of the foams.

- A surface approach:

Surface flame retarded foams consist of coatings applied on top of the materials to reduce their flammability. These coatings establish a protective barrier, hindering the flame spread. These coatings can be paints, varnishes, or fire-resistant coatings. I first used my post-doctoral knowledge on sol-gel process to develop an intumescent sol-gel coating for flexible open cell PU foams. The solution can penetrate the 3D network of the PU foam and the coated PU foam reached a V0 rating at UL-94 test. The formulation is a mix of different silica precursors and a phosphorous flame retardant. Different bio-based flame retardants were also studied to replace the phosphorous flame retardant, however, even if the foam reached a V0 rating at UL94 test, the mechanical properties of the foam were affected by the coating. The sol-gel coating was tested on closed-cell foams; however, the coating is too thin to be efficient and other types of thicker coatings have to be used. In the PhD work of M. Dilger, founded by the company JSP International, we managed, after plasma pre-treatment, to flame-retard expanded polypropylene (closed cells) and reach a V0 rating at vertical UL-94 test using commercially available FR paint or varnish.

- Inherently flame-retardant foams:

Inherently flame-retardant foams are materials inherently designed to resist fire, with a chemical composition that does not rely on additives or external coatings. They are frequently utilized in applications prioritizing fire safety, such as electrical cables, flame-resistant clothing, construction materials, and industrial equipment. Melamine and phenolic foams belong to this category. Low-

density phenolic foams are widely used for their flame-retardant properties and thermal stability. In the PhD work of S. Laidioui funded by BASF, Germany, low-density foams (around 15) were formulated using two types of acids, hydrochloric acid (HCl) and sulfuric acid (H_2SO_4), to evaluate their influence on fire and mechanical properties. Fire performances were analyzed using Mass Loss Cone (ISO 5660) at 50 kW/m^2, measuring the peak heat release rate (pHRR) and total heat release (THR). The results show that the foam formulated with HCl 7% exhibits a pHRR of 35 kW/m² and a THR of 3000 MJ/m², while the H_2SO_4-based foam with 18%wt has a pHRR of 22 kW/m² and a THR of 1600 MJ/m², revealing significant differences in combustion behavior. Additionally, mechanical tests indicate an elastic modulus of 0.69 MPa and a Young's modulus of 0.70 Pa for the HCl-based foam, compared to 0.18 MPa and 0.26 Pa, respectively, for the H_2SO_4-based foam. These findings highlight the impact of the acid choice on the mechanical performance properties and fire resistance, contributing to the optimization of phenolic foam formulations for demanding industrial applications.

All this research work carried out since 2008 led to numerous articles listed in section 5.

3.4. Conclusion

Despite being in charge of facilities, which represents a substantial investment of time and the need to meet deadlines, I know how to remain available for research collaborations for the development of new methodologies or the management of projects.
I manage the EPMA device, including maintenance, method development, customer research and services. I draw up quotations, carry out analyses, interpret results and write analysis reports. I promote the EPMA through training courses for companies (CNRS trainer since 2019) or students (ENSCL engineering students) but also by collaborating with numerous researchers and including EPMA results into numerous publications in international journals. My knowledge in managing a technical device allowed me to become technical adviser of two different facilities (Fire-Resist and PACTE).
I am also fully integrated into the UMET laboratory, and more particularly into the PReF team of UMET to develop my own research thematic on the flame retardancy of polymer foams. I am involved in numerous projects and my work led to numerous publications and communications. The list of contracts and project as well as publications and communications are listed in sections A4 and 5.

4. Contracts and projects

The laboratory was and still is heavily involved in collaborations with industrial and university partners.

When I was recruited in the laboratory as a research engineer, I was involved in a number of different research projects. I worked to maintain the existing collaborations but also to develop new ones.

Academic collaborations:

Thanks to my dual profile, "characterization of polymer materials by electron microscopy" and "flame retardancy of polymer materials", I have been involved in numerous academic projects (FUI, ANR or FP7, with or without industrials), since my arrival in the laboratory in 2005. With the implementation of the electron microanalyser facility, I was also able to quickly get to know the academic landscape of the University of Lille and collaborate with many laboratories of the University (PHLAM, UMET, UCCS). It allowed me to continue to be integrated into projects and broaden my research topics (surface

treatment of glasses, DrawspeedGlass or anti-fouling in dairy heat exchangers, Proteinopeps and Proteinolab).

Industrial collaborations:

In addition to collaborating with various industrial partners in national and international academic projects, the laboratory also works by the mean of research contracts with French and European companies. I first collaborated with BASF, Ludwigshafen, Germany, in 2018, for a three-year PhD contract, which I co-supervised (A. Gossiaux). The subject of this first PhD work was the systematic study of flame retarded polyurethane and polyisocyanurate foams. At the end of this first contract, I had the opportunity to write a second research project, that led to a second PhD work with BASF, starting in December 2022 (S. Laidioui). The aim of this second project was to study inherently flame-resistant polymers.

I was also able to collaborate with the company JSP International, France, in the context of a PhD study co-funded by ISITE and Université de Lille in 2020-2023, which I co-supervised. This work focuses on the subject of flame retardancy of expanded polypropylene and resulted in an article and a patent. Following this thesis, a third-year ENSCL student and a BUT2 student internship were hired to work with JSP, to complete the study on subjects not investigated during the three years of the PhD doctorate.

I also collaborated with Saint Gobain Recherche, France, to develop intumescent sol-gel coatings on glass, two master students were hired in that frame.

The complete list of all the projects I got involved in, as a co-supervisor or an expert, is given in the following section.

<u>Scientific co-supervisions:</u>

- 2023-2026: 3 years funded by ADEME/Region Hauts de France: "bio-based flame retardant foam: from the impact of the formulation to the application"
1 PhD student (Helena Arellano) hired in that frame
PhD supervisor: DR Anne-Laure Fameau
Supervision rate: 50%
Publication: 1 publication currently under revision
- 2023-2024: 5 months funded by the private company JSP international, France: Fire behavior of expanded polypropylene
1 student "BUT2" and 2 third year engineer students at ENSCL hired in that frame
Supervision rate: 100%
- 2022-2025: 3 years funded by the private company BASF, Germany: "inherently flame-retardant polymer foams"
1 PhD student (Soufyane Laidioui) hired in that frame
PhD supervisor: Prof. Sophie Duquesne
Supervision rate: 50%
Publication: 1 publication currently under revision

- 2020-2023: 3 years co-funded by ISITE, University of Lille and the private company JSP, France: "Flame retardant expanded polypropylene for applications in electric vehicles: design and mechanism of action"
1 PhD student (Melvin Dilger) hired in that frame
PhD supervisor: Maude Jimenez
Supervision rate: 50%
Publications: 1 article and 1 patent[81,82]
- 2018-2021: 3 years funded by the private company BASF, Germany: "Fire behavior study of rigid polyurethane foams: a systematic approach"
1 PhD student (Alexandre Gossiaux) hired in that frame
PhD supervisor: Prof. Sophie Duquesne
Supervision rate: 50%
Publications: 2 articles[51,52]
- 2018-2019: 1 year funded by Saint-Gobain Recherche, France: "Development of transparent intumescent fire-resistant sol-gel coatings for glass"
2 master students hired in that frame
Supervisor: Prof. Maude Jimenez
Supervision rate: 50%
Publication: confidential subject for 5 years, 2 articles in preparation

<u>Scientific expertise</u>: Characterization by electronic microscopy (SEM and TEM) and microanalysis (EPMA and EDS) and/or flame retardancy of polymer materials
- 2024-2028: 4 years ANR PRCE PREFIBIO in collaboration with the company BIOEX: "Multiscale and interdisciplinary approach to prevent and fight wildfires with low environmental impact biobased and biodegradable solutions"
Expertise in flame retardancy of polymer materials
- 2021-2025: 4 years ANR Chaire Industrielle project ProteinoPeps in collaboration with Ingredia company: "Characterization of the structure-functions of differentiated protein isolates"
Expertise in optical and electronic microscopy
Publication: 1 article currently being revised
- 2018-2021: 3 years ANR LabCom project in collaboration with Ingredia company: "Joint laboratory for the characterization of the structure-functions of differentiated protein isolates"
Expertise in optical and electronic microscopy
Publication: 2 articles[18,19]
- 2018-2021: 3 years ANR project ECONOMICS: "Eco-efficient and safe antifouling surfaces for milk and egg processing industries"
Expertise in optical and electronic microscopy
Publications: 8 articles[20,21,22,23,24,25,26,27]
- 2017-2020: 3 years founded by Institut Français des Matériaux Agrosourcés (IFMAS): "Bio-based self-stratifying coatings".
Expertise in optical and electronic microscopy
Publications: 2 articles[28,29]
- 2014-2017: 3 years ANR project STIC: "Self-stratifying intumescent coatings"
Expertise in optical and electronic microscopy and flame retardancy of polymer materials
Publications: 4 articles[30,31,32,33]

- **2013-2016: 3 years ANR project Hypopotaam**: "Flame retardant nanotalc based polymer composites".
Expertise in optical and electronic microscopy and flame retardancy of polymer materials
- 2012-2015: 3 years FP7 DEROCA project: "Development of safe and ecofriendly flame retardant materials based on CNT co-additives for commodity polymers"
Expertise in optical and electronic microscopy and flame retardancy of polymer materials
- 2011-2014: 3 years CIFRE founded by Arc International, France: "Deposition of metallicoxide coatings by atmospheric plasma"
Expertise in optical and electronic microscopy
- 2011-2014: 3 years scholarship from Irak, "Developpement of super hydrophobic coatings on stainless steel by atmospheric plasma treatment to limit dairy fouling – fundamental interactions between surface and fouling.
Expertise in optical and electronic microscopy
Publication: 1 article[34]
- 2011: 1-year Joint Technology Initiative CleanSky in the frame of the European Research project CleanSky Eco-Design in partnership with PPG Industries: "Characterization of oxide layers formed during anaphoretic paint electrodeposed on Al-alloys"
Expertise in optical and electronic microscopy
Publication: 1 article[35]
- 2010-2013: 3 years ANR Blanc international project: "Flame retarding nanoarchitectured fibers"
Expertise in optical and electronic microscopy and flame retardancy of polymer materials.
- 2009-2014: 4 years FUI project – Drawspeedglass in partnership with Saverglass – labeled by competitive cluster MAUD: "Development of organic coloring on glass at high speed"
Expertise in optical and electronic microscopy
- 2006-2008: 2 years FANsBAMED Project, in collaboration with "Groupe De Recherche BioMatériaux" and CERLA: "Functionalization, activation and nanostructuration of biomaterial surfaces for medical applications"
Expertise in optical and electronic microscopy

5. List of articles and communications

All my research works and collaborations allowed me to publish peer reviewed papers and participate to national and international conferences:

- ***Summary***

	Total	1st Author/presenter
Peer reviewed articles	91	11
Patents	2	0
Invited oral communications	16	4
Oral communications	53	12
Oral communications with peer reviewed article	25	1
Posters	14	4
Book chapters	2	0

- ***Publications (11 as first author)***

1- ***S. Bellayer**, M. Dilger, S. Duquesne, M. Jimenez, Flame-retardants for polypropylene: A review, Polymer Degradation and Stability, 230, 2024, DOI10.1016/j.polymdegradstab.2024.111008*

2- *F. Samyn, H. Ferreira, K. Bui, I. MuroPuente, C. Biget, A. Lebeau, S. Bellayer, M. Casetta, M. Jimenez, Eco-efficient, hydrophobic, self-healing and self-stratifying coating for polycarbonate Progress in Organic Coatings 196 2024, 108732, 10.1016/j.porgcoat.2024.108732*

3- *Saget, Manon; Nuns, Nicolas; Supiot, Philippe; Foissac, Corinne; Bellayer, Severine; Dourgaparsad, Kevin; Royoux, Pierre-Alexandre; Delaplace, Guillaume; Thomy, Vincent; Coffinier, Yannick; Jimenez, Maude Ultra-hydrophobic biomimetic transparent bilayer thin film deposited by atmospheric pressure plasma SURFACES AND INTERFACES 2023 42 10.1016/j.surfin.2023.103398*

4- *Masse, Morgane; Jimenez, Maude; Genay, Stephanie; Pettinari, Alice; Bellayer, Severine; Barthelemy, Christine; Decaudin, Bertrand; Blanchemain, Nicolas; Odou, Pascal Limitation of the migration of plasticizers from medical devices through treatment with low-pressure cold plasma, polydopamine coating, and annealing INTERNATIONAL JOURNAL OF PHARMACEUTICS 2023 646 10.1016/j.ijpharm.2023.123422*

5- *Gallos, Antoine; Lannoy, Oceane; Bellayer, Severine; Fontaine, Gaelle; Bourbigot, Serge; Allais, Florent Fire testing and mechanical properties of neat and elastomeric polylactic acid composites reinforced with raw and enzymatically treated hemp fibers GREEN CHEMISTRY LETTERS AND REVIEWS 2023 16 1 10.1080/17518253.2022.2164472*

6- *Gossiaux, Alexandre; Bellayer, Severine; Ortgies, Stefan; Wagener, Tobias; Koenig, Alexander; Duquesne, Sophie Systematic study of the condensed phase of phosphorus-based flame retarded foams POLYMER DEGRADATION AND STABILITY 2022 206 10.1016/j.polymdegradstab.2022.110208*

7- *Geiger, E.; Gueneau, C.; Alpettaz, T.; Bonnet, C.; Chatain, S.; Tougait, O.; Menut, D.; Bellayer, S.; Hunault, M. O. J. Y.; Corcoran, E. C. Fission products chemistry in simulated PWR fuel up to 2100°C: Experimental characterisation and TAF-ID modelling JOURNAL OF NUCLEAR MATERIALS 2022 572 10.1016/j.jnucmat.2022.154040*

8- *Thiery, Vincent; Dubois, Emmanuel; Bellayer, Severine The good, the bad and the ugly polishing: Effect of abrasive size on standardless EDS analysis of Portland cement clinker's calcium silicates MICRON 2022 158 10.1016/j.micron.2022.103266*

9- ***Bellayer**, Severine; Gossiaux, Alexandre; Duquesne, Sophie; Dewailly, Benjamin; Bachelet, Pierre; Jimenez, Maude Transparent fire protective sol-gel coating for wood panels POLYMER TESTING 2022 110 10.1016/j.polymertesting.2022.107579*

10- *Dufay, Malo; Jimenez, Maude; Casetta, Mathilde; Chai, Feng; Blanchemain, Nicolas; Stoclet, Gregory; Cazaux, Frederic; Bellayer, Severine; Degoutin, Stephanie PCL covered PP meshes plasma-grafted by sulfonated monomer for the prevention of postoperative abdominal adhesions MATERIALS TODAY COMMUNICATIONS 2021 26 10.1016/j.mtcomm.2020.101968*

11- *Scudeller, Luisa A.; Blanpain-Avet, Pascal; Six, Thierry; Bellayer, Severine; Jimenez, Maude; Croguennec, Thomas; Andre, Christophe; Delaplace, Guillaume Calcium Chelation by Phosphate Ions and Its Influence on Fouling Mechanisms of Whey Protein Solutions in a Plate Heat Exchanger FOODS 2021 10 2 10.3390/foods10020259*

12- *Gossiaux, Alexandre; Bachelet, Pierre; Bellayer, Severine; Ortgies, Stefan; Koenig, Alexander; Duquesne, Sophie Small-scale single burning item test for the study of the fire behavior of building materials FIRE SAFETY JOURNAL 2021 125 10.1016/j.firesaf.2021.103429*

13- *Liu, Weiji; Chen, Xiao Dong; Jeantet, Romain; Andre, Christophe; Bellayer, Severine; Delaplace, Guillaume Effect of casein/whey ratio on the thermal denaturation of whey proteins and subsequent fouling in a plate heat exchanger JOURNAL OF FOOD ENGINEERING 2021 289 10.1016/j.jfoodeng.2020.110175*

14- *Lemesle, Charlotte; Bellayer, Severine; Duquesne, Sophie; Schuller, Anne-Sophie; Thomas, Laurent; Casetta, Mathilde; Jimenez, Maude Self-stratified bio-based coatings: Formulation and elucidation of critical parameters governing stratification APPLIED SURFACE SCIENCE 2021 536 10.1016/j.apsusc.2020.147687*

15- *Lemesle, Charlotte; Fremiot, Jerome; Beaugendre, Agnes; Casetta, Mathilde; Bellayer, Severine; Duquesne, Sophie; Schuller, Anne-Sophie; Jimenez, Maude Life cycle assessment of multi-step versus one-step coating processes using oil or bio-based resins JOURNAL OF CLEANER PRODUCTION 2020 242 10.1016/j.jclepro.2019.118527*

16- *Louisy, Elodie; Bellayer, Severine; Fontaine, Gaelle; Rozes, Laurence; Bonnet, Fanny Novel hybrid poly(L-lactic acid) from titanium oxo-cluster via reactive extrusion polymerization EUROPEAN POLYMER JOURNAL 2020 122 10.1016/j.eurpolymj.2019.109238*

17- Bellayer, *Severine; Jimenez, Maude; Barrau, Sophie; Marin, Adeline; Sarrazin, Johan; Bourbigot, Serge Formulation of eco-friendly sol-gel coatings to flame-retard flexible polyurethane foam GREEN MATERIALS 2020 8 3 139-149 10.1680/jgrma.19.00059*

18- *Davesne, Anne-Lise; Bensabath, Tsilla; Sarazin, Johan; Bellayer, Severine; Parent, Fabrice; Samyn, Fabienne; Jimenez, Maude; Sanchette, Frederic; Bourbigot, Serge Low-Emissivity Metal/Dielectric Coatings as Radiative Barriers for the Fire Protection of Raw and Formulated Polymers ACS APPLIED POLYMER MATERIALS 2020 2 7 10.1021/acsapm.0c00399*

19- *Blanpain-Avet, P.; Andre, C.; Azevedo-Scudeller, L.; Croguennec, T.; Jimenez, M.; Bellayer, S.; Six, T.; Martins, G. A. S.; Delaplace, G. Effect of the phosphate/calcium molar ratio on fouling deposits*

generated by the processing of a whey protein isolate in a plate heat exchanger FOOD AND BIOPRODUCTS PROCESSING 2020 121 10.1016/j.fbp.2020.02.005

20- *Geoffroy, Laura; Davesne, Anne-lise; Bellayer, Severine; Blanchard, Florent; Richard, Elodie; Samyn, Fabienne; Jimenez, Maude; Bourbigot, Serge 3D printed sandwich materials filled with hydrogels for extremely low heat release rate POLYMER DEGRADATION AND STABILITY 2020 179 10.1016/j.polymdegradstab.2020.109269*

21- *Samyn, Fabienne; Vandewalle, Maxence; Bellayer, Severine; Duquesne, Sophie Sol-Gel Treatments to Flame Retard PA11/Flax Composites FIBERS 2019 7 10 10.3390/fib7100086*

22- *Davesne, Anne-Lise; Lazar, Simone; Bellayer, Severine; Qin, Shuang; Grunlan, Jaime C.; Bourbigot, Serge; Jimenez, Maude Hexagonal Boron Nitride Platelet-Based Nanocoating for Fire Protection ACS APPLIED NANO MATERIALS 2019 2 9 10.1021/acsanm.9b01055*

23- *Zouaghi, Sawsen; Bellayer, Severine; Thomy, Vincent; Dargent, Thomas; Coffinier, Yannick; Andre, Christophe; Delaplace, Guillaume; Jimenez, Maude Biomimetic surface modifications of stainless steel targeting dairy fouling mitigation and bacterial adhesion FOOD AND BIOPRODUCTS PROCESSING 2019 113 10.1016/j.fbp.2018.10.012*

24- *Beaugendre, A.; Lemesle, C.; Bellayer, S.; Degoutin, S.; Duquesne, S.; Casetta, M.; Pierlot, C.; Jaime, F.; Kim, T.; Jimenez, M. Flame retardant and weathering resistant self-layering epoxy-silicone coatings for plastics PROGRESS IN ORGANIC COATINGS 2019 136 10.1016/j.porgcoat.2019.105269*

25- *Zouaghi, S.; Abdallah, M.; Andre, C.; Chihib, N. E.; Bellayer, S.; Delaplace, G.; Celzard, A.; Jimenez, M. Graphite-based composites for whey protein fouling and bacterial adhesion management INTERNATIONAL DAIRY JOURNAL 2018 86 10.1016/j.idairyj.2018.07.004*

26- *Okyay, G.; Bellayer, S.; Samyn, F.; Jimenez, M.; Bourbigot, S. Characterization of in-flame soot from balsa composite combustion during mass loss cone calorimeter tests POLYMER DEGRADATION AND STABILITY 2018 154 10.1016/j.polymdegradstab.2018.06.013*

27- *Beaugendre, Agnes; Degoutin, Stephanie; Bellayer, Severine; Pierlot, Christel; Duquesne, Sophie; Casetta, Mathilde; Jimenez, Maude Self-Stratification of Ternary Systems Including a Flame Retardant Liquid Additive COATINGS 2018 8 12 10.3390/coatings8120448*

28- *Zouaghi, Sawsen; Barry, Mikayla E.; Bellayer, Severine; Lyskawa, Joel; Andre, Christophe; Delaplace, Guillaume; Grunlan, Melissa A.; Jimenez, Maude Antifouling amphiphilic silicone coatings for dairy fouling mitigation on stainless steel BIOFOULING 2018 34 7 10.1080/08927014.2018.1502275*

29- *Hansupo, N.; Tricot, G.; Bellayer, S.; Roussel, P.; Samyn, F.; Duquesne, S.; Jimenez, M.; Hollman, M.; Catala, P.; Bourbigot, S. Getting a better insight into the chemistry of decomposition of complex flame retarded formulation: New insights using solid state NMR POLYMER DEGRADATION AND STABILITY 2018 153 10.1016/j.polymdegradstab.2018.04.028*

30- *Zouaghi, Sawsen; Six, Thierry; Bellayer, Severine; Coffinier, Yannick; Abdallah, Marwan; Chihib, Nour-Eddine; Andre, Christophe; Delaplace, Guillaume; Jimenez, Maude Atmospheric pressure plasma spraying of silane-based coatings targeting whey protein fouling and bacterial adhesion management APPLIED SURFACE SCIENCE 2018 455 10.1016/j.apsusc.2018.06.006*

31- *Zouaghi, Sawsen; Six, Thierry; Nuns, Nicolas; Simon, Pardis; Bellayer, Severine; Moradi, Sona; Hatzikiriakos, Sawas G.; Andre, Christophe; Delaplace, Guillaume; Jimenez, Maude Influence of stainless-steel surface properties on whey protein fouling under industrial processing conditions JOURNAL OF FOOD ENGINEERING 2018 228 10.1016/j.jfoodeng.2018.02.009*

32- *Khaldi, M.; Croguennec, T.; Andre, C.; Ronse, G.; Jimenez, M.; Bellayer, S.; Blanpain-Avet, P.; Bouvier, L.; Six, T.; Bornaz, S.; Jeantet, R.; Delaplace, G. Effect of the calcium/protein molar ratio on β-lactoglobulin denaturation kinetics and fouling phenomena INTERNATIONAL DAIRY JOURNAL 2018 78 10.1016/j.idairyj.2017.10.002*

33- *Naik, Anil D.; Bourbigot, Serge; Bellayer, Severine; Touati, Nadia; Ben Tayeb, Karima; Vezin, Herve; Fontaine, Gaelle Salen Complexes as Fire Protective Agents for Thermoplastic Polyurethane: Deep Electron Paramagnetic Resonance Spectroscopy Investigation ACS APPLIED MATERIALS & INTERFACES 2018 10 29 10.1021/acsami.8b07323*

34- ***Bellayer****, S.; Jimenez, M.; Prieur, B.; Dewailly, B.; Ramgobin, A.; Sarazin, J.; Revel, B.; Tricot, G.; Bourbigot, S. Fire retardant sol-gel coated polyurethane foam: Mechanism of action POLYMER DEGRADATION AND STABILITY 2018 147 10.1016/j.polymdegradstab.2017.12.005*

35- *Souada, Malika; Louage, Christophe; Doisy, Jean-Yves; Meunier, Ludivine; Benderrag, Abdelkader; Ouddane, Baghdad; Bellayer, Severine; Nuns, Nicolas; Traisnel, Michel; Maschke, Ulrich Extraction of indium-tin oxide from end-of-life LCD panels using ultrasound assisted acid leaching ULTRASONICS SONOCHEMISTRY 2018 40 10.1016/j.ultsonch.2017.08.043*

36- *Beaugendre, A.; Saidi, S.; Degoutin, S.; Bellayer, S.; Pierlot, C.; Duquesne, S.; Casetta, M.; Jimenez, M. One pot flame retardant and weathering resistant coatings for plastics: a novel approach RSC ADVANCES 2017 7 65 10.1039/c7ra08028j*

37- *Lesaffre, Nicolas; Bellayer, Severine; Vezin, Herve; Fontaine, Gaelle; Jimenez, Maude; Bourbigot, Serge Recent advances on the ageing of flame retarded PLA: Effect of UV-light and/or relative humidity POLYMER DEGRADATION AND STABILITY 2017 139 10.1016/j.polymdegradstab.2017.04.007*

38- *Beaugendre, A.; Degoutin, S.; Bellayer, S.; Pierlot, C.; Duquesne, S.; Casetta, M.; Jimenez, M. Self-stratifying epoxy/silicone coatings PROGRESS IN ORGANIC COATINGS 2017 103 10.1016/j.porgcoat.2016.10.025*

39- *Prieur, B.; Meub, M.; Wittemann, M.; Klein, R.; Bellayer, S.; Fontaine, G.; Bourbigot, S. Phosphorylation of lignin: characterization and investigation of the thermal decomposition RSC ADVANCES 2017 7 27 10.1039/c7ra00295e*

40- *Beaugendre, A.; Degoutin, S.; Bellayer, S.; Pierlot, C.; Duquesne, S.; Casetta, M.; Jimenez, M. Self-stratifying coatings: A review PROGRESS IN ORGANIC COATINGS 2017 110 10.1016/j.porgcoat.2017.03.011*

41- *Zouaghi, Sawsen; Six, Thierry; Bellayer, Severine; Moradi, Sona; Hatzikiriakos, Savvas G.; Dargent, Thomas; Thomy, Vincent; Coffinier, Yannick; Andre, Christophe; Delaplace, Guillaume; Jimenez, Maude Antifouling Biomimetic Liquid-Infused Stainless Steel: Application to Dairy Industrial Processing ACS APPLIED MATERIALS & INTERFACES 2017 9 31 10.1021/acsami.7b06709*

42- *Fontaine, Gaelle; Desmarchelier, Hugo; Dupretz, Renaud; Naik, Anil; Bellayer, Severine; Duquesne, Sophie; Bourbigot, Serge Development of new flame retardants: application to polyurethane and polybutylene terephthalate ABSTRACTS OF PAPERS OF THE AMERICAN CHEMICAL SOCIETY 2016 252*

43- *Jimenez, Maude; Bellayer, Severine; Naik, Anil; Bachelet, Pierre; Duquesne, Sophie; Bourbigot, Serge Topcoats versus Durability of an Intumescent Coating INDUSTRIAL & ENGINEERING CHEMISTRY RESEARCH 2016 55 36 10.1021/acs.iecr.6b02484*

44- Bellayer, *S.; Jimenez, M.; Barrau, S.; Bourbigot, S. Fire retardant sol-gel coatings for flexible polyurethane foams RSC ADVANCES 2016 6 34 10.1039/c6ra02094a*

45- *Jimenez, Maude; Guin, Tyler; Bellayer, Severine; Dupretz, Renaud; Bourbigot, Serge; Grunlan, Jaime C. Microintumescent mechanism of flame-retardant water-based chitosan-ammonium polyphosphate multilayer nanocoating on cotton fabric JOURNAL OF APPLIED POLYMER SCIENCE 2016 133 32 10.1002/app.43783*

46- *Rachida Cherrak, Mohammed Hadje, Nouredine Benderdouche, Severine Bellayer, Michel Traisnel Treatment of recalcitrant organic pollutants in water by heterogeneous catalysis using a mixed material (TiO2-diatomite of algeria) Desalination and Water Treatment DESALINATION AND WATER TREATMENT 2016 57, 36, 17139-17148*

47- Bellayer, *S.; Jimenez, M.; Gardelle, B.; Delaplace, G.; Bouquerel, J.; Duquesne, S.; Bourbigot, S. The electron microanalyzer (EPMA): a powerful device for the microanalysis of filled polymeric materials POLYMERS FOR ADVANCED TECHNOLOGIES 2015 26 8 10.1002/pat.3523*

48- *Vandenbossche, Marianne; Derozier, Dominique; Casetta, Mathilde; Jimenez, Maude; Bellayer, Severine; Traisnel, Michel An innovative method to functionalize textiles for the remediation of polluted media APPLIED SURFACE SCIENCE 2015 330 10.1016/j.apsusc.2014.12.166*

49- *Naik, Anil D.; Fontaine, Gaelle; Bellayer, Severine; Bourbigot, Serge Salen based Schiff bases to flame retard thermoplastic polyurethane mimicking operational strategies of thermosetting resin RSC ADVANCES 2015 5 60 10.1039/c5ra06242j*

50- *Jimenez, Maude; Lesaffre, Nicolas; Bellayer, Severine; Dupretz, Renaud; Vandenbossche, Marianne; Duquesne, Sophie; Bourbigot, Serge Novel flame retardant flexible polyurethane foam: plasma induced graft-polymerization of phosphonates RSC ADVANCES 2015 5 78 10.1039/c5ra08289g*

51- *Naik, Anil D.; Fontaine, Gaelle; Bellayer, Severine; Bourbigot, Serge Crossing the Traditional Boundaries: Salen-Based Schiff Bases for Thermal Protective Applications ACS APPLIED MATERIALS & INTERFACES 2015 7 38 10.1021/acsami.5b05164*

52- *M.H. Staia, E.S. Puchi Cabrera, A. Iost, A. Zairi, S. Bellayer, A. Van Gorp Tribological response of AA 2024-T3 aluminium alloy coated with a DLC duplex coating TRIBOLOGY INTERNATIONAL 2015 85, 74-87 10.1016/j.triboint.2014.12.007*

53- *Degoutin, Stephanie; Jimenez, Maude; Chai, Feng; Pinalie, Thibaut; Bellayer, Severine; Vandenbossche, Marianne; Neut, Christel; Blanchemain, Nicolas; Martel, Bernard Simultaneous immobilization of heparin and gentamicin on polypropylene textiles: A dual therapeutic activity JOURNAL OF BIOMEDICAL MATERIALS RESEARCH PART A 2014 102 11 10.1002/jbm.a.35059*

54- *Vandenbossche, M.; Casetta, M.; Jimenez, M.; Bellayer, S.; Traisnel, M. Cysteine-grafted nonwoven geotextile: A new and efficient material for heavy metals sorption - Part A JOURNAL OF ENVIRONMENTAL MANAGEMENT 2014 132 10.1016/j.jenvman.2013.10.027*

55- *Naik, Anil D.; Fontaine, Gaelle; Samyn, Fabienne; Delva, Xavier; Louisy, Jeremie; Bellayer, Severine; Bourgeois, Yann; Bourbigot, Serge Mapping the multimodal action of melamine-poly(aluminium phosphate) in the flame retardancy of polyamide 66 RSC ADVANCES 2014 4 35 10.1039/c4ra02005g*

56- *Naik, Anil D.; Fontaine, Gaelle; Samyn, Fabienne; Delva, Xavier; Louisy, Jeremie; Bellayer, Severine; Bourgeois, Yann; Bourbigot, Serge Outlining the mechanism of flame retardancy in polyamide 66 blended with melamine-poly(zinc phosphate) FIRE SAFETY JOURNAL 2014 70 10.1016/j.firesaf.2014.08.019*

57- *Collinet-Fressancourt, Marion; Nuns, Nicolas; Bellayer, Severine; Traisnel, Michel Characterization by TEM and ToF-SIMS of the oxide layer formed during anaphoretic paint electrodeposition on Al-alloys APPLIED SURFACE SCIENCE 2013 277 10.1016/j.apsusc.2013.04.023*

58- *Gardelle, B.; Duquesne, S.; Vandereecken, P.; Bellayer, S.; Bourbigot, S. Resistance to fire of curable silicone/expandable graphite-based coating: Effect of the catalyst EUROPEAN POLYMER JOURNAL 2013 49 8 10.1016/j.eurpolymj.2013.04.021*

59- *Duquesne, Sophie; Bachelet, Pierre; Bellayer, Severine; Bourbigot, Serge; Mertens, William Influence of inorganic fillers on the fire protection of intumescent coatings JOURNAL OF FIRE SCIENCES 2013 31 3 10.1177/0734904112467291*

60- *Vandenbossche, M.; Jimenez, M.; Casette, M.; Bellayer, S.; Beaurain, A.; Bourbigot, S.; Traisnel, M.Chitosan-grafted nonwoven geotextile for heavy metals sorption in sediments REACTIVE & FUNCTIONAL POLYMERS 2013 73 1 10.1016/j.reactfunctpolym.2012.09.002*

61- *Gardelle, B.; Duquesne, S.; Vandereecken, P.; Bellayer, S.; Bourbigot, S. Resistance to fire of intumescent silicone-based coating: The role of organoclay PROGRESS IN ORGANIC COATINGS 2013 76 11 10.1016/j.porgcoat.2013.07.011*

62- *Jimenez, M.; Delaplace, G.; Nuns, N.; Bellayer, S.; Deresmes, D.; Ronse, G.; Alogaili, G.; Collinet-Fressancourt, M.; Traisnel, M. Toward the understanding of the interfacial dairy fouling deposition and growth mechanisms at a stainless-steel surface: A multiscale approach JOURNAL OF COLLOID AND INTERFACE SCIENCE 2013 404 10.1016/j.jcis.2013.04.021*

63- *Jimenez, M.; Bellayer, S.; Revel, B.; Duquesne, S.; Bourbigot, S. Comprehensive Study of the Influence of Different Aging Scenarios on the Fire Protective Behavior of an Epoxy Based Intumescent Coating INDUSTRIAL & ENGINEERING CHEMISTRY RESEARCH 2013 52 2 10.1021/ie302137g*

64- *Degoutin, S.; Jimenez, M.; Casetta, M.; Bellayer, S.; Chai, F.; Blanchemain, N.; Neut, C.; Kacem, I.; Traisnel, M.; Martel, B. Anticoagulant and antimicrobial finishing of non-woven polypropylene textiles BIOMEDICAL MATERIALS 2012 7 3 10.1088/1748-6041/7/3/035001*

65- *Gerard, Caroline; Fontaine, Gaelle; Bellayer, Severine; Bourbigot, Serge Reaction to fire of an intumescent epoxy resin: Protection mechanisms and synergy POLYMER DEGRADATION AND STABILITY 2012 97 8 10.1016/j.polymdegradstab.2012.05.025*

66- ***Bellayer**, Severine Patricia; Tavard, E.; Duquesne, S.; Piechaczyk, A.; Bourbigot, S. Natural mineral fire-retardant fillers for polyethylene FIRE AND MATERIALS 2011 35 3 10.1002/fam.1048*

67- *Fox, Douglas M.; Harris, Richard H., Jr.; Bellayer, Severine; Gilman, Jeffrey W.; Gelfer, Mikhail Y.; Hsaio, Benjamin S.; Maupin, Paul H.; Trulove, Paul C.; De Long, Hugh C. The pillaring effect of the 1,2-dimethyl-3(benzyl ethyl iso-butyl POSS) imidazolium cation in polymer/montmorillonite nanocomposites POLYMER 2011 52 23 10.1016/j.polymer.2011.09.016*

68- *Bouanis, F. Z.; Bentiss, F.; Bellayer, S.; Vogt, J. B.; Jama, C. Radiofrequency cold plasma nitrided carbon steel: Microstructural and micromechanical characterizations MATERIALS CHEMISTRY AND PHYSICS 2011 127 1-2 10.1016/j.matchemphys.2011.02.013*

69- *Jimenez, M.; Bellayer, S.; Duquesne, S.; Bourbigot, S. Improvement of heat resistance of high-performance fibers using a cold plasma polymerization process SURFACE & COATINGS TECHNOLOGY 2010 205 3 10.1016/j.surfcoat.2010.07.091*

70- *Podlesak, Harry; Pawlowski, Lech; d'Haese, Romain; Laureyns, Jacky; Lampke, Thomas; Bellayer, Severine Advanced Microstructural Study of Suspension Plasma Sprayed Hydroxyapatite Coatings JOURNAL OF THERMAL SPRAY TECHNOLOGY 2010 19 3 10.1007/s11666-010-9471-6*

71- *E.S. Puchi-Cabrera, M.H. Staia, M.J. Ortiz-Mancilla, J.G. La Barbera-Sosa, E.A. Ochoa Pérez, C. Villalobos-Gutiérrez, S. Bellayer, M. Traisnel, D. Chicot, J. Lesage, Fatigue behavior of a SAE 1045 steel coated with Colmonoy 88 alloy deposited by HVOF thermal spray, SURFACE AND COATINGS TECHNOLOGY 2010 205, 4, 1119-1126 10.1016/j.surfcoat.2010.01.011*

72- Bellayer, *S.; Tavard, E.; Duquesne, S.; Piechaczyk, A.; Bourbigot, S. Mechanism of intumescence of a polyethylene/calcium carbonate/stearic acid system POLYMER DEGRADATION AND STABILITY 2009 94 5 10.1016/j.polymdegradstab.2009.01.032*

73- Bellayer, *Severine; Viau, Lydie; Tebby, Zoe; Toupance, Thierry; Le Bideau, Jean; Vioux, Andre Immobilization of ionic liquids in translucent tin dioxide monoliths by sol-gel processing DALTON TRANSACTIONS 2009 8 10.1039/b814978j*

74- *Lunstroot, Kyra; Driesen, Kris; Nockemann, Peter; Van Hecke, Kristof; Van Meervelt, Luc; Goerller-Walrand, Christiane; Binnemans, Koen; Bellayer, Severine; Viau, Lydie; Le Bideau, Jean; Vioux, Andre Lanthanide-doped luminescent ionogels DALTON TRANSACTIONS 2009 2 10.1039/b812292j*

75- *Bourbigot, Serge; Turf, Thomas; Bellayer, Severine; Duquesne, Sophie Polyhedral oligomeric silsesquioxane as flame retardant for thermoplastic polyurethane POLYMER DEGRADATION AND STABILITY 2009 94 8 10.1016/j.polymdegradstab.2009.04.016*

76- *Ehora, G.; Daviero-Minaud, S.; Steil, M. C.; Gengembre, L.; Frere, M.; Bellayer, S.; Mentre, O. Ru-Pyrochlores: Compositional Tuning for Electrochemical Stability as Cathode Materials for IT-SOFCs CHEMISTRY OF MATERIALS 2008 20 24 10.1021/cm801942c*

77- *Suarez, M.; Bellayer, S.; Traisnel, M.; Gonzalez, W.; Chicot, D.; Lesage, J.; Puchi-Cabrera, E. S.; Staia, M. H. Corrosion behavior of Cr3C2-NiCr vacuum plasma sprayed coatings SURFACE & COATINGS TECHNOLOGY 2008 202 18 10.1016/j.surfcoat.2008.04.043*

78- *Bourbigot, Serge; Fontaine, Gaelle; Bellayer, Severine; Delobel, Rene Processing and nanodispersion: A quantitative approach for polylactide nanocomposite POLYMER TESTING 2008 27 1 10.1016/j.polymertesting.2007.07.008*

79- *Samyn, Fabienne; Bourbigot, Serge; Jama, Charafeddine; Bellayer, Severine; Nazare, Shonali; Hull, Richard; Fina, Alberto; Castrovinci, Andrea; Camino, Giovanni Characterisation of the dispersion in polymer flame retarded nanocomposites EUROPEAN POLYMER JOURNAL 2008 44 6 10.1016/j.eurpolymj.2008.03.018*

80- Bellayer, *S.; Gilman, J. W.; Rahatekar, S. S.; Bourbigot, S.; Flambard, X.; Hanssen, L. M.; Guo, H.; Kumar, S. Characterization of SWCNT and PAN/SWCNT films CARBON 2007 45 12 10.1016/j.carbon.2007.06.057*

81- *Le Bideau, J.; Gaveau, P.; Bellayer, S.; Neouze, M.-A.; Vioux, A. Effect of confinement on ionic liquids dynamics in monolithic silica ionogels:: ¹H NMR study PHYSICAL CHEMISTRY CHEMICAL PHYSICS 2007 9 40 10.1039/b711539c*

82- *Langat, J.; Bellayer, S.; Hudrlik, P.; Hudrlik, A.; Maupin, P. H.; Gilman, J. W., Sr.; Raghavan, D. Synthesis of imidazolium salts and their application in epoxy montmorillonite nanocomposites POLYMER 2006 47 19 10.1016/j.polymer.2006.06.067*

83- *Zammarano, M; Bellayer, S; Gilman, JW; Franceschi, M; Beyer, FL; Harris, RH; Meriani, S Delamination of organo-modified layered double hydroxides in polyamide 6 by melt processing POLYMER 2006 47 2 10.1016/j.polymer.2005.11.080*

84- *Lunstroot, Kyra; Driesen, Kris; Nockemann, Peter; Gorller-Walrand, Christiane; Binnemans, Koen; Bellayer, Severine; Le Bideau, Jean; Vioux, Andre Luminescent ionogels based on europium-doped ionic liquids confined within silica-derived networks CHEMISTRY OF MATERIALS 2006 18 24 10.1021/cm061704w*

85- *Neouze, Marie-Alexandra; Le Bideau, Jean; Gaveau, Philippe; Bellayer, Severine; Vioux, Andre Ionogels, new materials arising from the confinement of ionic liquids within silica-derived networks CHEMISTRY OF MATERIALS 2006 18 17 10.1021/cm060656c*

86- Bellayer, *S; Gilman, JW; Eidelman, N; Bourbigot, S; Flambard, X; Fox, DM; De Long, HC; Trulove, PC Preparation of homogeneously dispersed multiwalled carbon nanotube/polystyrene nanocomposites via melt extrusion using trialkyl imidazolium compatibilizer ADVANCED FUNCTIONAL MATERIALS 2005 15 6 10.1002/adfm.200400441*

87- *Zammarano, M; Franceschi, M; Bellayer, S; Gilman, JW; Meriani, S Preparation and flame resistance properties of revolutionary self-extinguishing epoxy nanocomposites based on layered double hydroxides POLYMER 2005 46 22 10.1016/j.polymer.2005.07.050*

88- *Kashiwagi, T; Du, FM; Winey, KI; Groth, KA; Shields, JR; Bellayer, SP; Kim, H; Douglas, JF Flammability properties of polymer nanocomposites with single-walled carbon nanotubes: effects of nanotube dispersion and concentration POLYMER 2005 46 2 10.1016/j.polymer.2004.10.087*

89- *Maupin, PH; Gilman, JW; Harris, RH; Bellayer, S; Bur, AJ; Roth, SC; Murariu, M; Morgan, AB; Harris, JD Optical probes for monitoring intercalation and exfoliation in melt-processed polymer nanocomposites MACROMOLECULAR RAPID COMMUNICATIONS 2004 25 7 10.1002/marc.200300262*

90- *Bourbigot, S; Vanderhart, DL; Gilman, JW; Bellayer, S; Stretz, H; Paul, DR Solid state NMR characterization and flammability of styrene-acrylonitrile copolymer montmorillonite nanocomposite POLYMER 2004 45 22 10.1016/j.polymer.2004.08.057*

91- *M. Lewandowski, M. Rochery, S. Bellayer, and S. Fourdrin, "Rheology of the Curing Process of Acrylic Latexes Used as Chemical Binders", Appl. Rheol. 12:4, 174-181, 2002.*

- ***Oral Communications***

Invited oral communications (4 as first author) :

1- *M. Jimenez, C. Lemesle, S. Bellayer, S. Duquesne, M. Casetta, A.-S. Schuller, J. Molina, Bio-based flame retardant self-stratifying coatings, SFRMT 2023, Beijing, Chine, Mar 2023*

2- *M. Jimenez, C. Lemesle, H. Ferreira, M. Casetta, F. Samyn, C. Biget, A. Lebeau, S. Bellayer, S. Duquesne, A.-S. Schuller, J. Molina, Eco-efficient, bio-based and smart self-stratifying coatings, 6th world congress on materials science engineering, Rome, Italie, Sep 2023*

3- *M. Jimenez, C. Lemesle, H. Ferreira, M. Casetta, F. Samyn, C. Biget, A. Lebeau, S. Bellayer, S. Duquesne, A.-S. Schuller, J. Molina, Smart fire protective thin coatings for plastics, Congrès AMI: Fire resistance in plastics, Berlin, Allemagne, Nov 2023*

4- ***S. Bellayer**, A. Gossiaux, S. Duquesne, M. Jimenez, Thin and Thick FR sol-gel coating, 2022 ACS Fire and Polymers, Napa Valley, CA, Etats-Unis d'Amérique, Juin 2022*

5- ***S. Bellayer**, M. Jimenez, B. Prieur, B. Dewailly, A. Ramgobin, J. Sarazin, B. Revel, G. Tricot, Fire retardant sol-gel coatings for flexible polyurethane foams, AMI Fire resistance in plastics, Cologne, Allemagne, Déc 2018*

6- *M. Jimenez, A. Beaugendre, S. Degoutin, S. Bellayer, C. Pierlot, S. Duquesne, M. Casetta, Flame retardant and weathering resistant self-stratifying coatings, European Coatings 2017 - Fire retardancy, Berlin, Allemagne, Oct 2017*

7- ***S. Bellayer**, M. Jimenez, S. Duquesne, S. Barrau, S. Bourbigot, Plasma and sol-gel flame retardant coatings for flexible PU foam, AMI Polymer Foam 2017, Cologne, Allemagne, Nov 2017*

8- *A. Beaugendre, S. Bellayer, S. Degoutin, C. Pierlot, R. Lebeuf, S. Duquesne, M. Casetta, M. Jimenez, Self-stratifying coatings, Eurocoat 2016, Paris, France, Mar 2016*

9- ***S. Bellayer**, M. Jimenez, S. Duquesne, F. Solarski, S. Bourbigot, Chemical characterization of flame retarded fibers and textiles, COST FLARETEX MP1105, Poznan, Pologne, Avr 2016*

10- *G. Fontaine, H. Desmarchelier, R. Dupretz, A.D. Naik, S. Bellayer, S. Duquesne, S. Bourbigot, Development of new flame retardants: application to Polyurethane and Polybutylene terephthalate, 252th National American Chemical Society Meeting, Philadelphia, Etats-Unis d'Amérique, Aout 2016*

11- *S. Duquesne, F. Solarski, M. Jimenez, S. Bellayer, S. Bourbigot, Similitude in fire testing : a realistic approach?, Fire Resistance in Plastics 2015, Trends and technical developments in the international flame retardant industry, Cologne, Allemagne, Déc 2016*

12- *G. Fontaine, A.D. Naik, S. Bellayer, S. Bourbigot, Salen based schiff bases: A new class of fire retardant, 26th Annual Conference on Recent Advances in Flame Retardancy of Polymeric Materials, Stamford, Etats-Unis d'Amérique, Mai 2015*

13- *S. Duquesne, F. Solarski, M. Jimenez, S. Bellayer, S. Bourbigot, Polyurethanes: a case study for the design of flame retardant materials, AMI Fire resistance in plastics, Cologne, Allemagne, Déc 2015*

14- *S. Bourbigot, F. Solarski, S. Bellayer, G. Fontaine, S. Duquesne, INFLUENCE OF THE NANOMORPHOLOGY ON THE REACTION TO FIRE OF FLAME RETARDED POLYMER, 5th International Seminar on Modern Polymeric Materials for Environmental Applications, Cracovie, Pologne, Mai 2013*

15- *M. Jimenez, S. Bellayer, S. Duquesne, S. Bourbigot, Weathering of intumescent coatings, 24rd Annual Recent Advances in Flame Retardancy of Polymeric Materials (BCC research Flame conference), Stamford, Etats-Unis d'Amérique, Mai 2013*

16- *G. Fontaine, C. Gérard, S. Bellayer, S. Bourbigot, POSS a synergist for fire retardant epoxy resin/APP SYSTEM: mechanism of action, 22th BCC Conference - Recent Advances in Flame Retardancy of Polymeric Materials, Stamford, USA, Mai 2011*

Oral communications (12 as first author) :

1- *S. Laidioui, S. Bellayer, L. Delepierre, A. Koenig, T. Heinz Steinke, S. Duquesne, Synthesis and study of the mechanical and fire behavior of phenolic foams, FRPM 2025, 3-6 june 2025, Madrid, Spain.*

2- ***S. Bellayer**, P. Bachelet, J. Sarazin, S. Bourbigot, Fire-Resist – a facility to perform and develop small scale fire tests, 4th école thématique des sciences des Incendies et applications, Stella Plage, France, April 2025.*

3- *G. Delaplace, W. Liu, M. Abdallah, L. Azevedo-Scudeller, A. Descamps, T. Six, P. Blanpain Avet, S. Bellayer, R. Jeantet, M. Jimenez, Role of calcium and casein micelle on the thermal denaturation of whey protein solutions and fouling mechanisms, International Congress on Engineering and Food, ICEF 14, Nantes, France, Mai 2024*

4- *M. Jimenez, C. Lemesle, S. Bellayer, S. Duquesne, M. Casetta, A.-S. Schuller, J. Molina, Eco-efficient flame retardant bio-based self-stratifying coatings, SICT Conference, Lisbon, Portugal, Avr 2023*

5- *K. Dourgaparsad, M. Saget, S. Zouaghi, N. Nuns, S. Bellayer, M. Grunlan, D. Balloy, C. GRUESCU, G. Delaplace, Surface engineering of stainless steel for dairy fouling management, 14th International Congress of Engineering and Food (ICEF14), Nantes, France, Juin 2023*

6- *K. Dourgaparsad, M. Saget, S. Zouaghi, N. Nuns, S. Bellayer, M. Grunlan, V. Thomy, Y. Coffinier, D. Balloy, C. GRUESCU, G. Delaplace, M. Jimenez, Surface engineering of stainless steel for dairy fouling management, Nature Inspired Creativity Engineers, Nice, France, Juin 2023*

7- *M. Jimenez, C. Lemesle, S. Bellayer, S. Duquesne, M. Casetta, A.-S. Schuller, J. Molina, Bio-based flame retardant self-stratifying coatings, ECOFRAM 2022, Alès, France, Mai 2022*

8- ***S. Bellayer**, A. Gossiaux, M. Jimenez, Transparent FR Sol-Gel coatings for wood panels, 3rd International Conference on ECO-friendly Flame Retardant Additives and Materials (ECOFRAM), Alès, France, Mai 2022*

9- *M. Jimenez, C. Lemesle, S. Bellayer, S. Duquesne, M. Casetta, A.-S. Schuller, J. Molina, Bio-based flame retardant self-stratifying coatings, Polymers 2022, Los Angeles, CA, Etats-Unis d'Amérique, Oct 2022*

10- *M. Dufay, F. Cazaux, F. Chai, N. Blanchemain, S. Bellayer, G. Stoclet, M. Casetta, M. Jimenez, S. Degoutin, Implants péritonéaux recouverts de nanofibres anticoagulantes pour la prévention des adhérences post-opératoires, Matériaux 2022, Lille, France, Oct 2022*

11- *S. **Bellayer**, A. Gossiaux, P. Bachelet, S. Duquesne, M. Jimenez, Transparent fire protective sol-gel coatings for wood panels, Workshop: Recent developments in flame-retardant materials by surface treatments, Mons/Belgique, Belgique, Nov 2022*

12- *M. Jimenez, C. Lemesle, S. Bellayer, S. Duquesne, M. Casetta, A.-S. Schuller, J. Molina, Bio-based flame retardant self-stratifying coatings, Workshop MateriaNova, Mons, Belgique, Nov 2022*

13- *M. Dufay, S. Degoutin, F. Cazaux, F. Chai, N. Blanchemain, S. Bellayer, G. Stoclet, M. Casetta, M. Jimenez, Plasma grafting or Coaxial electrospinning: comparison of functionalized PP meshes with anticoagulant activity, World Biomaterials Congress, Glasgow, Scotland, Royaume-Uni, Déc 2020*

14- *M. Dufay, S. Degoutin, F. Cazaux, F. Chai, N. Blanchemain, S. Bellayer, G. Stoclet, M. Casetta, M. Jimenez, PP peritoneal meshes covered with PCL nanofibers functionalized by cold plasma with antiadhesive properties, Frontiers in Biomedical Polymers, Tenerife, Espagne, Mai 2019*

15- *M. Dufay, S. Degoutin, F. Cazaux, L. Janus, F. Chai, N. Blanchemain, S. Bellayer, G. Stoclet, M. Casetta, M. Jimenez, Functionalized nanofibers with anticoagulant activity for postoperative adhesions prevention: plasma grafting or coaxial electrospinning, BIOMAT 2019, La Grande Motte, France, Juin 2019*

16- *W. Liu, X.D. Chen, R. Jeantet, R. Mercadé-Prieto, C. Andre, S. Bellayer, G. Delaplace, Role of casein on the heat-induced denaturation of whey proteins and subsequent fouling in plate heat exchanger, Heat Exchanger Fouling & cleaning conference XIII 2019, Jozefow, Pologne, Juin 2019*

17- *M. Dufay, S. Degoutin, F. Cazaux, L. Janus, F. Chai, N. Blanchemain, S. Bellayer, G. Stoclet, M. Casetta, M. Jimenez, Polypropylene peritoneal meshes functionalized by electrospinning and cold plasma treatment for anticoagulant properties, 47èmes Journées d'Études des Polymères, Latresne, France, Sep 2019*

18- *M. Jimenez, A. Beaugendre, C. Lemesle, S. Bellayer, S. Degoutin, C. Pierlot, M. Collinet, A.-S. Schuller, R. Saint-Loup, S. Duquesne, M. Casetta, S. Bourbigot, Eco-efficient flame retardant self-stratifying coatings for plastics, Ecofram 2018, Metz, France, Mar 2018*

19- ***S. Bellayer**, M. Jimenez, S. Barrau, P. Bachelet, B. Dewailly, A. Ramgobin, J. Sarazin, S. Bourbigot, Fire Retardant sol-gel coatings for flexible polyurethane foams, Ecofram 2018, Metz, France, Mar 2018*

20- S. Zouaghi, M. Barry, S. Bellayer, S. Moradi, S.G. Hatzikiriakos, T. Dargent, V. Thomy, Y. Coffinier, C. Andre, M.A. Grunlan, G. Delaplace, M. Jimenez, Surface modification of stainless steel targeting dairy fouling mitigation, Fouling and Cleaning in Food Processing 2018, Lund, Suède, Avr 2018

21- G. Okyay, S. Bellayer, F. Solarski, M. Jimenez, S. Bourbigot, Multi-scale assessment of soot using electron microscopy: applications on soot from bench-scale fire of polymers, Nanotech France 2018, Paris, France, Juin 2018

22- M. Jimenez, S. Zouaghi, M. Barry, S. Bellayer, S. Moradi, S.G. Hatzikiriakos, T. Dargent, V. Thomy, Y. Coffinier, C. Andre, M.A. Grunlan, G. Delaplace, Biomimetic approaches targeting dairy fouling mitigation of stainless steel, Smart Materials and Surfaces, Venise, Italie, Oct 2018

23- A. Hamieh, F. Ponchel, D. Remiens, S. Barrau, A. Addad, S. Bellayer, Synthèse de composites piézoélectriques céramique/polymère pour la réalisation des transducteurs électro-acoustiques, UGéPE 2018, Villeneuve d'Ascq, France, Nov 2018

24- G. Okyay, S. Bellayer, M. Jimenez, F. Solarski, S. Bourbigot, Light scattering properties of soot aggregates from fire scenarios of polymer burning, The 16th. Electromagnetic and Light Scattering Conference ELS-XVI, University of Maryland, Etats-Unis d'Amérique, Mar 2017

25- S. Zouaghi, T. Six, N. Nuns, A. Beaugendre, S. Bellayer, C. Andre, G. Delaplace, M. Jimenez, Antifouling silane-based coatings on stainless steel for dairy products processing, SurfKorea2017, Incheon, Corée du Sud, Mar 2017

26- A. Beaugendre, S. Bellayer, S. Degoutin, C. Pierlot, R. Lebeuf, S. Duquesne, M. Casetta, M. Jimenez, Design of flame-retardant self-stratifying coatings for plastics, SurfKorea2017, Incheon, Corée du Sud, Mar 2017

*27- S. **Bellayer**, M. Jimenez, M. Casetta, A. Beaugendre, S. Duquesne, S. Bourbigot, The microanalysis of polymer blends or filled polymers using electron probe microanalyzer, European Polymer Federation Congress, Lyon, France, Juil 2017*

28- S. Zouaghi, T. Six, N. Nuns, S. Bellayer, C. Andre, G. Delaplace, M. Jimenez, Antifouling surface modifications of stainless steel for dairy products processing, 16ème congrès de la Société Française de Génie des Procédés (SFGP), Nancy, France, Juil 2017

29- S. Duquesne, O. Galvis, F. Solarski, S. Bellayer, Flame Retardancy of Bio-Based Flax Composites : sol-gel and reactive approaches, BIOPOL 2017, Mons, Belgique, Sep 2017

30- F. Solarski, O. Galvis, S. Duquesne, S. Bellayer, Approches Innovantes D'ignifugation De Bio-Composites Thermoplastiques, Gdr Feux, 12-13 Octobre 2017, Toulouse, France, GDR Feux, Toulouse, France, Oct 2017

31- M. Jimenez, A. Beaugendre, S. Degoutin, S. Bellayer, C. Pierlot, S. Duquesne, M. Casetta, "one pot" flame retardant and weathering resistant coatings for plastics, AOFSM 2017, Shenzen, Chine, Oct 2017

*32- S**. Bellayer**, M. Jimenez, S. Bourbigot, Flame retardant coating for flexible PU foams, AMI Polymer Foam 2017, Cologne, Allemagne, Nov 2017*

33- A. Beaugendre, S. Bellayer, S. Degoutin, C. Pierlot, R. Lebeuf, S. Duquesne, M. Casetta, M. Jimenez, Self-stratifying coatings, Eurocoat, Paris, France, Mar 2016

34- A. Beaugendre, S. Bellayer, S. Degoutin, C. Pierlot, R. Lebeuf, S. Duquesne, M. Casetta, M. Jimenez, Epoxy/silicon self-stratifying coatings, The 12th Coatings Science International, Noordwijk, Pays-Bas, Juin 2016

35- M. Jimenez, A. Beaugendre, M. Casetta, S. Bellayer, S. Duquesne, S. Bourbigot, Solutions against weathering of intumescent fire resistant coatings?, ISPAC 2016, Singapour, Singapour, Juin 2016

36- S. Zouaghi, G. Ronse, N. Nuns, S. Bellayer, C. Andre, G. Delaplace, M. Jimenez, Toward the understanding of dairy fouling mechanisms in pasteurization conditions, Workshop Expert'Labs, Fuveau, France, Juin 2016

37- M. Jimenez, S. Bellayer, S. Duquesne, S. Bourbigot, Functional durability of intumescent coatings - Influence of topcoats, ISFRMT 2016, Changchun, Chine, Juin 2016

38- S. Zouaghi, G. Ronse, N. Nuns, S. Bellayer, C. Andre, G. Delaplace, M. Jimenez, Influence of roughness on heat-induced dairy fouling on stainless steel, Journées Nord-Ouest Européennes des Jeunes Chercheurs 2016, Villeneuve d'Ascq, France, Juil 2016

*39- S. **Bellayer**, M. Jimenez, B. Gardelle, A. Beaugendre, M. Casetta, J. Bouquerel, S. Duquesne, S. Bourbigot, Chemical imaging of polymers filled with wavelength dispersive spectrometer, 20th. European Symposium on polymer spectroscopy, Dresden, Allemagne, Sep 2016*

40- A. Beaugendre, S. Degoutin, S. Bellayer, C. Pierlot, S. Duquesne, M. Casetta, M. Jimenez, Eco-design of novel flame retardant coatings, Journée des jeunes chercheurs en Génie des Procédés GEPROD-UGéPe, Université catholique de Louvain, Louvain, Belgique, Oct 2016

41- N. Lesaffre, S. Bellayer, G. Fontaine, M. Jimenez, S. Bourbigot, Ageing of flame retarded PLA: development, characterization and modelling, Journée des Jeunes Polymeristes du Nord, Villeneuve d'Ascq, France, Juin 2015

42- G. Alogaili, M. Jimenez, S. Bellayer, N. Nuns, A. Allion-Maurer, A. Beaurain, G. Ronse, G. Delaplace, M. Traisnel, Development Anti-dairy fouling Surface of 316L 2B Stainless steel by Atmospheric Pressure Plasma Treatment, 41 International Conference On Plasma Science (ICOPS 2014) and 20th International Conference on High-Power Particle Beams, Washington, Etats-Unis d'Amérique, Mai 2014

43- *A.D. Naik, G. Fontaine, F. Solarski, X. Delva, J. Louisy, S. Bellayer, Y. Bourgeois, S. Bourbigot, Melamine integrated metal phosphates in the flame retardancy of polyamide-66, Modification, Degradation and Stabilisation : (MoDeSt 2014), Portoroz, Slovénie, Sep 2014*

44- *M. Jimenez, G. Delaplace, N. Nuns, S. Bellayer, D. Deresmes, G. Ronse, G. Alogaili, M. Traisnel, Toward a better understanding of the first stages of dairy fouling growth at a stainless steel surface, IVC19 congress, Paris, France, Sep 2013*

45- *M. Jimenez, G. Delaplace, N. Nuns, S. Bellayer, D. Deresmes, G. Ronse, G. Alogaili, M. Traisnel, Multiscale characterization of dairy fouling growth at a stainless steel surface, 15th European Conference on Applications of Surface and Interface Analysis 2013, ECASIA'13, Sardaigne, Italie, Oct 2013*

46- *M. Vandenbossche, M. Jimenez, M. Casetta, S. Bellayer, M. Traisnel, Greffage de chitosane sur des géotextiles pour fixer le cuivre présent dans les sédiments pollués, Journée des doctorants UGéPE, Roubaix, France, Mai 2012*

47- ***S. Bellayer**, S. Dipplel, M. Mora, M. Traisnel, « silica sol-gel coatings for titanium substrates », SFGP, Lille, 29 Nov- 01 Dec 2011.*

48- *G. Fontaine, C. Gérard, S. Bellayer, S. Bourbigot, Fire retarded epoxy resin: impressive synergistic effect of app/poss combination, 2010' International Symposium on Flame-Retardant Materials and Technologies - ISFRMT 2010, Chengdu, Chine, Sep 2010*

49- ***S. Bellayer**, M.H. Staia, M. Traisnel, E.S. Pushi-Cabrera, M. Suarez, J. Lesage, D. Chicot, « Microstructural characterization of post heat treated VPS Cr3C2-NiCr coatings », Projection Thermique – 4th RIPT, 3-4 Dec 2009.*

50- ***S. Bellayer**, S. Bourbigot, X. Flambard, M. Rochery, J. W. Gilman, E. Devaux, "POLYMER/MWNTs NANOCOMPOSITE YARNS AND FABRICS : Processing, Characterization, Flammability and Thermal Properties" AUTEX04 –World Textile Conference, Roubaix, France, 22 -24 June 2004.*

51- *Douglas M. Fox, Severine Bellayer, Walid H. Awad, Marius Murariu, Rick D. Davis, Jeffrey W. Gilman, Paul H. Maupin, Hugh C. De Long, and Paul C. Trulove, "The Use of Imidazolium Based Ionic Liquids for the Preparation of Polymer - Layered Silicate and Polymer - Carbon Nanotube Nanocomposites," EUCHEM Molten Salts Conference, Piechowice, Poland, 20 - 25 June 2004.*

52- *S. **Bellayer**, J. Gilman, S. Bourbigot, X. Flambard, D. Fox, P. Maupin, H. De Long, P. Trulove, N.Eidelman, "Trialkylimidazolium-Tetrafluoroborate Compatibilized, Multiwalled Carbon Nanotubes", 2004 Joint International Meeting : 206th Meeting of The Electrochemical Society (ECS), 2004 Fall Meeting of The Electrochemical Society of Japan (ECSJ), Honolulu, Hawaii, 3-8 October 2004.*

53- *S. **Bellayer**, S. Bourbigot, E. Devaux, X. Flambard, Etude et characterisation de textiles nanocomposites, Journées Jeunes Chercheurs, Villeneuve d'Ascq, France, Fev. 2003.*

Oral communications with publication (2 as first author):

1- *K. Dourgaparsad, M. Saget, S. Zouaghi, N. Nuns, S. Bellayer, M. Grunlan, V. Thomy, Y. Coffinier, D. Balloy, C. Gruescu, G. Delaplace, M. Jimenez, Surface engineering of stainless steel for dairy fouling management, Nature Inspired Creativity Engineers, Nice, France, Juin 2023*

2- *M. Jimenez, C. Lemesle, S. Bellayer, S. Duquesne, M. Casetta, A.-S. Schuller, J. Molina, Bio-based flame retardant self-stratifying coatings, ECOFRAM 2022, Alès, France, Mai 2022*

3- *M. Jimenez, C. Lemesle, S. Bellayer, S. Duquesne, M. Casetta, A.-S. Schuller, J. Molina, Bio-based flame retardant self-stratifying coatings, Polymers 2022, Los Angeles, Etats-Unis d'Amérique, Oct 2022*

4- *M. Jimenez, C. Lemesle, S. Bellayer, S. Duquesne, M. Casetta, A.-S. Schuller, J. Molina, Bio-based flame retardant self-stratifying coatings, Workshop MateriaNova, Mons, Belgique, Nov 2022*

5- *M. Jimenez, A. Beaugendre, S. Degoutin, S. Bellayer, C. Pierlot, S. Duquesne, M. Casetta, Flame retardant and weathering resistant self-stratifying coatings, Flame 2018, Stamford, Etats-Unis d'Amérique, Mai 2018*

6- ***S. Bellayer**, M. Jimenez, B. Prieur, B. Dewailly, A. Ramgobin, J. Sarazin, P. Bachelet, B. Revel, G. Tricot, S. Bourbigot, Fire retardant sol-gel coatings for flexible polyurethane foams, Flame 2018, Stamford, Etats-Unis d'Amérique, Mai 2018*

7- *M. Jimenez, S. Zouaghi, M. Barry, S. Bellayer, S. Moradi, S.G. Hatzikiriakos, T. Dargent, V. Thomy, Y. Coffinier, C. Andre, M.A. Grunlan, G. Delaplace, Biomimetic approaches targeting dairy fouling mitigation of stainless steel, Smart Materials and Surfaces, Venise, Italie, Oct 2018*

8- *A. Hamieh, F. Ponchel, D. Remiens, S. Barrau, A. Addad, S. Bellayer, Synthèse de composites piézoélectriques céramique/polymère pour la réalisation des transducteurs électro-acoustiques, UGéPE 2018, Villeneuve d'Ascq, France, Nov 2018*

9- *G. Okyay, A.D. Naik, P. TRANCHARD, S. Bellayer, M. Jimenez, F. Samyn, S. Bourbigot, Physical characterization of carbonaceous products from fire and fire retardants: assessment of the impact on fire performance, Fire and Materials 2017, San Francisco, CA, Etats-Unis d'Amérique, Fév 2017*

10- *G. Delaplace, Y. Gu, M. Khaldi, L. Bouvier, C. Andre, J. Petit, R. Guerin, G. Ronse, T. Six, A. Moreau, M. Jimenez, S. Bellayer, T. Croguennec, R. Jeantet, P. Blanpain Avet, Influence of calcium/beta-lactoglobulin molar ratio on plate heat exchanger fouling for various whey protein solutions, Conference on heat exchanger fouling and cleaning, Madrid, Espagne, Juin 2017*

11- *S. Zouaghi, T. Six, S. Bellayer, C. Andre, G. Delaplace, M. Jimenez, Antifouling silane-based coatings by plasma-assisted deposition for dairy products processing, XXXI International conference on surface modification Technologies (SMT31), Mons, Belgique, Juin 2017*

12- *S. Zouaghi, T. Six, S. Bellayer, S. Moradi, S.G. Hatzikiriakos, T. Dargent, V. Thomy, Y. Coffinier, C. Andre, G. Delaplace, M. Jimenez, Biomimetic nanostructured surfaces for antifouling in dairy processing, 23ème congrès français de mécanique, Lille, France, Sep 2017*

13- *S. Zouaghi, G. Ronse, N. Nuns, S. Bellayer, C. Andre, G. Delaplace, M. Jimenez, Influence of roughness on heat-induced dairy fouling on stainless steel, Journées Nord-Ouest Européennes des Jeunes Chercheurs 2016, Villeneuve d'Ascq, France, Juil 2016*

14- *S. Zouaghi, G. Ronse, N. Nuns, S. Bellayer, C. Andre, G. Delaplace, M. Jimenez, The impact of stainless steel polishing on heat-induced dairy fouling in pasteurization conditions, Journée Jeunes Chercheurs GEPROC : UGéPE 2016, Louvain, France, Oct 2016*

15- *G. Fontaine, A.D. Naik, S. Bellayer, S. Bourbigot, Salen based schiff bases: A new class of fire retardant, 26th Annual Conference on Recent Advances in Flame Retardancy of Polymeric Materials, Stamford, Etats-Unis d'Amérique, Mai 2015*

16- *M. Jimenez, S. Bellayer, S. Duquesne, S. Bourbigot, Weathering of intumescent coatings, ACS Fall Meeting, San Francisco, CA, Etats-Unis d'Amérique, Aout 2014*

17- *M. Vandenbossche, M. Jimenez, M. Casetta, S. Bellayer, S. Bourbigot, M. Traisnel, Heavy metal sorption on PP nonwoven geotextiles grafted with biomolecules, CIRAT-5, Monastir, Tunisie, Jan 2013*

18- *S. Bourbigot, F. Solarski, S. Bellayer, G. Fontaine, S. Duquesne, INFLUENCE OF THE NANOMORPHOLOGY ON THE REACTION TO FIRE OF FLAME RETARDED POLYMER, 5th International Seminar on Modern Polymeric Materials for Environmental Applications, Cracovie, Pologne, Mai 2013*

19- *M. Jimenez, S. Bellayer, S. Duquesne, S. Bourbigot, Weathering of intumescent coatings, 24rd Annual Recent Advances in Flame Retardancy of Polymeric Materials (BCC research Flame conference), Stamford, Etats-Unis d'Amérique, Mai 2013*

20- *S. Degoutin, M. Jimenez, M. Casetta, S. Bellayer, F. Chai, N. Blanchemain, C. Neut, B. Martel, Nonwoven polypropylene textiles with anticoagulant and antimicrobial properties, 5th conference of applied research on textile, Monastir, Tunisie, Juin 2013*

21- *M. Vandenbossche, M. Jimenez, M. Casetta, S. Bellayer, M. Traisnel, Greffage de Cystéine sur Géotextiles par plasma froid : Méthode Innovante de dépollution des Sédiments, 15ème Congrès des Sciences du Génie des Procédés pour une Industrie Durable (SFGP 2013), Lyon, France, Oct 2013*

22- *M. Hadjel, H. Douichen, S. Bellayer, M. Traisnel, Valorisation de la diatomite algérienne et son application dans le traitement des eaux, 14ième Congrès des Sciences du Génie des Procédés pour une Industrie Durable (SFGP 2013), Lyon, France, Oct 2013*

23- *M. Vandenbossche, M. Jimenez, M. Casetta, S. Bellayer, S. Bourbigot, M. Traisnel, Sorption of heavy metals on a chitosan-grafted-polypropylene nonwoven geotextile, ICHMET 2012, Rome, Italie, Sep 2012*

24- *G. Fontaine, C. Gérard, S. Bellayer, S. Bourbigot, POSS a synergist for fire retardant epoxy resin/APP SYSTEM: mechanism of action, 22th BCC Conference - Recent Advances in Flame Retardancy of Polymeric Materials, Stamford, Etats-Unis d'Amérique, Mai 2011*

25- *M. Hadjel, R. Cherrak, H. Djediai, S. Bellayer, M. Traisnel, Depollution and photocatalytic treatment of organic contaminants by synthesis of nano-composite (TiO_2-Diatomite)., Congrès SFGP, Lille, France, Déc 2011*

26- ***S. Bellayer**, S. Dippel, M. Mora, M. Traisnel, Sol-gel formulations and surface treatments for silicate coating on titanium substrates for biomaterial applications, Congrès SFGP Lille, Lille, France, Déc 2011*

- ***Posters:***

1- *S. Zouaghi, T. Six, S. Bellayer, S. Moradi, S.G. Hatzikiriakos, T. Dargent, V. Thomy, Y. Coffinier, C. Andre, G. Delaplace, M. Jimenez, Self-Cleaning Slippery Infused Surfaces for Dairy Processing, MicroNanoFluidics 2018, Grenoble, France, Mar 2018*

2- *M. Dufay, S. Degoutin, F. Cazaux, F. Chai, N. Blanchemain, S. Bellayer, M. Casetta, G. Stoclet, L. Janus, M. Jimenez, PP meshes covered with PCL nanofibers functionalized by cold plasma for biomedical application, ESB 2018, Maastricht, Pays-Bas, Sep 2018*

3- *A. Beaugendre, S. Bellayer, S. Degoutin, C. Pierlot, S. Duquesne, M. Casetta, M. Jimenez, Innovative self-stratifying *epoxy/silicone flame retardant coatings for plastics, Smart Coatings, Orlando, FL, Etats-Unis d'Amérique, Fév 2017*

4- *F. Samyn, S. Duquesne, S. Bellayer, Efficiency of sol-gel treatments of fibres to flame retard composites?, IAFSS 2017, Lund, Suède, Juin 2017*

5- *G. Okyay, S. Bellayer, M. Jimenez, F. Solarski, S. Bourbigot, In-flame Soot Characterization From Balsa Sandwhich During Mass Loss Cone Calorimeter Tests, FRPM 2017, Manchester, Royaume-Uni, Juil 2017 [LillOA]*

6- *S. **Bellayer**, M. Jimenez, The electron Probe Microanalyzer: a powerful device for microanalysis of flame retardant polymers and chars, 14th European Meeting of flame retardant materials (FRPM), Lille, France, Juil 2013 [LillOA]*

7- *M. Vandenbossche, M. Jimenez, M. Casetta, S. Bellayer, M. Traisnel, Greffage de Cystéine sur Géotextiles par plasma froid : Méthode Innovante de dépollution des Sédiments, 15ème Congrès des Sciences du Génie des Procédés pour une Industrie Durable (SFGP 2013), Lyon, France, Oct 2013 [LillOA]*

8- *M. Hadjel, H. Douichen, S. Bellayer, M. Traisnel, Valorisation de la diatomite algérienne et son application dans le traitement des eaux, 14ième Congrès des Sciences du Génie des Procédés pour une Industrie Durable (SFGP 2013), Lyon, France, Oct 2013*

9- *M. Hadjel, R. Cherrak, H. Djediai, S. Bellayer, M. Traisnel, Depollution and photocatalytic treatment of organic contaminants by synthesis of nano-composite (TiO2-Diatomite)., Congrès SFGP, Lille, France, Déc 2011*

10- *M. Suarez, S. Bellayer, M.Traisnel, J. Lesage, W. Gonzalez , M. Hadad, St. Siegmann, E. S. Puchi-Cabrera and M. H. Staia, Corrosion behavior of CrNi9.5C atmospheric plasma thermal sprayed coating, 3RIPT (3ième Rencontre Internationnel de Projection Thermique), December 6-7, 2007.*

11- *S. **Bellayer**, S. Bourbigot, X. Flambard, E. Devaux, M. Rochery, J. Gilman, Flame retardancy textile: Polymer/clay nanocomposite yarns, FRPM'03 9th European meeting on fire retardancy and protection of materials 17 - 19 September 2003*

12- *S. Bourbigot, J. W. Gilman, D. L. Vanderhart, R. D. Davis, S. Bellayer, M. Murariu, W. H. Awad, C. A. Wilkie, A. B. Morgan, H. Stretz and D. R. Paul, Recent advances in the development of polymer nanocomposites : processing, characterization, thermal stability and flammability, FRPM'03, 9th European meeting on fire retardancy and protection of materials, 17 - 19 September 2003*

13- *S. **Bellayer**, J. W. Gilman, N. Eidelman, S. Bourbigot, X. Flambard, D. M. Fox, H. C. De Long, and P. C. Trulove, Preparation of homogeneously dispersed trialkyl imidazolium compatibilized multiwalled carbon nanotubes/polystyrene nanocomposites via melt extrusion, 2nd NIST and NASA Joint Workshop on measurement issues in single wall carbon nanotubes : Purity and dispersion part II, Gaithersburg, MD, USA, January 26-28, 2005*

- ***Patents:***

1- *L. Védie, V. Kopf, A. Hira, M. Dilger, M. Jimenez, S. Bellayer, S. Duquesne, Polyolefin-based resin foamed particles, a component molded from the foamed particles, a method for producing the foamed particles, and a method of determining the flame-retarding properties of foamed particles, EP4563631A1, 2025-06-04*
2- *E. Devaux, S. Bellayer, S. Chlebicki, S. Bourbigot, A. Fonseca, J. Al-Asswad, J. B. Nagy, Continuous textile fibers and yarns made from a spinnable nanocomposite, US20070031662A1, Feb. 8, 2007*

- ***Book chapters:***

1- *S. Bourbigot, G. Fontaine, A. Gallos, C. Gérard, S. Bellayer, Functionalized-Carbon Multiwall Nanotube as Flame Retardant for Polylactic Acid, ACS symposium series, 2009*
2- *D. M. Fox, S. Bellayer, M. Murariu, J. W. Gilman, P.H. Maupin, H. C. De Long, P.C. Trulove, Application of Trialkylimidazolium Liquids and Salts to the Preparation of Polymer-Layered Silicate Nanocomposites and Polymer-Carbon Nanotube Nanocomposites, ACS symposium series, 2005*

Part B:
Detailed presentation of the research activities

Context

Synthetic foams find widespread applications in various industries, such as packaging, filtration, building, and household products, serving as essential materials for thermal and acoustic insulation. Their unique properties also make them valuable for specialized purposes, including decontamination (in nuclear and polluted water treatment) and even in the construction of space shuttles. The economic significance of foams is substantial, contributing significantly to the global insulation market, which is valued in billions of euros. The global building thermal insulation market size was valued at USD 24.51 billion in 2024 and is estimated to grow of 6.6% between 2025 and 2034.[36] Nowadays, foam insulation is a widely used type of insulation, and it has gained more popularity. It is well known as it offers a highly effective solution with resistance to heat transfer. Figure 1 shows the thickness required for a material to have the same insulating performance.[37] It is helpful in reducing undesired air infiltration. The foam insulation is considered the best solution to reduce greenhouse gas emission and lower utility bills. It can reduce energy consumption by minimizing air leakage that occurs on door frames, external walls, window frames, roof underlays, crawlspaces, floorings, and others. The most common types of materials used in making foam board include polystyrene, polyisocyanurate, and polyurethane.

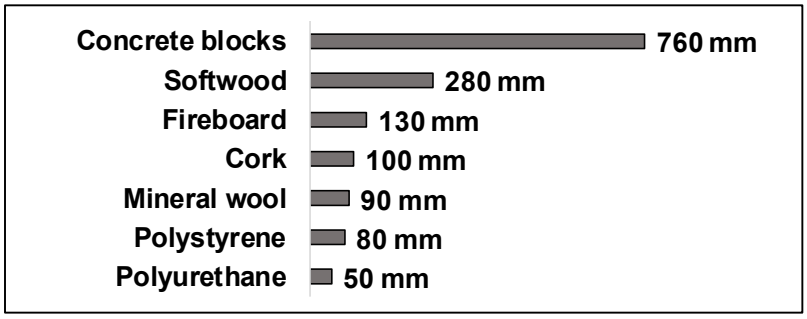

Figure 1: Material thickness to obtain the same insulating performance

Polymeric foams typically consist of a gaseous phase dispersed within a solid polymer matrix. These matrices can be composed of materials such as rubbers, elastomers, thermoplastics, or thermosets. Foams can be categorized based on their rigidity, falling into flexible, semi-flexible, semi-rigid, or rigid

materials, depending on the characteristics of the polymer matrix. These characteristics, including chemical composition, degree of crystallinity, and crosslinking, determine the rigidity of the foam.

Figure 2 provides a list of properties of foams and solids, particularly their density, Young's modulus, compression strength, and thermal conductivity. These properties are essential for understanding the characteristics and behavior of the materials. The range of these properties can vary depending on the composition of foams and solids.[38]

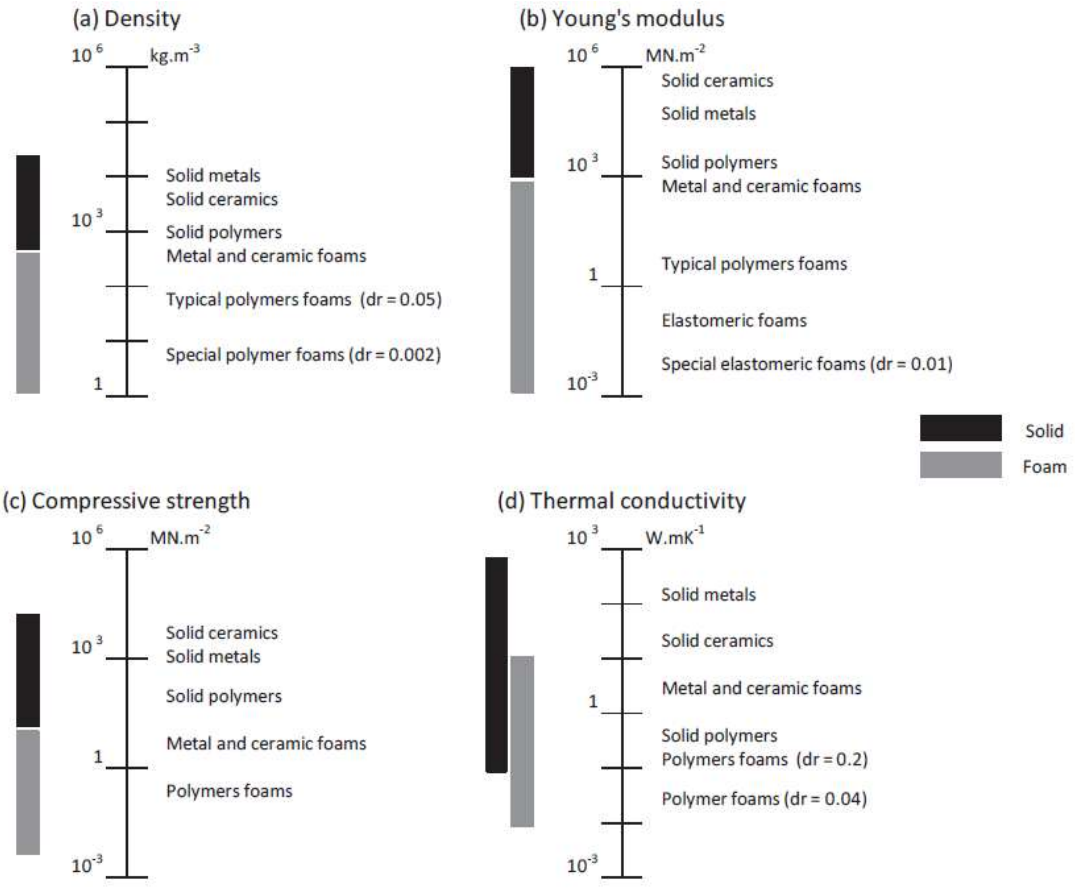

Figure 2: Range of properties of the foams depending on solids of which it is composed: (a) density (b) Young's modulus (c) compressive strength (d) thermal conductivity.

The cell geometry, including whether they are open or closed, their size and shape, significantly affects the final properties of foams. For instance, closed cells are better suited for thermal insulation applications as they act as a barrier to heat transfer through the material. On the other hand, open cells are preferred for acoustic insulation applications as they allow sound waves to penetrate the material and get trapped within it, reducing the amount of sound transmitted through the material.

The size and shape of cells can also influence foam material properties, such as mechanical strength, density, and porosity. Therefore, understanding and controlling cell geometry are essential aspects of foam material design and development.

Unfortunately, most organic polymers have a higher vulnerability to fire than their non-organic equivalents and can cause devastating fires. In 2017, the horrific Grenfell tower fire killed 79 people.[39,40] This fire was caused by the explosion of a refrigerator in a studio on the 4th floor. The fire has become uncontrollable because of expanded polyethylene foam used as thermal insulator. According to a report by the National Fire Protection Association (USA) in the same year, 499,000 fires occurred in home structures. 10,600 people were injured and 2,630 died. $10.7 billion in property damage occurred in structure fires, including $7.7 billion in property loss in home fires.[41] Thus, it is an economic and social need to use FR (fire retardant) synthetic materials and not only a scientific issue. Therefore, the importance of having high-performance fire retardant insulative materials is crucial.

Fire resistance standards vary according to application and country, but they are crucial to guarantee the safety of building occupants. Foams intended to be used in applications where there is a risk of fire must comply with specific fire classification standards, such as classes A1, A2, B, C, etc. (Appendix 2), depending on their fire behavior. Flame retardancy has therefore become a critical performance parameter to be considered in the design of polymers. Analysis of the evolution of flame-retardant polymers involves exploring the role of conventional as well as new flame-retardant systems used in polymer technology. Difficulties have also been encountered in understanding the flame retardant performance of additives in polymer matrices as a consequence of the lack of a universal criterion for the analysis of experimental data, combined with some judgments arbitrarily made on small datasets. Moreover, the circumstances of modern material design and people's high expectations, combined with the legislation imposed by governments to protect human beings, buildings, and the environment against fire. The development of increasingly complex and sophisticated flame-retardant systems is the result of the adaptation of the plastics industry to various societal changes and evolutions. A study conducted by a consulting firm (IHS Market) showed that in 2017 the global consumption of flame retardants amounted to more than 2.25 million tons per year.[42] In 2016, halogenated compounds accounted for 22% of world production (17% for brominated derivatives and 5% for chlorinated derivatives).[43] However, over the last 10 years, the production of halogenated derivatives has tended to decrease in order to be replaced by non-halogenated products that are considered to be less toxic to the environment and human health. Indeed, certain types of halogenated FR have a high bioaccumulation capacity and were found in the food chain network. They are also present in the atmosphere. A study showed that traces of FR were found in nature as far as in the Arctic Ocean.[44] In the case of brominated FR, most are lipophilic, i.e., they prefer fatty phases found in the food chain.

Traces of these products have been found in blood and breast milk. Some of these compounds disrupt the endocrine system, thyroid, and reproductive functions. A study conducted on animals has shown the negative impact of brominated FR on infant metabolism and brain development.[45] Therefore, the European Union has adopted laws to reduce or totally prohibit the use of certain FR that can possibly be harmful to human health and the environment. The collective awareness of the need to conserve the environment, together with public and occupational health and safety, led to the prohibition of some materials. This is the case of some halogenated flame-retardant additives that have been banned from the European market because of toxicological and environmental issues.

Unfortunately, the halogenated FR were highly effective at relatively low incorporation content; therefore, their replacement has proved to be complicated and often relatively ineffective, especially in some applications like foams, fabrics and films.[46,47] In parallel, fire safety rules are undergoing major changes, with which it is very difficult for the development of new FR to keep pace.[48] Consequently, the industry is looking for efficient, cost-effective, and environmentally-friendly flame-retardant systems.[49] The development of highly efficient FR materials is a state-of-the-art issue that needs to critically meet the requirements of new technologies. For example, in the case of electric cars, the development of new generations of batteries, which will provide higher energy density, faster charging, requires the development of new materials capable of securing the transmission of data and energy at high voltages using lighter and safer casing.[50] These challenging new materials must therefore present good mechanical, electrical, and fire properties to protects the cell's sensitive internal components from external damage. Depending on the processing method, there are some additional requirements to be satisfied for choosing the correct additives and processing conditions, such as the toxicity of materials, processing limitations, and safety requirements.

In this context, the foam manufacturing industry (transportation, building and construction) is continuously looking for new ways to flame retard materials. Various approaches exist to flame retard foams such as:

- A bulk approach:

The bulk approach is the most used in industry, it is a well-known process, which is most of the time the easiest and less expensive process to flame retard a polymer matrix. This approach is conducted by the introduction of FR additives or reactive agents to diminish the material combustibility. The additives or reactive agents act by limiting the combustion reaction or by releasing gases that suppress the flame. This way is the most commonly used in the production of items like upholstered foams for furniture, mattresses, or fire-resistant flooring.

- A surface approach:

Surface flame retarded foams consist of coatings applied on top of the materials to reduce their flammability. These coatings establish a protective barrier, hindering the flame spread. They can be paints, varnishes or fire-resistant coatings. This approach is used to flame retard foams; however, the limitations are those already known for coatings such as adherence problem or aging problems. Depending on the type of foams, open-cell foams of closed-cell foams, the coating penetrates the 3D network or stay on top determining the thickness of coating to deposit on the foam.

- Inherently flame-retardant foams:

Inherently flame-retardant foams are materials inherently designed to resist fire, with a chemical composition that does not rely on additives or external coatings. They are frequently utilized in applications prioritizing fire safety, such as electrical cables, flame-resistant clothing, construction materials, and industrial equipment. This approach seems appealing; however, the production of such foams remains expensive and their use are therefore limited. Moreover, to obtain adequate mechanical and flame retardant properties can be a problem.

Thus, there is still room for research in the FR foams field and since my arrival at UMET (Unité Matériaux et Tranformations, Appendix 1) at Centrale Lille, Villeneuve d'Ascq, in 2006, my research work has been devoted to develop fire retardant solutions for polymer foams.

This manuscript sums up my research work carried out at UMET. Chapter one focuses on the difficulties to improve the fire properties in the bulk using polyurethane (PU) and polyisocyanurate (PIR) foams as examples. It is a work carried out during the PhD research of A. Gossiaux in collaboration with BASF, Germany, using rigid PUR and PIR foams as raw materials. This work highlights the difficulties encountered to find new effective FR for foams when introduced in the polymer during the fabrication process. Different foam formulations were characterized using various analytical tools to fully understand the mechanism of action of each FR. The following chapter sums up results on how to improve the flame retardant properties of polymer foams using coatings to flame retard foams. In the case of surface coatings, different cases are studied, open-cell and closed-cell foams and hydrophilic and hydrophobic surfaces. Thin sol-gel coatings and thick paints and varnishes were studied. Finally, the last part deals with the use of intrinsic flame retardant foams that are part of the most recent research to avoid toxicity and safety problems due to the use of FR.

In each part of the manuscript the formulated materials are fully characterized and tested to fire with different fire tests and discussion will be made to highlight the difficulties encountered in each case.

Chapter I: FR bulk modification of foams

The topic developed in this chapter was carried out in the frame of a collaboration with BASF, Germany (PhD A. Gossiaux 2018-2021) and led to two papers.[51,52]

I.1. Introduction

In many fields, synthetic polymers are replacing traditional compounds such as wool, metal and glass because of their advantageous functional properties: lightness, easy process, mechanical strength, choice of shape, low density, acoustic and thermal resistance and above all their low cost. This is especially true in the case of insulation material. Polyurethane foams and especially rigid polyurethane foams (PUR) are one of the most efficient and high-performance insulation materials. It is the perfect candidate to enable effective energy saving with minimal occupation of space. Thus, over the years, PUR foam has become a perfect candidate for thermal insulation due to its efficiency, relatively low cost compared to competitors, and high degree of modularity in terms of properties. Unfortunately, the dramatic Grenfell tower fire killed 79 people in London because non-fireproofed insulative materials were used in the building construction.[39,40] Thus, the use of fireproof synthetic materials has become not only a scientific issue but an economic and social need as well. Therefore, the importance of having high-performance and fire-resistant materials is crucial. Since most polymeric materials are flammable, flame retardants (FR) have to be used in their formulation to prevent the outbreak of a fire. For the most part, FR are added in the bulk material during synthesis.

A lot of literature exists on flame retardancy of polyurethane (PUR) or polyisocyanurate (PIR) foams (Appendix 3). So, in this work, the goal was not to synthesize or find new FR but mainly to stimulate the emergence of new FR by studying the influence of different parameters of the flame retardants on the fire behavior of the foams. It will help to better understand their mechanism of action and give direction for potential new research for the synthesis of FR adapted to PIR and PUR foams. Model FR were chosen with different oxidation states, boiling points as well as substituents and a systematic study has been developed to characterize their efficiency.

I.2. Choice of materials

I.2.1. Choice of model flame retardants molecules

The phosphorous FR (P-FR) were chosen based on the literature and on practical issues. It has been shown in the literature that the oxidation state of the phosphorus can play an important role in the mode of action of the FR[53,54,55]. For instance, it has been shown in an epoxy resin that a flame inhibition

phenomenon is observed for phosphine oxide and that a low oxidation state of the phosphorous FR promotes a gas phase action. On the other hand, the boiling point as well as the decomposition of the polymer can also play an important role in the mode of action of the FR. Indeed, two phosphorus FR with two different oxidations state can both act in the gas phase if their boiling temperature is lower than the decomposition temperature of the polymer (example of triethyl phosphate and dimethyl methyl phosphonate). Conversely, if the oxidation degrees of the P-FR are different but their decomposition point is close to that of the polymer, then the P-FR with a lower oxidation state may show action in the condensed and gas phase while those with a high oxidation state (+V) will act primarily in the condensed phase. Therefore, several characteristic parameters of the P-FR have to be taken into account when investigating their mode of action. Four chemical groups based on a triethylphosphate structure were chosen. Figure 3 shows their chemical structure and Table 1 their main properties.

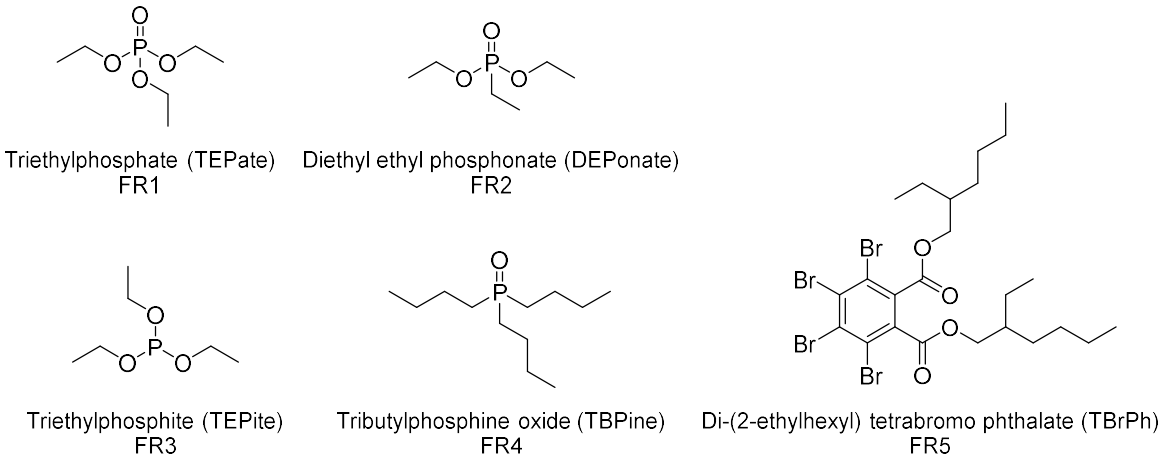

Figure 3: Chemical structure of TEPate, DEPonate, TEPite, TBPine and TBrPh.

TEPate is the FR additive with the highest oxidation degree (+V). It is a flame retardant commercially used in PUR and PIR foams. Similar structures were chosen for the other FR, i.e., having ethyl substituents but changing the oxidation state of the phosphorus or the boiling point. The diethyl ethyl phosphonate (DEPonate), the triethylphosphite (TEPite) but also the tributyl phosphine oxide were chosen. TEPate has the highest oxidation state (+V) and TBPine oxide has the lowest (-I), while the oxidation state of DEPonate and TEPite are intermediate (+III). These FR are liquid at room temperature except TBPine, which is solid (Mp = 60°C). Finally, TEPite has the lowest boiling point (158°C), while TBPine has the highest boiling point (300°C). Due to the high cost of the ethyl molecule, TBPine has been chosen instead of TEPine: it increases its boiling point temperature. In comparison, the boiling point of TBPine is almost twice that of TEPite.

Table 1: Physico-chemical and thermal properties of TEPate, DEPonate, TEPite, TBPine and TBrPh.

Parameters	**TEPate**	**DEPonate**	**TEPite**	**TBPine**	**TBrPh**
CAS number	78-40-0	78-38-6	122-52-1	814-29-9	26040-51-7
Molecular formula	$C_6H_{15}O_4P$	$C_6H_{15}O_3P$	$C_6H_{15}O_3P$	$C_{12}H_{27}OP$	$C_{24}H_{34}Br_4O_4$
Molecular weight ($g.mol^{-1}$)	182	166	166	218	706
Mp (°C)	-56.4	-	-112	64	-
Bp (°C)	215	198	158	300	584*
Oxidation degree	+ V	+ III	+ III	- I	-

* Calculated using Advanced Chemistry development (ACD/Labs) Software V11.02

Diethyl ethyl phosphonate is an organic phosphorus flame retardant that is well known in the field of fire retardancy and especially in the formulation of polyurethane foam. DEPonate has a double role as it can be used both as a flame retardant and as a plasticizer. Concerning TEPite, this molecule was not initially used as a flame retardant. Indeed, this molecule is used in the industrial production of insecticide or in organic chemistry as a reagent for the synthesis of alkenes, alkynes, or nitrogenous heterocycles. Triethyl phosphite is quite sensitive to oxidation and hydrolysis. In the case of tributylphosphine oxide (TBPine), the choice of FR with ethyl substituents was not possible due to a very high cost. The FR with the butyl substituents from the same group was cheaper and was therefore selected since it is potentially applicable from an industrial point of view if it proves to be effective. TBPine is rarely used as a flame retardant. A study carried out by Hastie et al. in 1975[56] showed that triphenylphosphine oxide could be used as a FR in a poly(ethyleneterephthalate) polymer. Its action was mainly attributed to the gas phase action. However, no other study has shown that TBPine could be used efficiently as a FR. Finally, di-(2-ethylhexyl) tetrabromo phthalate (TBrPh) is a brominated FR, which is commonly used in addition to phosphorus FR in a PUR system. Despite the desire to reduce the use of halogenated FR because of the potential toxicity of some of them, no acceptable solution exists for some PUR foam applications. Brominated FR are thus still used in PUR systems to reach the desired classification. TBrPh was selected because it is a non-reactive additive, it does not contain any phosphorus species, it has a defined structure and it is not a mixture of several brominated monomers. It is a liquid flame retardant that is easy to handle and which presents a high bromine content. Finally, it offers very low volatility combined with superior thermal stability.

I.2.2. Choice of foams

All the PUR and PIR foams are provided by BASF company. Eight types of foam are presented in this study and prepared with FR (Table 2). The PIR foam is a rigid polyisocyanurate formulated with a

polyol polyether and a polymeric methylene diphenyl diisocyanate. Additional additives are also used, like stabilizers, catalysts, and chemical and physical blowing agents. Apparent density is close to 39 kg/m^3 and closed cell content near 93%. The percentages are calculated to keep the NCO/OH ratio and the apparent density constant. PIR foam contains around 3.0 wt% of FR including phosphorus (around 0.58 wt%) compounds. PUR foam is a rigid polyurethane foam formulated with a polyol polyether and a polymeric methylene diphenyl diisocyanate. Additional additives are also used, like stabilizers, catalysts, and chemical and physical blowing agents. Apparent density is close to 39 kg/m^3 and closed cell content near 91%. PU Foam contains 13.0 wt% of FR including phosphorus (around 3.0 wt%) and bromine (around 1.1 wt%) compounds.

Table 2: Weight percentage of FR within each system.

System	Br (wt%)	P (wt%)	FR content (wt%)
PIR Foam without FR	0	0	0
PIR Foam with TEPate	0	0.58	3.4
PIR Foam with DEPonate	0	0.59	3.2
PIR Foam with DBPite	0	0.55	2.9
PIR Foam with DBPine	0	0.59	4.1
PUR Foam without FR	0	0	0
PUR Foam with TBrPh	3.02	0	6.7
PUR Foam with TEPate	2.95	1.11	13.0
PUR Foam with DEPonate	3.01	1.13	12.7
PUR Foam with DBPite	3.01	1.14	12.7
PUR Foam with DBPine	2.96	1.10	14.2

All the apparent densities are close to 40 kg.m^{-3}. The addition of the different FR does not affect the density except for the PIR TBPine system, which has a slightly lower apparent density (37 kg.m^{-3}). Regarding the closed cell content, PIR foams show a high rate, close to 90 %, while PUR foams show a slightly lower closed cell content, around 85 %. Finally, the NCO/OH ratio is 3.4 to 1 for the PIR system, which corresponds to the ratio needed to obtain polyisocyanurate polymers, while the ratio is 1.05 to 1 for polyurethane foam.

I.3. Thermal stability of the modified foams

TG analysis

This section deals with thermogravimetric analyses (TGA) carried out under nitrogen atmosphere by varying the temperature from 40°C to 800°C with a temperature ramp of 10°C.min^{-1}. TGA measurements were conducted under inert atmosphere aim to mimic the decomposition that can occur at the interface between the material and the flame where the oxygen rate is close to zero.[57]

TGA thermograms of PIR systems are presented in Figure 4 and PUR TGA measurements are presented in Figure 5.

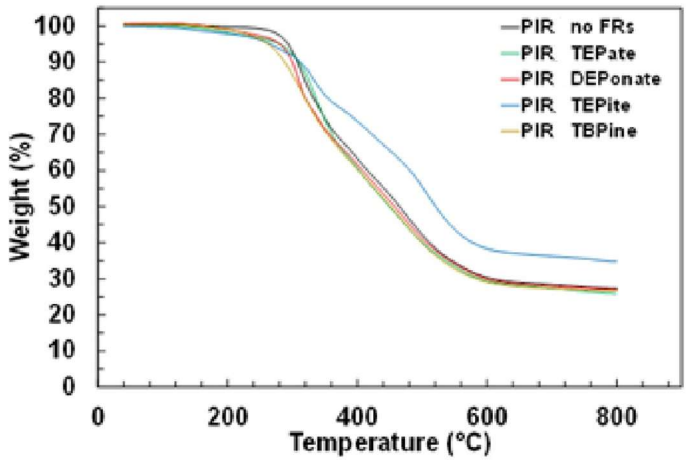

Figure 4: TGA curves of PIR systems under nitrogen atmosphere – 10°C.min^{-1}.

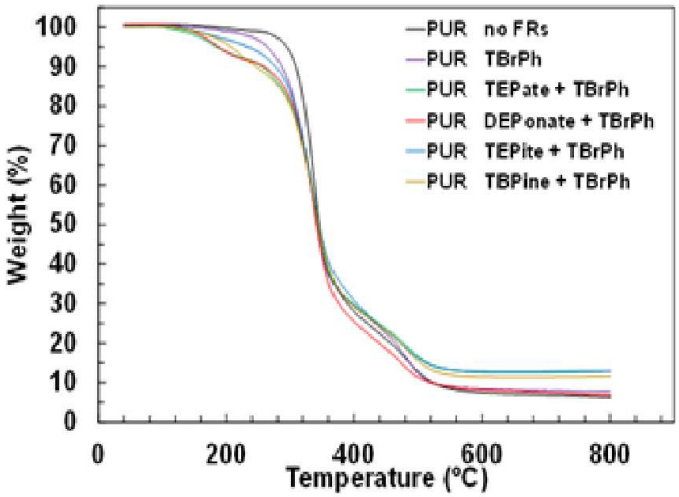

Figure 5: TGA curves of PUR systems under nitrogen atmosphere – 10°C.min^{-1}.

Table 3 shows all the characteristic data from the TGA analysis such as $T_{5wt\%}$, $T_{50wt\%}$ and residual weight at 800°C.

Table 3: Main characteristic TGA data of PIR and PUR systems under nitrogen atmosphere -10°C.min^{-1}.

	$T_{5wt\%}$ (°C)	$T_{50wt\%}$ (°C)	Res. weight $_{800°C}$ (%)	Bp_{FR} (°C)
PIR no FR	292	463	27.3	-
PIR TEPate	279	449	25.9	215
PIR DEPonate	276	455	27.0	198
PIR TEPite	267	521	34.8	158
PIR TBPine	260	450	26.8	300
PUR no FR	292	345	6.4	-
PUR TBrPh	261	341	7.7	-
PUR TEPate + TBrPh	185	342	13.0	215
PUR DEPonate + TBrPh	183	341	6.8	198
PUR TEPite + TBrPh	231	345	13.0	158
PUR TBPine + TBrPh	207	342	11.7	300

In the case of PIR systems, the decomposition takes place at a lower temperature when FR are used. This can be explained by the fact that the FR volatilize and act before the decomposition of the polymer itself ($T_{5wt\%}$ = 292°C). The PIR TEPate shows the closest $T_{5wt\%}$ compared to the one of the polymer (279°C), while the PIR TBPine shows the furthest from the decomposition of the polymer (260°C). As a reminder, the TBPine has the highest boiling point. Thus, TBPine decomposes before reaching its boiling point or interact with the polymer leading to decomposition of the polymer and/or the additives. It can be concluded from a general point of view that in the case of PIR systems, the $T_{5wt\%}$ decreases when FR are added compared to the $T_{5wt\%}$ of the polymer without FR, but in a limited way (maximum decrease is about 32°C). Moreover, whatever the FR used, the $T_{5wt\%}$ are close. Similarly, concerning the $T_{50wt\%}$, the values are relatively close to each other (between 449°C and 463°C) and similar to that of PIR without FR. An exception is noted for the PIR TEPite, which shows a $T_{50wt\%}$ at a higher temperature (521°C) than the neat PIR system. This increase of $T_{50wt\%}$ is linked to an increase of the residual weight at 800°C reaching a value of 34.8 % compared to 26-27 % for the other PIR systems. Therefore, adding TEPite in a PIR system seems to favor an action in the condensed phase contrary to the other FR, which should then favor an action in the gas phase.

In the case of PUR systems, the $T_{5wt\%}$ of PUR with no FR (292°C) is identical to that of PIR with no FR (292°C); however, the $T_{50wt\%}$ is much lower (345°C), i.e., 118°C lower. Indeed, polyurethane foams are less thermally stable than polyisocyanurate systems. Secondly, the $T_{5wt\%}$ of PUR TBrPh (261°C) is close to that of the system without FR, whereas the $T_{5wt\%}$ values for the other FR are much lower (between

183°C and 231°C). PUR DEPonate shows the lowest $T_{5wt\%}$ (183°C) while PUR TEPite shows a higher $T_{5wt\%}$ (231°C). On the other hand, in the case of PUR systems, the residual weight varies depending on the FR used. In particular, PUR DEPonate shows one of the lowest residual weights (6.8 wt%), while PUR TEPite shows one of the highest residual weights (13.0 wt%). These results are consistent with the literature since several studies have shown that the use of DEPonate or DEPonate-like molecules such as dimethyl propylphosphonate tends to volatilize at temperatures between 180°C and 200°C in rigid polyurethane systems[58,59]. DEPonate tends to have a predominant action in the gas phase.

Thus, according to these initial results, TEPite seems to increase the residual weight of the PIR and PUR systems, which favors a condensed phase action. Otherwise, the other FR appear to act differently depending on the system in which they are added. For example, TEPate and TBPine increase the residual weight of PUR foams at 800°C, showing a potential condensed phase action, while their residual weights are decreased in the case of PIR foams.

Rheology measurements

To further characterize the condense phase, a rheometer is used. It allows to access the expansion of the material when submitted to a temperature ramp. The furnace is heated up to 500°C using a ramp of 10°C.min^{-1}. A constant force of 10 g is applied on the material during the whole experiment and the gap between the two plates is recovered to measure the expansion or collapsing of the material during its decomposition.[60] Figure 6 presents a schematic representation of the test.

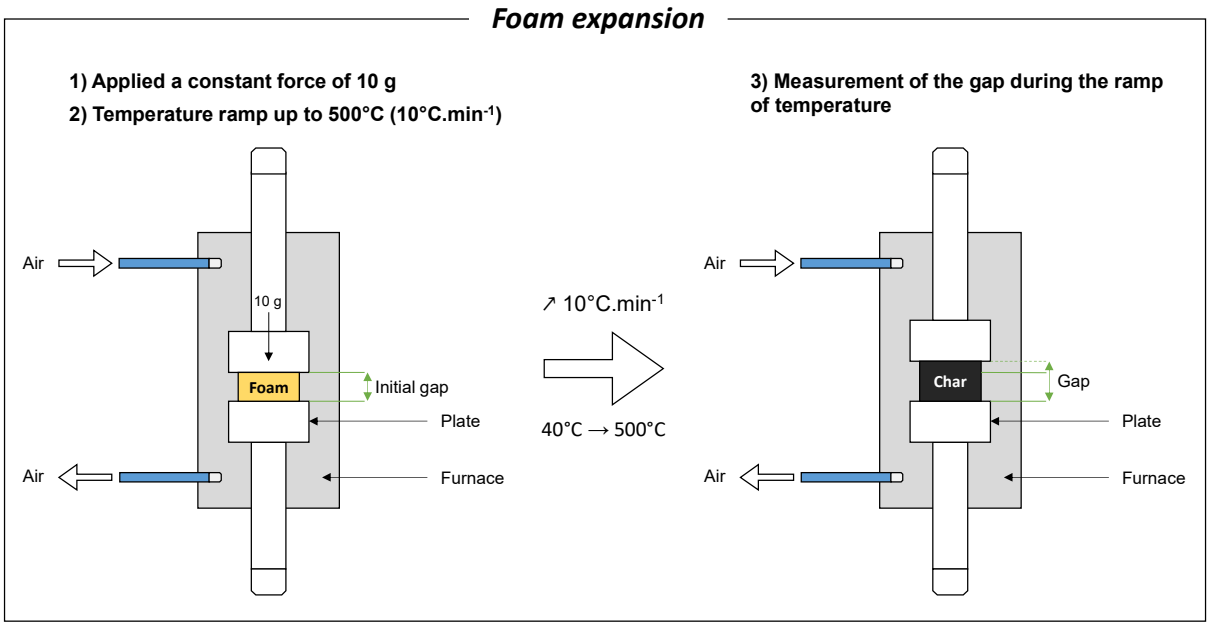

Figure 6: Schematic representation of the measurement of foam expansion.

The expansion of the material is calculated using Equation 1.

$$\% \, exp_{(t)} = 100 - \left(\frac{gap_{(t)}}{gap_{(t_0)}} \times 100 \right) \qquad \textbf{Equation 1}$$

$$\% \, exp_{(t)} = expansion \, of \, the \, material \, at \, time \, t \, (\%)$$

$$gap_{(t)} = thickness \, of \, the \, material \, at \, time \, t \, (mm)$$

$$gap_{(t_0)} = thickness \, of \, the \, material \, at \, t = 0 \, s \, (mm)$$

Figure 7 compares the expansion of the PIR systems. Table 4 presents the characteristic data obtained during this experiment, i.e., the expansion of the material at 500°C ($Exp._{500°C}$), the maximum of expansion (Max exp.) and the temperature of the maximum of expansion ($T_{Max\ exp.}$).

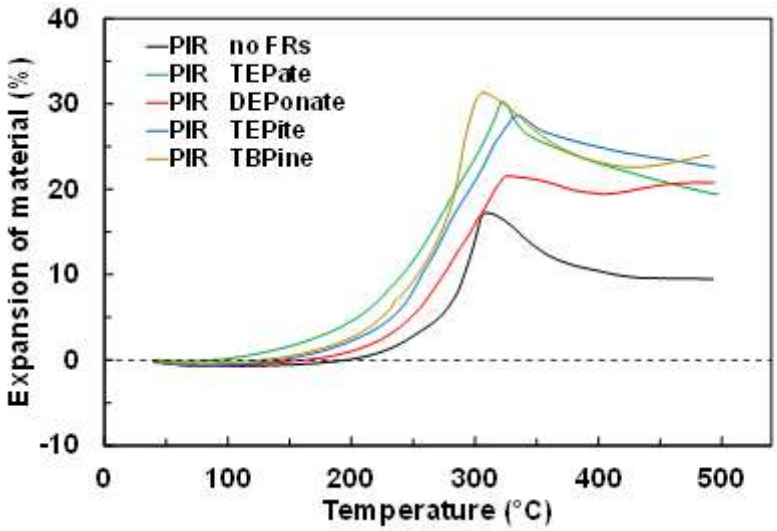

Figure 7: Expansion of PIR systems.

Table 4: Main characteristic data of expansion measurements for PIR systems.

	PIR no FR	PIR TEPate	PIR DEPonate	PIR TEPite	PIR TBPine
$Exp._{500°C}$ (%)	9.5	19.4	20.8	22.6	24.0
Max exp. (%)	17.2	30.2	21.5	28.6	31.3
$T_{Max\ exp.}$ (°C)	310	322	327	336	306

All PIR systems show positive expansion over the whole temperature range (from 40°C to 500°C). Similarly, all the systems with FR show a higher expansion at 500°C than the PIR system without FR. Their expansion at 500°C is between 19.4 % and 24 % while the system without FR shows an expansion at 500°C of almost half the value (close to 10 %). We have shown using TGA that the charring is not significantly promoted in presence of FR. It is noteworthy that the rheology test has been performed

in an uncontrolled atmosphere: the oven is not ventilated and the degradation products can accumulate in the oven, lowering the air content and allowing pyrolysis and charring. Consequently, it may be proposed that the expansion of PIR with FR is due to the release of FR in the gas phase. Therefore, in addition to the pentane initially present in the foam, the volatilizing FR induce a swelling of the polymer as it decomposes. This is in agreement with the fact that the maximum expansion is obtained in a temperature range between 306°C and 336°C, which corresponds to temperatures slightly higher than $T_{5wt\%}$ observed in TGA. However, since TGA have been carried out under N_2 atmosphere, it is normal to have a slight shift of temperature. When the polymer starts to decompose, the expansion of PIR with FR decreases slightly to reach an average value close to 21.7 %, whatever the FR. In conclusion, it can be said that the addition of FR in a PIR system increases the expansion of the material. However, despite the number of experiments carried out, the measurements could not differentiate the different systems with FR.

When looking at the starting point of the expansion, it can be seen that all the systems have a different starting point. However, it is difficult to draw a clear mode of action. It is clear that the swelling starts when the FR start to degrade, since the FR degrade before the neat PIR foam. The FR starts to degrade, and the released products induce a swelling of the material. The charring phenomenon is strong enough to avoid the collapse of the structure. The temperature difference of the starting of the swelling corresponds to the degradation point of the FR; however, the small temperature difference prevents the interpretation of the results.

Figure 8 compares the expansion of the PUR systems and Table 5 presents the characteristic data.

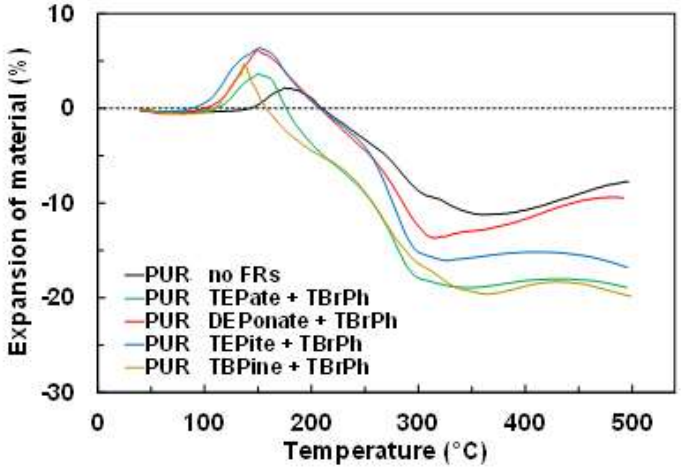

Figure 8: Expansion of PUR systems.

Table 5: Main characteristic data of expansion measurements for PUR systems.

	PUR no FR	PUR TEPate + TBrPh	PUR DEPonate + TBrPh	PUR TEPite + TBrPh	PUR TBPine + TBrPh
$Exp._{500°C}$ (%)	-7.7	-18.9	-9.5	-16.8	-19.9
Max exp. (%)	2.1	3.6	6.2	6.4	4.7
$T_{Max\ exp.}$ (°C)	172	150	149	151	137

The expansion at 500°C of PUR systems is negative, meaning that the foams collapse. At first, an expansion can be observed in a temperature range between 40°C and 210°C. The maximum expansion reached is between 2.1 % and 6.4 %, and the maximum expansion temperature between 137°C and 172°C. Thus, the different expansions are low in contrast to the PIR systems and occur at lower temperatures. On the other hand, the expansion at 500°C of PUR without FR is -7.7 %. The use of FR causes a higher foam collapse, down to -19.9 % for the PUR TBPine system. PUR DEPonate shows the lowest collapse of the PUR systems with FR with a negative expansion of -9.5 %. It can thus be assumed that even if the FR promote the formation of a residue at high temperature as shown by TGA, its cohesiveness is poor. When looking at the starting point of the swelling in the case of the PUR system, a similar mechanism appears: the swelling starts sooner when FR are present because of a temperature of degradation lower for FR than for PUR foam. However, the built structure is not strong enough even with the FR and the char collapses.

Tests were also conducted to quantify the resistance of the char at 500°C when it is subjected to a constraint. The upper plate of the rheometer is brought in contact with the char, then the upper plate goes down at a constant speed of 0.02 $mm.s^{-1}$ and the compression force is monitored as a function of the distance between the two plates (gap).[61] This technique allows us to determine if a FR has an action in the condensed phase building a more compact and cohesive char. The Figure 9 presents a schematic illustration of the test.

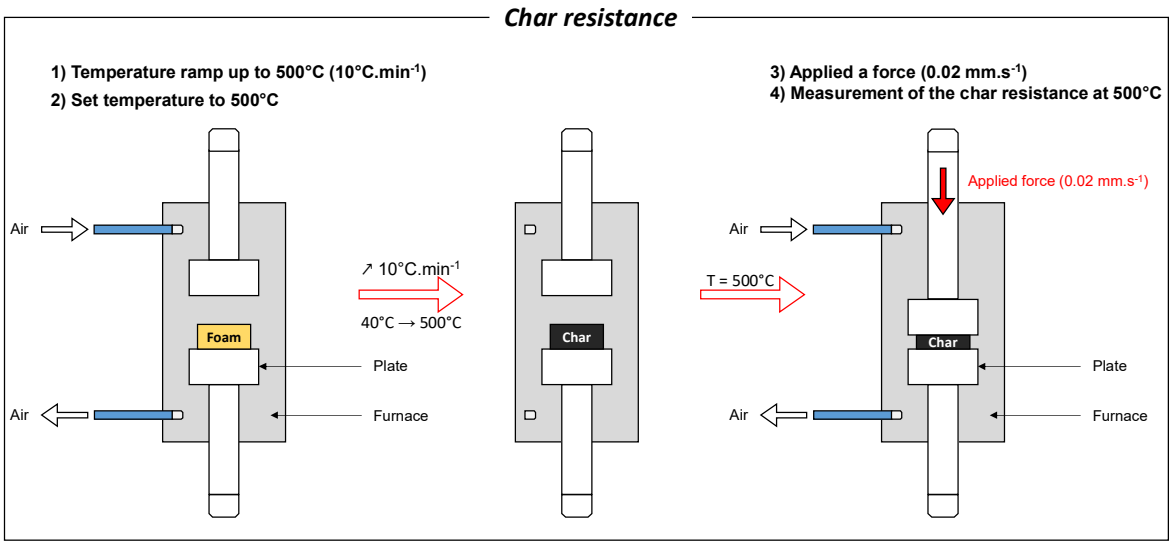

Figure 9: Schematic representation of the measurement of char mechanical resistance.

Figures 10 and 11 show the evolution of the char strength as a function of the gap for the PIR and PUR systems, respectively.

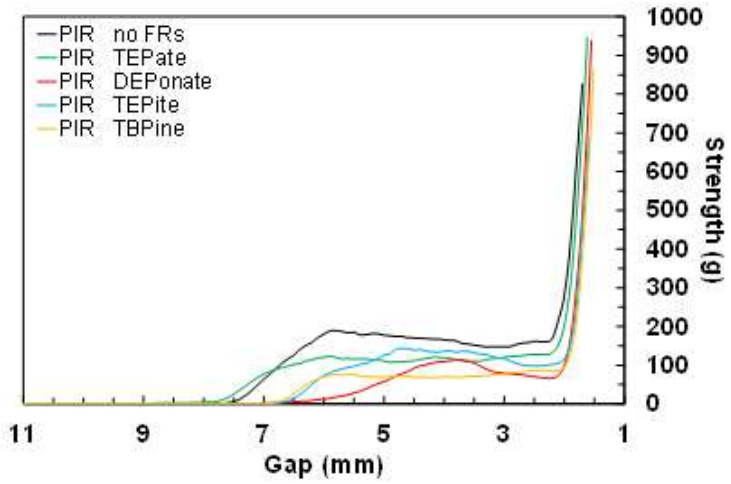

Figure 10: Evolution of char strength as a function of gap for PIR systems.

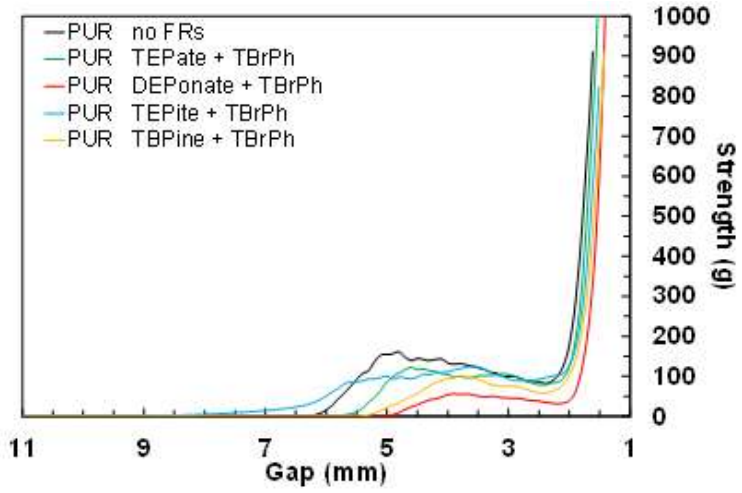

Figure 11: Evolution of char strength as a function of gap for PUR systems.

When the upper plate of the rheometer is not in contact with the char, the strength is zero. As soon as the upper plate is in contact with the char, the strength increases and varies according to the mechanical properties and the shape of the char (its ability to be compressed). It can be admitted that the higher the resistance, the more compact and resistant the char. Below a 2 mm gap, the force value increases strongly since the char is fully compressed.

Figure 12 shows the average compression force of the char. This value is obtained determining the average value of the strength from the first positive value down to around 2 mm (just before the strong rise of the force). For example, for the PIR without FR system, the average force will be between the gap 7.5 mm and the gap 2.25 mm.

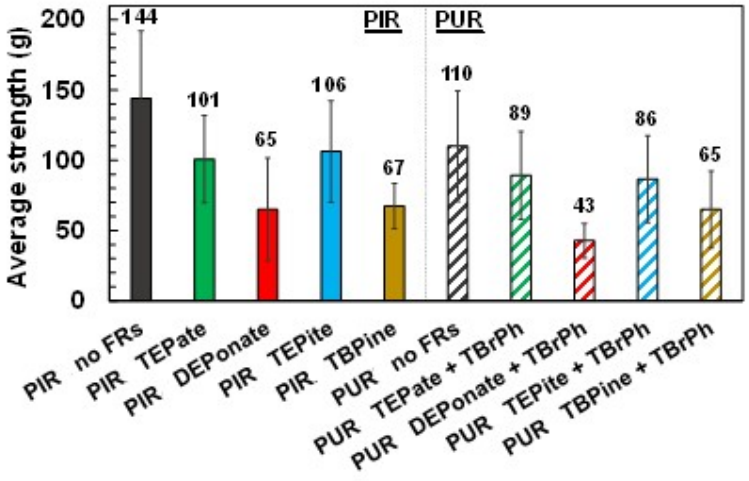

Figure 12: Average strength of PIR and PUR systems.

In the case of PIR systems, the system without FR shows the highest average strength (144 g), which indicates a char which is rather resistant to compression. Then, PIR TEPate and PIR TEPite present an intermediate average strength of 101 g and 106 g, respectively, while PIR DEPonate and PIR TBPine systems show average strength of the char equal to 65 g and 67 g, respectively. These results show that when PIR degrades in the presence of FR, the char formed is more easily compressible. It shows that the char is easily mechanically degraded by an external source. However, the char is also less brittle and could deform to accommodate an internal stress (gas release).

The same tendency can be observed for the PUR systems compared to PIR and thus the same conclusions can be drawn. PUR with no FR shows a char which is more resistant to compression, while PUR TEPate and PUR TEPite present a lower compression strength. Finally, the PUR DEPonate and PUR TBPine systems show the lowest compression strength.

In conclusion, these values reveal that the addition of FR leads to the formation of a char that is easier to compress. Figure 12 shows that TEPate and TEPite lead to char structures slightly less resistant than the system without FR. The compression force is also strongly decreased for DEPonate and TBPine.

According to the analyses carried out on the foams by TGA and rheology, two FR demonstrate either an action in condensed phase or in gas phase. First, the TEPite favours the increase of the residual weight under TGA conditions for the PIR and PUR systems. Moreover, among all the FR, TEPite presents a slight decrease of the average strength of the char, which corresponds to a resistant char. Thus, it may be proposed that TEPite may act predominantly in the condensed phase. On the contrary, it appears that DEPonate seems not to act mainly in the condensed phase but rather in the gas phase. Indeed, under TGA analyses, the use of DEPonate leads to the formation of the lowest residual weight in the PIR system as well as in the PUR system. Moreover, the use of this FR leads to the lowest average compression strength of the char indicating the formation of a weak char. Finally, concerning TEPate and TBPine, the action of these FR does not seem to be as obvious as that of TEPite and DEPonate. More characterizations are needed to make conclusions on their mode of action.

I.4. Study of the fire behavior using mass loss cone

I.4.1. Heat release

In order to compare the efficiency of the different FR molecules in terms of fire properties, MLC tests were performed. The apparatus used in the lab is a mass loss calorimeter (MLC) provided by FTT (Appendix 4). A sample of 10 cm × 10 cm × 4 cm is placed on a support located below the conical heater. The distance between the surface of the sample and the conical heater is set up at 25 mm. Tests were carried out with a flux of 35 $kW.m^{-2}$. A spark igniter is placed above the sample to ignite the

gases released by the degradation of the foam. The test is thus performed under forced ignition. The cone is equipped with four thermocouples located in the chimney. This constitutes a thermopile that was previously calibrated with methane allowing the heat release rate (HRR) to be determined from a calibration curve. An opacimeter is placed at the exit of the chimney to determine the smoke released during combustion. A TRDA Smoke density device supplied by NETZSCH Taurus Instruments was used to characterize the smoke released during a test.

Figure 13 and Figure 14 show the evolution of the heat release rate (HRR) versus time for the PIR and PUR systems respectively.

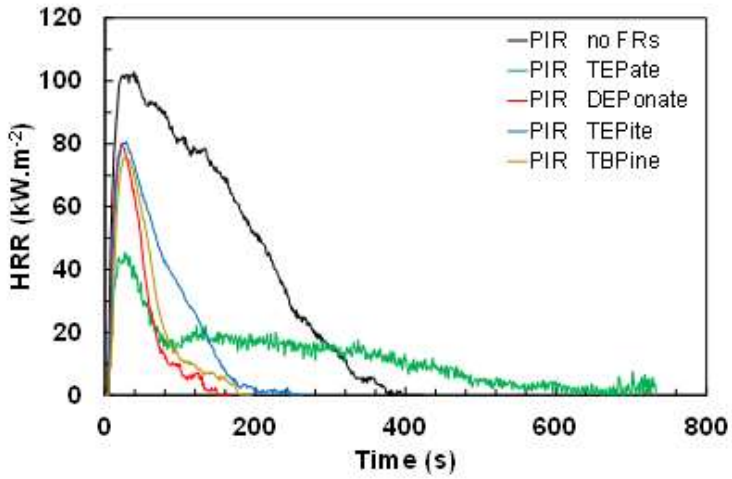

Figure 13: Heat release rate measurements for PIR systems (from MLC test at 35 kW.m^{-2}).

Concerning the PIR systems, all the FR used show a lower pHRR and flaming time compared to PIR without FR. The only exception is for the PIR TEPate system, which exhibits a much higher flaming time than the system without FR. Regarding the PUR systems, it obviously appears that the PUR DEPonate system shows a much lower pHRR and flaming time than the PUR without FR. All the other FR additives show a limited effect on pHRR and flaming time.

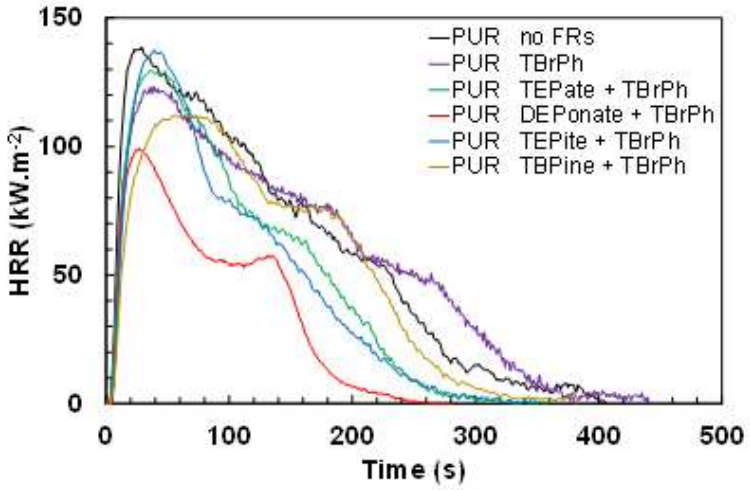

Figure 14: Heat release rate measurements for PUR systems (from MLC test at 35 kW.m^{-2}).

Figure 15 presents more precisely the main characteristic data obtained with the MLC test, i.e., the pHRR and the THR. It will help to refine the comparison of the effect of each FR on the fire behavior of the foams.

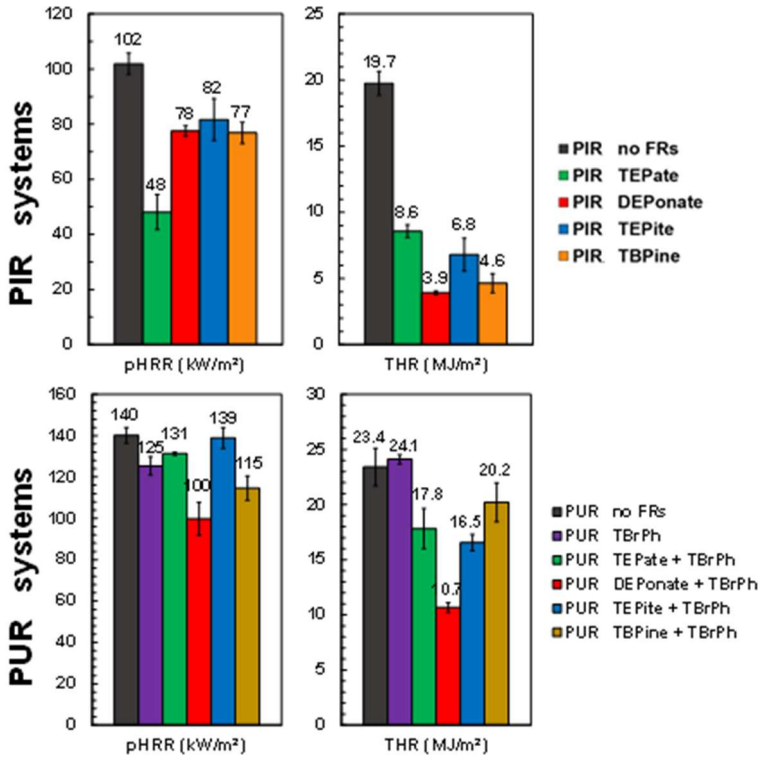

Figure 15: pHRR and THR measurements for PIR and PUR systems (from MLC test at 35 kW.m^{-2}).

First, regarding the PIR systems, the use of TEPate in PIR shows the best performance - highest reduction of the pHRR (-53 %) - while the three other FR have an identical action on the pHRR,

decreasing the value by around 20 %. Concerning the THR, all the FR that have been considered in this study have a positive effect on the total energy released during combustion. However, even if the PIR TEPate presents the best action on the pHRR, it presents the THR with the lowest decrease (-56 %). The lowest THR is obtained for PIR DEPonate (3.9 $MJ.m^{-2}$), which presents a decrease of 80 % compared to the value obtained for PIR without FR. Concerning the mode of action of the FR, the strong decrease of the pHRR of PIR TEPate and the fact that no charring effect is reported using TGA, we can imagine that TEPate acts mainly in the gas phase. However, this action is not sufficient to stop the combustion. Indeed, as shown in Figure 13, the flaming time is much higher for PIR TEPate than for the other systems.

Concerning the PUR systems, the effects of the FR seem to be different from those observed for PIR systems. Indeed, it is no longer TEPate that shows the best decrease of the pHRR but DEPonate. The pHRR of PUR DEPonate decreases by 29 %. TBPine also shows good efficiency in PUR foam for the reduction of the pHRR (decrease of 18 %). Otherwise, the other FR do not show any significant action on the pHRR. If the THR result is taken into account, PUR DEPonate shows the lowest THR (10.7 $MJ.m^{-2}$) followed by PUR TEPite (16.5 $MJ.m^{-2}$) and PUR TEPate (17.8 $MJ.m^{-2}$), and finally PUR TBPine (20.2 $MJ.m^{-2}$). TBrPh used alone shows little effect on the pHRR and THR, i.e., a small decrease of the pHRR (-11 %) and even an increase of the THR (+ 3 %). As in the PIR system, DEPonate shows good performance.

These results are in good agreement with the literature. Concerning TEPate, in 2016, Xu *et al.* also showed that the use of TEPate in a PUR system resulted in a decrease in both pHRR and THR.[62] In 2014, Zhang *et al.*[58] showed that the use of DEPonate in a PUR system resulted in lower pHRR and THR. Studies on polyisocyanurate systems are much less common in the literature. However, it has been shown that dimethyl methyl phosphonate has the effect of decreasing the pHRR and THR on a PIR system[63,64,65]. As dimethyl methyl phosphonate and DEPonate have relatively close boiling points, 181°C and 198°C respectively, we can assume that DEPonate has the same type of action here.

I.4.2. Flaming time

Figure 16 presents the main characteristic time of combustion, i.e., the ignition times, the times to reach the maximum HRR (t pHRR), and the flaming times (time to total flame extinguishment). The objective here is to compare the actions of the phosphorus FR on these parameters.

First, whatever the materials, ignition is very rapid, and combustion starts almost instantaneously after placing the spark igniter above the samples (around 5 s). Therefore, this parameter cannot discriminate the systems.

Then, regarding the PIR systems, the addition of FR allows us to slightly decrease the t pHRR (from 5 s to 9 s). However, this decrease remains low. Concerning the effect on the flaming time, the FR act differently. The PIR TEPate shows the highest flaming time, with an increase of 226 s compared to the PIR system without FR. On the other hand, DEPonate and TBPine show the best action since they allow the decrease of the burning time by 271 s and 258 s respectively. TEPite acts in an intermediate way by decreasing the combustion time by 193 s. Here again, DEPonate shows the best effect by decreasing the flaming time in the most efficient way.

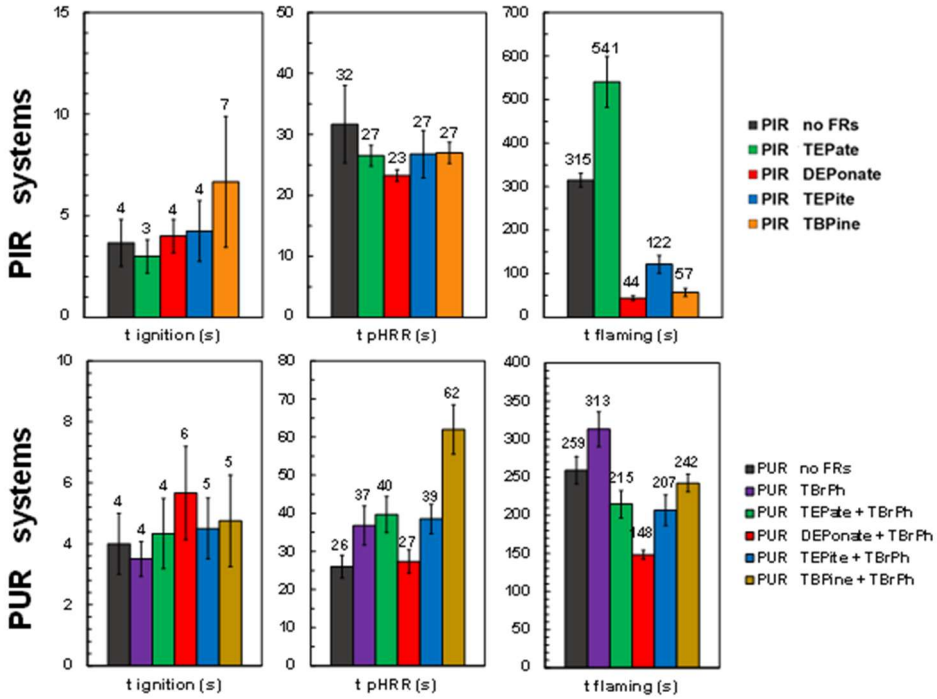

Figure 16: Ignition time, pHRR time and flaming time measurements for PIR and PUR systems (from MLC test at 35 kW.m^{-2}).

Finally, about the PUR systems, the addition of FR increases the t pHRR unlike the PIR systems. Indeed, this increase is in the range of 11 s to 36 s excluding the PUR DEPonate, for which t pHRR remains identical to that of the system without FR. Still with respect to the t pHRR, TBPine shows the highest value. Indeed, if we look at the HRR curve (yellow – Figure 14), we observe that the HRR values remain high and quite close, between 50 s and 100 s. Finally, the addition of FR enables the decrease of the flaming time, except for the TBrPh alone, which increases it by 54 s. TEPate, TEPite and TBPine decrease the flaming time by about 34 s, while DEPonate confirms its effectiveness in the studied systems.

I.4.3. Visual observations

Figure 17 shows the surface and the core structure of the residues of the PIR and PUR systems collected after the MLC tests, while Table 6 presents the residual weights.

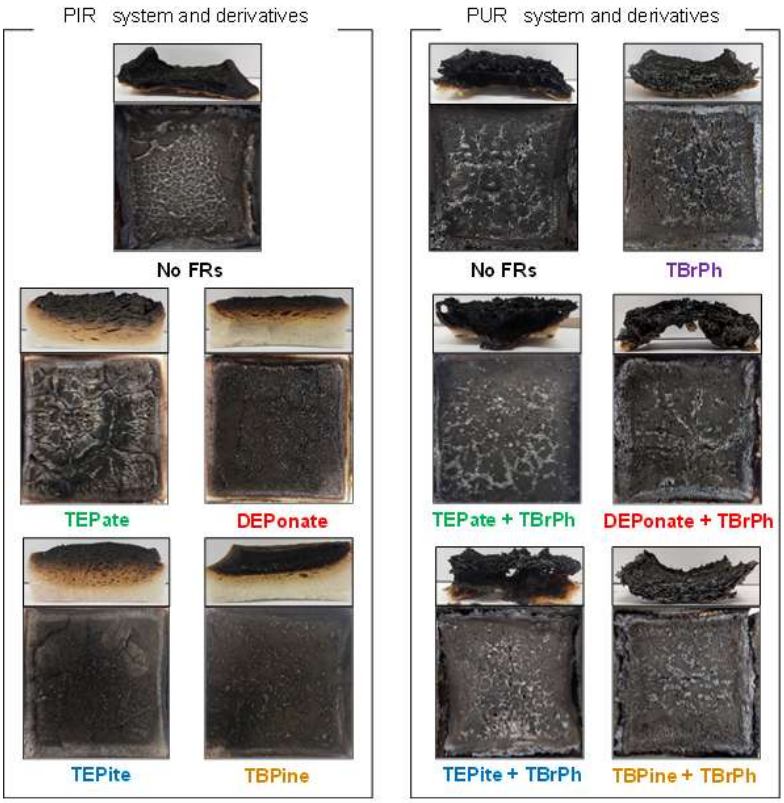

Figure 17: Images of the surface and the core of the PIR systems and the PUR systems after the MLC test at 35 kW.m^{-2}.

Concerning the PIR systems, the PIR without FR has a surface with many cracks and the surface looks like "fish-scales". The core of the material is entirely decomposed and does not show any swelling or unburned material. The residual weight of this carbonaceous residue is much lower than all the flame retarded counterparts (48.5 wt%). This confirms that the structure is much more degraded when no FR is added. Concerning TEPate, it is the only system to present large cracks on the surface of the sample. This could be correlated with the fact that the flaming time is the highest among all the systems studied. When the surface presents cracks, it permits the release of the combustible gases and does not limit the input of oxygen promoting the combustion. Looking more closely at the core of the material, the upper half is black, showing the degradation of the foam, while the lower half is brown, showing the beginning of its decomposition. TEPate also has the lowest residual weight of the PIR systems with FR (65.2 wt%) but its flaming time is much higher compared to the PIR without FR.

The residue collected from PIR DEPonate does not present a cracked surface, but rather a smooth surface with some very thin cracks. The core of the material is also different from the one observed for TEPate. Indeed, the black part corresponding to the char is smaller and the brown part is also thinner but shows a swelling behavior with the appearance of holes. In that case, a large part of the material is not decomposed. As shown before, the material only burns for a short time, which is why not much of the material is burned. It can also be linked with the fact that PIR DEPonate has the highest char residual weight (82.1 wt%).

The use of TBPine leads to a relatively identical surface compared to PIR DEPonate. However, when looking at the core, the brown intermediate part is not observed. No swelling is visible. Despite this difference, their fire behavior is identical and the residual mass after the MLC is relatively close to that of DEPonate (80.1 wt%).

Finally, TEPite shows a surface identical to that of DEPonate and TBPine, but presents a core closer to that of TEPate. TEPite has an intermediate residual mass of 74.6 wt%.

These results thus demonstrate that it seems important to obtain a smooth surface, avoiding cracks in order to limit the mass transfer and avoid an increase of the combustion time.

Table 6: Residual weight of PIR systems and PUR systems from MLC trials.

	Residual weight (%)	**Std. dev.**
PIR no FR	48.5	0.9
PIR TEPate	65.2	4.6
PIR DEPonate	82.1	1.6
PIR TEPite	74.6	3.2
PIR TBPine	80.1	1.0
PUR no FR	43.0	0.6
PUR TBrPh	38.1	3.5
PUR TEPate + TBrPh	37.6	4.1
PUR DEPonate + TBrPh	49.9	1.1
PUR TEPite + TBrPh	33.1	3.0
PUR TBPine + TBrPh	32.2	1.2

Concerning the PUR system, the visual observation of the surface of the material or the core is less obvious. Indeed, the surfaces show several holes and the cores show a material, which is always strongly decomposed. The examination of the cores does not allow us to draw any precise conclusion

on the carbonization process. Regarding the residual weights, the PUR DEPonate system has the highest residual weight (49.9 wt%). It can be related to the fact that the THR obtained with PUR DEPonate is the lowest.

When compared, it appears that the MLC and TGA weight residues do not correlate well. The weight residue rate is higher after MLC test than TGA. For PIR foams, the different systems are not fully pyrolyzed during MLC tests, which explains why the residue content is higher. For PUR foams, the pyrolysis seems more pronounced; however, the weight residue is still higher when performing MLC test than TGA analyses. Different reasons can explain this result: the thermal transfer occurring in the MLC test as well as the atmosphere are different from the one occurring in TGA, and also the fact that MLC test allows thermal insulation of the under layer of the sample from the heat source, inducing more charring than in TGA.

I.4.4. Smoke production

In the PU foam field, it is well known that PU produces toxic opaque smoke. Thus, smoke release measurements were performed depending on the chosen molecules. Figure 18 compares the total amount of smoke released during combustion of the PIR and PUR systems. It is calculated by integrating the air under the curve representing the light attenuation versus time curve. The value of the total smoke released is therefore relative (semi-quantitative). Figure 18 also reports the total amount of smoke released during combustion by the THR. The total light attenuation was divided by the THR in order to “normalize” the smoke production and get the amount of smoke emitted per unit of energy delivered since the amount of foam that is burned strongly varies from one system to another.

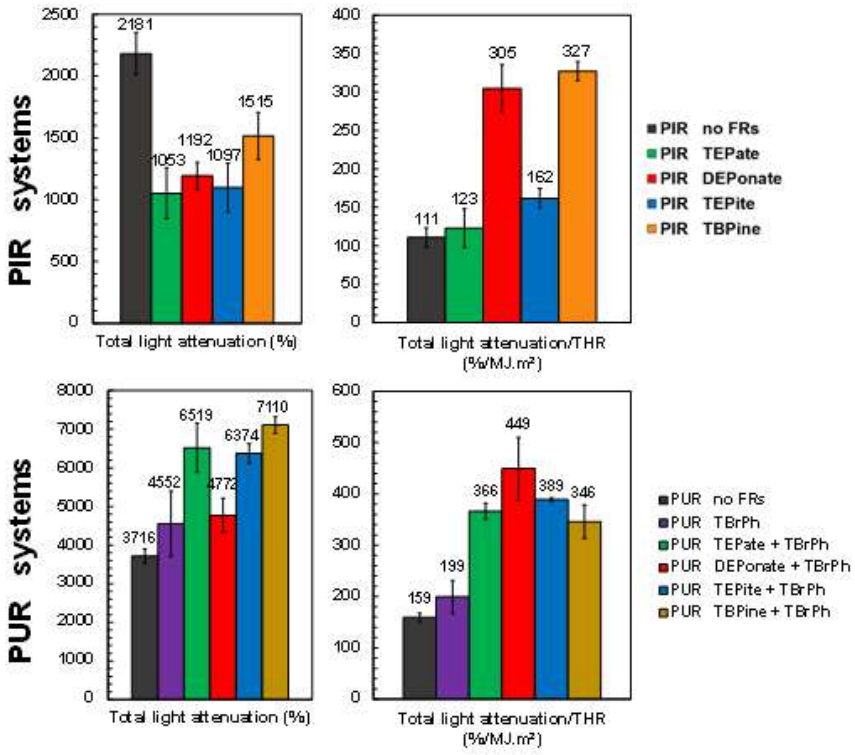

Figure 18: Total light attenuation for PIR and PUR systems (from MLC test at 35 kW.m^{-2}).

Regarding the PIR systems, the addition of FR allows us to strongly decrease the total smoke produced during the combustion. This is due to a very low THR of each of the systems with FR and a high residual weight after the tests compared to the system without FR. Since less foam burns, the total amount of smoke decreases. TEPate, DEPonate and TEPite show the lowest total light attenuation, close to 1100%, while TBPine is slightly more significant with a value of 1515%. When the normalized value *vs.* THR are considered, it can be seen that TEPate (123 %.MJ^{-1}.m^2) and TEPite (162 %.MJ^{-1}.m^2) release slightly more smoke compared to the system without FR, while DEPonate (305 %.MJ^{-1}.m^2) and TBPine (327 %.MJ^{-1}.m^2) release 3 times more smoke per unit of energy than the system without FR.

Concerning the PUR system, contrary to the PIR systems, the addition of FR increases the total light attenuation in each case, even if the THR is equal to or much lower than the system without FR. TBrPh only slightly increases the smoke production (4552 %) as if its action was relatively weak. As seen previously, TBrPh has a very low effect on the pHRR and slightly increases the THR and flaming time. Used alone, TBrPh does not act efficiently on any of the studied parameters. DEPonate also shows a slight increase in total smoke production. However, considering that the THR decreases strongly, the normalized value is high. Finally, TEPate, TEPite and TBPine lead almost to the same value considering the total smoke evolved (around 6700 %) as well as the normalized values. The total amount of smoke evolved is almost twice that obtained for the system without FR. Finally, if we consider the total light attenuation per unit of energy emitted, the DEPonate shows the highest value (449 %.MJ^{-1}.m^2)

compared to its counterpart without FR (159 %.MJ^{-1}.m^2). Those results are in good agreement with the study of Singh *et al.* showing that the use of phosphorus FR in PUR systems has the tendency to decrease the thermal decomposition temperature of foams, resulting in an increase of the smoke density[66].

I.5. Comprehension of the decomposition phenomena

I.5.1. ^{31}P solid state NMR

^{31}P solid state nuclear magnetic resonance (NMR) spectroscopy is used to characterize the foams before and after their decomposition and help to understand degradation phenomenon occurring during combustion. Figure 19 shows the ^{31}P spectra of each of the PIR and PUR systems before burning. On each of the spectra, the spinning sidebands are represented by an asterisk and shifted from a spin rate of 12.5 kHz for each of the corresponding peaks.

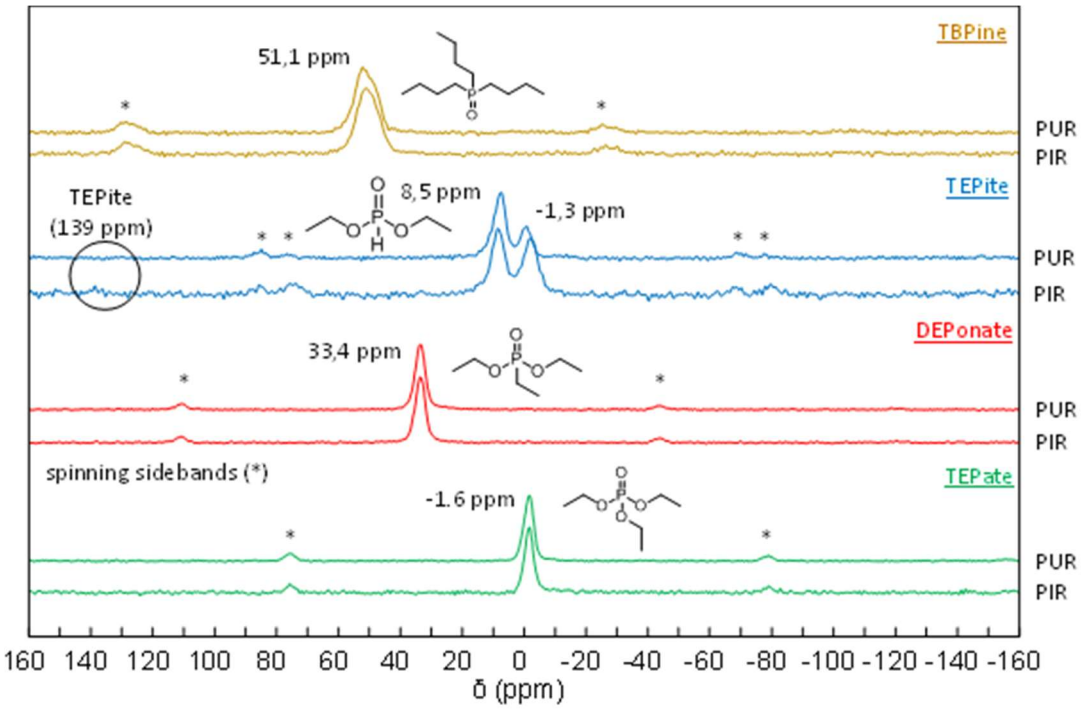

Figure 19: ^{31}P solid state NMR spectra of PIR systems and PUR systems before burning.

The spectra of TEPate containing foams show a single peak at -1.6 ppm corresponding to its chemical structure[67]. Those of DEPonate foams also show a single characteristic peak at 33.4 ppm corresponding to a phosphonate[68], as well as in the case of TBPine foam spectra, which show a single peak at 51.1 ppm corresponding to a phosphine oxide[69]. Contrary to the others, TEPite foam spectra show two peaks located at 8.5 ppm and - 1.3 ppm. These peaks do not correspond to TEPite (which should be located at around 139 ppm) [70]. This result was not expected. However, it can be proposed that since, triethyl phosphite is extremely sensitive to hydrolysis and acidic environments, triethyl phosphite

decomposes during the preparation of the foam in the presence of the acidic chemical blowing agent (formic acid for PIR) or water (PUR). It thus decomposes into diethyl phosphonate and ethanol[71]. The diethyl phosphonate corresponds to the peak located at 8.5 ppm and is different from the FR DEPonate used in the study, which is a diethyl ethyl phosphonate. The second peak is more difficult to attribute. The peak at -1.3 ppm may correspond to the oxidation of triethyl phosphite into triethyl phosphate. Since the ^{31}P solid state NMR experiment are semi-quantitative (possibility to compare the ratio), it can be said that PIR contains almost as much diethyl phosphonate as triethyl phosphate, while PUR has more diethyl phosphonate than triethyl phosphate. Thus, it is necessary to keep in mind that for each of the tests previously carried out using TEPite, it is in fact a mixture of diethyl phosphonate and triethyl phosphate instead of TEPite. However, the mixture will still be denominated TEPite. It can be seen that TEPite systems lead to intermediate results at MLC test, between TEPate and TEPonate systems. It is coherent with the fact that TEPite is hydrolyzed into a mixture of TEPate and a diethylphosphonate. However, the use of TEPite into PUR or PIR foams must be avoided because it leads to uncontrolled hydrolysis of the FR.

Since foams were characterized and the peaks assigned to the structure of the FR, it is now possible to characterize the corresponding carbonaceous residues obtained after MLC test. Only the top and completely black part of the MLC residues was analyzed. A High Power Decoupling (HPDEC) sequence was used for the ^{31}P solid state NMR experiments. The use of this type of sequence allows the calculation of the ratio of each of the phosphorus structures existing in the foam and their comparison. Each system with FR has the same shape of spectrum made of three peaks. Figure 20 shows, as an example, the ^{31}P spectra of the carbonaceous residue of PIR TEPate.

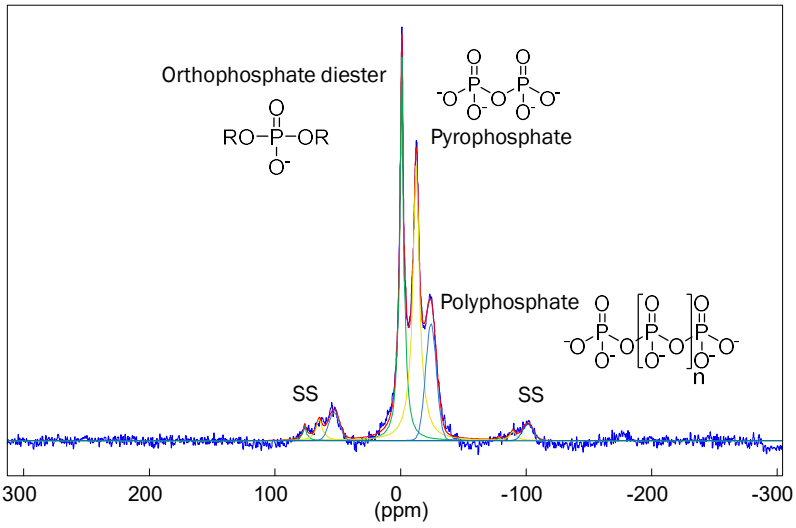

Figure 20: ^{31}P solid state NMR spectra of PIR residue.

For each of the systems with FR, three different structures are obtained in the char corresponding to orthophosphate diester at -1 ppm, pyrophosphate at -11 ppm and polyphosphate at -23 ppm[72,73,74]. The characteristic peaks of the native FR structures shown in Figure 19 have disappeared, corresponding to a complete decomposition of the FR during combustion and the oxidation of the phosphorus. The area under all peaks can be determined and the ratio of the different phosphorus structures found in the charred residues can be compared. Figure 21 presents the ratio of the different phosphorus structures found in the charred residues. It allows for a better understanding of which type of phosphorus structure is promoted in the charring phenomenon during combustion for each system.

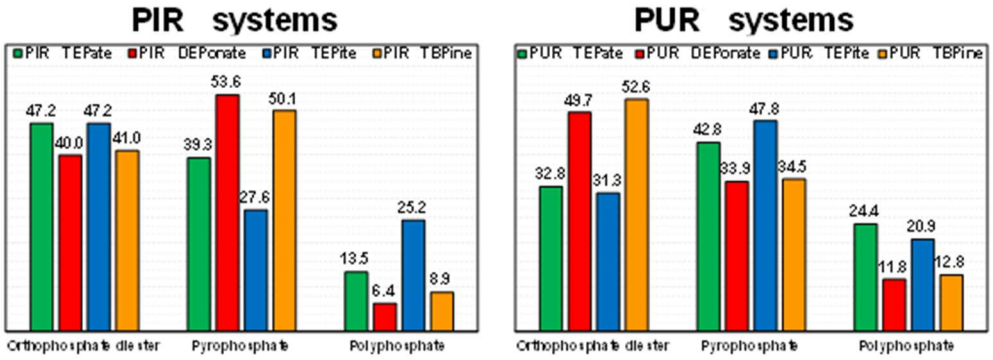

Figure 21: Ratio of orthophosphate diester, pyrophosphate and polyphosphate in each residue of PIR and PUR systems.

On general matters, it can be found in literature that the pyrophosphate and polyphosphate created during decomposition participate and promote the formation of the carbonaceous structure (char). They can play a role in a condensed phase, for example, in intumescent systems. At higher exposition time or higher temperature, more polyphosphorus structures are formed. It will be considered that a more developed char structure will be constituted of more polyphosphate.

When looking at the results of the PIR systems, the PIR TEPite system leads to the highest polyphosphate content in the char (25.2 %). Thus, it would be the system with the most developed and most thermally resistant char. If we correlate with TGA analysis, TEPite leads to the formation of the best charring phenomenon with the highest increase of residual weight at 800°C, which is consistent with those results. Then, if we look at the mechanical properties of the char (compression force), TEPite also showed a more mechanically resistant char compared to DEPonate or TBPine, for example. Thus, it is possible to assume that TEPite tends to act mainly in the condensed phase. However, it could also be assumed that its action is too quick to permit to achieve the best improvement of the fire-retardant properties of the foams as measured using the MLC test. Therefore, even if the FR additive improves the charring effect, the action in the gas phase seems to be

predominant to obtain good performance in PIR foams. Indeed, even if the polycondensation of DEPonate is 4 times less than that of TEPite, DEPonate yields better results using MLC test (RHR, THR, Figure 13). We can therefore conclude that, despite an improvement of the char structure, TEPite is not sufficient to stop the combustion or to reduce its intensity efficiently.

The study of PUR systems confirms the observations and assumptions previously discussed. Indeed, polyphosphate structures are more present in the TEPate (24.4 %) and TEPite (20.9 %) systems than in DEPonate (11.8 %) and TBPine (12.8 %) systems. Thus, even if there is a promotion of the charring effect with TEPite in PUR system, the action in not strong enough to obtain good results using MLC test.

I.5.2. Chemical analysis of the charred residues

The objective of the chemical analysis is to measure the evolution of the content of carbon, hydrogen, nitrogen, oxygen, and phosphorus before and after the combustion. The goal is to compare the concentration of elements remaining in the char of the different samples after combustion and better understand the mode of action of the FR.

Figure 22 shows the weight percentage of carbon, hydrogen, nitrogen, oxygen, and phosphorus in the char of the PIR systems before and after burning. The weight percentages are absolute and not relative.

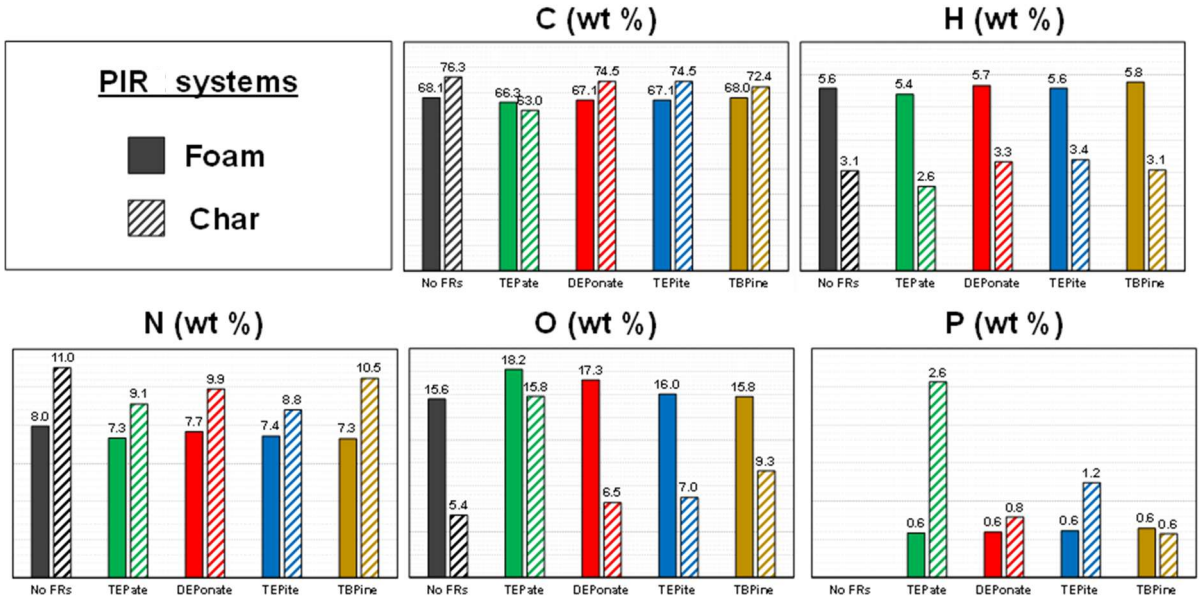

Figure 22: Carbon, hydrogen, nitrogen, oxygen, and phosphorus content in each system before and after the combustion for PIR system.

First, concerning hydrogen, the absolute amount of hydrogen in the chars is around 2 times lower than in the foam before combustion. None of the FR promote an increase of the hydrogen content. This observation is coherent with the fact that during charring, the aromatic molecules become predominant, reducing the amount of H.

Then, concerning the carbon content, all foams and chars are predominantly composed of carbon. The carbon content varies depending on the system studied. For each of the foams before combustion, the carbon content is between 66 wt% and 68 wt%. After combustion, the carbon content of the chars increases slightly to between 72 wt% and 76 wt% except for PIR TEPate, which decreases from 66.3 wt% to 63.0 wt%. The differences remain small.

As far as the nitrogen content is concerned, it is lower for each of the foams compared to their corresponding char after combustion. Foams before combustion have a percentage close to 8 wt% and their corresponding chars have a percentage between 9 wt% and 11 wt%. This variation is low, and no significant difference exists from one system to another.

Finally, concerning oxygen and phosphorous contents, foams lose a lot of oxygen during combustion. This is mainly due to the loss of isocyanate functions and polyol functions that decompose more quickly and easily when polyisocyanurate bonds break. PIR without FR, PIR with DEPonate and TEPite show a drop of oxygen content from about 15 wt% to 5 wt%. The oxygen content of TBPine decreases slightly less from about 15 wt% down to 9.3 wt%. Finally, TEPate shows the smallest decrease from 18.2 wt% to 15.8 wt%. This small decrease can be linked to the strong increase of the phosphorus content in the char (from 0.6 wt% up to 2.6 wt%). The phosphorus content increases only in the cases of the TEPite and TEPate systems. This result indicates that the phosphorus remains in the condensed phase and can improve the charring phenomenon. These observations confirm the results obtained previously with TGA and ^{31}P solid state NMR analyses, demonstrating an action for TEPite and TEPate mainly occurring in the condensed phase compared to DEPonate or TBPine.

Figure 23 shows the weight percentage of carbon, hydrogen, nitrogen, oxygen and phosphorus in the foams and chars of PUR systems.

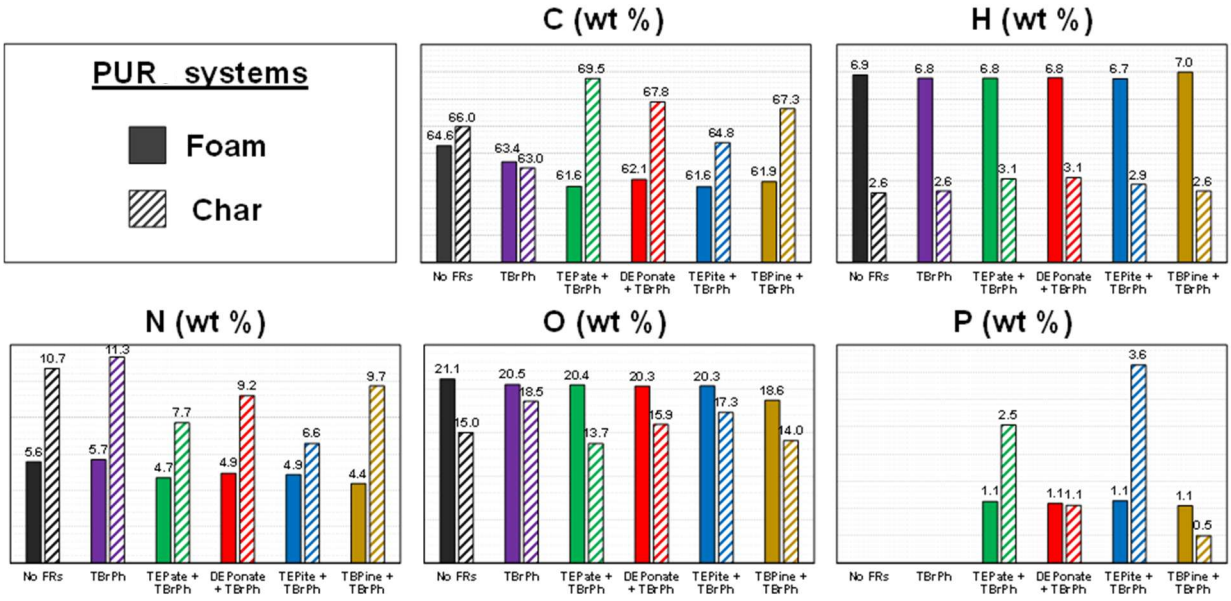

Figure 23: Carbon, hydrogen, nitrogen, oxygen, and phosphorus content in each system before and after the combustion for PUR system.

The same trends as those obtained for PIR systems can be observed for PUR foams. Carbon and nitrogen content increases after combustion, while hydrogen and oxygen content decreases. The initial phosphorus content of 1.1 wt% increases for TEPate (2.5 wt%) and TEPite (3.6 wt%), while it remains stable for DEPonate (1.1 wt%) and decreases for TBPine (0.5 wt%). Here again, it is TEPate and TEPite that show a higher concentration of phosphorus after combustion. This indicates a much more pronounced action of TEPate and TEPite in the condensed phase than for DEPonate and TBPine.

^{31}P solid state NMR and elemental analysis have shown a more pronounced action of TEPate and TEPite to promote the charring phenomenon compared to DEPonate or TBPine. Indeed, when TEPate and TEPite are used, the concentration of phosphorus in the carbonaceous residue increases and polycondensation of the phosphorus structures occurs.

The study of model FR molecules changing oxidation state and boiling point temperature showed that DEPonate is the most efficient of the tested phosphorus molecules when using MLC test. The study of the chars showed that the main mode of action of this FR occurs in the gas phase rather than in the condense phase. Indeed, even if the action of TEPate and TEPite is effective in the condense phase, promoting charring, the effect is not strong enough to improve the FR properties efficiently. It should also be noted that the FR do not have the same action depending on the polymer in which it is incorporated. Between PIR and PUR systems, PIR systems always have better fire behavior because, in addition to the potential gas phase activity of the FR, the creation of a stronger and more resistant char during combustion was noticed.

The second step of the study was to study the effect of the substituent of the model FR, replacing their aliphatic substituents by aromatic ones.

I.6. Modification of the substituents of the model FR

In the previous section, a series of phosphorus flame retardants of different chemical nature and oxidation state were tested on a PIR and PUR system. This series of flame retardants had aliphatic substituents. The objective of this part is to keep this series of phosphorus flame retardants, i.e. keeping the same chemical groups, but replacing their aliphatic substituents by aromatic ones. The modification of these substituents will obviously modify the boiling points and melting points of the FR. For this new series of tests, only the MLC was used. Indeed, the objective is to quickly highlight if these modifications have a direct impact on the fire behavior of the foam. Moreover, only the PIR system has been kept because it is the most efficient system.

I.6.1. Chosen model FR molecules

Regarding the composition of the PIR systems and the aromatics phosphorus derivatives, only the amount of FR added has been modified to obtain 0.6 wt% of phosphorus. The exact formulation and the physical properties (apparent density, closed cell content and cell size) of the foams remain confidential and are not provided in details. However, it is possible to mention that the properties as well as the general composition vary but very slightly.

Figure 24 shows the chemical structure of the flame retardants. Each of the ethyl or butyl substituents has been replaced by a phenyl group, except for DEPPonate, where only the ethyl groups not attached to an oxygen has been replaced by a phenyl group. Indeed, the diphenyl phenyl phosphonate molecule is too expensive and would not be a good candidate even just for laboratory purpose.

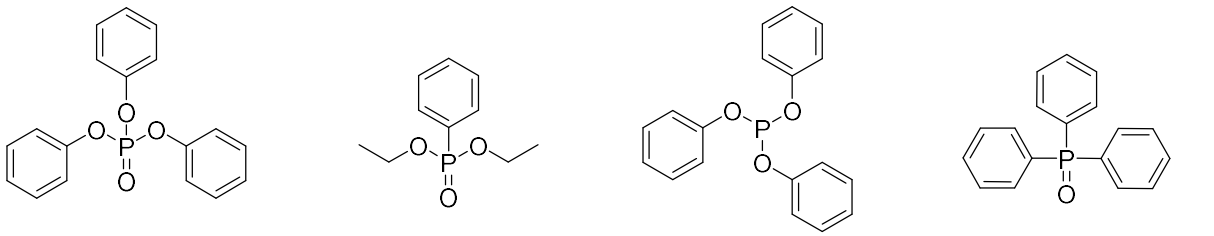

Figure 24: Chemical structure of TPPate, DEPPonate, TPPite and TPPine.

General information:

Table 7 shows the main characteristic information of the four new aromatic FR presented in Figure 24. TPPate is known to be used as a flame retardant and as a plasticizer, as TEPate. The use of DEPPonate

is not defined and is, in any case, not used as a flame retardant. TPPite is used as an antioxidant and complexing agent for synthetic resins, rubber and oils. Finally, TPPine is commonly used to induce crystallization of chemical compounds, but is not used as FR. It has to be mentioned that TPPate, DEPPonate and TPPine are classified as very toxic to aquatic life with long lasting effects. Therefore, they are mainly studied for a fundamental point of view.

Table 7: Physico-chemical and thermal properties of TPPate, DEPPonate, TPPite and TPPine.

Parameters	**TPPate**	**DEPPonate**	**TPPite**	**TPPine**
CAS number	115-86-6	1754-49-0	101-02-0	791-28-6
Molecular formula	$C_{18}H_{15}O_4P$	$C_{10}H_{15}O_3P$	$C_{18}H_{15}O_3P$	$C_{18}H_{15}OP$
Molecular weight ($g.mol^{-1}$)	326	214	310	278
Mp (°C)	49	< 20	25	156
Bp (°C)	412*	267	360	462*
Oxidation degree	+ V	+ III	+ III	- I
GSH classification		-		

* Calculated using Advanced Chemistry development (ACD/Labs) Software V11.02

Contrary to the aliphatic FR used in the first part of the chapter, the aromatic FR show high melting point due to the aromatic substituents. Thus, TPPate, TPPite and TPPine are solid at room temperature (20°C). They are the only solid compounds in the formulation. On the contrary, DEPPonate is liquid at room temperature. Considering that the boiling temperatures are higher than those of the aliphatic compounds, it can be assumed that the gas phase action would be less predominant.

I.6.2. Study of the fire behavior using mass loss cone

I.6.2.1. Heat release

Figure 25 presents the main characteristic data obtained from the MLC test (pHRR and THR) for both aliphatic and aromatic FR.

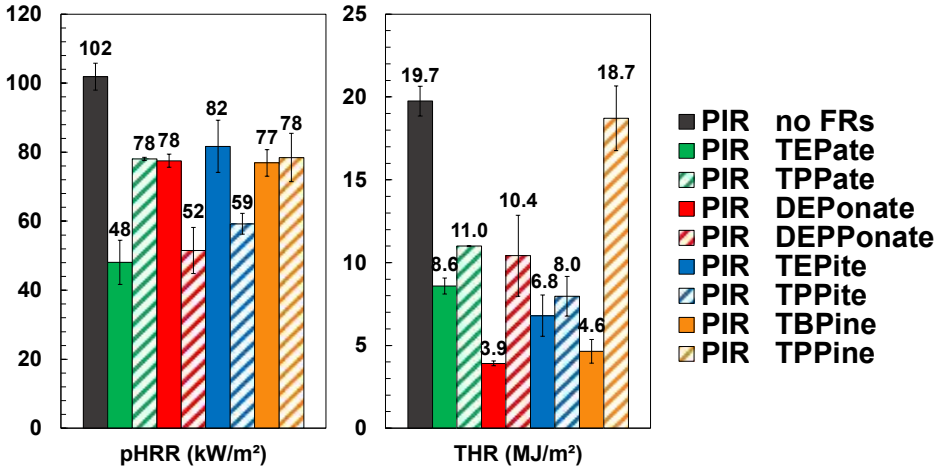

Figure 25: pHRR and THR measurements for PIR system with aliphatic and aromatic FR compounds (from MLC tests at 35 kW.m^{-2})

First, whether aliphatic or aromatic FR, they allow to permit a decrease of the pHRR and of the THR except for the PIR TPPine, which presents a THR close to the reference system without FR. Indeed, TPPine system shows a pHRR that does not vary (78 kW.m^{-2}) compared to TBPine (77 kW.m^{-2}), however the THR is multiplied by 4 (from 4.6 MJ.m^{-2} to 18.7 MJ.m^{-2}). The increase of the THR is related to the increase of the flaming time (the results are exposed in the next section). DEPPonate (52 kW.m^{-2}) and TPPine (59 kW.m^{-2}) systems show a significant decrease of their pHRR compared to DEPonate (78 kW.m^{-2}) and TEPine (82 kW.m^{-2}) systems respectively, however, their THR increases. In the same way, the increase of the THR, despite a decrease of the pHRR is linked to a significant increase of the flaming time. Finally, in the case of TPPate system, the aromatic FR leads to a significant increase of the pHRR (from 48 kW.m^{-2} to 78 kW.m^{-2}) whereas the THR increases slightly.

As a conclusion, despite the positive action of the aromatic FR on the pHRR (except for the phosphate), the THR increases in the case of all aromatic FR compared to their aliphatic counterpart. Therefore, it appears that it is more favorable to use the aliphatic FR to improve the fire behavior of the PIR foam. This result is consistent with the previously discussed results showing that a gas phase action has first to occur to be efficient. When aromatic FR are considered, their boiling point is too high and their action in the gas phase decreases as well as their efficiency. In 2020, Akdogan *et al.* discussed about the effect of TPPate as a flame retardant in a PUR system. TPPate action allows to decrease the pHRR and THR of the system with FR[75]. They also showed in this study that the action of TPPate is very effective in the gas phase and that there is also a weak action in the condensed phase, but less significant. This observation is also confirmed by another study conducted by Thirumal *et al.* in 2009 on a polyurethane system[76]. However, those results should be taken with caution since PIR system and a PUR system are complex formulation that could differ sharply.

I.6.2.2. Flaming time

Figure 26 shows the characteristic time collected at the MLC i.e. the ignition times, the times when the pHRR (t pHRR) is reached and the flaming times. The objective here is to observe the actions of the FR on these parameters.

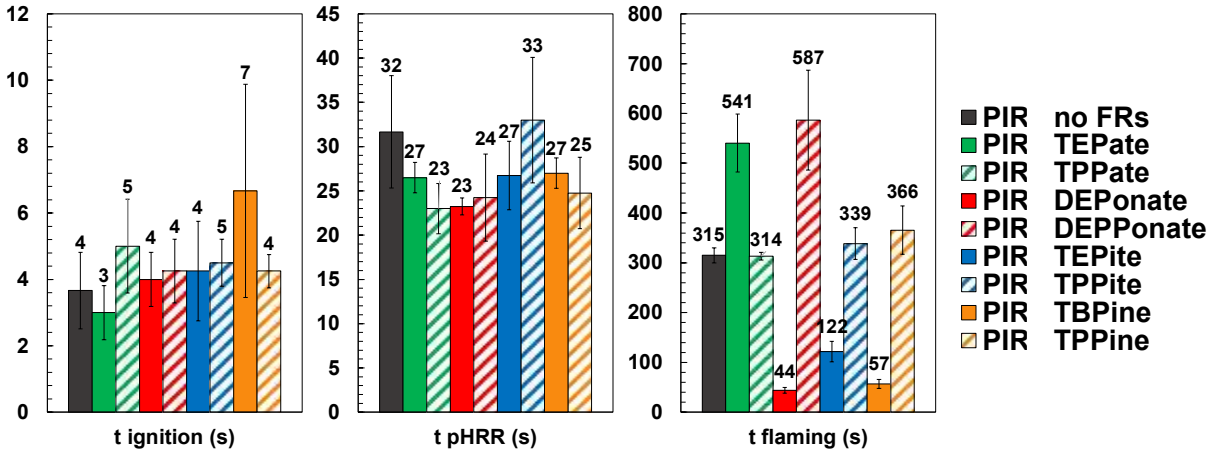

Figure 26: Ignition time, pHRR time and flaming time measurements for PIR with aliphatic and aromatic FR (from MLC test at 35 kW.m^{-2}).

As previously discussed, whether with or without FR, the material always ignites quickly, in less than 10 seconds. Thus, it is not possible to discriminate the action of FR using the time to ignition.

Then, regarding the t pHRR, the use of aromatic FR only slightly modifies the t pHRR compared to its aliphatic counterpart. The main difference is observed for PIR TEPite and PIR TPPite. However, the difference remains small and in the margin of error.

Finally, concerning the flaming time, the use of aromatic FR sharply increases it (except for TPPate). Indeed, for DEPPonate, TPPite and TTPine, a huge increase of the flaming time is observed. The flaming time varies from 44 s for DEPonate to 587 s for DEPPonate. Thus, even if the combustion is very weak and only small flames are visible on the surface of the sample during the test, it lasts a longer time. In a real fire, this long burning time may contribute to flame propagation and it is therefore not an interesting behavior. In the case of TPPine, the pHRR does not vary and the energy released during combustion remains relatively high. Thus, a very high THR close to the system without FR is observed. As a conclusion, DEPonate, TBPine and TEPite remain the most interesting FR with respect to flaming time. These FR have aliphatic substituents and boiling point temperatures much lower than those of the FR with aromatic substituents confirming that a gas phase action should be promoted.

I.6.2.3. Visual observations

The last results obtained in MLC concern the visual observation of the residue collected at the end of the test. Figure 27 shows the surface and core of the PIR systems (aliphatic and aromatics FR) after the MLC trials whereas Table 8 presents the residual weights.

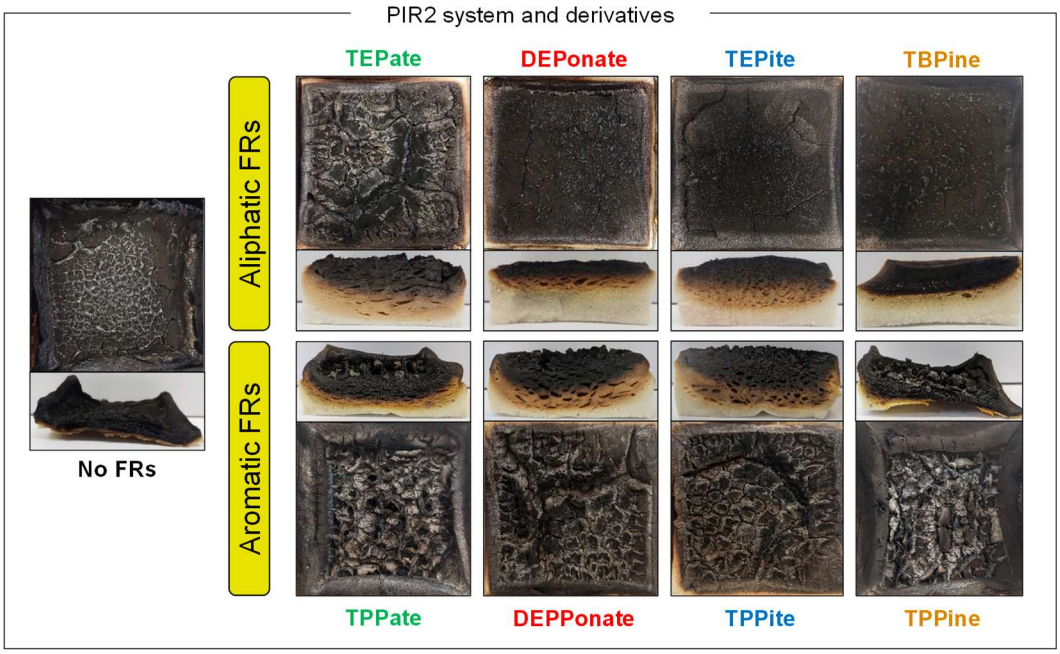

Figure 27: Images of the surface and of the core of PIR residues with aliphatic and aromatic FR (from MLC test at 35 kW.m^{-2}).

Table 8: Residual weights obtained after MLC tests at 35 kW.m^{-2} for PIR with aliphatic and aromatic FR.

	Residual weight (%)	**Std. dev.**
PIR no FR	48.5	0.9
PIR TEPate	65.2	4.6
PIR TPPate	63.7	0.8
PIR DEPonate	82.1	1.6
PIR DEPPonate	63.1	3.4
PIR TEPite	74.6	3.2
PIR TPPite	72.5	2.0
PIR TBPine	80.1	1.0
PIR TPPine	48.1	4.8

Each of the aromatic FR series presents large cracks and shows "fish-scale" shapes at the surface of the residues. These cracked surfaces (TEPate, TPPate, DEPPonate, TPPite and TPPine) are characteristic of a long burning time equal, at least, to the time of the system without FR (314 s) and up to 587 s for the DEPPonate system. The more the foam burns, the more cracks appear. Moreover, if the residual weights are compared, the systems with a very cracked surface have residual weights lower than 70 wt% and can even drop down to 48.1 wt% for TPPine system, which has the highest THR of all systems with FR. Only TPPite has a high residual weight (above 70 wt%) even though it has a surface with many cracks. On the contrary, the smoothest surfaces correspond to the systems with the aliphatic FR, which also present low THR and high residual weights.

In order to go further on the understanding, Figure 28 presents the correlation between the residual weights of the chars collected at the end of MLC experiment and the THR. We notice that the R^2 is high (0.9611) and thus a linear correlation between the THR and the residual weights within the same system (PIR) can be proposed.

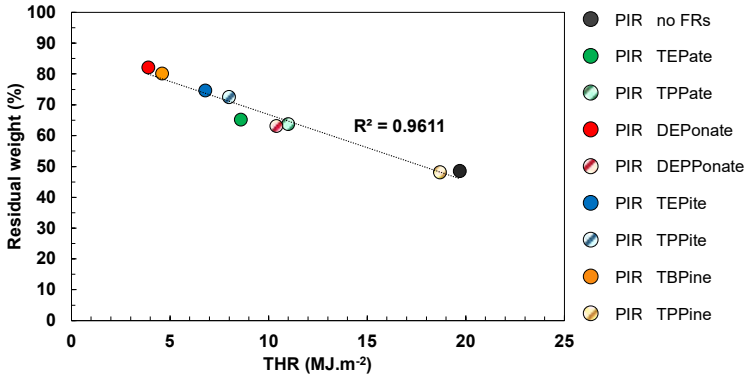

Figure 28: Correlation between residual weight and THR for the PIR systems (aliphatic and aromatics FR).

Finally concerning the core of the materials, TPPine shows a totally decomposed core, while the other aromatic FR show a core with a large charcoal part (black part), but also a large brown part, which corresponds to an intermediate state of degradation of the foam. Comparing all the cores, DEPonate and TBPine residues has the thinnest black charcoal part and the thinnest brown part. This can be related to the fact that they have the highest residual weights and the lowest THR.

I.6.2.4. Smoke production

Figure 29 compares the total amount of smoke released during combustion. It is calculated by integrating the air under the curve representing the light attenuation versus time curve. The value of the total smoke released is therefore relative (semi-quantitative).

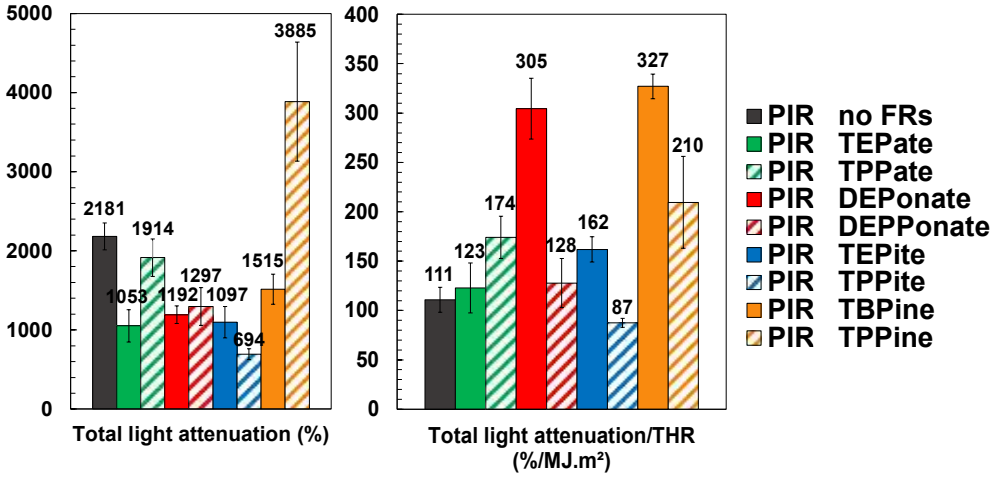

Figure 29: Total light attenuation obtained during MLC tests at 35 kW.m^{-2} for PIR with aliphatic and aromatic FR.

When considering the amount of smoke released, each of the systems with aromatic FR, with the exception of TPPite, has higher total light attenuation than its aliphatic counterpart. However, if we normalize the total light attenuation to the amount of energy released during combustion, all systems with aromatic FR are more efficient than the aliphatic systems (except for the phosphate). This could be explained by the fact that the THR as well as the flaming time increases when aromatic FR are used.

I.7. Conclusion and outlook

The main objective of this study was to investigate the influence of a series of phosphorus flame retardants characterized by different oxidation degrees, boiling temperature and substituents.

First, a series of model phosphorus flame retardants were studied using MLC tests to compare the different FR. The results showed that DEPonate is more efficient that the commercially available TEPate. The foams before and after burning were characterized, and the results showed that the main mode of action of the FR occurs in the gas phase, rather than in the condense phase. Indeed, even if the action of TEPate and TEPite is effective in the condense phase, promoting charring, the effect is not strong enough to improve the FR properties efficiently. It should also be noted that the FR do not have the same action depending on the polymer in which it is incorporated. Between PIR and PUR systems, PIR systems always have a better fire behavior because, in addition to potential gas phase activity of the FR, the creation of a stronger and more resistant char during combustion was noticed.

Then, the effect of the substituents of the FR were studied in PIR systems. Aliphatic substituents were replaced by aromatic substituents and the systems were submitted to MLC tests. The fire behavior of

the PIR foams were not improved by the aromatic FR. Indeed, since the boiling points of the aromatic FR are significantly increased, the gas phase action is probably less effective for these FR.

Thus, some interesting results were obtained by changing the oxidation rate, the boiling point or the substituents of FR. However further studies are necessary to conclude on the real efficiency of the different FR. Indeed, concerning the FR, the quantity used was based on having the same quantity of phosphorus in the systems, allowing to compare the PIR and PUR systems between them. However, it would be interesting to modify the amount of the FR considered as the most efficient (DEPonate) and try to mix it with other FR with different mode of action to try to promote synergistic effects.

In this work, another factor that has been seen to have a strong impact on the fire behavior of rigid PU and PIR foam is the choice of the blowing agent. Due to time constraint, no real study could be performed. Preliminary results showed that the modification of blowing agents can play an important role in the burning intensity of foams. The physical blowing agent used in the PUR and PIR systems is a commercial n-pentane. Indeed, n-pentane is a hydrocarbon, which boiling point is close to room temperature (36°C). However, since it is a hydrocarbon, it is extremely flammable. N-pentane is still currently used because it is an efficient gas to decrease the thermal conductivity of the material at a low cost of use, however other kind of physical blowing agents exist and can be used in foam formulations. Those can be mixtures of pentane isomers, liquid carbon dioxide, hydrofluorocarbons (HFC) or hydrochlorofluoroolefin (HCFO). The use of hydrofluorocarbons (HFO) is increasingly prohibited because of the harmful effect that these gases have on the destruction of the ozone layer. Thus, it would be interesting to study and compare the effect of pentane, isopentane or cyclopentane and liquid carbon dioxide as blowing agent.

Finally, the test used is the MLC test, however, in the foam industry, FR foams have to pass the SBI test to have a fire classification. The SBI test allows to measure the flame propagation (in addition to the pHRR and THR), which is a parameter that the MLC cannot evaluate. Since the SBI test is a large-scale test necessitating a large amount of material, it is not available for research and development purpose. In order to overcome this problem and to allow further investigation of the formulated foams, a mini SBI test has been developed during this project and detailed in a published article.[51] The mini SBI test has been developed, but up to now, no correlation study between the real SBI and the mini SBI was carried out, as a consequence, comparisons between samples can be performed but no conclusion can be drawn concerning the results that could be obtained with the real SBI. It would be interesting to pursue the study and find a correlation between the two tests.

As seen in this chapter, the development of new FR for foams remains a challenge because many parameters need to be taking into account, such as the efficiency of the FR but also its toxicity and above all, its cost. Thus, in parallel, other flame retardant processes are also investigated, such as flame-retardant surface coatings.

Chapter 2: Surface modification by FR coatings

The topic of the sol-gel inorganic-organic coating was first developed through personal research and then supported by two master students in collaboration with Saint Gobain Research, France. It led to four papers.[77,78,79,80] The organic coatings study was carried out through a PhD student (PhD M. Dilger 2019-2022) in collaboration with JSP International company. This work led to one paper[81] and one patent.[82]

II.1. Introduction

When it comes down to flame retard foams with coatings, contrary to bulk modification, closed and open cell foams needs to be studied as completely different materials. In the first case, the coating stays on top of the foam but in the second case the coating penetrates into the foam and coats the internal 3D network of the foam. Open and closed cell foams are two completely different types of foams, they have different strengths and weaknesses, but one is not necessarily better than the other, the choice goes to the type of foam that fits the needs. Open-cell foam (Figure 30) is made of cells that are deliberately left open. This makes the foam a softer, more flexible material. Closed-cell foam is made up of cells that are completely closed. The cells are pressed together, so air and moisture are unable to get inside the foam. Because of this, closed-cell foam is much more rigid and stable than open-cell foam. Closed-cell foam is much denser than open cell foam making this type of foam highly suited for shock absorption and thermal insulation. Open-cell foam has small cells that are not completely sealed and allow air to fill the space or take on water if soaked. This means the foam can be easily compressed and then naturally recover back to its original shape. As a result, open-cell PU foam is widely known for its use in the mattress and furniture industry as sofa cushion foam, foam mattresses, campervan foam, upholstery, headboards, etc. Open-cell foam is also excellent for soundproofing.

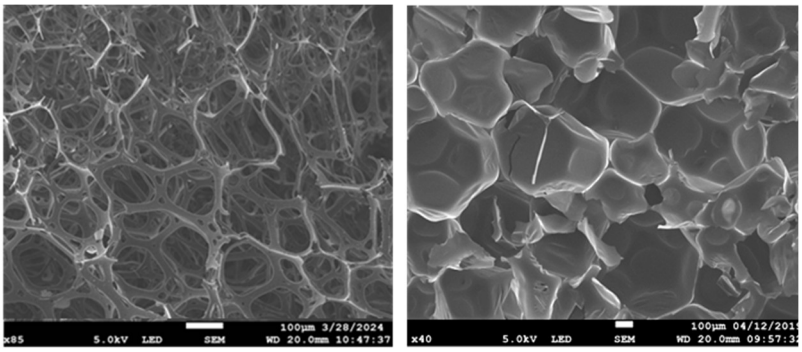

Figure 30: Open-cell foam (left) and closed-cell foam (right)

Thus, in this chapter, the coating of open and closed cell foams will be studied. In a first part, open-cell flexible PU foam will be coated and in second part expanded closed-cell polypropylene (PP) materials will be coated. For the expanded PP, surface treatment prior to coating will also be studied to improve the adhesion of the FR coating.

II.2. Open-cell foams: thin sol-gel coatings

II.2.1. Introduction

Flexible polyurethane foams (FPUF) are mainly used in furniture, mattresses or vehicle seat cushions. Because of the high flammability of FPUF, Europe, the USA and other developed countries and regions have formulated a series of mandatory regulations and standardized testing methods to promote the use of flame retardants in the foams. Indeed, untreated polyurethane flexible foams are prone to rapid fire growth and to the production of highly opaque and toxic fumes (in particular carbon monoxide and hydrogen cyanide) (Figure 31).

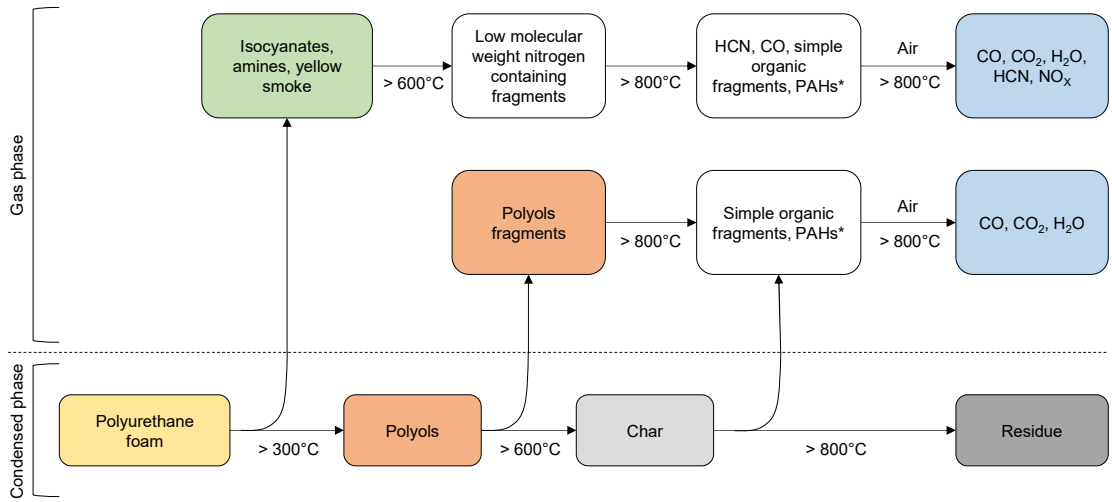

**PAHs: polycyclic aromatic hydrocarbons.*

Figure 31: Mechanism of decomposition of polyurethane foam under air atmosphere

Furthermore, the low viscosity of the decomposition products generates smoldering and severe dripping that increases the fire hazard related to the combustion of such foams. In fact, this flow of flaming liquid often results in a pool fire that promotes flame propagation and boosts the rate of heat release (HRR).[83] As a result, FPUF in furniture and bedding is capable of setting a room to flashover in as little as 5-10 minutes once ignited.[84]

The flame retardant (FR) additives used initially were mainly aliphatic chlorinated phosphate esters, compatible with foam processing. The choice of FR materials suitable for use in FPUFs is reduced due

to the combined requirements of 1) combustion modifying performance, 2) compatibility with the foaming process and 3) effect on the physical properties and aging performance of the foam.[85]

When a low fire requirement is needed (e.g. self-extinguishment after small flame exposition), even if many materials have been tested over several years,[86,87,88] the main technology still involves the use of halogenated compounds (polybrominateddiphenyl ethers, for example) in conjunction with organic phosphorus compounds (tris (2-chloroethyl) phosphate),[89] despite their tendency to increase the ratio of toxic fumes during burning. Some special high-performance foam products (able to withstand an intense flame source) include the use of expandable graphite, large amounts of melamine, or ammonium polyphosphate.[90,91] Other FR organic or mineral additives that have been evaluated individually are generally not able to provide the performance given by the combination of halogenated and phosphorus compounds. For example, some additives (such as borates or alumina trihydrate), known to be used in other types of plastics, have so far not been found effective in flexible foams. Nanotechnologies have also been evaluated and found completely unsuitable in the foam production process. As a result, high-performance foam products generally require a high level of additives, which results in substantially greater costs as well as processing issues (abrasive effect of fillers on machines, decantation) and reduced physical properties (increase of density, faster aging).[92,93,94] Researchers are now focused on the treatment of the end product to fire retard FPUF.[95,96,97,98,99]

In this work, sol-gel process was selected as the surface treatment as it has already proven its great potential in making coatings that can penetrate an entire network. The sol-gel technique is based on a two-step reaction (hydrolysis and condensation), starting from (semi-)metal alkoxides (usually tetraethoxysilane, tetramethoxysilane, titanium tetraisopropoxide, or aluminum isopropoxide) that leads to the formation of completely inorganic or hybrid organic–inorganic coatings at or near room temperature (Figure 32). It was found to be a wet-chemical technique for the fabrication of environmentally friendly flame retardant coatings on textiles ;[100] however, at the time this process had not been evaluated for foams yet.

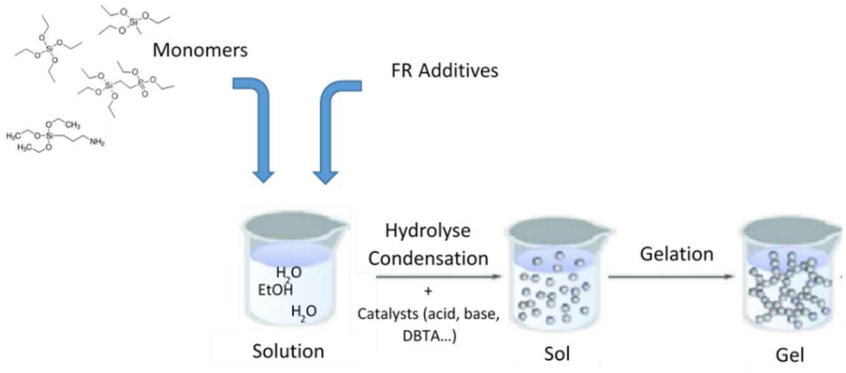

Figure 32: Scheme of a sol-gel process

It has been clearly demonstrated for textiles that sol–gel-derived hybrid architectures are capable of protecting the polymer surface acting as a thermal insulator, thus improving the flame retardant (FR) properties of the treated substrates. However, sol-gel-derived architectures cannot be fully considered effective flame retardant systems, whatever the flaming test considered. Indeed, they operate only in the condensed phase during the combustion of a polymeric material and not in the gas phase, since they are not able to interact with the released gases and smokes. To overcome this limitation, synergistic or joint effects achieved by combining the sol–gel oxidic phases with active species (phosphorus and/or nitrogen) can be imagined.

For this study, various sol-gel formulations using different catalysts and monomers were applied on open-cell FPUFs. The FR properties of the treated foams were assessed by mass loss calorimeter (MLC) and UL94 tests to demonstrate the potential of the sol-gel process for FPUF substrates.

II.2.2. Sol-gel formulation and process:

No literature existed on sol-gel coating on FPUF, thus, different sol-gel formulations were tested (Table 9). A mixture of tetraethoxysilicate (TEOS, 98% purity) and methyltriethoxysilicate (MTES, 95% purity) was used as the basis of all formulations.

MTES was added to TEOS in order to limit shrinkage and cracks of the coating during drying. However, since MTES is also known to increase gelation time, its amount was kept low.[101]

In all formulations, 10.8 ml ethanol with 5.8 ml TEOS and 1.44 ml MTES were mixed for 10 min in a 250 ml beaker. Then, flame retardant precursors were added to the mixture and stirred for 5 min before the addition of 216 ml of deionized water. Diethylphosphatoethyltriethoxysilane (DPTES, 92% purity), 3-amino propyl triethoxysilane (APTES, 97% purity) or diethyl phosphite (DEP, 99% purity). DPTES has to be added in a formulation containing TEOS, the presence of a crosslinking agent like TEOS being necessary to build a 3D network.[102] The highest DPTES concentration that can be introduced in such mixed organic-inorganic systems in order to obtain a monolithic and transparent gel is 30% molar ratio, which is the ratio used in this work. After 5 minutes' stirring, 0.3 ml of the catalyst was added.

The first sol-gel solutions were made in an acidic medium to catalyze the reaction; however, FPUFs degrade in acidic solutions and the foams showed major discoloration (turning from yellow to pink). To avoid any damage to the foams, other catalysts were employed. Different catalysts have been studied in the literature.[103,104] Following the state of the art, three different catalysts were tested (dibutyltindiacetate (DBTA, technical grade), titanium diisopropoxydebis(acetylacetonate) (TDIPA, 75% purity in isopropanol) and Tin II 2 ethylhexanoate (TEH, 92.5-100% purity)). Foams were immersed after

3 min stirring of the catalyzed formulation and pressed several times for solution absorption without stirring. The foams were finally left to drip-dry for 1 hour at 70°C in a convection air oven and 2 days at room temperature before characterization.

Samples (10 cm x 10 cm x 1.5 cm for mass loss calorimeter (MLC) and 10 cm x 5 cm x 1.5 cm for UL94) were cut from open-cell flexible molded polyurethane foams provided by Saira Seats, France and were used as received without further cleaning. The Saira Seats foams are composed of more than 98 wt% polyurethane and less than 2 wt% bis-chloromethylenebis(bis- 2-chloroethyl)phosphate (Amgard V6, CAS no. 38051-10-4). They are obtained by 1) polymerization of a polyol on an isocyanate and 2) release of carbon dioxide resulting from the polycondensation of an isocyanate on a water molecule. Both reactions occur simultaneously, and the components are added in stoichiometric amounts, in order to guarantee the total polymerization and neutrality of each reactive function (hydroxyl, amine, isocyanate), resulting in an inert polymer without any free monomer.

Table 9 sums up the different formulation tested to find a flexible FR coating that can protect FPUF.

Table 9: The different sol-gel coatings formulations

Formulations	TEOS (ml)	MTES (ml)	DPTES (ml)	APTES (ml)	DEP (ml)	Catalysts (ml)		
						TEH	DBTA	TDIPA
Sol/TEH	5.8	1.44				0.3		
Sol/DBTA	5.8	1.44					0.3	
Sol/TDIPA	5.8	1.44						0.3
Sol/DPTES	5.8	1.44	3.6			0.3		
Sol/DPTES/APTES	5.8	1.44	3.6	25		0.3		
Sol/APTES2/DEP1	5.8	1.44		6	3.2	0,3		
Sol/APTES4/DEP2	5.8	1.44		12	6.5	0.3		
Sol/APTES8/DEP4	5.8	1.44		25	13	0.3		
APTES8/DEP4				25	13	0.3		
APTES8/DEP4 without catalyst				25	13			
Sol/DEP4	5.8	1.44			13	0.3		

II.2.3. Coating morphologies

The FPUFs coated with the different sol-gel formulations were first observed by SEM to check the aspect of the coating (cracks and homogeneity). Some preliminary tests (not shown) revealed that using a sol-gel solution using only TEOS monomers - whatever the catalyst - was not able to provide a

crack-free coating; this is why MTES was added to TEOS. It has been shown in the literature[105] that a high content of MTES reduces the shrinkage during thermal treatments. Si-CH_3 groups reduce the network connectivity, thus increasing the compliance of the gel and allowing a better densification during drying. As mentioned in the experimental part, the amount of MTES was kept low to avoid an increase of the gelation time.

The influence on the coating morphology of the three different catalysts (DBTA, TDIPA and TEH) selected to prepare the sol-gel solutions was analyzed by SEM. The parameter used to differentiate the catalysts was their ability to form a homogeneous crack-free coating. It is noteworthy that this is the first time that TEH and TDIPA catalysts were tested in sol-gel processes. Indeed, these catalysts were initially used to reticulate silicons.[106] However, the reticulation reaction of silicon is similar to the condensation sol-gel reaction as it is a chemical reaction between the hydroxyl functions from curable silicone resin and the alkoxy groups of the cross linker. Figure 33 shows the SEM pictures of the coatings obtained at the surface of the FPUFs. The TEH catalyst gives the best results (Figure 33c) in terms of coating homogeneity: barely any cracks are observed compared to coatings obtained with the catalysts TDIPA and DBTA (Figures 33a and b).

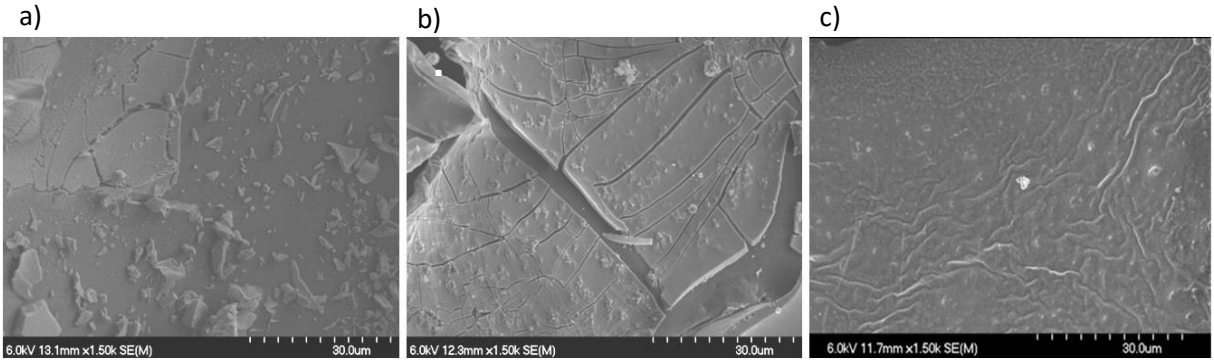

Figure 33: SEM pictures of FPUFs coated with a) sol/TDIPA, b) sol/DBTA and c) sol/TEH

As the TEH catalyst showed the most promising results in obtaining a crack-free sol-gel coating on FPUF, this catalyst was selected.

Even if the FPUF seems to keep its color and hand touch softness, SEM imaging was carried out to check the coating homogeneity. Figures 34a and 34b show the open-cell structure of the virgin FPUF. When FPUF is coated with the basic TEOS/MTES (Sol) formulation without FR monomers, it is possible to see in Figures 34c and 34d that the FPUF keeps its open cell structure and that the obtained coating is wrinkled but remains crack free. In the same manner, Figures 34e and 34f show the FPUF coated with formulation Sol/APTES4/DEP2: at low magnification the FPUF does not exhibit any difference compared to virgin FPUF; the open-cell structure is still visible. At higher magnification, a crack-free coating is visible, however, the coating is not perfectly homogenous, some parts without coating being

still visible (red circle). When increasing FR monomer concentrations (formulation Sol/APTES8/DEP4) the coating is even less homogeneous but remains crack-free (Figure 34g and 34h).

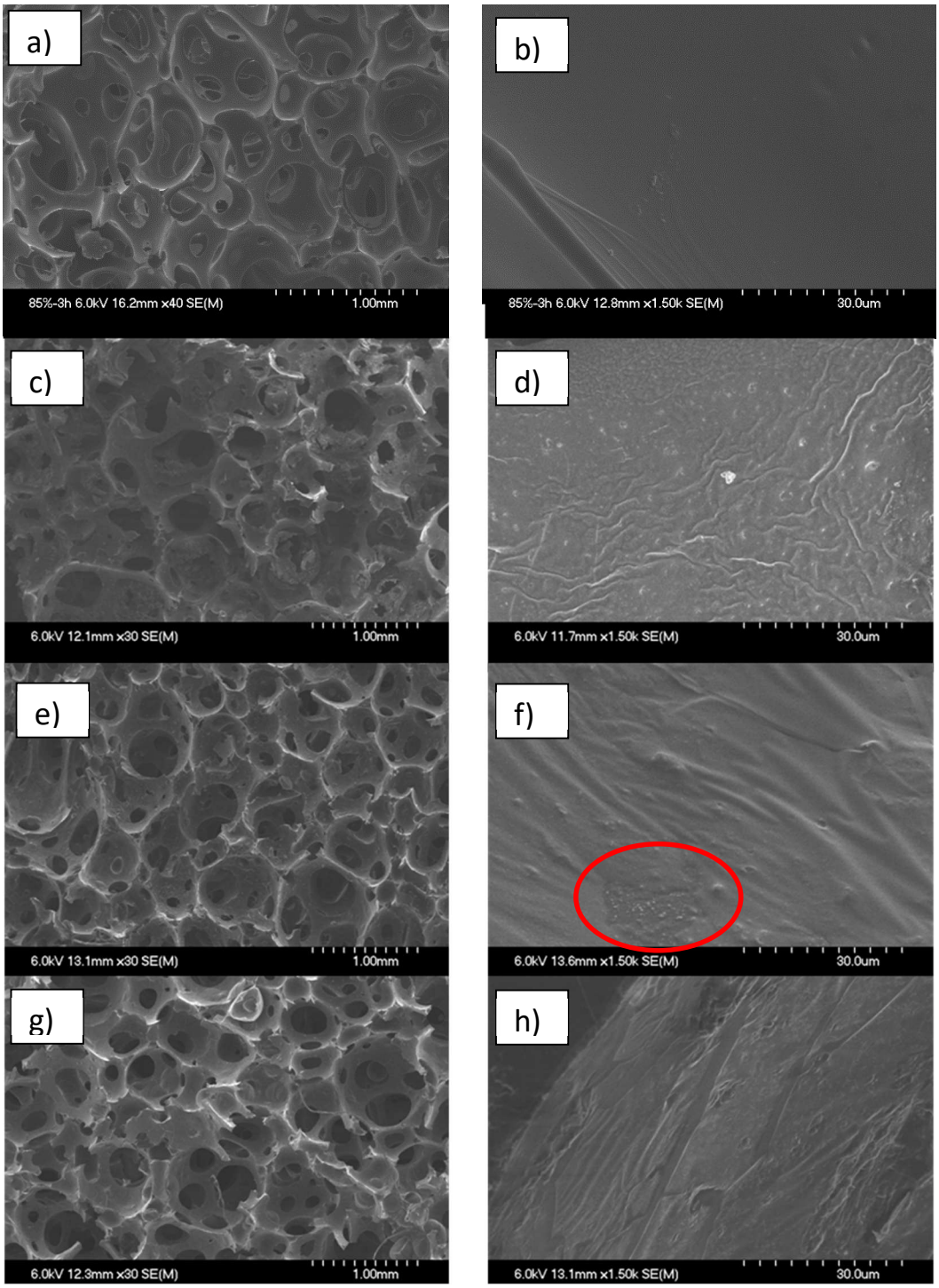

Figure 34: SEM images at low and high magnification of virgin FPUF (a and b), FPUF treated with Sol (c and d), Sol/APTES4/DEP2 (e and f) and Sol/APTES8/DEP4 (g and h). Inhomogeneities of the Sol/APTES4/DEP2 coating are shown in the red circle.

EPMA, which allows to perform X-ray mappings of elements at the surface of a sample, of the cross section of the coated foam confirms the fact that the coating is quite homogenous on the surface of the FPUF. Figure 35 shows X-ray mappings of a cross section of the sample Sol/APTES4/DEP2. The P and Sn elements were analyzed and found to be well distributed on the surface of the FPUF. Phosphorus EPMA mapping shows that the coating remains on the surface of the whole 3D FPUF; it does not penetrate inside the PU polymer chains, as can be seen in the literature for other kinds of formulations.[99]

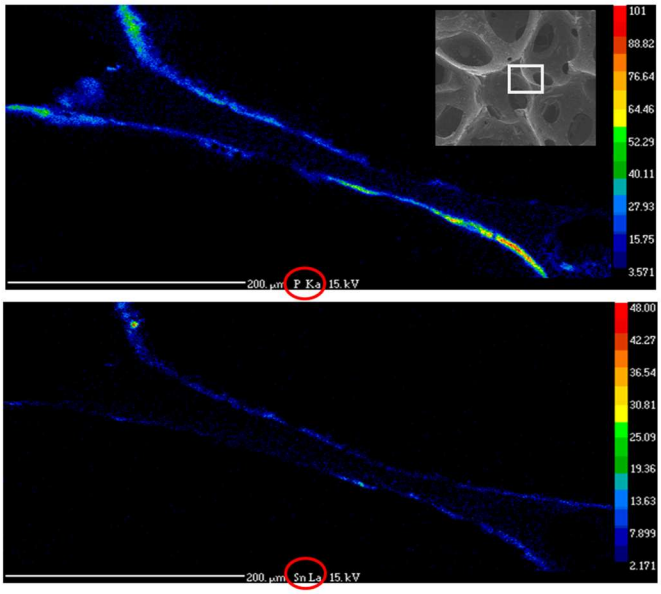

Figure 35: EPMA X-ray mappings of P and Sn elements on a part of the cross section of the sample coated with Sol/APTES4/DEP2.

II.2.4. Study of the fire behavior

- *MLC Test (Appendix 4):*

It is reported in the literature that silica sol-gel coatings are capable of protecting polymer surfaces, acting as thermal insulators, and thus improving the flame retardancy of the treated substrate;[100] however, it is also known that such architectures operate only in the condensed phase during the combustion of a polymeric material and not in the gas phase, providing limited FR properties to the substrate. Thus, in this work, potential additional FR monomers were incorporated into the sol-gel formulation.

Nitrogen or phosphorus monomers can enhance the fire properties of the silica coating. The monomers studied in this work are DPTES and APTES with or without DEP at different ratios. The first experiment chosen to differentiate the formulations was the MLC at a high heat flux (50kw/m^2) to simulate a fully developed fire. Different formulations were tested and the HRR and THR curves obtained are shown in figure 36 (each complete formulation is summarized in table 9).

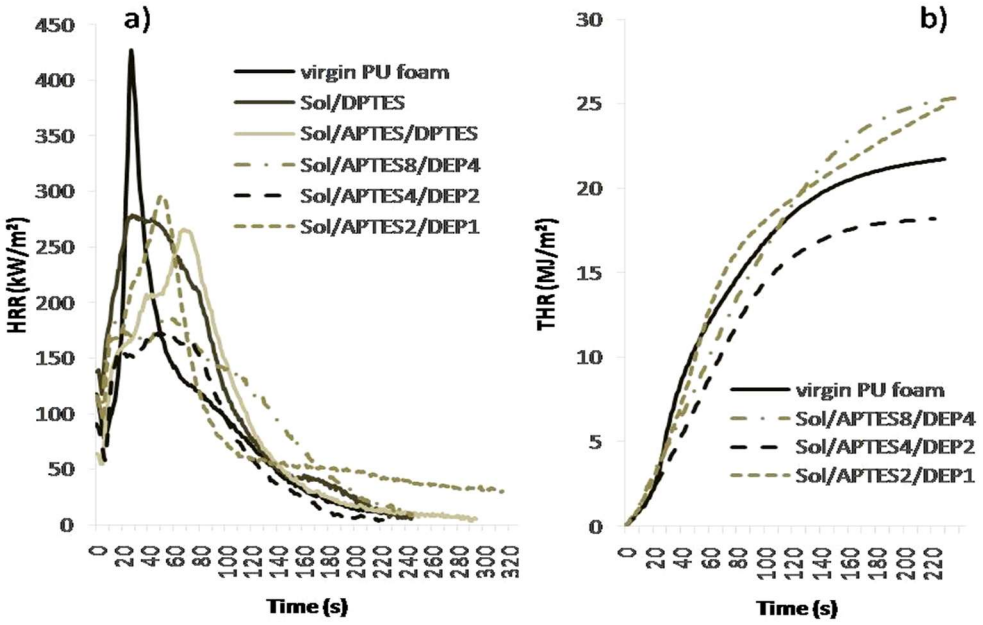

Figure 36: a) HRR curves of virgin FPUF, FPUF treated with Sol/DPTES, Sol/DPTES/APTES, Sol/APTES2/DEP1, Sol/APTES4/DEP2 and Sol/APTES8/DEP4 and b) corresponding THR curves.

The virgin FPUF shows a sharp HRR curve and a high pHRR (425 kW/m^2). Under MLC conditions, virgin FPUF starts to melt and burns very quickly without leaving any char at the end of the experiment. When the phosphorus silica coating, sol/DPTES, is applied on the FPUF, the HRR curve is wider and pHRR is smaller (280 kW/m^{2}compared to 425 kw/m^2, 40% reduction). As already seen in the literature for textile substrates, pure silica coating acts as a thermal insulator and slows down the heat transfers from the surface to the inside of the material, and DPTES builds a good organosilicate coating with improved flame retardant properties. It is also probably the same behavior in the present case for FPUF, which explains the reduction of pHRR. However, in order to avoid the destabilization of the silica network, it has been seen that the DPTES ratio cannot be increased in the sol formulation to improve the flame retardant properties (30% molar ratio DPTES maximum). As a consequence, DPTES was tested in association with a nitrogen monomer (APTES) to improve the FR properties of the coating.[107] In terms of pHRR, there is no difference between Sol/DPTES/APTES and sol/DPTES (pHRR around 280kW/m^2). However, more interestingly, the pHRR is shifted to a higher time when APTES is added. Some hypotheses to explain this behavior are that the release of decomposition products is slowed down with the addition of APTES in addition of DPTES, or that the decomposition products are less flammable in those conditions.

Instead of DPTES, DEP can be used in combination with APTES to improve FR properties. Thus, DPTES was replaced by DEP.[108] When FPUF is coated with Sol/APTES4/DEP2, the MLC tests show a 60%

reduction of pHRR compared to virgin FPUF. The limit amount of APTES and DEP potentially used in such sol is not documented, and thus different amounts of APTES and DEP were tested. However, no better results were obtained. When less FR monomer is used (Sol/APTES2/DEP1), the obtained pHRR is higher (not enough FR properties) as well as when too much is added (extra fuel is given to the flame). The ratio needs to be adjusted to optimize protection of the FPUF. This is confirmed by the THR curves (Figure 36), which show that Sol/APTES4/DEP2 is the only formulation that induces a reduction of the THR compared to virgin FPUF.

In order to better understand the role of each additive, further MLC experiments were carried out (Figure 37). Coatings were made with Sol/DEP4 (without APTES), with APTES8/DEP4 solution without the Sol mixture and with APTES8/DEP4 without a catalyst. It appears that when DEP is not associated with APTES, APTES has almost no FR effect (HRR peak reduced from 425 kW/m^2 to 360 kW/m^2). APTES can potentially form an organosilicate network by itself; however, the results show that it is better to add TEOS/MTES (pHRR at 170 kW/m^2 with TEOS/MTES versus 220 kW/m^2 without TEOS/MTES). When no TEOS/MTES is added to APTES/DEP the coating remains sticky even after several days of drying - the silica network is probably not sufficiently cross-linked or stable to protect the FPUF. Indeed, TEOS/MTES sol even at low concentration creates a stronger silicate coating. In order to confirm this hypothesis, the experiment was carried out with APTES/DEP without any catalyst to have a very low reticulation ratio. There is no FR effect of the coating when the catalyst is not added to the formulation. The coating is not reticulated enough to be stable in the MLC conditions and show FR properties.

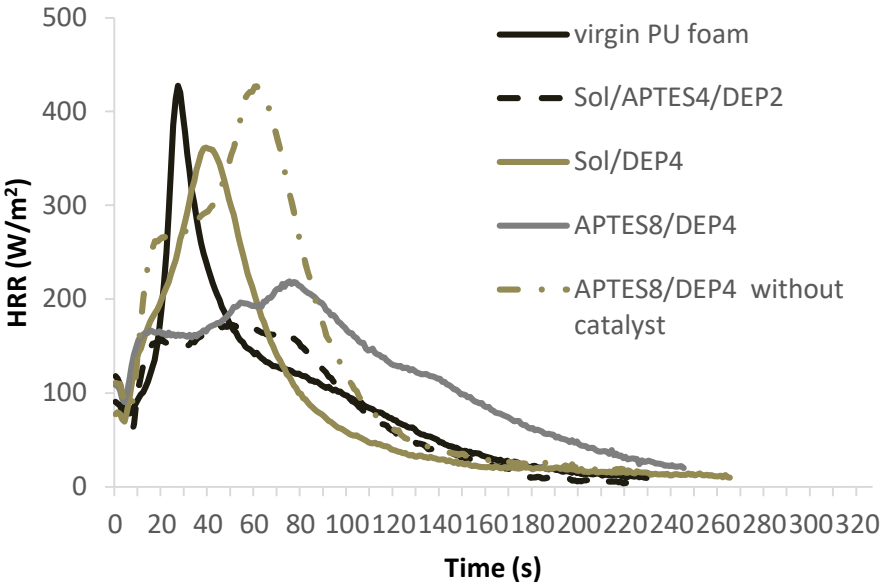

Figure 37: HRR curves of virgin FPUF, FPUF treated with Sol/APTES4/DEP2, Sol/DEP4, APTES8/DEP4 and APTES8/DEP4 without catalyst

- *UL 94 test (Appendix 5):*

In order to test the coated FPUF in a different fire scenario than the MLC, UL94 experiments were carried out. Samples were in the vertical position and a flame is applied 10s twice. Four formulations were tested: Virgin, Sol/DPTES, Sol/APTES4/DEP2 and Sol/APTES8/DEP4on FPUFs. Virgin FPUF melts and drips as soon as the flame is applied and Sol/DPTES FPUF burns entirely; only a small black and brittle char remains after the experiment. FPUFs coated with Sol/APTES4/DEP2 and Sol/APTES8/DEP4 do not burn, even after 30s exposition to the flame. The surface of the FPUF coated with Sol/APTES4/DEP2 becomes black at the flame position and above (Figure 38a) but the flame does not spread and self-extinguishes after removing the burner. The Sol/APTES8/DEP4 coated FPUF does not burn at all (Figure 38b).

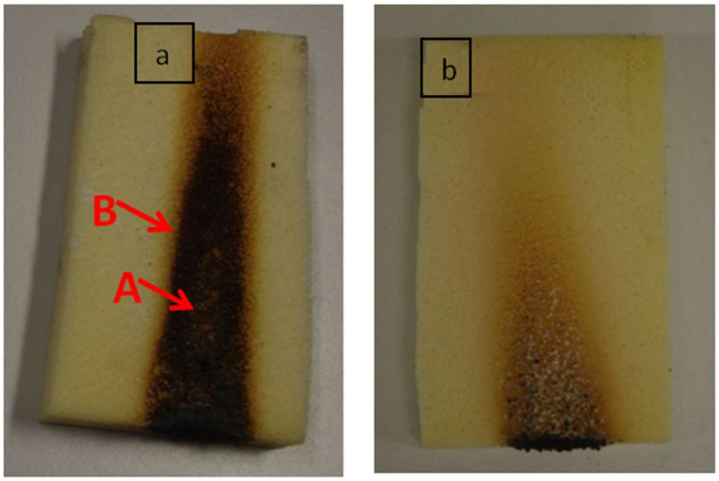

Figure 38: UL94 test results after 30 second flame exposition in vertical position of sample coated with a) Sol/APTES4/DEP2 and b) Sol/APTES8/DEP4. Arrows A and B show the area where SEM analyses were performed.

- *Burner test (Appendix 6):*

Since good behaviour were obtained with UL94 and MLC tests, a burner test with a higher heat flux was used to test the sol-gel treated foam. Ten-by-ten centimeter treated and not treated samples were positioned in front of a 116 kW burner and the behaviour was recorded with a video camera. After few seconds, a hole appears in the untreated sample, however for the treated samples, even if the sample turns black very quickly, the char remains stable for more than 3 minutes under the burner heat flux, no hole appears. Figure 39 shows the resulting samples.

Figure 39: Untreated sample after few seconds in front of a 116 kW burner (left) and sol-gel treated sample after 3 minutes in front of a 116 kW burner (right)

Characterizations were carried out to understand the mechanism of action of the sol-gel coating when temperature rise.

II.2.5. Characterization of the intumescent behaviour

SEM analyses were carried out, after MLC test, on the most promising sample, i.e. the Sol/APTES4/DEP2 sample (Figure 40). A black char remains (whereas no remaining char is obtained for virgin FPUF) and big bubbles are visible even at low magnification. Even if the same kind of chemical systems have already been studied in the literature for cotton,[107,108] this intumescent behavior has not been reported for foams yet. At higher magnification, it is possible to see that the bubbles are in fact composed of a network of small particles. Chemical analysis (Figure 41a) shows the presence of a high amount of Si and O and the presence of C, P, Sn and N. The small particles are probably SiO_2 particles. This hypothesis was confirmed by ATR FTIR analyses. FTIR spectrum (Figure 41b) exhibits a peak at 1070 cm^{-1} ascribed to the Si-O-Si stretching mode (arrow 1) and a band at 800 cm^{-1} due to the Si-O-Si bending vibration (arrow 2), which confirm the presence of the inorganic SiO_2 matrix. Thus, the sol-gel coating is homogenous enough on the whole surface of the FPUF to be able to build a 3D silica structure during burning, preventing the char from collapsing.

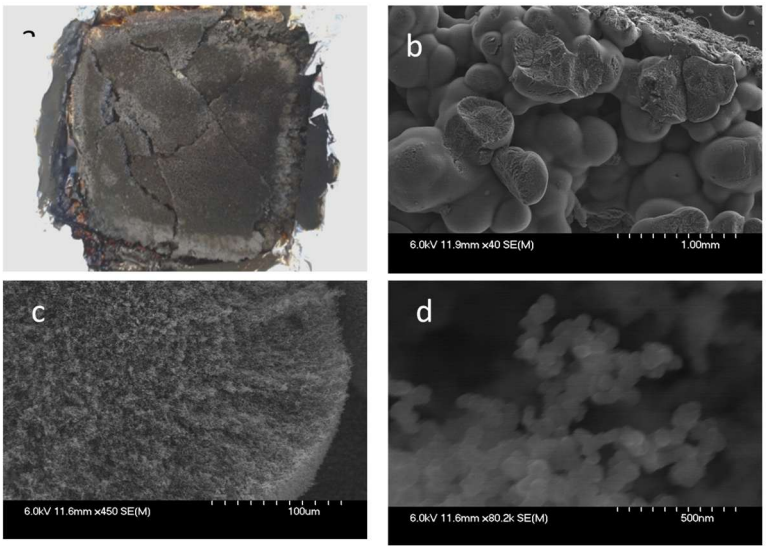

Figure 40: a) Numerical picture of the char of the sample coated with Sol/APTES4/DEP2; b) and c) SEM pictures of the char of the sample coated with Sol/APTES4/DEP2 at low magnification, and d) at high magnification.

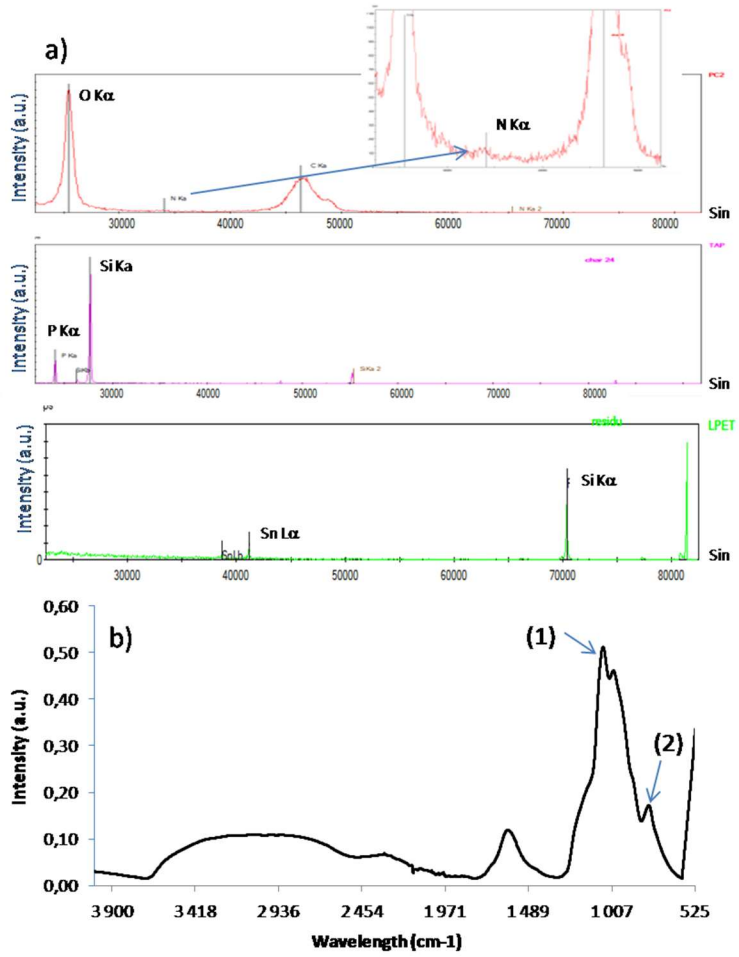

Figure 41: a) Chemical analysis of the FPUF char coated with Sol/APTES4/DEP2 and b) its FTIR spectrum

SEM analyses were also carried out after the UL94 test on the burnt part of the Sol/APTES4/DEP2 coated FPUF. As in MLC experiments, large bubbles are visible on the surface of the FPUF when exposed to the flame. However, Figure 42 shows that these bubbles do not have the same structure in the center of the black burned part of the sample (Figure 38, arrow A) and next to the not degraded part of the sample (Figure 38, arrow B). In the black part (Figure 42 a,b,c), the bubbles correspond to those observed after the MLC tests. Next to the unburnt part of the sample (Figure 42 d,e) the bubbles look smoother; the coating has not been degraded yet. Between the bubbles (arrows in Figure 42d), the open cell structure of the unburned sample is still visible. The bubbles form a layer protecting the underlying part of the sample from the heat and flame.

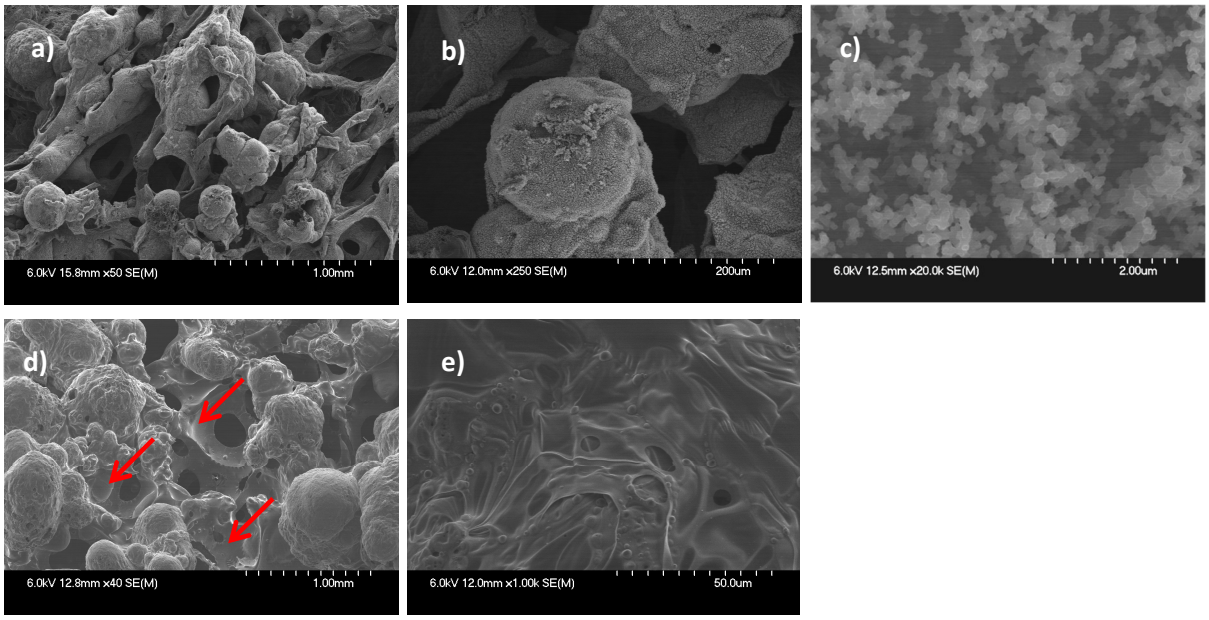

Figure 42: SEM pictures at low and high magnification of a), b) and c) the black burned part of the sample coated with Sol/APTES4/DEP2 and d) and e) next to the unburned part of the sample. The red arrows show the unburned part of the FPUF.

MLC and UL94 experiments demonstrate that a significant residue is built during burning when Sol/APTES/DEP formulations are applied on the FPUF. In terms of MLC and UL94 results, the formulation Sol/APTES4/DEP2 gives the best compromise. Thus, the study will focus on this formulation from now on.

II.2.6. Thermal analysis

TGA experiments were carried out under nitrogen gas flow to quantify the amount of residue and to determine how the FR sol-gel formulations influence the thermal degradation of the FPUF (Figure 43a).

Different formulations were tested: Virgin, Sol and Sol/APTES4/DEP2 coated FPUF. The virgin FPUF degrades in two steps at 230°C and 380°C, as well as all the other treated samples (see Table 10). The thermal decomposition of virgin FPUF and the formation of its various decomposition products are well described in the literature.[109,110] The first stage of decomposition leads to depolymerization reactions, which are characteristic of urethane and substituted urea bond cleavage, to form isocyanate, polyol, primary or secondary amine. The following stages of decomposition are mainly due to subsequent degradation of the remaining polyol chains and dimerization and trimerization of isocyanates. The more significant difference is the weight loss of the samples at the end of the experiment. The virgin FPUF does not exhibit any residue at the end of the TGA and the Sol sample exhibits only 5wt% residue at 800°C.The Sol/APTES4/DEP2 sample shows increased amounts of residue, i.e. 18wt% (see Table 10). This residue is correlated with the weight gain of the coated FPUF after drying.

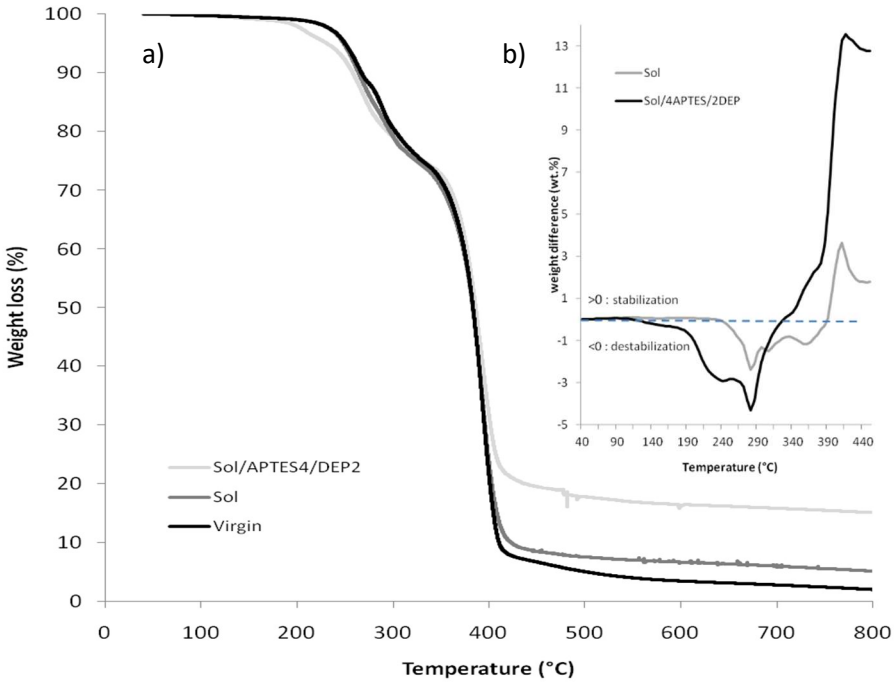

Figure 43: a) TGA analyses of Virgin, Sol and Sol/APTES4/DEP2coated FPUFs and respective weight difference curves between Sol and Sol/APTES4/DEP2 coated FPUFs and virgin FPUF TGA curves (10°C min^{-1}, nitrogen flow).

Table 10: Weight gain of coated FPUF after drying, and degradation temperature of each sample and the corresponding percentage of residue under TGA conditions

Samples	Weight gain after drying (wt%)	Degradation temperature 1 (°C)	Degradation temperature 2 (°C)	Residue (wt%)
Virgin FPUF	/	230	380	0
Sol	14	230	380	5
Sol/APTES4/DEP2	28	190	380	18

When looking at the weight difference curves (Figure 43b), it is noticeable that the destabilization is less significant for the Sol coating; indeed, the two TGA thermograms are almost overlapping. The Sol/APTES4/DEP2FR coating starts to degrade at around 190°C, sooner than the virgin FPUF (230°C). However, after 290°C the stabilization is more significant for the Sol/APTES4/DEP2FR coating. Thus, the protective intumescent behavior probably occurs between 190°C and 290°C.

II.2.7. Study of the chemistry of the network:

Figure 44 reports the FTIR spectra of Sol and Sol/APTES4/DEP2 coatings. One may notice the presence of absorption bands associated with hydrolyzed APTES, illustrated by different vibrational modes related to NH_2, CH_2 and SiO bonds. The spectral region (3700-2800 cm^{-1}) is characterized by two peaks at 3300 cm^{-1} and 3290 cm^{-1} related to the asymmetric and symmetric stretching modes of NH_2, respectively. The broad band ranging from 3700 to 3200 cm^{-1} is associated with the stretching mode of hydrogen in OH bonds, where it is possible to point out the stretching modes of CH_2 at 2932 cm^{-1} and 2883 cm^{-1}. The 1562 cm^{-1} and 1484 cm^{-1} peaks are assigned to the NH_2 deformation modes of the amine groups.

It is also possible to notice the deformation mode of the Si-CH_2 at 1410 cm^{-1} and the asymmetric stretching modes of the Si-O-Si bond at 1130 cm^{-1} and 1044 cm^{-1}. Diethyl phosphite revealed intense absorptions at 980, 1042, 1258 and 2355 cm^{-1}. The peaks at 980 and 1042, 1258 and 2355 cm^{-1} are due to vP–O–C, P=O and P-H stretching vibrations, respectively.

The disappearance of the typical DEP, P=O stretching band[111] at 1250 cm^{-1}, suggests a coordination of all the phosphoryl oxygens to amino-protonated nitrogen via hydrogen bonding (Figure 44), as reported in the literature.[112,113]

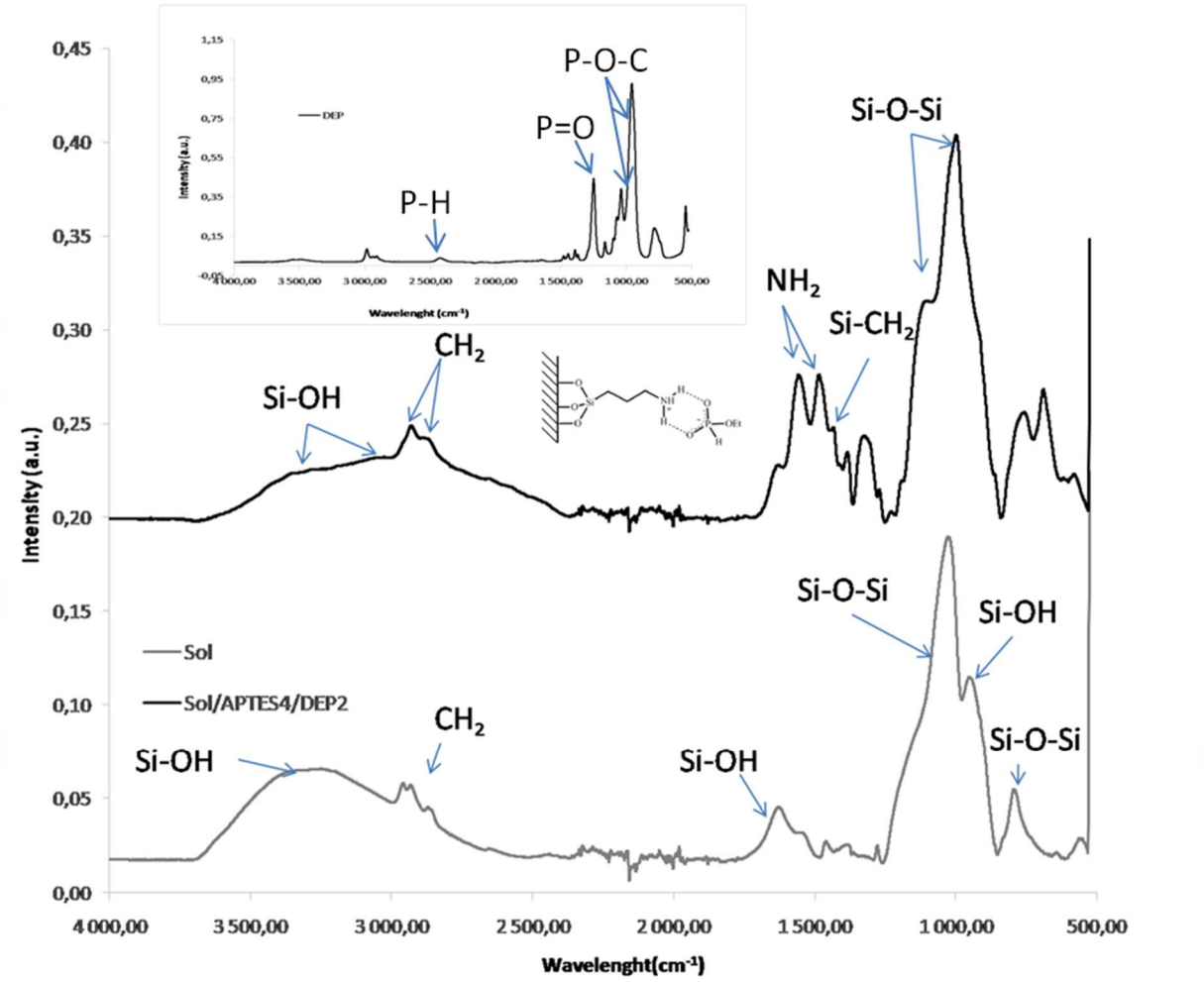

Figure 44: FTIR spectra of Sol and Sol/APTES4/DEP2 films and as received DEP and a scheme of hydrogen bonding between APTES and DEP.

As seen by FTIR, DEP is not covalently linked in the network and can potentially be unstable. That is why the UL94 test was carried out again on treated FPUF samples (Sol/APTES4/DEP2) stored for three months at room temperature in the lab. Similar FR behavior was observed compared to the unaged samples. The FPUF FR foam still self-extinguishes after a 30-second flame exposition. This means that the DEP is well integrated in the Si-O-Si network.

II.2.8. Mechanical properties of the coated foam:

In order to check how the coating affects the mechanical properties of the FPUF, stress/strain experiments were carried out on FPUF. Results (Figure 45) showed that the elastic mechanical property of the FPUF is not lost. Indeed, the characteristic shape of the elastic behavior curve is kept when the coating is applied on the FPUF. However, since the initial slope of the curve is proportional to the elastic

modulus of the tested material, there is a slight increase of the elastic modulus of the coated FPUF compared to virgin FPUF.

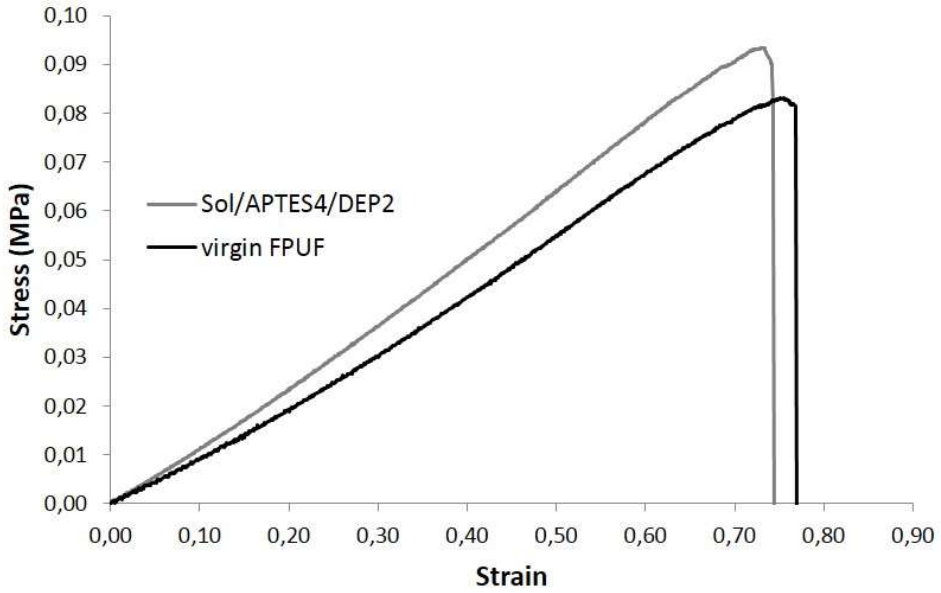

Figure 45 : Stress/Strain curves of virgin FPUF and Sol/APTES4/DEP2 coated FPUF.

SEM analyses were carried out on the broken samples used for the stress/strain experiments in order to verify the stability of the coating after a strong deformation. Figure 46 shows that the cells are still well-defined and that the coating still adheres well to the PU foam; only few cracks are visible on some parts of the sample. Thus, the sol/APTES4/DEP2 coated FPUF seems to keep the mechanical properties of a virgin FPUF even if more tests are necessary to fully characterize its mechanical properties.

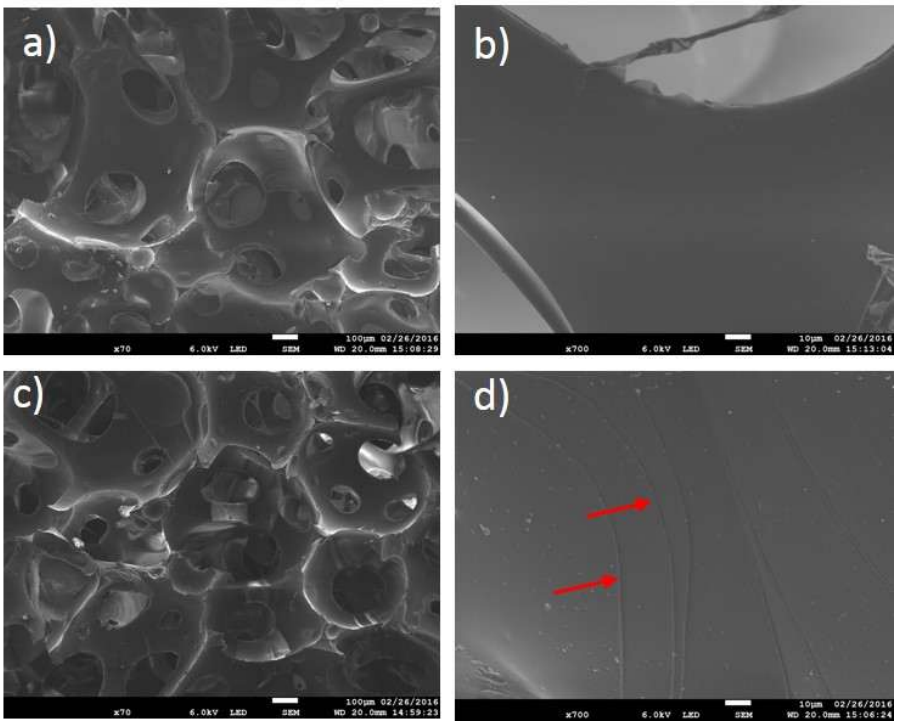

Figure 46 : SEM images of virgin FPUF (a and b) and FPUF coated with Sol/APTES4/DEP2 (c and d) after deformation. A few cracks can be observed on the FPUF coated with Sol/APTES4/DEP2 (red arrows)

As a conclusion, for the first time, sol-gel coatings were applied on FPUF to confer FR properties to FPUF. Several sol gel formulations with different catalysts and FR monomers were selected. A non-acidic route was preferred in order to avoid foam discoloration, and a mixture of TEOS and MTES was applied to minimize crack formation in the coating. Instead of an acidic catalyst, tin II 2 ethylhexanoate catalyst was chosen to reticulate the network. It was noticed that DPTES is not sufficient enough to obtain good FR properties. An association of a proper ratio of APTES with DEP in a TEOS/MTES solution is necessary to achieve self-extinguishment in the UL94 test and 60% HRR peak reduction in the MLC test. The mechanical properties of the foam were checked and seemed not to be altered by the coating. The stable coating has an intumescent behavior and builds a 3D silicon network during burning, slows down the release of degradation products and protects the underlying FPUF from burning.

The full mechanism of action has been investigated in our lab using different analytical tools, such as solid-state NMR, Py-GCMS or TGA FTIR. The following section sums up the mechanism of action.

II.2.9. Study of mechanism of action

The flame retardant mechanism of action has been studied in a published article.[114]

In this paper, both the coating alone and the coated PU foam have been studied using solid state magic angle spinning nuclear magnetic resonance (MAS-NMR), rheology, thermogravimetric analyses coupled with infrared detection (TGA-FTIR), microcalorimetry (MCC), smoke box and Pyrolysis Gas chromatography coupled with mass spectrometry (Py-GCMS), in order to build a FR mechanism of action and understand the phenomena occurring both in the condensed and gas phases during combustion.

Thanks to all the chemical analyses of the condensed and gas phases, a FR mechanism of action can be built (Figure 47).

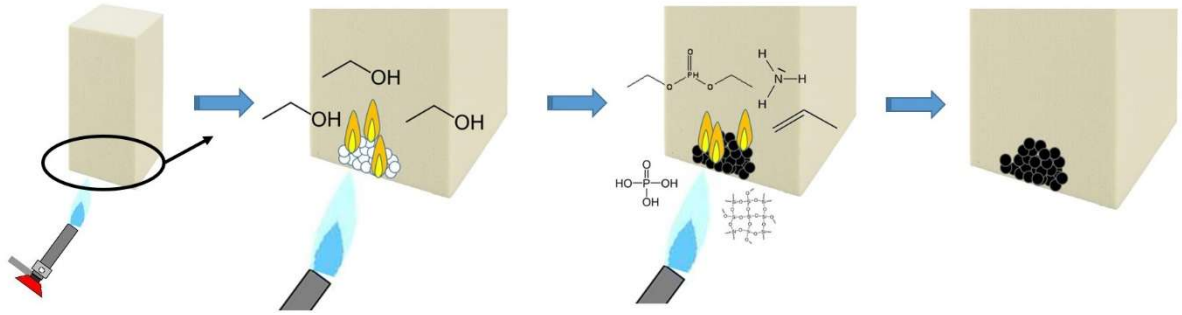

Figure 47: Schema of the mechanism of action of the Sol/4APTES/2DEP FR coating when a flame is applied.

Around 190°C, a first expansion step is observed by rheological test, it is due to the release of ethanol (Py GC-MS, TGA-FTIR). It produces a white and fragile foamy residue. Then, around 380°C, during a second expansion phase, three different gases are released by the coating, i.e. ammonia, propene and non-degraded DEP (Py GC-MS, TGA-FTIR). A black and strong char is obtained. As proven by solid-state NMR, this char is composed of a Si-O-Si network mixed with phosphoric acid and silicophosphate. Thus, in the presence of a heating source, one part of DEP is released in the gas phase and contributes to the flame out, and another part turns into phosphoric acid (charring agent) in the intumescent system, while APTES plays the role of a swelling agent, releasing ammonia in particular. The intumescent char obtained, composed of a foamed glassy layer of Si-O-Si, silicophosphate (Si-O-P) and phosphoric acid, stops the decomposition process (pyrolysis) and prevents the release of flammable gases, essentially cutting off fuel to the flame. Thus, the flame retardant mechanism occurs in the condensed phase for the most part through an intumescent phenomenon. However, as revealed by Py-GCMS and TGA-FTIR analyses, a large quantity of non-degraded DEP and ammonia passes in the gas phase, which participates in the flame retardant effect in the gas phase through chemical mechanisms (radical scavenger mechanisms, dilution effect, modification of the degradation path) and explain the significant decrease of HRR peak during the MCC test.

II.2.10. Conclusion and Outlooks:

A sol-gel coating containing APTES and DEP was developed as an effective flame retardant for PU foam. The mechanism was studied by carrying out solid state NMR, rheometry, Py-GCMS, PCFC, TGA-FTIR and smoke box test. Solid state NMR showed that the residue was mainly a Si-O-Si and Si-O-P network mixed with phosphoric acid. An intrinsic intumescent phenomenon of the sol-gel coating was evidenced by rheological tests. Py-GCMS shows the release of ethanol, propene, ammonia and non-degraded DEP, which was confirmed by TGA-FTIR. The mechanism of action was determined to be a combination of a condense phase and a chemical mechanism. Indeed, the degradation of the coating gives all the ingredients for the intumescent phenomenon to occur, phosphoric acid (charring agent), ammonia (swelling agent) and DEP (acid source). When the coating is applied on PU foam, it builds a strong residue that slows down and even prevents the gas of degradation from being released in the gas phase, which protects the underlying PU foam from the flame. DEP and ammonia are released in the gas phase and can also act as a flame suppressant through chemical mechanisms (radical scavengers, dilution, modification of the degradation pathways). The formulated sol-gel coating is flame retardant by itself and does not require the PU foam substrate to be intumescent. It can potentially be applied on any substrate. However, the coating is very thin and must penetrate the 3D network to be effective, thus, such coating could not be effective on closed-cell foams. Thicker coating needs to be investigated.

Since the formulated sol-gel coating is intumescent and transparent, it has also been tested on wood. It demonstrated some efficiency and it is the subject of a paper published in 2022,[77] however, wood is exposed to weathering and the sol-gel, as it is, is susceptible to humidity. Thus, it necessitates further work to formulate a sol-gel resistant to humidity or find a suitable topcoat to deposit on its surface, in order for the sol-gel coating to be usable to flame retard wood. For some applications, glass also needs to be fire resistant, thus, it would be interesting to test the formulated transparent sol-gel coating on glass. Preliminary researches were conducted with Saint Gobain Research (two master students), which still need further investigation.

It has been seen in this section that sol-gel coatings containing diethylphosphite can protect efficiently polyurethane foam from fire. However, diethylphosphite can cause allergic skin reaction and produce toxic fumes during combustion. Thus, alternative additives were screened to replace diethylphosphite, it was the subject of a paper published in 2020.[115] Screened flame retardant molecules were phosphorus donors of low toxicity compared to halogenated compound, such as resorcinol bis (diphenyl phosphate) (RDP) and bisphenol A bis(diphenyl phosphate) (BDP), and bio-based additives with potential flame

retardant functional groups such as chitosan. UL94 and mass loss calorimeter (MLC) tests were used to examine the reaction to fire of the different formulations. It was noticed that RDP is as effective as diethylphosphite to produce flame retardant coatings. Chitosan can also be used, but it needs to be mixed with RDP to provide acceptable flame retardant properties. Mechanical tests show that the addition of chitosan in the coatings increases the young modulus of the FPUF foam and decreases the tensile strength. Due to time constrain, other green alternatives could not be tested (such as starch, lignin, cyclodextrin or tannic and phytic acids) but still need to be investigated.

II.3. Closed-cells foams: thick coatings

II.3.1 Introduction

When designing cars, manufacturers strive to reduce their weight, to reduce fuel consumption and achieve better energy efficiency. It is now estimated that about 15% of a vehicle's total weight is made up by plastic parts. Expanded polypropylene (EPP) is a very lightweight plastic material that fits into limited space and makes it possible to achieve the appropriate shape defined by the client's specifications. This makes it easier to obtain properly designed products, headrests and arm rests, for example. However, the use of electrical cars is rapidly increasing and with the transition to electric transportation comes a new challenge: vehicles with lithium-ion batteries are dangerous when they catch fire. New regulations are on the way for material used in such electric vehicles. Thus, in this section, the deposition of a flame retardant coating on expanded polypropylene is discussed. Contrary to open-cell foams, coating applied to closed-cell foams cannot penetrate through the network, the coating stayed on top. Thicker coating than sol-gel coatings are investigated.

A second problematic is also assessed in this section, PP is a hydrophobic polymer and poor adhesion is obtained on PP, thus the increase of the adhesion of PP is investigated through plasma treatment to increase its adhesion.

II.3.2. Expended polypropylene coatings

This section investigates the coating of EPP materials. ARPRO 5142 EPP is supplied by JSP, France (Figure 48).

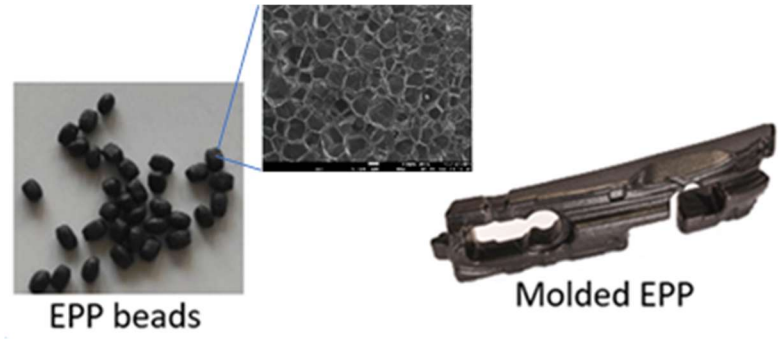

Figure 48: EPP beads with the corresponding SEM image of the closed cells inside (left) and a molded EPP piece (right)

The work consists in applying a flame retardant coating directly on top of the molded EPP pieces. To do so, it is mandatory to ensure good adhesion (high surface energy and wettability) of the coating on EPP. Since PP is hydrophobic and has poor adhesion properties (low surface energy and poor wettability), a study was carried out to increase the hydrophilicity of EPP and to enhance the adhesion of the coating. For this purpose, a low-pressure plasma treatment was carried out prior to coating. In a second step, coating formulations were optimized. The goal was to reach a V0 classification at UL-94 (self-extinguishment after 10s exposition to a flame, sample in vertical position).

II.3.2.1 EPP functionalization: Low pressure plasma treatment

The literature related to surface treatments of PP can be translated to EPP. As PP, EPP is an inert material, without functional and polar groups. PP has low surface energy (30-32mN/m), poor wettability (contact angle between 85-100°) preventing good adhesion of coatings on its surface[116,117]. Therefore, the surface of the EPP must be treated and functionalized to increase its surface energy and wettability, and thus facilitate adhesion of further flame retardant coatings. Several methods to modify the PP surface have been described in the literature, including acidic treatments, flaming treatment and plasma treatments[118,119,120,121,122]. In this study low-pressure cold plasma (Appendix 7) has been chosen for surface treatment to achieve the lowest contact angle possible with the lowest treatment time and power. The equipment used is a low-pressure cold plasma CD 1200 manufactured by Europlasma, equipped with a CESAR radio frequency power generator from Advanced Energy (13,56 MHz). The functionalization was characterized via wettability by measuring the water contact angle. A Krüss DSA25 drop shape analyzer with an AD4021 software is used with a water drop of 0.5µL. Raw EPP is hydrophobic, showing contact angles of 85±2° (Figure 49).

The objective is to decrease the water contact angle of PP to the minimum value possible without degrading the polymer. First, the influence of the different plasma parameters (treatment time, plasma power, argon flow) was studied and is described hereafter. This study was carried out in order to

identify the working range of each parameter, in order to carry out an experimental design to optimize the treatment.

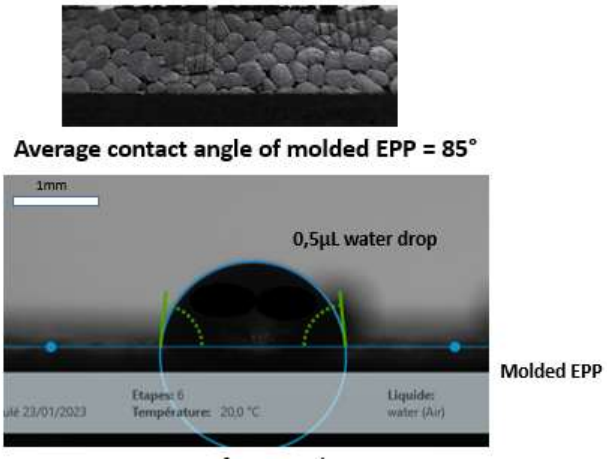

Figure 49: Contact angles of molded EPP

- Influence of time of treatment

The time of treatment is an important parameter for industrial applications. Here, the plasma power, the gas flow and the composition of the gas (pure Argon) were fixed and only the time of treatment was changed. The power was fixed at 100W for a gas flow of 20sccm and the time varied between 50s and 210s. A decrease in water contact angle was observed when increasing the time. It was observed that doubling the time from 50s (test 5) to 100s (test 6) halved the contact angle, showing a decrease from 60° to 30° (Table 11). However, a time limit is reached, the treatment time in test 7 was doubled compared to test 6, but the contact angle only decreased of 4° (contact angle 26°) (Table 11).

Table 11: Contact angle of the EPP beads and molded EPP at several times of treatment

Substrate	N° of test	Time (s)	Flow (sccm) 100% Ar	Power (W)	Contact angle (°)	Standard deviation (°)
Molded EPP bar	5	50	20	100	60	2
	6	100			30	2
	7	210			26	1

- Influence of power

Here, the time of treatment and flow are fixed and the parameter studied is the power. The increase of power leads to a decrease of the contact angle and a limit is observed. For a fixed time (100s) and

flow (20sccm), the power increase reduces the water contact angle from 51° to 30° [test 13: **51°** (60W) > test 14: **34°** (80W) >test 7: **30°** (100W)] (Table 12).

Table 12 Influence of the power on the water contact angle of EPP beads and molded EPP

Substrate	N° of test	Time (s)	Flow (sccm) 100% Ar	Power (W)	Contact angle (°)	Standard deviation (°)
Molded EPP bar	13	100	20	60	51	3
	14			80	34	2
	7			100	30	2

- Influence of gas flow

Finally, the influence of the argon flow was looked at. The other parameters (treatment time and power) were fixed. It is observed that the contact angle decreases when the Ar flow decreases. Good results were obtained at 20 sccm, as a consequence, there is no need to increase the flow above this value.

For fixed time parameters of 100s and power of 100W, a decrease of the flow from 30 to 20sccm leads to a decrease in the contact angle of 12° (from 42° to 30°) (*Table 13*).

Table 13: Influence of the gas flow on the water contact angle of EPP

Substrat	N° of test	Time (s)	Flow (sccm) 100% Ar	Power (W)	Contact angle (°)	Standard deviation (°)
Molded EPP bar	18	100	30	100	42	4
	7		20		30	1

To conclude, increasing the time of treatment and power as well as decreasing the gas flow leads to a decrease in water contact angle (Figure 50). The parameters all depend on each other. The different parameters for EPP were optimized at 100s time, 20sccm gas flow (100% Ar) and 100W power. It allowed to reach a contact angle of 30°. These parameters were thus chosen for the study.

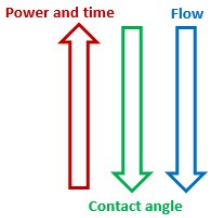

Figure 50: Summary diagram: Influence of the parameters on the water contact angle

- Ageing of the plasma treatment

After treatment, samples were let to age under ambient conditions and water contact angle was measured regularly to evaluate potential ageing of the treatment. Different treatment conditions were performed to study the influence of one parameter on the ageing of the treatment. After 15min ageing, the contact angle increases by about 5° regardless the treatment parameters, after 45min a further increase of about 5° is measured (*Table 14*). The contact angle reaches only 43° after 2h and 50° after 24h.

Table 14: Water contact angle over the time according to different parameters

	Plasma settings				**Contact angle (°)**				
Substrate	**N° of test**	**Time (s)**	**Flow 100% Ar (sccm)**	**Power (W)**	**t=0**	**t=15min**	**t=45min**	**t=2h**	**t=24h**
Molded EPP	**6**	100	20	100	30	36	38	43	50

The contact angle increases over time due to several modifications on the surface. Indeed, during the plasma treatment, free radicals are formed on the surface that can recombine and rearrange over time. In addition, the adhesion of the surface is increased, but can also be easily and quickly polluted[123]. In conclusion, ageing is quick and the coating must be applied within the first 15min.

- Conclusion

The influence of the main plasma parameters, such as time, power and gas flow rate were evaluated. It has been established that when the power and time increase and the flow decreases, the contact angle decreases. The parameters for the EPP were selected, 210s/20sccm/150W allowing to reach a contact angle of 30°. However, it was also shown that the treatment is not permanent: regardless the parameters, after 15min, the contact angle starts to increase and after 24h it reaches 50° for EPP.

After plasma treatment optimization, the objective was to coat the plasma treated pieces with a FR coating to obtain V0 rating at UL-94

II.3.2.2 Flame-retardant coatings

In this section, the application of a flame retardant coating on plasma treated EPP bars are studied. The influence of the plasma treatment on the adhesion of the coating is studied as well as the choice of the type of coating.

- Influence of the plasma treatment on the adhesion of a coating

In order to validate the good adhesion of the resin or coating on the surface, SEM observations of the coated samples were performed.

SEM characterisations were carried out on the coated EPP. The EPP was spray-coated with an intumescent coating (IFR) formulated from PVA Emultex FR 797 resin. After drying, the sample was cut for analysis. The coating applied on the surface of EPP without plasma treatment showed no adhesion, it peeled off (Figure 51). On the other hand, for the plasma treated samples with a contact angle of 30°, the coating was well adherent despite the asperities of the surface (Figure 51).

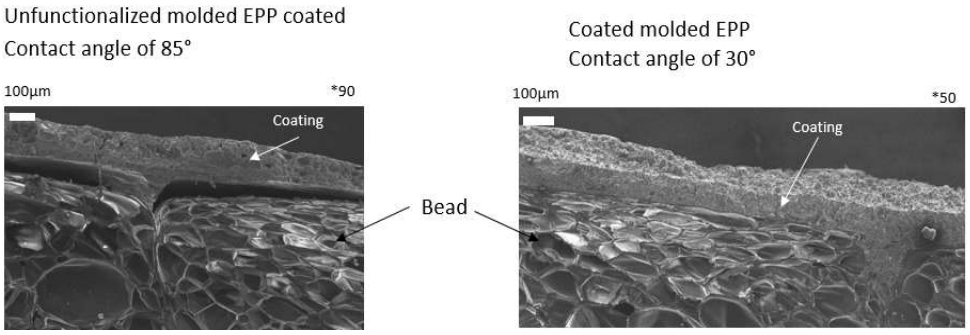

Figure 51: SEM of un-treated (left) with poor adhesion and pretreated coated molded EPP (right) with good adhesion

As assumed from the beginning of the study, functionalization of the surface by plasma treatment is mandatory to ensure good adhesion of the coatings.

- Coating application and choice of the FR resin

In this section, two different commercial resins formulated with FR additives and a commercial FR varnish are compared in terms of adhesion on the plasma treated surfaces.

The application of the coating can be performed using dip coating or spray coating depending on the difficulty to optimize the spray process. Dip coating is a quick and easy way to coat the EPP bars,

however, it makes it difficult to control the mass applied and the coating thickness, thus spraying was preferred to coat the EPP bars.

As seen in literature, different resins or varnishes can be used to obtain FR coatings. PVA (polyvinylacetate) resins (Emultex FR 728 and 797) were chosen as they are easy to formulate to obtain flame retardant properties and similar formulated resins already proved their efficiency on PP.[124] The FR 728 enables the formation of a quick char, which is particularly adapted for UL-94 test, since a quick FR reaction is needed to pass the test. In contrast, the FR 797 provides a slower char formation but it has a higher water resistance. The glass transition temperature (Tg) of the FR 797 (Tg=13°C) is lower than the one of the FR 728 (Tg=23°C), which provides a higher flexibility to the resulting coating. These two resins were compared to a commercial varnish, the Pyroplast HW 100, an intumescent flame retardant (IFR) coating designed to protect wood. The Pyroplast is already formulated, transparent and has also shown effective flame retardant properties for PP.[125] Moreover, a top coat to protect the Pyroplast against climate constraints also exists on the market.

The two PVA based resins chosen, i.e. FR 728 and FR 797 were formulated as shown in Table 15 in order to have a ratio of 50% solution (resin and water) and 50% FR with a ratio 3/1/1/1 of APP/DPER/Mel/TiO_2 respectively.[124] The EPP bars (100s, 20sccm, 100W for a contact angle of 30°) were then sprayed with formulated coating (FR 728 (1), FR 797 (1) or Pyroplast, diluted or not) and dried.

Table 15: Formulated resins and Pyroplast diluted or not

Formulation	FR 728 (%)	FR 797 (%)	Water (%)	Pyroplast HW 100	AP 422 (%)	DPER (%)	Melamine (%)	TiO_2 (%)
FR 728 (1)	25		25		25.1	8.3	8.3	8.3
FR 797 (1)		25	25		25.1	8.3	8.3	8.3
Pyroplast HW 100				100				
Diluted Pyroplast HW 100			50	50				

The coating adhesion was assessed by SEM (not shown). A good adhesion of the resin is obtained when the FR 797 (1) formulation is applied on the plasma treated EPP bar. No cracks are visible on the surface (Figure 52).

Figure 52: Coated molded EPP with FR 797 (1)

The application of FR 728 (1) coating on the EPP bars shows a lot of surface cracks (Figure 53). which confirms the poorer adhesion of FR 728 (1) compared to FR 797 (1) due to the lack of flexibility of the resin FR 728.

Figure 53: Coated molded EPP with FR 728 (1)

The undiluted Pyroplast has a good adhesion on the molded EPP bars, no crack is observed (Figure 54).

Figure 54: Coated EPP with undiluted Pyroplast

To perform fire tests, the FR 797 resin was chosen as it shows the best adhesion and is more scrub resistant. Furthermore, according to the supplier's information, FR 797 is more water resistant than the FR 728. The FR 797 resin will be compared to the Pyroplast varnish, which also showed good adhesion at low thickness and has a smoother appearance, no particles are observed on the surface.

II.3.2.3 Fire test on EPP pieces

The final section refers to the objective of obtaining a V0 rating at UL-94 test with the coated EPP bars. The tests were carried out on 125mm*13mm*10mm bars for both. Table 16 sums up the results obtained at UL-94 test.

Both the coated EPP bars (1) and coated EPP bars (2) achieved a V0 rating without drop, even if the FR coating applied on EPP bars (2) is thinner than (1) and contains less FR (Table 16). However, for the EPP bars (2bis) the amount of coating is even more decreased (from 60wt% down to 35wt%) and a V2/NR result is obtained, a limit is thus reached between 35wt% and 60wt%. The coated EPP bars with Pyroplast obtained a V0 rating for an amount above 18wt%. The Pyroplast showed better flame retardant properties on EPP than formulated FR 797, since less coating is needed to have similar results.

Since the coated bars achieved a V0 result (Figure 55), it proves that the coating provides a good fire protection.

Table 16: UL-94 test results

Coated samples	**Formulation**						**Increase of mass (%)**	**Thickness (µm)**	**Rating**
	FR 797	**Water**	**AP 422**	**DPER**	**MEL**	**TiO_2**			
EPP bars (1)	25	25	25.1	8.3	8.3	8.3	~130	≤200	**V0**
EPP bars (2)	36.25	36.25	15	5	5	2.5	~60	≤100	**V0**
EPP bars (2bis)							~35	≤60	V2/NR
EPP bars (A)	**Pyroplast**						~70	≤100	**V0**
EPP beads (A)							~33 After molding	≤100 before molding	NR
EPP bars (B)							~30	≤60	**V0**

Figure 55: Coated sample with formulated FR 797 after UL-94 test

II.3.3. Conclusion and outlooks

The objective was to obtain a V0 rating at UL-94 by coating EPP pieces (UL-94 bar) with IFR coatings. Several steps are necessary, the first one is to perform a plasma treatment at the surface of EPP to increase the adhesion properties of EPP. Indeed, EPP has a low surface energy, leading to poor coating adhesion. EPP bars were functionalized using a low-pressure cold plasma and the results were characterized by measuring the water contact angle. Using 100s /20sccm (100%Ar) / 100W plasma conditions, a contact angle of 30° was obtained. The flexibility and scrub resistance of the resins allowed a very good adhesion of the coatings on the surface. The varnish has also a good adhesion.

FR properties of the obtained bars were tested following vertical UL-94 test. V0 results were obtained using 100µm thickness of Emultex FR 797 coating containing fewer FR and with a 60µm thickness of Pyroplast coating. The coatings are effective when applied on EPP pieces.

Pyroplast is highly effective, but it appears to be sensitive to water. A top coat exists on the market for Pyroplast, the next step would be to test this topcoat and verify that it does not alter the fire properties of the coated materials.
The IFR system (APP/DPER/Melamine/TiO2) used in Emultex FR 797 resin also showed its effectiveness when applied on EPP. However, compare to the thickness of the coating, the particle size needs to be reduced for the coating to be more homogeneous.

II.4. Conclusion and outlooks:

When talking about coating foams, it is important to specify which kind of foam has to be coated. Indeed, foams can be divided into different groups, such as open-cell and closed-cell foams, which both of them are also divided into two under groups; flexible and rigid foams. Each of these groups can not be coated with the same kind of coating. Rigid closed-cell foams can be coated with a thick layer without compromising the mechanical property of the foam, but it is not the case when talking about flexible foams, which will lose their flexible property when coated with a thick coating. In this

chapter, two cases have been studied, open-cell flexible foam and rigid closed-cell foam. A sol-gel thin FR coating has been developed to coat the entire 3D network of the open-cell flexible PU foam. The coating is adherent to the foam and is not affected by mechanical constraint that can be applied to the foam. The coating allows to reach a V0 rating at UL94. The mechanism of action has been elucidated, the intumescent properties of the coating allow to quickly protect the underlayers of the foam and a gas phase action of the additives help to extinguish the flame.

In the case of a rigid closed-cell foam a thicker coating is necessary to protect the foam since the coating can not penetrate the foam network. In the case studied, the polymer used was PP. Contrary to PU, PP is apolar and has no adhesion property. Thus, a surface pretreatment is need before coating deposition. Two different commercially available coating were studied. V0 rating were obtained at UL94 test using 100µm thickness of Emultex FR 797 coating containing few FR and with only 60µm thickness of Pyroplast coating.

As a conclusion, it is possible to find FR coatings for foams, however, it has to be adapted to the foam used. The major issue, not studied here, is the ageing of the coatings under real end use conditions, especially humidity. Mechanical properties and fire-retardant properties can also be altered after scratching the coating. Thus, the study of the coating stability under different ageing conditions still needs to be carried out.

Chapter III: Inherent fire-resistant foams

The topic developed in this chapter was carried out in the frame of a collaboration with BASF, Germany (PhD S. Laidioui 2022) and led to one paper currently being revised.

III.1. Introduction

As seen in chapter 1, effective FR additives exist and can be incorporated in foams during synthesis. However, these additives can be controversial and it is difficult to find alternative to these existing FR. Thus, new synthetic foams are developed for building application. Those systems do not require the use of FR additives but are intrinsically flame retardant. Phenolic foams are foams belonging to this category.

On the contrary to PU or PS foams, phenolic foams (PF) stand out in the construction industry due to their excellent fire resistance, low production of smoke and toxic gases, and high thermal stability. These properties make them ideal materials for applications requiring strong fire protection (wall, roof, pipe or ventilation insulation). Moreover, these foams offer a unique combination of lightness, structural rigidity and thermal insulation, making them ideal for a variety of applications. Their closed-cell structure and ability to preserve their mechanical properties at elevated temperatures make them the preferred choice in environments where fire safety is paramount.

Phenolic foams are processed from phenolic resins. Phenolic resins are synthetic polymers produced by polycondensation between phenol (P) and formaldehyde (F) (Figure 56). When using an acid catalyst with a molar ratio F/P lower than 1, novolac-type resins are obtained. They are only reactive in the presence of catalysts, and therefore they are considered relatively stable. Under basic conditions and with a molar ratio of (F/P) higher than 1, resol-type resins are obtained. This family is reactive due to the presence of methylol groups at the end of the chains and can be cured once exposed to temperature. Hence, precautions have to be taken for the storage of these resins in order to avoid their polymerization. Resol-type resins are used for foam processing[126,127].

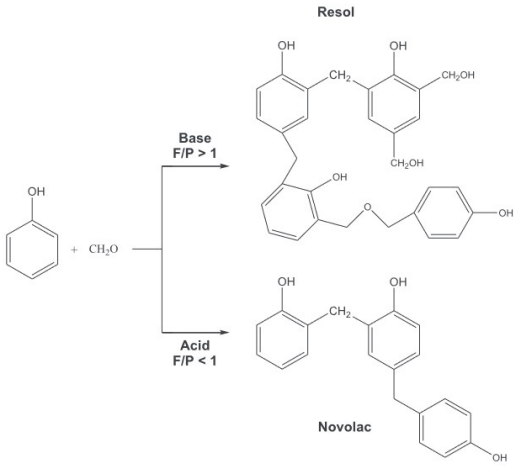

Figure 56: Novolac-type and resol-type phenolic resins

Phenolic foam can be manufactured using various methods, including mechanical, physical, or chemical approaches[128,129]. The formation of phenolic foam involves a delicate balance between two competing mechanisms: the expansion and the curing of the resin, which can occur simultaneously. Key parameters influencing this process include the viscosity and reactivity of the phenolic resin.

Viscosity plays a crucial role in phenolic foam formation. Low viscosity is essential for effective mixing. Conversely, higher viscosity can influence cell growth and potentially prevent coalescence. Researchers have found that viscosity can affect structural aspects of phenolic foam, such as cell wall thickness, cell size, and the formation of macro-defects. Excessively high viscosity can impede foam expansion, leading to a density higher than desired[127,130,131]. Reactivity is another critical factor that controls the curing and foaming processes of phenolic foam. If reactivity is too high, foams may cure before complete foaming is achieved, resulting in unexpected final foam densities. Other resin parameters, including pH, water and monomer content, can influence the ultimate foam properties[126,132].

The preparation of phenolic foam involves the use of an emulsifier, blowing agent, catalyst, and optionally, various additives. Among these additives, plasticizers, fibers[133], micro- or nanoparticles[134] are frequently utilized. Emulsifiers play a pivotal role in controlling the quality and properties of phenolic foam. They facilitate the creation of a stable and homogeneous oil-in-water emulsion between the blowing agent and phenolic resin, which governs foam cell characteristics. Emulsifiers must maintain emulsion stability throughout the foaming process, considering factors like temperature variations, viscosity changes, and phase transition of the blowing agent. Tween 80, a non-ionic surfactant also known as polyethylene glycol sorbitan monooleate, is a commonly used emulsifier. Silicon oil has been explored as an alternative to Tween 80. In some cases, a combination of two emulsifiers (one in water and one in oil) is employed to achieve the desired emulsion quality.

These emulsifiers facilitate the opening of foam cells, help break resin droplets encapsulating the blowing agent, and promote the creation of an interconnected open-cell pore structure[131,135,136,137,138,139,140].

Blowing agents play a crucial role in inducing the foaming of phenolic resin through either physical or chemical processes. Carbon dioxide (CO_2) can be formed in situ as a blowing agent, particularly in resol foam formulations. Its formation can result from the reaction of carbonates with an acid catalyst or the reaction of water with a small amount of isocyanate. Blowing agents that operate through physical processes are typically low-boiling-point liquids (such as n-pentane) that evaporate as the temperature rises due to heating. This evaporation induces the formation of gas bubbles within the phenolic matrix[127,141,142].

Some studies have investigated the fire behavior of these foams, two fire tests are mainly used to evaluate it, the Limit Oxygen Index (LOI) (ISO 458) and the cone calorimeter test. With LOI values between 28.5vol.-% and 52vol.-%, PF is classified as a non-flammable material[135]. However, as rigid thermosetting foams, PF foams suffer from inherent brittleness, which limits their broader use. To overcome this limitation, it is crucial to enhance their mechanical properties while maintaining their fire-retardant qualities. A key factor in this improvement is the foam's density as mechanical properties improve with increasing density, which directly affects its durability and ease of handling. In the construction and transportation sectors, optimizing this density can not only enhance the performance of PF foams but also expand their use by improving their ease of manipulation.

The objective of this study is to find a process to formulate low density PF (around 20 kg/m^3) with good mechanical and flame retardant properties. In this work the density of PF will be studied as a function of the curing agent (HCl or H_2SO_4) concentration and as a function of the temperature of the foaming process. The up-scaling of the process is also studied to see the impact of the size of the mold on PF density. The aim is to obtain a foam with the lowest density without compromising the mechanical and fire-resistant properties.

III.2. Foaming process

A commercial phenolic resin is used as a precursor to obtain phenolic foam, it is a Prefere 91 5353V industrial resol resin provided by Prefere phenolics. The foaming process is a complex process where several parameters need to be adjusted. Indeed, the phenolic foaming process has to be carried out above room temperature to insure a quick reticulation of the resin after foaming. However, the temperature needs to be adjusted for the viscosity of the system to be controlled and avoid that the

resin reticulates before foaming Then, it is possible to vary the mass percentage of each of the reagents (blowing agent, emulsifier and acid), their nature, as well as the order in which they are added to the mix. The mix step is also an important step, as it is possible to vary the type of mixing process (by hand, magnetic bar or blender) the temperature and the mixing time. The last parameters concern the curing; it can be carried out using an oven, a microwave or an oil bath. The heating temperature and duration are crucial to obtain the desired foam.

The process used in this work is described in Figure 57. It involves a foaming carried out in an oil bath heated up between 80 and 130°C. First, the resol resin (5g) is mixed and homogenized with the blowing agent, the n-pentane (0.5g), using Tween-80 (0.6g) at ambient temperature. Then the curing agent (2.5g) is added to the mixture. The mixing of the different additives is performed in the mold placed in the oil bath, at a temperature above room temperature. The foaming can take from 10 minutes up to 1 hour depending on the size of the sample. Finally, an annealing step is carried out in an oven between 80 and 150°C, overnight.

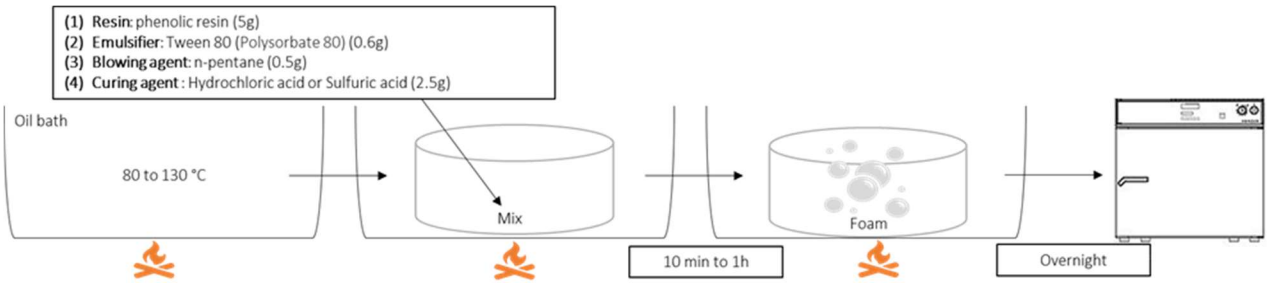

Figure 57: Foaming process

III.3. Process and formulation optimization

The phenolic foaming process has to be carried out above room temperature but not too high to avoid reticulation before foaming. TG analysis has been carried out to better know the onset of reticulation. Figure 58 shows the TG analysis of the resol resin used to determine the working temperature range for the foaming process. The results show that there is a mass loss of 20% from 80 to 200°C,

corresponding to the cross-linking of the resin[143], so it is preferable to work at the beginning of this step. Three oil bath temperatures were investigated to reticulate the PF foam i.e., 80, 100 and 130°C.

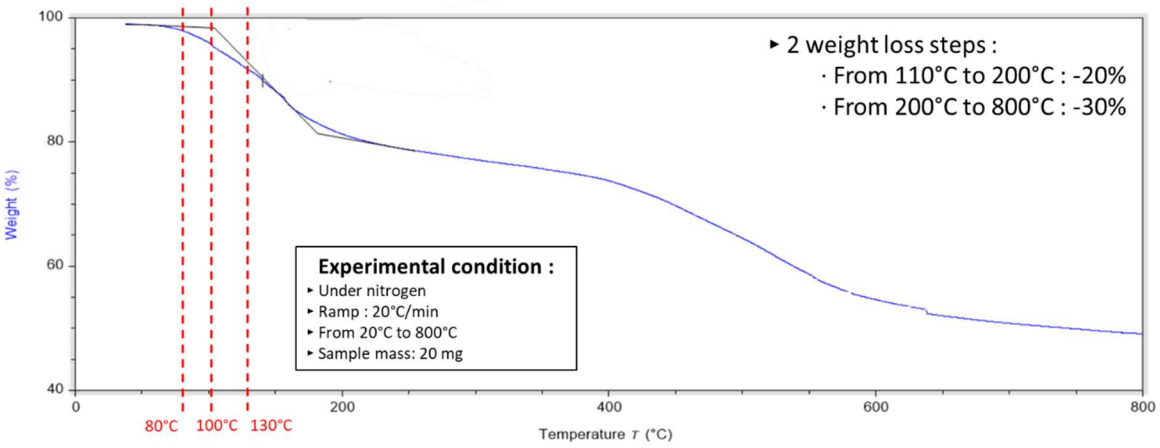

Figure 58: TGA of Resol resin

Table 17 shows the density of the obtained foam in function of HCl concentration and temperature of the oil bath. The concentration of HCl has been varied from 2 to 37wt% for three temperatures of the oil bath (80, 100 and 130°C). The results show that no foam is obtained at 2% of HCl for all the temperatures. The concentration of HCl is not high enough for the reticulation to occur, the foam collapses after the release of all the n-pentane. In the contrary, for 27%wt of HCl and above, the concentration of HCl is too high and the resin reticulates too quickly to obtain a foam. At 130°C, no foaming occurs at 17%wt and 22%wt of HCl. Reticulation of the resin occurs too quickly at 130°C, temperature increases the reticulation rate.

When the temperature and HCl concentration are adequate, a foam is obtained and density can be measured. Results in table 17 show that the density decreases with temperature, from around 120 kg/m^3 at 80°C down to 55 kg/m^3 at 130°C. HCl concentration seems to not affect the density of the foam.

Table 17: Density(kg/m^3) of the foams versus HCl concentration and oil bath temperature

[HCl] (%wt) / T°oil bath	2%	7%	12%	17%	22%	27%	32%	37%
80°C	X	124	107	126	120	X	X	X
100°C	X	99	80	109	117	X	X	X
130°C	X	58	55	X	X	X	X	X

Since the goal is to obtain a low-density foam, it would be interesting to work at 130°C, however, as Figure 59 shows, when the temperature increases, the homogeneity of the foam cell size decreases. The temperature of the foaming process is thus a compromise between density and cell homogeneity. It is to note that the foaming phenomenon occurs only up to the oil bath top level and then stops, whatever the conditions.

The chosen working temperature is 100°C, because the obtain foam density is lower than for formulations at 80°C, but the cell sizes of the foam are more homogeneous than those formulated at 130°C. Since HCl concentration seems to have a limited impact on the foam reticulation, HCl concentration is kept as low as possible (7%).

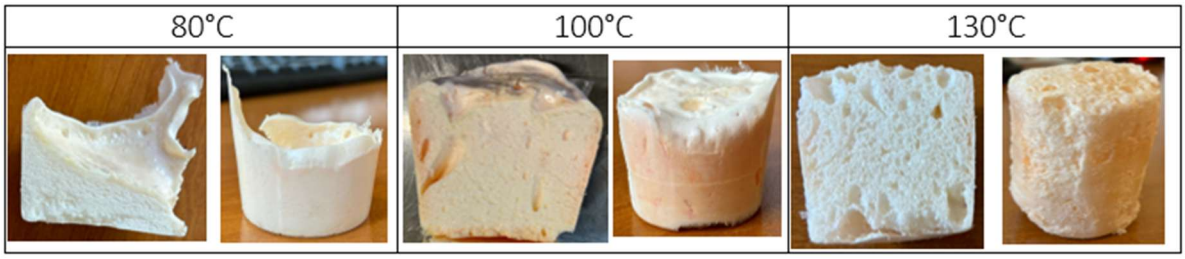

Figure 59: images of PF formulated at 80, 100 and 130°,C with 7% HCl

After having screened different foaming formulations at different temperature process conditions, the up-scaling of the process is investigated with the chosen conditions (7% HCl, 100°C oil-bath temperature).

The goal of the up-scaling step is to obtain larger samples and characterize their mechanical and fire-retardant properties. This approach also allows us to determine whether the homogeneity of the cell size and the density is maintained when larger samples are produced. A stainless-steel mold is used and the quantity of resin, emulsifier and curing agent is multiplied by 5. It was noticed that with only 5 time more blowing agent, foaming does not occur, thus 10 times more blowing agent is added.

Figure 60 presents the foam obtained with 7%wt HCl at 100°C. The produced foam is homogeneous and its density is about 22 kg/m^3. The density is much lower that when the foam is produced in a smaller mold. In the case of the stainless-steel mold, the foaming continues to occur even higher than the oil bath top level, which was not the case in the small polymer mold. Since the larger mold is made of stainless steel, the whole mold is at 100°C and the foam can expend more, which is not the case for the polymer mold. Polymers, such as PP, are not good thermal conductor. If the temperature in the mold decreases above the oil bath level, it induces a decrease of the temperature of the resin and thus a change in viscosity, which is not adapted anymore for the foaming to occur.

Figure 60: PF formulated with 7%wt HCl

Thus, the up-scaling does not alter the foam homogeneity, but density can be lowered by changing the material of the mold to favor the foaming growth.

After the foaming process, the foam is annealed in an oven overnight to end the reticulation process and evaporate water and other reaction products. Figure 61 shows the density variation of the foam (7% HCl, 100°C) at different annealing temperatures overnight. Before the annealing step, the obtained density is around 20 kg/m^3. The results show that at 60°C, the density of the foam remains unchanged, but at 80°C and above the density decreases down to 15 kg/m^3. A major change in color is also observed at 150°C, which may indicate foam degradation.

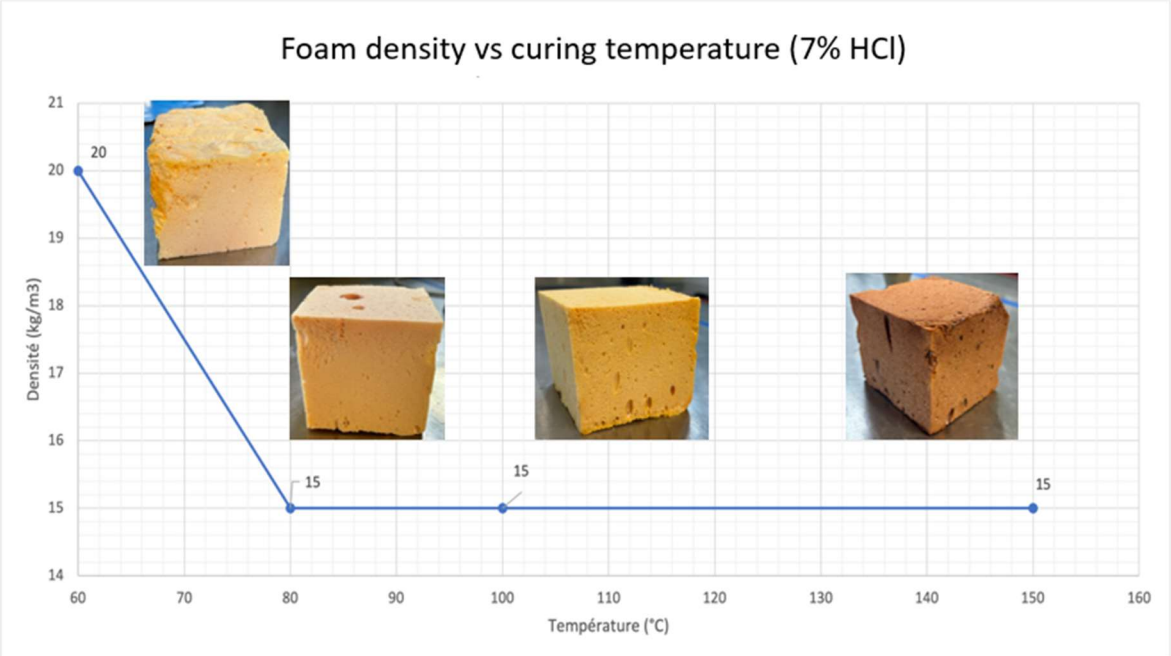

Figure 61: Density of PF (7% HCl) versus curing temperature

Homogeneous phenolic foams are obtained using HCl as curing agent and using 100°C as working temperature for foaming. When up-scaling the process, density as low as 15 kg/m^2 can be obtained. It has been seen that the oil bath temperature as well as the mold type and the conditioning temperature of the foam influence the density of the PF foam, but not the concentration of the curing agent used (HCl). The concentration of the curing agent did not seem to influence the density of the foam. In the litterature, other type of acid curing agent can be used, such as sulfuric acid. Thus, sulfuric acid has been tryied with the same foaming process as for HCl.

The conditions used for foaming are the same as for HCl, but 18% of H_2SO_4 was used to obtain the same pH value in the mixture. Figure 62 shows a foam obtained after annealing the foam at 80°C overnight. The obtained density is 16 kg/m^3. As a conclusion, changing the curing agent does not seem to influence significantly the density of the formulated foam. However, the foam formulated with H_2SO_4 seems more brittle than when produced with HCl, thus, the mechanical properties of the foams were characterized.

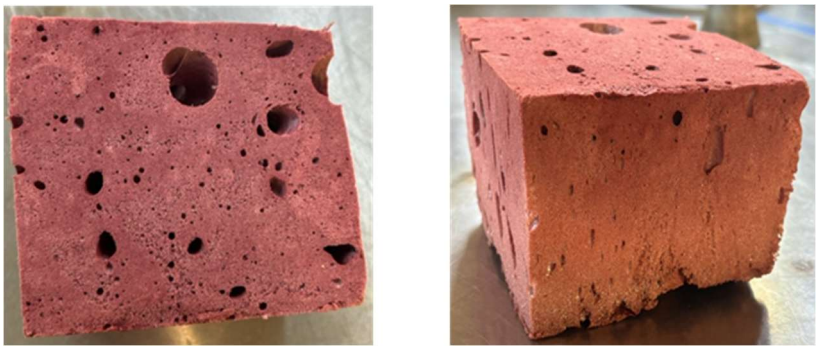

Figure 62: PF formulated with 18%wt H_2SO_4

III.4. Characterization of mechanical and fire properties

III.4.1. Effect of the curing agent on the compressive strength

To study the mechanical properties obtained for the different foams, compressive tests were carried out on the foams with and without annealing step (Figure 63). The foams produced with 7% HCl and 18% H_2SO_4 at 100°C are studied.

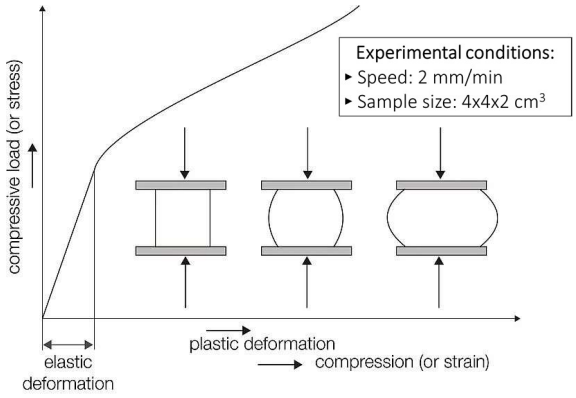

Figure 63: Compression experiments carried out on phenolic foams

Figure 64 shows that the Young's modulus has a slight tendency to increase with increasing the annealing temperature (20% variation between the sample treated at 60°C, 0,75 Pa and 150°C, 1.0 Pa). The PF formulated with H_2SO_4 has a lower young's modulus than PF with HCl (60°C, 0.3 Pa and 80%, 0.26 Pa). The yield points, which are the transition point between the elastic and plastic areas, are presented in Figure 65. It shows that the PF sample with HCl annealed at 80°C has an average yield point of 0.70 MPa, which is higher than samples annealed at 60, 100 and 150°C, which have average breaking points of 0.50, 0.51 and 0.42 MPa, respectively. This can be explained by the fact that before 80°C, there is still foaming by-products to evaporate or that the reticulation is not yet completed, which would make defects in the structure. After 80°C, the decrease of the yield point can be due to a too high reticulation rate, which would make the structure more brittle. For PF formulated with H_2SO_4, the Yield point is lower than for PF foams formulated with HCl. It is to note that for H_2SO_4, the Yield point is higher for the sample annealed at 80°C (0.23 MPa) than that at 60°C, 0.18MPa.

To conclude on the mechanical properties of the formulated samples, PF foams obtained with HCl have higher Young's moduli and Yield points than those obtained with H_2SO_4, leading to the conclusion that PF foams formulated with HCl have better mechanical properties.

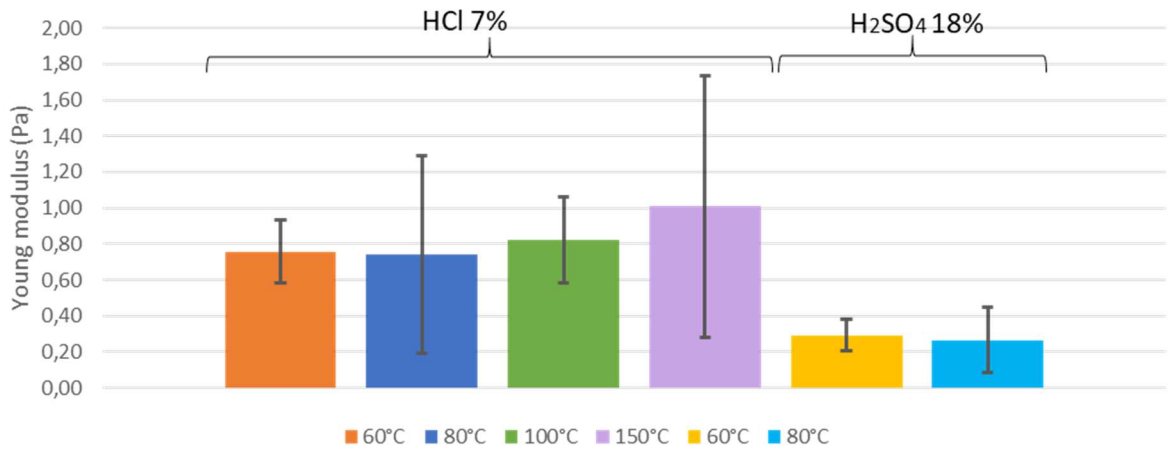

Figure 64: Young modulus diagram of PF 7%wt and H_2SO_4 18%wt at different curing temperature.

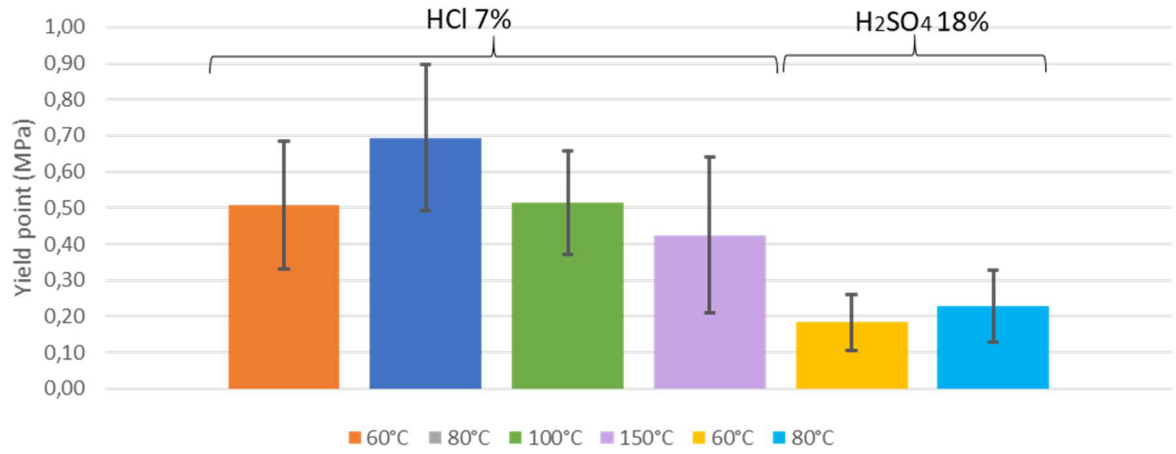

Figure 65: Yield point diagram of PF 7%wt and H2SO4 18%wt at different curing temperature

Since the curing agent can influence the mechanical of the formulated foam, the fire properties were also investigated.

III.4.2. Effects of the curing agent on the fire properties

In term of flame retardancy properties, the same foams (7% HCl and H_2SO_4 18%, 100°C with and without annealing step) were tested under the condition of the mass loss cone test. Figure 66 shows the impact of the annealing temperature on the peak of heat released rate (pHRR) and on the total heat release rate (THR). The sample conditioned at 60°C has an average pHRR of 54 kW/m^2, which is the highest pHRR compared to the sample conditioned at 80, 100 and 150°C, 34, 43 and 32 kW/m^2, respectively for PF formulated with HCl. This can be explained by the fact that, by products of the foaming mixture (such as n-pentane or formaldehyde), has not yet completely evaporated. For PF

obtained with H_2SO_4, pHRR values are lower than those obtained for foams formulated with HCl. For samples annealed at 60 and 80°C, the pHRR values obtained are 42 and 21 kW/m^2, respectively. As for those with HCl, there is a decrease of the pHRR between the samples annealed at 60 and 80°C.

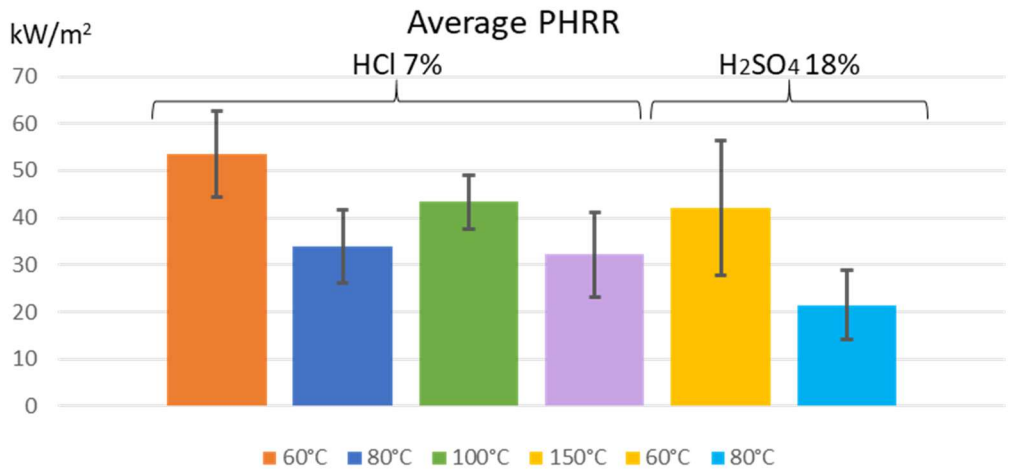

Figure 66: Average pHRR diagram of PF 7%wt and H_2SO_4 18%wt at different curing temperature

For the THR in Figure 67, the same trend is observed, a decrease of the THR is observed with the increase of annealing temperature. For PF formulated with HCl, the maximum is for the sample annealed at 60°C with an average THR of 4500 kW/m^2, and a minimum for the sample at 150°C, with an average THR of 1800kW/m^2. For PF formulated with H_2SO_4, the average of the THR also decreases as the annealing temperature rises from 60 to 80°C, with values of 3700 and 1600 kJ/m^2, respectively. Those values are lower than those obtained for foams produced with HCl.

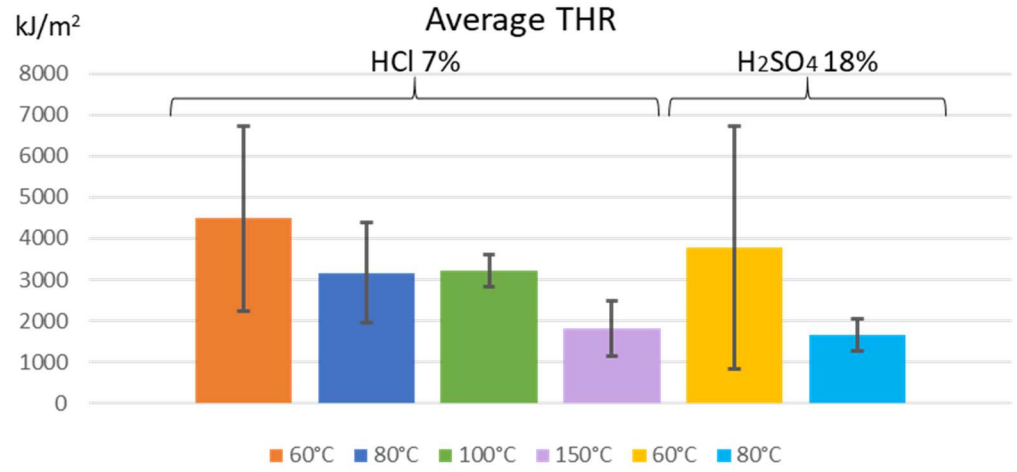

Figure 67: Average THR diagram of PF 7%wt and H_2SO_4 18%wt at different curing temperature

During mass loss cone experiments, gas analyses were carried out using an Antaris FTIR spectrometer (Figure 68). Regardless of the acid used for the formulation (HCl or H_2SO_4), the spectra obtained display similar features. In all cases, characteristic bands can be assigned to gaseous products such as carbon dioxide (CO_2) and carbon monoxide (CO). CO_2 is evidenced by the intense asymmetric stretching band ν(C=O) around 2340 cm^{-1}, while CO is identified by its stretching vibration ν(C≡O) observed at 2100–2140 cm^{-1}. In addition, a sharp band observed at 3650 cm^{-1} corresponds to free O–H stretching, characteristic of hydroxyl groups generated during the oxidative degradation of the phenolic network. Two finer bands located at 1430 and 1460 cm^{-1} can be assigned respectively to aromatic ring vibrations or carboxylate modes (~1430 cm^{-1}), and to CH_2 bending vibrations (~1460 cm^{-1}). The recurrence of these signals, regardless of the acid used, demonstrates that the decomposition mechanism during MLC systematically leads to the release of CO_2 and CO, together with the formation of hydroxyl functionalities and aromatic residues, confirming that the acid type does not significantly influence the products detected by FTIR.

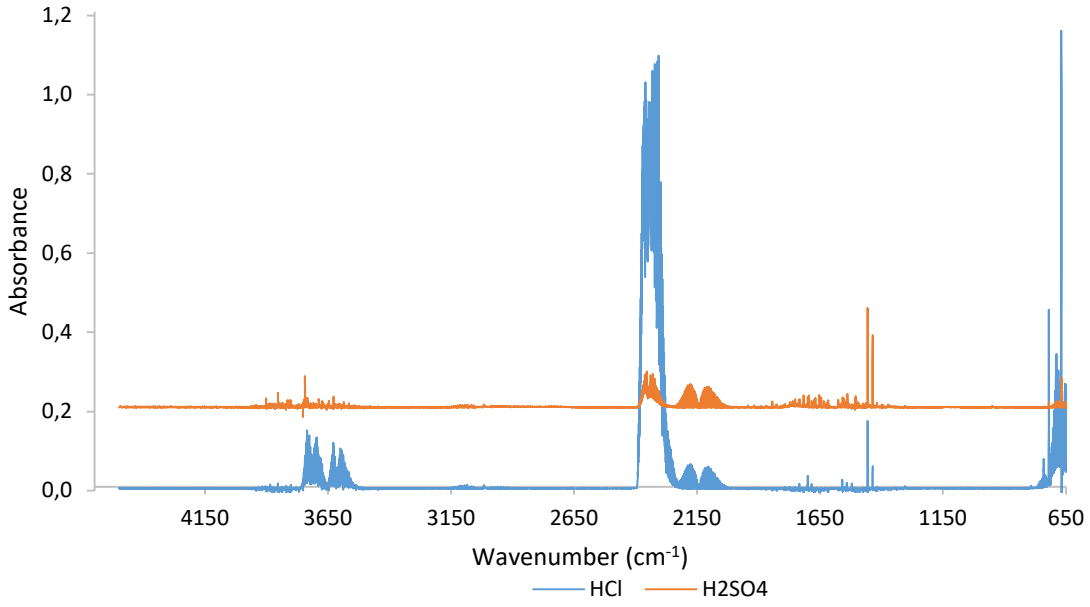

Figure 68 FTIR spectra of the gas released during MLC test for PFF

As a conclusion, the mechanical and fire properties are influenced by the curing agent. the foams obtained with HCl have better mechanical properties than those using H_2SO_4, but H_2SO_4 foams have better flame retardant properties than those obtained with HCl. No difference is observed in terms of gas released, only CO, CO_2 and H_2O are observed. Compare to conventional rigid polyurethane or polyisocyanurate foams, phenolic foams have lower gas release production and toxicity, indeed no HCN is released.

III.4.3. SEM observation of PF formulated with HCl and H_2SO_4

- **Comparison of PF foams formulated with HCl and H_2SO_4**

Figure 69 and Figure 70 show the SEM images of the foam obtained with HCl and H_2SO_4. The closed-cell structures are quite similar between the two foams, however at high magnification, the surface of the cell-walls seems less smooth for the foam with H_2SO_4.

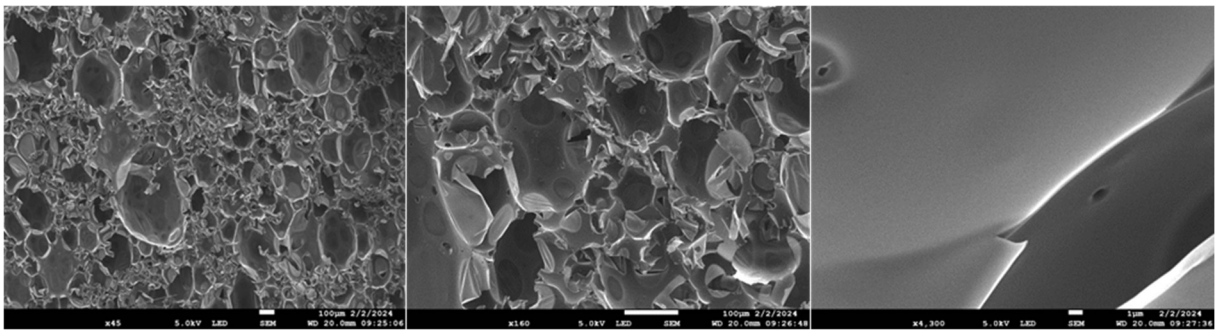

Figure 69: SEM images of PF with 7wt% HCl annealed at 80°C

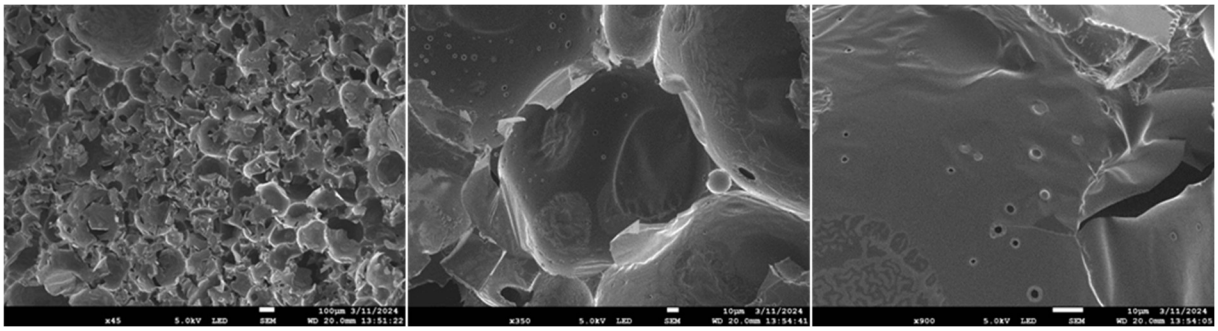

Figure 70: SEM images of PF with 18wt% H_2SO_4 annealed at 80°C

- **SEM observation of a PF char**

The SEM images presented in Figure 69 and Figure 70 show the foam before fire test. The foam has a closed-cell structure of fairly homogeneous size. Figure 71 shows a cross section of the upper part of the foam after mass loss cone test. The lower part (which was not exposed to the heat flow) has a structure similar to Figure 69 with closed-cells, but the upper part, which has directly faced the heat flow has an open cell structure. The heat degrades the foam starting by the cell walls leading to a structure corresponding to an open-cell structure foam at the top of the degraded foam.

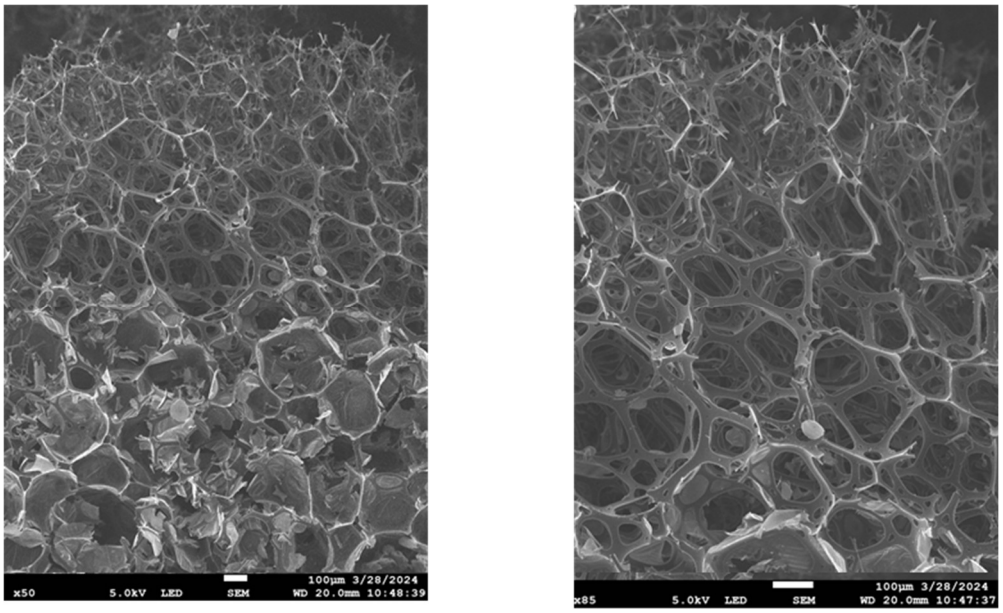

Figure 71: SEM images of PF char cross section formulated with HCl

III.5. Conclusion and outlooks

Phenolic foams were produced by mixing a resol phenolic resin with a blowing agent (n-pentane), an emulsifier (Tween 80) and a curing agent (HCl or H_2SO_4). The goal is to produce a foam with the lowest density for an end-use in the building industry. A screening of different formulations and process conditions was performed and showed that an oil bath at 100°C, an annealing step at 80°C overnight can produce a foam with a density as low as 15 kg/m^2. Mechanical and flame retardant properties were characterized. Excellent flame retardant properties were obtained. Since the concentration of the curing agent did not seem to affect the density of the foam, it has been decided to change the curing agent with H_2SO_4 instead of HCl. The variation of the curing agent did not change the obtained density either, however the mechanical and flame retardant properties were affected compared to those obtained with HCl. Indeed, the foams obtained with HCl have better mechanical properties than those using H_2SO_4, but H_2SO_4 foams have better flame retardant properties than those obtained with HCl. Thus, for the same density, the type of acid has an influence on the properties of the obtained foams.

Literature on inherent flame retardant foams is rather poor and lots of work still have to be done on the subject. As it has been shown with phenolic foams, the flame retardant properties are excellent, unfortunately, the mechanical properties need to be adjusted. The study is still ongoing in our lab and since it has been shown that acid can play a role on the obtained mechanical properties, other acid will be tested, such as paratoluene sulfonic acid or mixtures of acids, including phosphoric acid. Rheological

studies versus temperature also need to be conducted to try to correlate the viscosity of the medium with the swelling rate. The goal is to find the ideal pH were the foam swells homogeneously but not too much, to avoid defects, which strongly affect the mechanical properties.

Thermal conductivity measurements are also to be performed to determine how the foaming process affect the thermal properties of the foam. Due to closed-cell morphology, phenolic foams have adapted thermal conductivity properties for insulative building materials.

General conclusion and outlooks:

After an engineer diploma from ENSAIT, Roubaix, in 2001, I started a PhD at the University of Lille in the fields of polymer nanocomposites and flame retardancy, for which I spend 2.5 years at NIST, Gaithersburg, USA. During that time, I became the contact to perform transmission electronic microscopy for the group and carried out an international volunteering contract with the French ambassy. I graduated in 2005, and started a one-year CNRS post-doctoral position in Montpellier, at the Charles Gerhart Institute in the field of silica ionogels. In 2006, due to my knowledge in the electronic microscopy field, I began as a post-doctoral researcher at ENSCL, Villeneuve d'Ascq. I was recruited to organize the arrival of a new electron probe microanalyser at ENSCL and to be the dedicated engineer.

The arrival of the EPMA at ENSCL in 2007 was a success and the apparatus is still in use up to now. However, the EPMA is aging and starts to get obsolete, thus, I have the project to renew it in the frame of the CPER CHEMACT, with FEDER fundings. The project (1 500 000 €), supported by Chevreul Institute, is to get the latest generation of electron microprobes, equipped with a SXES (Soft X-ray emission spectrometer) detectors, which would provide access to elemental imaging at the nanometer scale and to elemental detection starting from lithium (Li) element. A key advantage of the device lies in the quantitative determination of light elements (Li, Be, B, C, N, O) or trace elements in the 100 ppm range, providing rapid access to quantitative elemental analysis and multi-scale X-ray mapping from the extreme surface to the core of the material. This project is part of a highly competitive context for the development of innovative materials, where characterization techniques must keep pace with the evolution of new materials production processes. Since the "Hauts-de-France" region is fully committed to innovation through the establishment of battery production and recycling plants, a microprobe enabling the detection and mapping of lithium in materials would be fully integrated into the socio-economic landscape of the "Hauts-de-France" region. It will break down a number of technological barriers. The electron microprobe will be installed at the Institut Chevreul, on the campus of the University of Lille, and will be part of the electron microscopy facility. This electron microprobe will be the only one north of Paris and the second in France equipped with an SXES detector, enabling the University of Lille to strengthen the relevance of its research resources and remain a leading and attractive international research cluster.

In parallel to this responsibility, I continued my research in the field of flame retardancy of polymers. I became a permanent research engineer at ENSCL, in 2008 and I am still doing research in the field of

flame retardancy of polymers. During the whole period of academic research, I was able to collaborate with numerous persons and publish more than 90 papers (11 as first author) and be part of more than 90 oral communications (14 as first author). I already co-supervised two PhD students and I am also currently co-supervising two PhD students in the frame of flame retardant polymer materials. My technical competences and knowledge acquired all these years allowed me to become technical adviser of two facilities, one in the evaluation of flame retardant materials (FIRE RESIST) and the other one on the analysis and elaboration of materials (PACTE). These facilities are a great help to develop and characterize materials. FIRE RESIST allows the development and the use of the fire test benches necessary in research projects.

We are currently working on the development of a small wood crib test to evaluate the efficiency of fire extinguishing foams and we will be working soon on a new small-scale test to evaluate long term fire retardants.

Even if my research has changed over time, it has always been in the field of flame retardancy. I was able to specialize my knowledge in the field of flame retardancy of polymer foams. FR foams are not new, many FR, as well as paths to flame retard foams exist to comply with the current fire regulation for foams. Unfortunately, very effective FR are controversial because of their toxicity for the environment or human health. Thus, researches are still ongoing to find efficient FR alternatives. There are different ways to flame retard foams, 1) in the bulk with FR, 2) with a surface coating or 3) by manufacturing inherently flame-retardant foams. These three routes were investigated in this manuscript. It has been shown with model phosphorous FR in PU and PIR foam that some phosphorous molecules can be more efficient that the one commercially available. To be effective, the main mode of action of the FR needs to occur in the gas phase, rather than in the condense phase. Indeed, even if the action is effective in the condense phase, by promoting charring, the effect is not strong enough to improve the FR properties of the foam efficiently. It should also be noted that the FR do not have the same action depending on the polymer in which it is incorporated. Between PIR and PUR systems, PIR systems always have a better fire behavior because, in addition to potential gas phase activity of the FR, the creation of a stronger and more resistant char during combustion was noticed. In this study, the quantity of FR used was based on having the same quantity of phosphorus in the different systems, to compare the PIR and PUR systems between them. However, it would have been interesting to modify the amount of the FR considered as the most efficient and try to mix it with other FR with different modes of action to try to promote synergistic effects. Moreover, the test used for the study is the MLC test. It is easy to use for rapid screening of a large quantity of formulations. However, in the

foam industry, FR foams have to pass the SBI test to have a fire classification. The SBI test allows to measure the flame propagation (in addition to the pHRR and THR), which is a parameter that the MLC cannot evaluate. Unfortunately, the SBI test is a large-scale test necessitating a large amount of material, it is not available for research and development purpose. Thus, in order to overcome this problem and to allow further investigation of the formulated foams, a mini SBI test has been developed in our lab, but due to time constraint the different system could not be evaluated with the new mini SBI bench test.

Foam can also be coated to be FR, but it is important to take into account the kind of foam to be coated. The coating has to be adapted to the foam used. In this manuscript, an open-cell flexible foam and a rigid closed-cell foam were studied. A thin sol-gel FR coating has been developed to coat the entire 3D network of the open-cell flexible PU foam. The coating is adherent to the foam and is not affected by mechanical constraint that can be applied to the foam. The coating allows to reach a V0 rating at UL94. The mechanism of action has been elucidated, the intumescent properties of the coating allow to quickly protect the underlayers of the foam and a gas phase action of the additives help to extinguish the flame. A thicker coating is necessary to protect the rigid closed-cell foam since the coating can not penetrate the foam network. In the case studied, the polymer used was PP. Contrary to PU, PP is apolar and has no adhesion property. Thus, a surface pretreatment is needed before coating deposition. Two different commercially available coatings were studied. V0 ratings were obtained at UL94 test using 100µm thickness of Emultex FR 797 coating containing few FR and with only 60µm thickness of Pyroplast varnish. The major issue with coating foams, which is not studied in this work, is the ageing of the coatings under real end-use conditions. Mechanical properties and fire-retardant properties can be altered after scratching the coating or because of humidity and lose their properties.

The choice of manufacturing inherently FR foams can be a good alternative to bulk FR or coatings because there is less toxicity problems due to FR or ageing problems. FR properties of phenolic foam are excellent; however, the mechanical properties of the formulated foams need to be well characterized and compromise needs to be found between fire and mechanical properties. There are only few publications in the field of inherently FR foam, but a lot of industrial patents. Lots of work still can be done, such as changing the acid catalyst or study the addition of plasticizer. It is to note that the industrial cost to formulate this kind of foams still remains higher than regular PU foam.

These studies allowed me to work in the flame retardancy of synthetic polymer foams for building and upholstered applications and to gain expertise in the wide field of flame retardant foams. Foams can be flame retarded following different ways, however the driving force of the current research to flame retard foam is the reduction of toxicity for human health and the environment.

Thus, my researches topics are now oriented toward finding more sustainable ways to flame retard foams, finding greener FR compatible with foaming process or coating application process, and synthesizing FR foams without flame retardant.

My involvement in the research of more sustainable FR enables me to collaborate with PIHM lab of INRAE to ***develop a new research topic on ecofriendly firefighting foams against wild fire****. The project is a PhD project (Helena Arellano) funded by ADEME and the "Hauts de France" region.*

Forest fires are a growing concern in France and around the world, due to the current climate change. Each fire season, wildfires devastate some 350 million hectares of forest worldwide, an area six times the size of France. The objective of the project is to develop new, efficient Class A foams, based on renewable biomass resources and with low environmental impact. Class A foams have two special features to consider. The first is that formulations must be obtained from a so-called concentrated formula, which is mixed with water at the dosage ratio (usually 1% by volume), instantaneously before foam generation. Concentrating formulas enable firefighters to transport much smaller quantities of product. All current dosing equipment therefore requires the use of a concentrated formula that is easily dilutable and has adjusted rheological properties (very low viscosity liquid) to obtain the desired foam quality. The second special feature of fire-resistant foams is their ability to wet the wood. The minimum requirement for an effective Class A foam solution is a surface tension lower than that of the wood, so that it can be wetted. This is generally achieved using a mixture of surfactants, polymers, proteins and/or solvents. Thus, the development of new Class A foams must take into account these two parameters to be effective and rapidly deployed on the market.

To achieve this goal, the research program has four main objectives:
1) The formulation of fully biobased and biodegradable foams from a blend of biomass-derived components (biobased surfactants, biopolymers, bioparticles and commercially available plant proteins), respecting the ecosystem and promoting germination where possible to restore the environment after a fire. These foams will be based on the principle of the sol-gel transition, so as to obtain foams that are easy to produce in the liquid state (sol), but which gel once applied to the fire area.
2) The development of a laboratory-scale evaluation system for forest fire-fighting foams, to assess their effectiveness and discriminate between different formulations.
3) The evaluation of the biodegradability of formulas and their impact on soils, thanks to collaborations with expert laboratories (INRAe Avignon and Université de Nantes).
4) Testing the effectiveness of the most promising formulas on a larger scale, thanks to a partnership with BIOEX, a French company specializing in fire-fighting foams.

This project is now part of a larger ANR PRC project (2025-2029) between 7 partners (INRAe Lille, INRAe Avignon, University of Lille, University of Corte, University of Nantes, Institut Agro Rennes-Angers) and the company BIOEX (leader in the production of fire fighter solutions) to produce short-term and long-term flame-retardant solutions for class A fire. I take part in this project as co-supervisor of Helena Arellano PhD thesis but also as the technical adviser of the Fire-Resist facility for the whole duration of the project.

***In the same frame of developing bio-based materials, it would be interesting to continue the work on biobased coatings to fire retard biobased materials used for building applications**. Indeed, environmentally friendly materials manufactured for soundproofing applications already exist and can be obtained from renewable resources or recycled textile wastes.[144] They can be materials composed of fibers of jute, hemp, coconut, linen and textile waste. The first step would be to evaluate their FR properties and then try to flame-retard them using biobased FR surface modifications. As already seen in the sol-gel coating section, the use of biobased FR is highly attractive due to their low cost, wide availability and ease of access.*

Numerous biobased materials can be used as FR in coatings:

- *Chitosan (CS), it is a natural, biodegradable polysaccharide derived from the deacetylation of natural chitin. It can be extracted from crab, shrimp and mushroom shells.[145,146,147] The multiple hydroxyl and reactive amino groups in the CS molecular chain make it a positively charged polymer with excellent coordination capabilities, enabling its phosphorylation. CS is rich in carbon and can therefore be used as a carbon source for IFR.[148,149,150]*
- *Starch, it is used as a derivative for green char formation. The activation temperatures of starch derivatives are considerably lower than the decomposition temperatures of pure starch. The ammonia released by the thermal degradation of the derivative contributes to starch's flame-retardant properties. As a result, starch becomes a promising candidate for sustainable and environmentally friendly flame retardants.[151]*
- *Lignin, it is also a promising complex organic polymer with flame-retardant properties. Lignin is a key structural material located in the supporting tissues of most plants.[152] It plays a particularly important role in the formation of wood cell walls. Lignin is used to improve the fire-retardant properties of synthetic polymers because of its excellent thermal properties. Indeed, its decomposition occurs at temperatures between 200 and 500°C, depending on the nature of its production and the chemical modifications of its structure.[153,154]*
- *Cyclodextrin (CD), it is another class of bio-based material (oligosaccharides) usable for flame retardancy. Oligosaccharides are formed by the enzymatic modification of starches and are*

composed of several glucose units arranged in the shape of a truncated hollow cone. Their simple structure and high thermal stability make them an even better choice for use as carbonizing agents. Among the available CDs, β-cyclodextrin (β-CD) is the most popular and widely used.[155]

- *Flame retardants containing tannic acid (TA) are also an emerging and promising area of research in sustainable fireproofing. TA can be obtained from the seeds, bark and other parts of many tree species.*[156] *It is a non-toxic, inexpensive and abundant polyphenolic compound that can be characterized by the presence of hydroxyl groups linked to a benzene ring, as well as other groups such as organic acids and sugars.*[157] *Due to its specific aromatic structure, TA has high chemical and thermal stability.*[158] *Natural fire resistance is mainly attributed to their phenol-like reactivity. Phenoxy radicals can quench oxygen free radicals when the polymer decomposes during heating. In addition, TA promotes char production during combustion, resulting in the formation of a protective char layer that can block oxygen and heat transfer, as well as the release of flammable gases.*[159]
- *Phosphorus-containing biomass such as phytic acid (PA), it is also an excellent candidate as a flame retardant. Phytic acid has a phosphorus content of 28% and is the main source of phosphorus in plant tissues. Found mainly in plant seeds, roots and stems, PA can release phosphorus/polyphosphate during heating, accelerating carbonization of the polymer matrix and forming a protective carbonization layer. In the gas phase, PA decomposes into PO° and HPO° radicals to capture H° and OH° radicals, thus ending the chain reaction and achieving the flame-retardant effect. As a result, PA acts in both the gas and condensation phases and has rapidly become a good candidate for flame retardancy.*[160]

Among these natural products, chitosan, lignin, cyclodextrin, starch and tannin stand out. Studies have shown that they can be dehydrated and carbonized. The carbonization layer not only forms an external heat and oxygen shield for the polymer matrix, but also prevents flammable and volatile gases generated by the polymer from entering the gas phase, thus preventing flame propagation and achieving a flame-retardant effect.[161,162,163,164]

Contrary to chitosan, lignin, cyclodextrin, starch or tannin, which act as charring agent to enhance char production during combustion and limit the degradation of the polymer, phytic acid has also an action in the gas phase acting as radical scavengers. Thus, bio-based FR are very promising materials for the flame retardant field. However, the development of bio-based flame retardants still faces many challenges. Indeed, when not modified, bio-based materials have low flame retardant efficiency, and high amount of them is usually needed in order to reach satisfying flame retardant properties. Unfortunately, high loading of additives usually greatly affects the mechanical properties of the

material. Moreover, modifying bio-based materials induces a more complex fabrication process and thus a higher cost of production. Thus, researches are still on going to find proper flame retardant solutions with bio-based materials. This is still a promising and sustainable approach worthful to investigate in future studies especially in the case of bio-based substrates.

APPENDICES

I/ UMET Laboratory

The laboratory "Unité Matériaux Et Transformations" was created in January 2010 following the merger of four former laboratories of the Lille campus. The UMET laboratory now hosts a large portion of the research in Materials Science of the the Université de Lille. The laboratory includes approximately 80 professors and assistant professors, and CNRS researchers, 40 technical and administration staff, 60 PhD students, and 15 temporary contracts researchers or emeritus faculty.

There are seven research groups:

- Matériaux Moléculaires et Thérapeutiques
- Earth and Planetary Materials
- Métallurgie Physique et Génie des Matériaux ;
- Polymer Systems Engineering
- Plasticity
- Interface Processes and Hygiene of Materials
- Recycling and Functionalization processes

All work on materials science, but with different applications.

The UMET laboratory belongs to larger consortium, the “fédération de recherche” Michel-Eugène Chevreul, that hosts laboratories related to materials science in Northern France. The UMET is one of the three large members of the consortium, that also includes the Unité de Catalyse et de Chimie du Solide (UCCS) and the Laboratoire de Spectroscopie pour les Interactions, la Réactivité et l'Environnement (LASIRE). Among other tasks, the consortium is in charge of running large scale experimental facilities (NMR, electron diffraction, X-ray diffraction, mass spectroscopy, vibrationnal spectroscopy...). The UMET is hosting the Plateforme de Microscopie Électronique de Lille (PMEL) within its building and provides the associated technical staff. The consortium also runs the large-scale project ARCHI-CM (Chimie et Matériaux Architecturés) financed by the state and the local government.

One of the internationally well-recognized expertise of UMET is flame retardancy of material. The fields of expertise in this thematic are summed up in Figure A1.

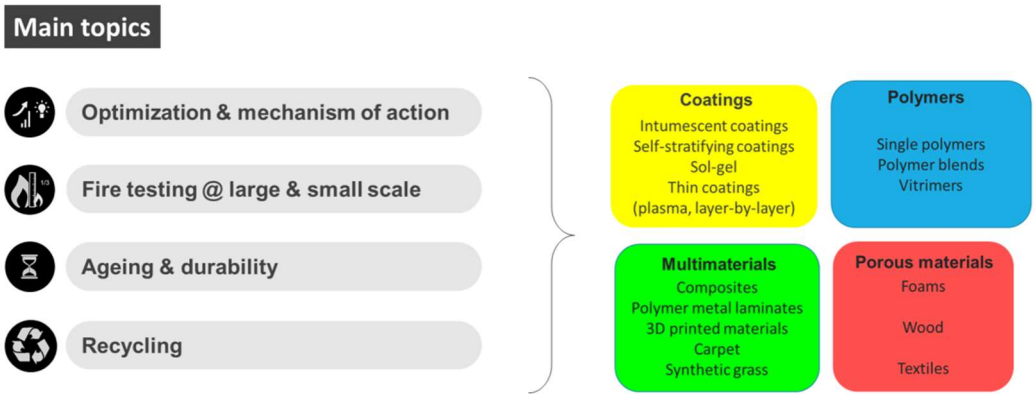

Figure A1: Expertise of UMET in flame retardancy of materials

Executive committee

- Director: Guillaume Delaplace
- Deputy directors: Sophie Duquesne, Damien Jacob
- Officers: Sophie Barrau (Training program-research link), Séverine Bellayer, Franck Béclin (Quality of work life), Gaëlle Le Fer (Communication and scientific animation), Sébastien Merkel (Open science, data management and IT security)

Former members of the executive committee

- Woisel Patrice: Director, 2017-2023
- Affouard Frédéric: Deputy director, 2017-2023
- Legris Alexandre: Director, 2010-2017
- Leroux Hugues: Deputy director, 2010-2017

II/ Regulatory framework in European Union

Two types of fire behavior are considered in European regulations to control the products. The first corresponds to its **resistance to fire** [36] and the second corresponds to its **reaction to fire** [37].

Fire resistance standard tests allow to understand the propagation of fire and its behavior after flashover, i.e. during a fully-developed fire step. This stage of regulation provides an understanding of the material ability to contain a fire. These tests are important in the development and design of a product because they assess its ability to spread a fire [38]. However, only the part concerning the reaction to fire will be discussed here since it is the purpose of this PhD work.

Reaction to fire standard allows to measure how a material contribute to the fire before the flashover, i.e. before the fully-developed fire. These tests will determine the impact of the product on the speed at which the flashover is reached. In the case of building construction product, a first series of tests is applied to all products that will be used in the European Union. The regulation is called Euroclasses. The standards used for the classification are detailed in Table A1.

Table A1*: Tests performed for Euroclasses.*

ISO	Test	Description	Required for class
EN ISO 11925	Ignitability test	Punctual attack by a small flame	A, B, C, D and E
EN 13823	Single Burning Item (SBI)	Solicitation by an isolated burning item	A, B, C and D
EN ISO 1716	Calorimeter bomb	Fully developed fire in the room	A1 and A2
EN ISO 1182	Furnace		

In that frame, building materials are classified from A to F according to EN 13501-1 (Table A2).

***Table A2**: Classification from A to F according to the standard EN 13501-1.*

Class	Test method(s)	Classification criteria	Additional classification
A1	EN ISO 1182 (1); and	$\Delta T \leq 30°C$; and $\Delta m \leq 50$ %; and $t_f = 0$ (i.e. no sustained flaming)	-
	EN ISO 1716	PCS ≤ 2.0 MJ.kg^{-1} (1); and PCS ≤ 2.0 MJ.kg^{-1} (2) (2[a]); and PCS ≤ 1.4 MJ.m^{-2} (3); and PCS ≤ 2.0 MJ.kg^{-1} (4)	
A2	EN ISO 1182 (1); or	$\Delta T \leq 50°C$; and $\Delta m \leq 50$ %; and $t_f \leq 20$ s	
	EN ISO 1716; and	PCS ≤ 3.0 MJ.kg^{-1} (1); and PCS ≤ 4.0 MJ.m^{-2} (2); and PCS ≤ 4.0 MJ.m^{-2} (3); and PCS ≤ 3.0 MJ.kg^{-1} (4)	
	EN 13823 (SBI)	-FIGRA ≤ 120 W.s^{-1} -$THR_{600\ s}$ ≤ 7.5 MJ -LFS < edge of specimen	Smoke production (5); and flaming droplets/particles (6)
B	EN 13823 (SBI); and	-FIGRA ≤ 120 W.s^{-1} -$THR_{600\ s}$ ≤ 7.5 MJ -LFS < edge of specimen	Smoke production (5); and flaming droplets/particles (6)
	EN ISO 11925-2 (8): exposure = 30s	Fs ≤ 150 mm within 60 s	
C	EN 13823 (SBI); and	-FIGRA ≤ 250 W.s^{-1} -$THR_{600\ s}$ ≤ 15 MJ -LFS (lateral flame spread) < edge of specimen	Smoke production (5); and flaming droplets/particles (6)
	EN ISO 11925-2 (8): exposure = 30s	Fs ≤ 150 mm within 60 s	
D	EN 13823 (SBI); and	FIGRA ≤ 750 W.s^{-1}	Smoke production (5); and flaming droplets/particles (6)
	EN ISO 11925-2 (8): exposure = 30s	Fs ≤ 150 mm within 60 s	
E	EN ISO 11925-2 (8): exposure = 15s	Flame spread (Fs) ≤ 150 mm within 20 s	Flaming droplets/particles (7)
F	No performance determined		

(1) For homogeneous products and substantial components of non-homogeneous products
(2) For any external non-substantial component of non-homogeneous products
(2a) Alternatively, any external non-substantial component having a PCS ≤ 2.0 MJ.m^{-2}, provided that the product satisfies the following criteria of SBI: FIGRA ≤ 20 W.s^{-1}; and LFS < edge of specimen; and $THR_{600\ s}$ ≤ 4.0 MJ; and s1; and d0
(3) For any internal non-substantial component of non-homogeneous products
(4) For the product as a whole
(5) s1 = SMOGRA ≤ 30 m^2.s^{-2} and $TSP_{600\ s}$ ≤ 50 m^2; s2 = SMOGRA ≤ 180 m^2.s^{-2} and $TSP_{600\ s}$ ≤ 200 m^2; s3 = not s1 or s2
(6) d0 = no flaming droplets / particles in SBI within 600 s; d1 = no flaming droplets / particles persisting longer than 10 s in SBI within 600 s; d2 = not d0 or d1; Ignition of the paper in EN ISO 11925-2 results in a d2 classification
(7) Pass = no ignition of the paper (no classification); Fail = ignition of the paper (d2 classification)
(8) Under conditions of surface flame attack and, if appropriate to the end-use application of the product, edge flame attack

The order of the classification is from F to A, A being the best ranking. First, the material must pass the ignitability test (EN ISO 11925-2), which consists of setting a flame for 15 seconds to 30 seconds on a sample and observing its propagation. The test is performed to determine the classification of the material between F and E.

If the flame spread is lower to 150 mm within 60 s, the other test corresponding to the class D, C and B is performed. It corresponds to the Single Burning Item (SBI) (EN 13823). The purpose of the SBI test is to examine the contribution of a material to the development of a fire (the test is further discussed in chapter 5), in a scenario simulating the combustion of an isolated object in the corner of a room. Thus, a specimen, consisting of two panels forming a right angle, is exposed to the flame of a burner placed at the bottom of the corner. The flame is produced by burning propane gas and spreads through a sand bed to produce a heat flux of about 30 kW. The performance of the material is measured by its heat production and smoke production. Depending on the SBI results, the material will be ranking between B and D. Finally, if the material has the ranking B, it will have to pass two other tests (calorimeter bomb (EN ISO 1716) and furnace tests (EN ISO 1182)), to reach the A ranking.

III/ Polyurethane and polyisocyanurate

The synthesis of polyurethane is a polyaddition reaction between a diisocyanate and a diol (Figure A2), was discovered by Otto Bayer in 1937. Polyurethanes result from the reaction between alcohols with two or more reactive hydroxyl groups (polyol) per molecule and isocyanates that have more than one reactive isocyanate group per molecule.

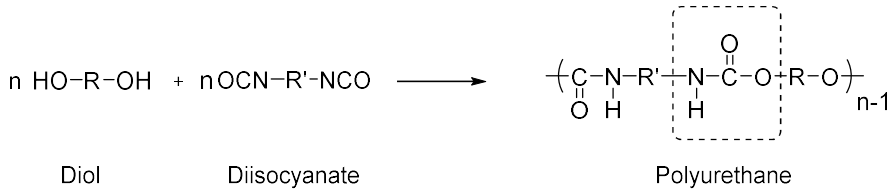

Figure A2: Polyaddition reaction between a diol and a diisocyanate.

This is only true if the number of hydroxyl groups is the same as the number of isocyanate groups (with a minimum of two functions available for both). If the ratio is modified, secondary reactions can occur that can be done intentionally to control the properties of the foams. In the case of polyisocyanurate foams, a ratio of three isocyanate groups to one single hydroxyl group is needed (Figure A3).

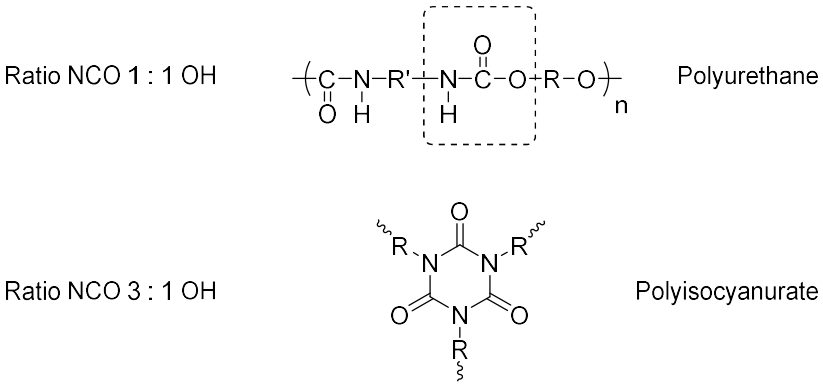

Figure A3: Difference of ratio between NCO and OH groups to obtain polyurethane and polyisocyanurate.

IV/ Mass loss cone test including smoke and gas measurements

The cone calorimeter test (ISO 5660) and the mass loss calorimeter test (ISO13927) are two small scale tests used to determine the heat release rate (HRR) of a material in the event of a fire. The first technique determines the HRR based on oxygen consumption (Hugget's formula) while the second uses a thermopile located in the chimney that is calibrated with methane. In this project, the mass loss cone was used. This test allows to compare the fire behavior of materials and in our case, to study the impact of flame retardants.

The apparatus used in the project is a mass loss calorimeter (MLC) provided by FTT (Figure A4). A sample of 10 cm × 10 cm × 2 or 4 cm is placed on a support located below the conical heater. The distance between the surface of the sample and the conical heater is set up at 25 mm. The define radiative flux used were 35 $kW.m^{-2}$ and 50 $kW.m^{-2}$. A spark igniter is placed above the sample to ignite the gases release by the degradation of the foam. The test is thus performed under forced ignition. The cone is equipped with four thermocouples located in the chimney. It constitutes a thermopile that is previously calibrated with methane allowing to determine the heat release rate (HRR) from a calibration curve.

A FTIR spectrometer can be coupled with the MLC test. It is connected to a sample probe placed in the chimney. This technique permits to determine and to quantify (semi-quantification) the gases released during combustion. A heat gun is placed at the outlet of the MLC chimney in order to collect the combustion gases. The heat gun (185°C) contains glass wool for soot filtration and is directly connected to a sampling line heated to 185°C. This line is connected to a pump to control the extraction. A drying system removes water and avoids pollution in the infrared spectrometer. The internal pressure of the system is set at 650 torr. Infrared spectra were recorded in a range between 550 and 4500 cm^{-1} with an ANTARIS IGS Fourier transformed infrared spectrometer gas analyzer from ThermoScientific, in real time mode with a resolution of 0.5 cm^{-1}. The number of scans was set at 64.

To quantify gases, spectra need to be recorded at different concentrations for targeted gases and a quantification method needs to be created using TQ Analyst. When creating a method, representative regions in the IR spectra of the selected gas need to be chosen and interactions with other gases have to be taken into account. The following gases can be quantified in our case: carbon monoxide, carbon dioxide and hydrogen cyanide. Quantification is reproducible within 10 %.

Finally, an opacimeter is placed at the exit of the chimney to determine the smoke released during combustion. A TRDA Smoke density device supplied by NETZSCH Taurus Instruments is used to characterize the smoke released during a test. The light emitter sensor is composed of a 10 W halogen light source and tempered with heatproof optics. The light receiver sensor is constituted of silicon

photo receiver, also tempered and with heatproof optics. A spectral filter and measuring light amplifier are also added.

Using three different equipment, the parameters measured during a MLC test are:

- Peak of heat release rate (pHRR) (kW.m^{-2})
- Ignition time, flaming time, time of pHRR (t pHRR) (s)
- Residual weight (wt%)
- Total Heat Release (THR) (MJ)
- Total light attenuation (%)
- Gases concentration (ppm)

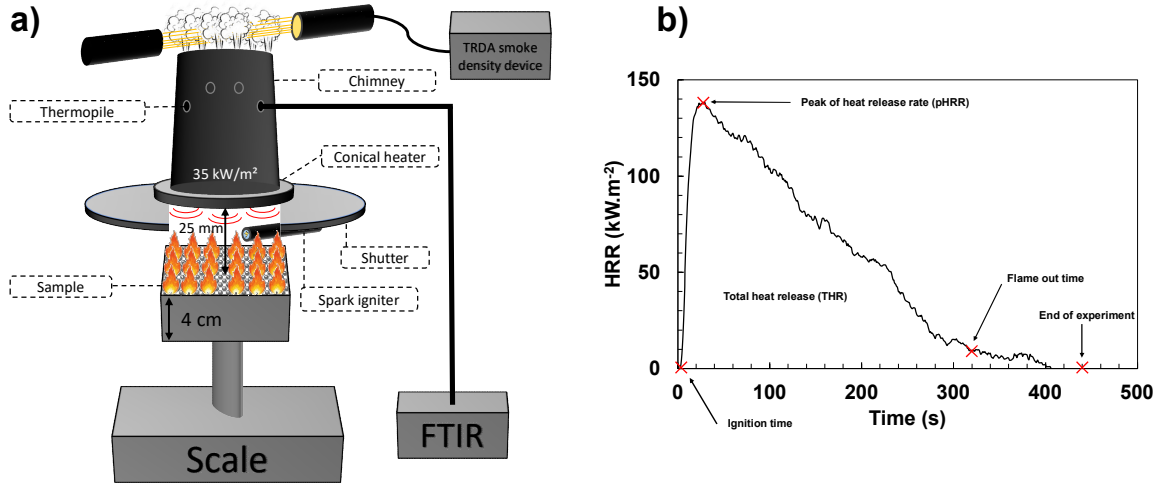

Figure A4: a) Mass loss calorimeter including smoke and gas measurements. b) Example of a theoretical HRR vs time curve with the main determined parameters.

Figure A4b shows a theoretical curve obtained from the MLC test. It allows to visualize how the parameters such as, pHRR, time to ignition, THR or flaming time are obtained. The data acquisition is performed from when the sample is irradiated by the MLC test resistor until 120 s after the extinction of the flame. The ignition time is obtained at the moment of the flame appearance at the surface of the sample, while the flaming time corresponds to the time during which the material had a flame at the surface. The pHRR is the maximum value of the HRR over the whole test. The total light attenuation is the sum of the light attenuation values measured during the whole test. The higher this value is, the more smoke the system releases. The residual weight is obtained by measuring the mass of the carbonaceous residue with a scale at the end of the experiment. All the measured parameters will be criteria used to differentiate the action of FR on the fire behavior of PUR and PIR foams.

V/ UL94 test

UL-94 vertical test allows investigating the vertical propagation of a flame and the dripping of the sample. The melt dripping of plastics is indeed one of the most important issues in the UL-94 classification.

The test is carried out following the method mentioned in the standards ASTM D3801, IEC 707 or ISO 1210. It determines the tendency of a material either to extinguish or to spread the flame once the specimen has been ignited. It also evaluates the melt dripping behavior of samples, which is not the case for many other conventional tests.

UL-94 vertical tests illustrated in Figure A5 were carried out on a Fire Testing Technology Limited equipment on bars, in accordance with the recommendations of the standards. Specimens are clamped vertically and exposed from the bottom, to a defined flame ignition source of 50W, for 10 sec. The power of the flame (50W) has been previously calibrated by heating a specific thermocouple type K with a copper head (5.5mm±0.01mm of diameter and 1.76g±0.01g) from 100°C to 700°C in 44s±2s. Then the flame is applied twice if the sample self-extinguishes after the first ignition. Cotton is also placed below the sample to evaluate the presence or not of flaming drops.

The specimens are ignited by a blue flame (without cone) of 20mm. The flame is generated by a methane burner having a gas flow rate of 105mL/min with a back pressure less than 10 mm of water. Three classifications are assigned to the materials based on their behavior during burning, the flame propagation and dripping: V0, V1, V2 (Table A3), V0 being the best rating. If the material does not meet these criteria, it is no rating (NR) at the UL-94 test. The obtained ratings depend on the extinction time after the first and second flame application (self-extinguishment ability), on the dripping and on the burning rate.

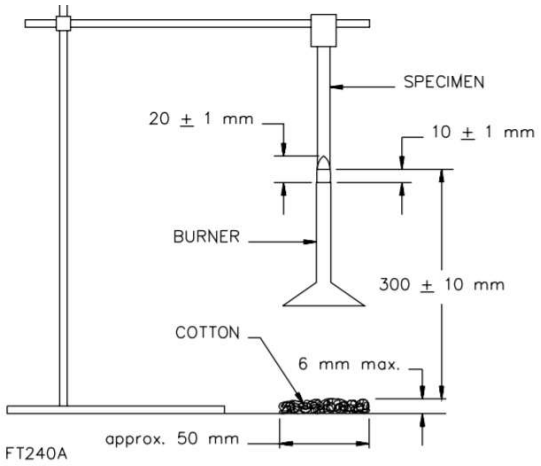

Figure A5: Scheme of the vertical UL-94 test.

Table A3: The different criteria conditions when using the vertical UL-94 test (30)

Criteria conditions	V-0	V-1	V-2
Afterflame time for each individual specimen t_1 or t_2	≤10s	≤30s	≤30s
Total afterflame time for any condition set (t_1 plus t_2 for the 5 specimens)	≤50s	≤250s	≤250s
Afterflame plus afterglow time for each individual specimen after the second flame application (t_2+t_3)	≤30s	≤60s	≤60s
Afterflame or afterglow of any specimen up to the holding clamp	No	No	No
Cotton indicator ignited by flaming particles or drops	No	No	Yes

VI/ 116 kW burner test

A sample is fixed vertically on a moving panel that can bring the sample in front of a 116 kW burner test. During experiments, regular video cameras or InfraRed cameras can be positioned on the front or back side of the sample. Results are recorded and recovered on a computer.

Figure A6: Experimental set up of the 116 kW burner test

VII/ Low pressure cold plasma process

A rotary low-pressure radiofrequency cold plasma generated in a chamber was chosen in order to functionalize the whole surface of EPP beads or molded EPP pieces. The temperature of the treatment is close to ambient temperature and the beads are in a closed chamber and can not be blown away from the plasma area.

The equipment used is a low-pressure cold plasma CD 1200 manufactured by Europlasma, equipped with a CESAR radio frequency power generator from Advanced Energy (13,56 MHz) and a drum to apply a rotation. The functionalization process is applied as follow: samples are loaded in the chamber with or without the drum, the processing chamber is set under vacuum to about 50 mTorr (0.066 mbar) and the process gas is introduced (argon or a mix argon/oxygen) at 20sccm *(standard cm^3/min)* for 60s. The gas flow is set and the power is turned on for a selected time depending on the sample (beads, molded EPP) and the environment (with or without drum, quantity of beads). Then, the power source and the gas supply are switched off. Finally, the chamber is set back to atmospheric pressure and the sample is recovered. Two set up have been used, a static set up without rotation and a dynamic set up with a drum to apply a rotation (Figure A7).

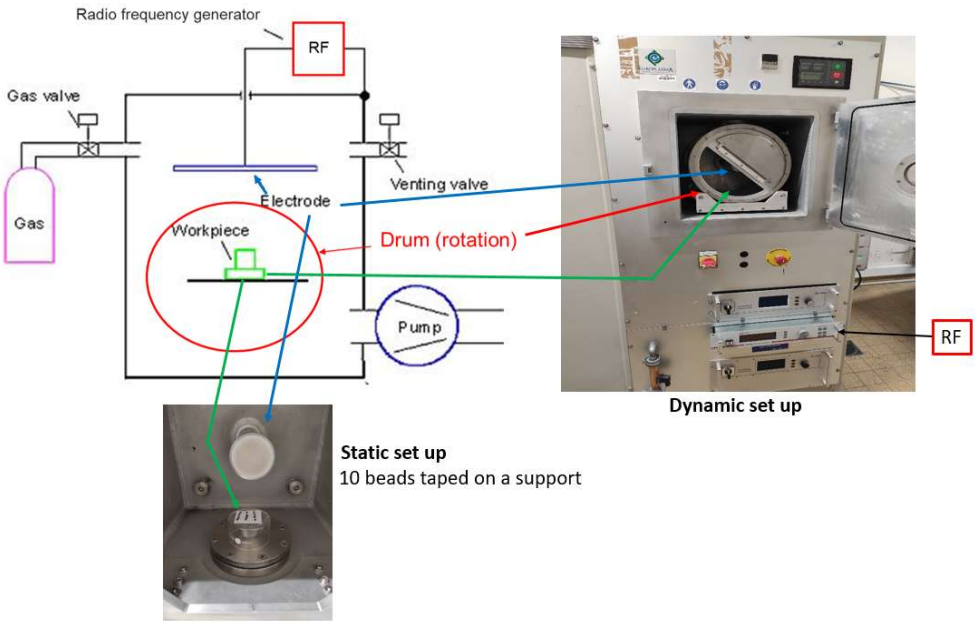

Figure A7: Schematic representation of the plasma chamber (left), image of the plasma in dynamic set up (right) and static set up of the plasma (below)

REFERENCES

[1] Bourbigot, S; Vanderhart, DL; Gilman, JW; Bellayer, S; Stretz, H; Paul, DR Solid state NMR characterization and flammability of styrene-acrylonitrile copolymer montmorillonite nanocomposite POLYMER 2004 45 22 10.1016/j.polymer.2004.08.057

[2] Maupin, PH; Gilman, JW; Harris, RH; Bellayer, S; Bur, AJ; Roth, SC; Murariu, M; Morgan, AB; Harris, JD Optical probes for monitoring intercalation and exfoliation in melt-processed polymer nanocomposites MACROMOLECULAR RAPID COMMUNICATIONS 2004 25 7 10.1002/marc.200300262

[3] Kashiwagi, T; Du, FM; Winey, KI; Groth, KA; Shields, JR; Bellayer, SP; Kim, H; Douglas, JF Flammability properties of polymer nanocomposites with single-walled carbon nanotubes: effects of nanotube dispersion and concentration POLYMER 2005 46 2 10.1016/j.polymer.2004.10.087

[4] Zammarano, M; Franceschi, M; Bellayer, S; Gilman, JW; Meriani, S Preparation and flame resistance properties of revolutionary self-extinguishing epoxy nanocomposites based on layered double hydroxides POLYMER 2005 46 22 10.1016/j.polymer.2005.07.050

[5] Bellayer, S; Gilman, JW; Eidelman, N; Bourbigot, S; Flambard, X; Fox, DM; De Long, HC; Trulove, PC Preparation of homogeneously dispersed multiwalled carbon nanotube/polystyrene nanocomposites via melt extrusion using trialkyl imidazolium compatibilizer ADVANCED FUNCTIONAL MATERIALS 2005 15 6 10.1002/adfm.200400441

[6] Zammarano, M; Bellayer, S; Gilman, JW; Franceschi, M; Beyer, FL; Harris, RH; Meriani, S Delamination of organo-modified layered double hydroxides in polyamide 6 by melt processing POLYMER 2006 47 2 10.1016/j.polymer.2005.11.080

[7] Langat, J.; Bellayer, S.; Hudrlik, P.; Hudrlik, A.; Maupin, P. H.; Gilman, J. W., Sr.; Raghavan, D. Synthesis of imidazolium salts and their application in epoxy montmorillonite nanocomposites POLYMER 2006 47 19 10.1016/j.polymer.2006.06.067

[8] Bellayer, S.; Gilman, J. W.; Rahatekar, S. S.; Bourbigot, S.; Flambard, X.; Hanssen, L. M.; Guo, H.; Kumar, S. Characterization of SWCNT and PAN/SWCNT films CARBON 2007 45 12 10.1016/j.carbon.2007.06.057

[9] Fox, Douglas M.; Harris, Richard H., Jr.; Bellayer, Severine; Gilman, Jeffrey W.; Gelfer, Mikhail Y.; Hsaio, Benjamin S.; Maupin, Paul H.; Trulove, Paul C.; De Long, Hugh C. The pillaring effect of the 1,2-dimethyl-3(benzyl ethyl iso-butyl POSS) imidazolium cation in polymer/montmorillonite nanocomposites POLYMER 2011 52 23 10.1016/j.polymer.2011.09.016

[10] E. Devaux, S. Bellayer, S. Chlebicki, S. Bourbigot, A. Fonseca, J. Al-Asswad, J. B. Nagy, Continuous textile fibers and yarns made from a spinnable nanocomposite, US20070031662A1, Feb. 8, 2007

[11] Neouze, Marie-Alexandra; Le Bideau, Jean; Gaveau, Philippe; Bellayer, Severine; Vioux, Andre Ionogels, new materials arising from the confinement of ionic liquids within silica-derived networks CHEMISTRY OF MATERIALS 2006 18 17 10.1021/cm060656c

[12] Lunstroot, Kyra; Driesen, Kris; Nockemann, Peter; Gorller-Walrand, Christiane; Binnemans, Koen; Bellayer, Severine; Le Bideau, Jean; Vioux, Andre Luminescent ionogels based on europium-doped ionic liquids confined within silica-derived networks CHEMISTRY OF MATERIALS 2006 18 24 10.1021/cm061704w

[13] Le Bideau, J.; Gaveau, P.; Bellayer, S.; Neouze, M.-A.; Vioux, A. Effect of confinement on ionic liquids dynamics in monolithic silica ionogels:: ¹H NMR study PHYSICAL CHEMISTRY CHEMICAL PHYSICS 2007 9 40 10.1039/b711539c

[14] Lunstroot, Kyra; Driesen, Kris; Nockemann, Peter; Van Hecke, Kristof; Van Meervelt, Luc; Goerller-Walrand, Christiane; Binnemans, Koen; Bellayer, Severine; Viau, Lydie; Le Bideau, Jean; Vioux, Andre Lanthanide-doped luminescent ionogels DALTON TRANSACTIONS 2009 2 10.1039/b812292j

[15] Bellayer, Severine; Viau, Lydie; Tebby, Zoe; Toupance, Thierry; Le Bideau, Jean; Vioux, Andre Immobilization of ionic liquids in translucent tin dioxide monoliths by sol-gel processing DALTON TRANSACTIONS 2009 8 10.1039/b814978j

[16] Bellayer, S.; Tavard, E.; Duquesne, S.; Piechaczyk, A.; Bourbigot, S. Mechanism of intumescence of a polyethylene/calcium carbonate/stearic acid system POLYMER DEGRADATION AND STABILITY 2009 94 5 10.1016/j.polymdegradstab.2009.01.032

[17] Bellayer, Severine Patricia; Tavard, E.; Duquesne, S.; Piechaczyk, A.; Bourbigot, S. Natural mineral fire-retardant fillers for polyethylene FIRE AND MATERIALS 2011 35 3 10.1002/fam.1048

[18] Liu, Weiji; Chen, Xiao Dong; Jeantet, Romain; Andre, Christophe; Bellayer, Severine; Delaplace, Guillaume Effect of casein/whey ratio on the thermal denaturation of whey proteins and subsequent fouling in a plate heat exchanger JOURNAL OF FOOD ENGINEERING 2021 289 10.1016/j.jfoodeng.2020.110175

[19] Blanpain-Avet, P.; Andre, C.; Azevedo-Scudeller, L.; Croguennec, T.; Jimenez, M.; Bellayer, S.; Six, T.; Martins, G. A. S.; Delaplace, G. Effect of the phosphate/calcium molar ratio on fouling deposits generated by the processing of a whey protein isolate in a plate heat exchanger FOOD AND BIOPRODUCTS PROCESSING 2020 121 10.1016/j.fbp.2020.02.005

[20] Scudeller, Luisa A.; Blanpain-Avet, Pascal; Six, Thierry; Bellayer, Severine; Jimenez, Maude; Croguennec, Thomas; Andre, Christophe; Delaplace, Guillaume Calcium Chelation by Phosphate Ions and Its Influence on Fouling Mechanisms of Whey Protein Solutions in a Plate Heat Exchanger FOODS 2021 10 2 10.3390/foods10020259

[21] Zouaghi, Sawsen; Bellayer, Severine; Thomy, Vincent; Dargent, Thomas; Coffinier, Yannick; Andre, Christophe; Delaplace, Guillaume; Jimenez, Maude Biomimetic surface modifications of stainless steel targeting dairy fouling mitigation and bacterial adhesion FOOD AND BIOPRODUCTS PROCESSING 2019 113 10.1016/j.fbp.2018.10.012

[22] Zouaghi, S.; Abdallah, M.; Andre, C.; Chihib, N. E.; Bellayer, S.; Delaplace, G.; Celzard, A.; Jimenez, M. Graphite-based composites for whey protein fouling and bacterial adhesion management INTERNATIONAL DAIRY JOURNAL 2018 86 10.1016/j.idairyj.2018.07.004

[23] Zouaghi, Sawsen; Barry, Mikayla E.; Bellayer, Severine; Lyskawa, Joel; Andre, Christophe; Delaplace, Guillaume; Grunlan, Melissa A.; Jimenez, Maude Antifouling amphiphilic silicone coatings for dairy fouling mitigation on stainless steel BIOFOULING 2018 34 7 10.1080/08927014.2018.1502275

[24] Zouaghi, Sawsen; Six, Thierry; Bellayer, Severine; Coffinier, Yannick; Abdallah, Marwan; Chihib, Nour-Eddine; Andre, Christophe; Delaplace, Guillaume; Jimenez, Maude Atmospheric pressure plasma spraying of silane-based coatings targeting whey protein fouling and bacterial adhesion management APPLIED SURFACE SCIENCE 2018 455 10.1016/j.apsusc.2018.06.006

[25] Zouaghi, Sawsen; Six, Thierry; Nuns, Nicolas; Simon, Pardis; Bellayer, Severine; Moradi, Sona; Hatzikiriakos, Sawas G.; Andre, Christophe; Delaplace, Guillaume; Jimenez, Maude Influence of stainless-steel surface properties on whey protein fouling under industrial processing conditions JOURNAL OF FOOD ENGINEERING 2018 228 10.1016/j.jfoodeng.2018.02.009

[26] Zouaghi, Sawsen; Six, Thierry; Bellayer, Severine; Moradi, Sona; Hatzikiriakos, Savvas G.; Dargent, Thomas; Thomy, Vincent; Coffinier, Yannick; Andre, Christophe; Delaplace, Guillaume; Jimenez, Maude Antifouling Biomimetic Liquid-Infused Stainless Steel: Application to Dairy Industrial Processing ACS APPLIED MATERIALS & INTERFACES 2017 9 31 10.1021/acsami.7b06709

[27] Saget, Manon; Nuns, Nicolas; Supiot, Philippe; Foissac, Corinne; Bellayer, Severine; Dourgaparsad, Kevin; Royoux, Pierre-Alexandre; Delaplace, Guillaume; Thomy, Vincent; Coffinier, Yannick; Jimenez, Maude Ultra-hydrophobic biomimetic transparent bilayer thin film deposited by atmospheric pressure plasma SURFACES AND INTERFACES 2023 42 10.1016/j.surfin.2023.103398

[28] Lemesle, Charlotte; Bellayer, Severine; Duquesne, Sophie; Schuller, Anne-Sophie; Thomas, Laurent; Casetta, Mathilde; Jimenez, Maude Self-stratified bio-based coatings: Formulation and elucidation of critical parameters governing stratification APPLIED SURFACE SCIENCE 2021 536 10.1016/j.apsusc.2020.147687

[29] Lemesle, Charlotte; Fremiot, Jerome; Beaugendre, Agnes; Casetta, Mathilde; Bellayer, Severine; Duquesne, Sophie; Schuller, Anne-Sophie; Jimenez, Maude Life cycle assessment of multi-step versus one-step coating processes using oil or bio-based resins JOURNAL OF CLEANER PRODUCTION 2020 242 10.1016/j.jclepro.2019.118527

[30] Beaugendre, A.; Degoutin, S.; Bellayer, S.; Pierlot, C.; Duquesne, S.; Casetta, M.; Jimenez, M. Self-stratifying epoxy/silicone coatings PROGRESS IN ORGANIC COATINGS 2017 103 10.1016/j.porgcoat.2016.10.025

[31] Beaugendre, A.; Saidi, S.; Degoutin, S.; Bellayer, S.; Pierlot, C.; Duquesne, S.; Casetta, M.; Jimenez, M. One pot flame retardant and weathering resistant coatings for plastics: a novel approach RSC ADVANCES 2017 7 65 10.1039/c7ra08028j

[32] Beaugendre, Agnes; Degoutin, Stephanie; Bellayer, Severine; Pierlot, Christel; Duquesne, Sophie; Casetta, Mathilde; Jimenez, Maude Self-Stratification of Ternary Systems Including a Flame Retardant Liquid Additive COATINGS 2018 8 12 10.3390/coatings8120448

[33] Beaugendre, A.; Lemesle, C.; Bellayer, S.; Degoutin, S.; Duquesne, S.; Casetta, M.; Pierlot, C.; Jaime, F.; Kim, T.; Jimenez, M. Flame retardant and weathering resistant self-layering epoxy-silicone coatings for plastics PROGRESS IN ORGANIC COATINGS 2019 136 10.1016/j.porgcoat.2019.105269

[34] Jimenez, M.; Delaplace, G.; Nuns, N.; Bellayer, S.; Deresmes, D.; Ronse, G.; Alogaili, G.; Collinet-Fressancourt, M.; Traisnel, M. Toward the understanding of the interfacial dairy fouling deposition and growth mechanisms at a stainless steel surface: A multiscale approach JOURNAL OF COLLOID AND INTERFACE SCIENCE 2013 404 10.1016/j.jcis.2013.04.021

[35] Collinet-Fressancourt, Marion; Nuns, Nicolas; Bellayer, Severine; Traisnel, Michel Characterization by TEM and ToF-SIMS of the oxide layer formed during anaphoretic paint electrodeposition on Al-alloys APPLIED SURFACE SCIENCE 2013 277 10.1016/j.apsusc.2013.04.023

[36] A. Singh, S. Singh, Building Thermal Insulation Market Size Report, ID GMI1755, Dec 2024

[37] Woods, G. The ICI Polyurethanes Book, Second Edition.; Wiley; 1990.

[38] Mougel, C.; Garnier, T.; Cassagnau, P.; Sintes-Zydowicz, N. Phenolic Foams: A Review of Mechanical Properties, Fire Resistance and New Trends in Phenol Substitution. Polymer 2019, 164, 86–117. https://doi.org/10.1016/j.polymer.2018.12.050.

[39] H. Siddique, Grenfell Tower fire: police considering manslaughter charges, The Guardian. (2017). https://www.theguardian.com/uk-news/2017/jun/23/grenfell-tower-fire-police-considering-manslaughter-charges (accessed April 8, 2020).

[40] M. McKee, Grenfell Tower fire: why we cannot ignore the political determinants of health, British Medical Journal Publishing Group, 2017.

[41] Evarts, B. Fire Loss in the United States During 2017. 2017, 23

[42] The flame retardants market | FLAMERETARDANTS-ONLINE, (n.d.). https://www.flameretardants-online.com/flame-retardants/market (accessed June 18, 2019).

[43] Flame Retardants - Specialty Chemicals Update Program (SCUP) | IHS Markit, (n.d.). https://ihsmarkit.com/products/chemical-flame-retardants-scup.html (accessed June 18, 2019).

[44] Y. Ma, Z. Xie, R. Lohmann, W. Mi, G. Gao, Organophosphate Ester Flame Retardants and Plasticizers in Ocean Sediments from the North Pacific to the Arctic Ocean, Environ. Sci. Technol. 51 (2017) 3809–3815.

[45] E.W.Y. Tung, A. Kawata, M. Rigden, W.J. Bowers, D. Caldwell, A.C. Holloway, B. Robaire, B.F. Hales, M.G. Wade, Gestational and Lactational Exposure to an Environmentally-Relevant Mixture of Brominated Flame Retardants: Effects on Neurodevelopment and Metabolism: Gestational and Lactational Exposure to Flame Retardants, Birth Defects Res. 109 (2017) 497–512.

[46] A.R. Horrocks, Polymer Degradation and Stability 96 (2011) 377-392.

[47] K.A. Salmeia, S. Gaan, G. Malucelli, Polymers 8 (2016) 319.

[48] J.W. Mitchell, Non-Halogenated Flame Retardant Handbook (2014) 1-16.

[49] Y. Hu, X. Wang, Flame Retardant Polymeric Materials: A Handbook, CRC Press, 2019.

[50] A. Perujo, G. Van Grootveld, H. Scholz, New Generation of Electric Vehicles (2012) 3-28.

[51] Gossiaux, Alexandre; Bachelet, Pierre; Bellayer, Severine; Ortgies, Stefan; Koenig, Alexander; Duquesne, Sophie Small-scale single burning item test for the study of the fire behavior of building materials FIRE SAFETY JOURNAL 2021 125 10.1016/j.firesaf.2021.103429

[52] Gossiaux, Alexandre; Bellayer, Severine; Ortgies, Stefan; Wagener, Tobias; Koenig, Alexander; Duquesne, Sophie Systematic study of the condensed phase of phosphorus-based flame retarded foams POLYMER DEGRADATION AND STABILITY 2022 206 10.1016/j.polymdegradstab.2022.110208

[53] U. braun, A.I. Balabanovich, B. Schartel, U. Knoll, J. Artner, M. Ciesielski, M. Dorïng, R. Perez, J.K.W. Sandler, V. Altstädt, T. Hoffman, D. Pospiech, Influence of the oxidation state of phosphorus on the decomposition and fire behavior of flame-retarded epoxy resin composites, Polymer. 47 (2006) 8495-8508.

[54] A. Lorenzetti, M. Modesti, S. Besco, D. Hrelja, S. Donadi, Influence of phosphorus valency on thermal behaviour of flame retarded polyurethane foams, Polym. Degrad. Stab. 96 (2011) 1455–1461.

[55] B. Schartel, Phosphorus-based flame retardancy mechanisms—old hat or a starting point for future development? Materials. 3 (2010) 4710–4745.

[56] J.W. Hastie, C.L. McBee, Mechanistic studies of triphenylphosphine oxide-poly (ethyleneterephthalate) and related flame retardant systems, 0 ed., National Bureau of Standards, Gaithersburg, MD, 1975.

[57] D. Drysdale, An introduction to fire dynamics, John Wiley & Sons, 2011.

[58] M. Zhang, J. Zhang, S. Chen, Y. Zhou, Synthesis and fire properties of rigid polyurethane foams made from a polyol derived from melamine and cardanol, Polym. Degrad. Stab. 110 (2014) 27–34.

[59] F. Feng, L. Qian, The flame retardant behaviors and synergistic effect of expandable graphite and dimethyl methylphosphonate in rigid polyurethane foams, Polym. Compos. 35 (2014) 301–309.

[60] S.Duquesne, S.Magnet, C.Jama, R.Delobel Thermoplastic resins for thin film intumescent coatings – towards a better understanding of their effect on intumescence efficiency Polymer Degradation and Stability 88, 1, 2005, 63-69.

[61] M. Muller, S. Bourbigot, S. Duquesne, R.A. Klein, G Giannini, C.I. Lindsay, Measurement and investigation of intumescent char strength: Application to polyurethanes, Journal of Fire Sciences, 2013, 31 4 293-308

[62] W. Xu, G. Wang, Influence of thermal behavior of phosphorus compounds on their flame retardant effect in PU rigid foam: Influence of phosphorus compounds on PU rigid foam, Fire Mater. 40 (2016) 826–835.

[63] X. Liu, Y. Zhou, J. Hao, J. Du, Smoke and toxicity suppression by zinc salts in flame-retardant polyurethane-polyisocyanurate foams filled with phosphonate and chlorinated phosphate, J. Appl. Polym. Sci. 132 (2015) n/a-n/a.

[64] X. Liu, D.-M. Xu, Y.-L. Wang, Y. Zhou, J.-W. Hao, Smoke and toxicity suppression properties of ferrites on flame-retardant polyurethane–polyisocyanurate foams filled with phosphonate, J. Therm. Anal. Calorim. 125 (2016) 245–254.

[65] X. Liu, J.-Y. Wang, X.-M. Yang, Y.-L. Wang, J.-W. Hao, Application of TG/FTIR TG/MS and cone calorimetry to understand flame retardancy and catalytic charring mechanism of boron phosphate in flame-retardant PUR–PIR foams, J. Therm. Anal. Calorim. 130 (2017) 1817–1827.

[66] H. Singh, A.K. Jain, Ignition, combustion, toxicity, and fire retardancy of polyurethane foams: A comprehensive review, J. Appl. Polym. Sci. (2008) NA-NA. https://doi.org/10.1002/app.29131.

[67] Phosphoric acid, triethyl ester - 31P NMR - Chemical Shifts - SpectraBase, (n.d.). https://spectrabase.com/spectrum/I7axrn0GNGb (accessed August 5, 2021).

[68] ethyl phosphonic acid, diethyl ester - 31P NMR - Chemical Shifts - SpectraBase, (n.d.). https://spectrabase.com/spectrum/9dLWfRekCGO (accessed August 5, 2021).

[69] R. Guthrie, I. Jenkins, The mechanism of the Mitsunobu reaction. A 31P N.M.R. study, Aust. J. Chem. 35 (1982) 767.

[70] Phosphorous acid, triethyl ester - 31P NMR - Chemical Shifts - SpectraBase, (n.d.). https://spectrabase.com/spectrum/FMRcI4SELqZ (accessed August 5, 2021).

[71] C.L. Chernick, H.A. Skinner, 285. Thermochemistry of organophosphorus compounds. Part II. Triethyl phosphate, tripropylphosphine oxide, and tributylphosphine oxide, J. Chem. Soc. Resumed. (1956) 1401–1405.

[72] M. Jimenez, N. Lesaffre, S. Bellayer, R. Dupretz, M. Vandenbossche, S. Duquesne, S. Bourbigot, Novel flame retardant flexible polyurethane foam: plasma induced graft-polymerization of phosphonates, RSC Adv. 5 (2015) 63853–63865. https://doi.org/10.1039/C5RA08289G.

[73] M. Le Bras, S. Bourbigot, B. Revel, Comprehensive study of the degradation of an intumescent EVA-based material during combustion, J. Mater. Sci. 34 (1999) 5777–5782.

[74] P. Sannigrahi, E. Ingall, Polyphosphates as a source of enhanced P fluxes in marine sediments overlain by anoxic waters: Evidence from 31P NMR, Geochem. Trans. 6 (2005) 52.

[75] E. Akdogan, M. Erdem, M.E. Ureyen, M. Kaya, Rigid polyurethane foams with halogen-free flame retardants: thermal insulation, mechanical, and flame retardant properties, J. Appl. Polym. Sci. 137 (2020) 47611.

[76] M. Thirumal, N.K. Singha, D. Khastgir, B.S. Manjunath, Y.P. Naik, Halogen-free flame-retardant rigid polyurethane foams: Effect of alumina trihydrate and triphenylphosphate on the properties of polyurethane foams, J. Appl. Polym. Sci. 116 (2010) 2260–2268.

[77] Bellayer, Severine; Gossiaux, Alexandre; Duquesne, Sophie; Dewailly, Benjamin; Bachelet, Pierre; Jimenez, Maude Transparent fire protective sol-gel coating for wood panels POLYMER TESTING 2022 110 10.1016/j.polymertesting.2022.107579

[78] Bellayer, Severine; Jimenez, Maude; Barrau, Sophie; Marin, Adeline; Sarrazin, Johan; Bourbigot, Serge Formulation of eco-friendly sol-gel coatings to flame-retard flexible polyurethane foam GREEN MATERIALS 2020 8 3 139-149 10.1680/jgrma.19.00059

[79] Bellayer, S.; Jimenez, M.; Prieur, B.; Dewailly, B.; Ramgobin, A.; Sarazin, J.; Revel, B.; Tricot, G.; Bourbigot, S. Fire retardant sol-gel coated polyurethane foam: Mechanism of action POLYMER DEGRADATION AND STABILITY 2018 147 10.1016/j.polymdegradstab.2017.12.005

[80] Bellayer, S.; Jimenez, M.; Barrau, S.; Bourbigot, S. Fire retardant sol-gel coatings for flexible polyurethane foams RSC ADVANCES 2016 6 34 10.1039/c6ra02094a

[81] S. Bellayer, M. Dilger, S. Duquesne, M. Jimenez, Flame-retardants for polypropylene: A review, Polymer Degradation and Stability, 230, 2024, DOI10.1016/j.polymdegradstab.2024.111008

[82] L. Védie, V. Kopf, A. Hira, M. Dilger, M. Jimenez, S. Bellayer, S. Duquesne, Polyolefin-based resin foamed particles, a component molded from the foamed particles, a method for producing the foamed particles, and a method of determining the flame-retarding properties of foamed particles, EP4563631A1, 2025-06-04

[83] M. Zammarano, S. Matko, W.M. Pitts, D.M. Fox, R.D. Davis, *Polymer Degradation and Stability*, 2014, 106, 97-107
[84] R.H. Krämer, M. Zammarano, G.T. Linteris, U.W. Gedde, J.W. Gilman, *Polymer Degradation and Stability*, 2010, 95, 1115-1122.
[85] Z. Lan, R. Daga, R. Whitehouse, S. McCarthy , D. Schmidt *Polymer* 2014, 55, 11, 27, 2635-2644
[86] S.V. Levchik, E.D. Weil, *Polymer International*, 2004, 53, 1585-1610.
[87] M. Modesti, A. Lorenzetti, *Polymer Degradation and Stability*, 2002, 78, 167-173.
[88] H. Singh, A.K. Jain, *Journal of Applied Polymer Science*, 2009, 111, 1115-1143.
[89] S.D. Shaw, A. Blum, R. Weber, K. Kannan, D. Rich, D. Lucas, C.P. Koshland, D. Dobraca, S. Hanson, L.S. Birnbaum. *Rev Environ Health*. 2010, 25(4), 261-305.
[90] R. Bashirzadeh, A. Gharehbaghi, *Journal of Cellular Plastics* 2010, 46, 2, 129-158
[91] L. Gao, G. Zheng, Y. Zhou, L. Hu, G. Feng, Y. Xie, *Industrial Crops and Products* 2013, 50, 638–647
10
[92] A. König, A. Malek, U. Fehrenbacher, G. Brunklaus, M. Wilhem, T. Hirth *Journal of Cellular Plastics*, 2010, 46, 395-413
[93] J. Jang, H. Chung, M. Kim, H. Sung, *Polymer Testing*, 2000, 19, 269-279.
[94] M. Demirel, V. Pamuk, N. Dilsiz, *Journal of Applied Polymer Science*, 2010, 115, 2550-2555.
[95] M. Haile, S. Fomete, I. D. Lopez, J. C. Grunlan, *J Mater Sci*, 2016, 51, 375–381
[96] 14 K. M. Holder, M. E. Huff, M. N. Cosio, J. C. Grunlan, *J Mater Sci*, 2015, 50, 2451–2458
[97] A. M. Borreguero, P. Sharma, C. Spiteri, M. M. Velencoso, M. S. Carmona, J. E. Moses, J. F. Rodríguez, *Reactive & Functional Polymers* 2013, 73, 1207–1212
[98] Davis, R., Li, Y-C., Gervasio, M., Luu, J., Kim, Y.S. *ACS Applied Materials and Interfaces* 2015, 7, 11, 6082-6092
[99] M. Jimenez, N. Lesaffre, S.Bellayer, R.Dupretz, M.Vandenbossche, S. Duquesne, S. Bourbigot, *RSC Adv.*, 2015, 5, 63853
[100] J. Alongi, G. Malucelli, *Journal of Materials Chemistry*, 2012, 22 (41), 21805-21809
[101] P. Innocenzi, M.O. Abdirashid, M. Guglielmi, *Journal of Sol-Gel Science and Technology* 1994, 3, 47-55
[102] A. Cardenas, N. Hovnanian and M. Smaihi, *Journal of Applied Polymer Science*, 1996, 60, 2279-2288
[103] J. Alongi, G. Malucelli, *Polymer Degradation and Stability* 2013, 98, 1428 -1438
[104] B. Gardelle, S. Duquesne, P. Vandereecken, S. Bellayer, S. Bourbigot, *European Polymer Journal*, 2013, 49, 8, 2031-2041
[105] P. Innocenzi, M.O. Abdirashid, M. Guglielmi, *Journal of Sol-Gel Science and Technology* 1994, 3, 47-55
[106] B. Gardelle, S. Duquesne, P. Vandereecken, S. Bellayer, S. Bourbigot, *European Polymer Journal*, 2013, 49, 8, 2031-2041
[107] J.Alongi, C. Colleoni, G.Rosace, G.Malucelli, *J Therm Anal Calorim* 2012, 110, 1207–1216
[108] G. Brancatelli, C. Colleoni, M.R. Massafra, G. Rosace, *Polymer Degradation and Stability* 2011, 96, 483-490
[109] A.W. Benbow, C.F. Cullis, *Combustion and Flame*, 1975, 24, 217-230
[110] S. Liang, M. Neisius, H. Mispreuve, R. Naescher, S. Gaan, *Polymer Degradation and Stability*, 2012, 97, 2428-2440
[111] L. Jiang, X. Mao, J. Yu, A. Lin, Anti Corr Meth Mater 2009, 56, 13.
[112] G. Guerrero, P.H. Mutin, A. Vioux, *Chem Mater* 2001 13 11 4367-4373.
[113] M.B. Mitchell, V.N. Sheinker, E.A. Mintz*, J PhysChem* B, 1997, 101, 11192-11203.
[114] S. Bellayer M. Jimenez B. Prieur B. Dewailly A. Ramgobin J. Sarazin B. Revel G. Tricot S. Bourbigot Fire retardant sol-gel coated polyurethane foam: Mechanism of action, *Polymer Degradation and Stability,* 147, 2018, 159-167
[115] S. Belayer, M. Jimenez, S. Barreau, A. Marin, J. Sarazin, S. Bourbigot, Formulation of eco-friendly sol–gel coatings to flame-retard flexible polyurethane, Green Materials, (2020) 8 (3): 139–149
[116] Schreier P, Trassl C, Altstädt V. Surface modification of polypropylene based particle foams. In Nuremberg, Germany; 2014 [cited 2021 Oct 27]. p. 378–82. Available from: http://aip.scitation.org/doi/abs/10.1063/1.4873804
[117] Liang CH, Li C, Chen TH, Cheng CY, Huang C. Surface evaluation of reactive plasma-modified microporous polypropylene membrane by static contact angle analysis. Polymer Degradation and Stability. 2019 Feb;160:89–95.
[118] Liston EM, Martinu L, Wertheimer MR. Plasma surface modification of polymers for improved adhesion: a critical review. Journal of Adhesion Science and Technology. 1993 Jan;7(10):1091–127.
[119] Etat de l'art sur différents aspects des traitements plasma, IMMM-UMR CNRS 6283. 2016.
[120] Fávaro SL, Rubira AF, Muniz EC, Radovanovic E. Surface modification of HDPE, PP, and PET films with KMnO4/HCl solutions. Polymer Degradation and Stability. 2007 Jul;92(7):1219–26.

[121] Duquesne S, Jimenez M, Bourbigot S. Aging of the flame-retardant properties of polycarbonate and polypropylene protected by an intumescent coating. J Appl Polym Sci. 2014 Feb 5;131(3). Available from: http://doi.wiley.com/10.1002/app.39566

[122] Jimenez M, Duquesne S, Bourbigot S. Fire protection of polypropylene and polycarbonate by intumescent coatings. Polym Adv Technol. 2012 Jan;23(1):130–5.

[123] Slepička P, Vasina A, Kolská Z, Luxbacher T, Malinský P, Macková A, et al. Argon plasma irradiation of polypropylene. Nuclear Instruments and Methods in Physics Research Section B: Beam Interactions with Materials and Atoms. 2010 Jun;268(11–12):2111–4.

[124] Jimenez M, Duquesne S, Bourbigot S. Fire protection of polypropylene and polycarbonate by intumescent coatings. Polym Adv Technol. 2012 Jan;23(1):130–5

[125] Duquesne S, Jimenez M, Bourbigot S. Aging of the flame-retardant properties of polycarbonate and polypropylene protected by an intumescent coating. J Appl Polym Sci. 2014 Feb 5;131(3). Available from: http://doi.wiley.com/10.1002/app.39566

[126] Mougel, C.; Garnier, T.; Cassagnau, P.; Sintes-Zydowicz, N. Phenolic Foams: A Review of Mechanical Properties, Fire Resistance and New Trends in Phenol Substitution. *Polymer* 2019, *164*, 86–117. https://doi.org/10.1016/j.polymer.2018.12.050.

[127] Auad, M. L.; Zhao, L.; Shen, H.; Nutt, S. R.; Sorathia, U. Flammability Properties and Mechanical Performance of Epoxy Modified Phenolic Foams. *J. Appl. Polym. Sci.* 2007, *104* (3), 1399–1407. https://doi.org/10.1002/app.24405.

[128] Landrock, A. H. *Handbook of Plastic Foams: Types, Properties, Manufacture and Applications*; Elsevier, 1995.

[129] Forest, C.; Chaumont, P.; Cassagnau, P.; Swoboda, B.; Sonntag, P. Polymer Nano-Foams for Insulating Applications Prepared from CO2 Foaming. *Prog. Polym. Sci.* 2015, *41*, 122–145. https://doi.org/10.1016/j.progpolymsci.2014.07.001.

[130] Jing, S.; Li, T.; Li, X.; Xu, Q.; Hu, J.; Li, R. Phenolic Foams Modified by Cardanol through Bisphenol Modification. *J. Appl. Polym. Sci.* 2014, *131* (4). https://doi.org/10.1002/app.39942.

[131] Yang, C.; Zhuang, Z.-H.; Yang, Z.-G. Pulverized Polyurethane Foam Particles Reinforced Rigid Polyurethane Foam and Phenolic Foam. *J. Appl. Polym. Sci.* 2014, *131* (1). https://doi.org/10.1002/app.39734.

[132] Song, S. A.; Chung, Y. S.; Kim, S. S. The Mechanical and Thermal Characteristics of Phenolic Foams Reinforced with Carbon Nanoparticles. *Compos. Sci. Technol.* 2014, *103*, 85–93. https://doi.org/10.1016/j.compscitech.2014.08.013.

[133] Desai, A. FIBER REINFORCED HYBRID PHENOLIC FOAM.

[134] Li, Q.; Chen, L.; Li, X.; Zhang, J.; Zheng, K.; Zhang, X.; Tian, X. Effect of Nano-Titanium Nitride on Thermal Insulating and Flame-Retardant Performances of Phenolic Foam. *J. Appl. Polym. Sci.* 2016, *133* (32). https://doi.org/10.1002/app.43765.

[135] Ma, Y.; Wang, J.; Xu, Y.; Wang, C.; Chu, F. Effect of Zinc Oxide on Properties of Phenolic Foams/Halogen-Free Flame Retardant System. *J. Appl. Polym. Sci.* 2015, *132* (44). https://doi.org/10.1002/app.42730.

[136] Yuan, J.; Zhang, Y.; Wang, Z. Phenolic Foams Toughened with Crosslinked Poly (n-Butyl Acrylate)/Silica Core-Shell Nanocomposite Particles. *J. Appl. Polym. Sci.* 2015, *132* (40). https://doi.org/10.1002/app.42590.

[137] Yang, H.; Wang, X.; Yu, B.; Yuan, H.; Song, L.; Hu, Y.; Yuen, R. K. K.; Yeoh, G. H. A Novel Polyurethane Prepolymer as Toughening Agent: Preparation, Characterization, and Its Influence on Mechanical and Flame Retardant Properties of Phenolic Foam. *J. Appl. Polym. Sci.* 2013, *128* (5), 2720–2728. https://doi.org/10.1002/app.38399.

[138] Yuan, H.; Xing, W.; Yang, H.; Song, L.; Hu, Y.; Yeoh, G. H. Mechanical and Thermal Properties of Phenolic/Glass Fiber Foam Modified with Phosphorus-Containing Polyurethane Prepolymer. *Polym. Int.* 2013, *62* (2), 273–279. https://doi.org/10.1002/pi.4296.

[139] Preparation and Characterization of Phenolic Foams Modified by Castor Oil-based Polyurethane Prepolymer. http://www.cifp.ac.cn/EN/10.3969/j.issn.0253-2417.2015.04.002 (accessed 2023-11-27).

[140] Xu, Q.; Gong, R.; Cui, M.; Liu, C.; Li, R. Preparation of High-Strength Microporous Phenolic Open-Cell Foams with Physical Foaming Method. *High Perform. Polym.* 2015, *27* (7), 852–867. https://doi.org/10.1177/0954008314564197

[141] Rader, S. L.; Va, W. USE THEREOF FOR IN PLACE FOAMING.

[142] Rangari, V. K.; Hassan, T. A.; Zhou, Y.; Mahfuz, H.; Jeelani, S.; Prorok, B. C. Cloisite Clay-Infused Phenolic Foam Nanocomposites. *J. Appl. Polym. Sci.* 2007, *103* (1), 308–314. https://doi.org/10.1002/app.25287.

[143] Liu, X. H.; Fu, S. Y.; Xu, Y. Z.; Wang, C. P.; Chu, F. X. Effect of Acid Curing Agent on the Foaming of Liquefied Bamboo-Based Resol Resin. *Adv. Mater. Res.* 2013, *724–725*, 231–235. https://doi.org/10.4028/www.scientific.net/AMR.724-725.231.

[144] J Fontoba-Ferrándiz, E Juliá-Sanchishttps, JE Crespo Amorós, J Segura Alcaraz, JM Gadea Borrell, and F Parres García, Panels of eco-friendly materials for architectural acoustics, 54, 25, 2020, 3743-3753

[145] Y. Xiao, Y. Zheng, X. Wang, Z. Chen, Z. Xu Preparation of a chitosan-based flame-retardant synergist and its application in flame-retardant polypropylene J. Appl. Polym. Sci., 131 (19) (2014)
[146] Z.A. Raza, S. Khalil, A. Ayub, I.M. Banat Recent developments in chitosan encapsulation of various active ingredients for multifunctional applications Carbohydr. Res, 492 (2020) (2020), 108004
[147] X. Huo, W. Li, Y. Wang, N. Han, J. Wang, N. Wang, X. Zhang Chitosan composite microencapsulated comb-like polymeric phase change material via coacervation microencapsulation Carbohydr. Polym., 200 (2018) (2018), 602-610
[148] S. Hu, L. Song, H. Pan, Y. Hu Thermal properties and combustion behaviors of chitosan based flame retardant combining phosphorus and nickel Ind. Eng. Chem. Res., 51 (9) (2012), pp. 3663-3669
[149] S. Hu, L. Song, Y. Hu Preparation and characterization of chitosan-based flame retardant and its thermal and combustible behavior on polyvinyl alcohol Polym. -Plast. Technol. Eng., 52 (4) (2013), 393-399
[150] M. Hassan, M. Nour, Y. Abdelmonem, G. Makhlouf, A. Abdelkhalik Synergistic effect of chitosan-based flame retardant and modified clay on the flammability properties of LLDPE Polym. Degrad. Stab., 133 (2016) (2016), 8-15
[151] Passauer L (2019) Thermal characterization of ammonium starch phosphate carbamates for potential applications as bio-based flame-retardants. Carbohyd Polym 211:69–74
[152] Saake, Bodo; Lehnen, Ralph, Lignin Ullmann's Encyclopedia of Industrial Chemistry. Weinheim: Wiley-VCH 2007. ISBN 978-3527306732.
[153] Wu W., He H., Liu T., Wei R., Cao X., Sun Q., Venkatesh S., Yuen K.K.R., Roy V.A., Li R.K.Y. Synergetic enhancement on flame retardancy by melamine phosphate modified lignin in rice husk ash filled P34HB biocomposites. Compos. Sci. Technol. 2018;168:246–254
[154] Borysiak S. Fundamental studies on lignocellulose/polypropylene composites: Effects of wood treatment on the transcrystalline morphology and mechanical properties. J. Appl. Polym. Sci. 2013;127:1309–1322.
[155] S. Ding, P. Liu, S. Zhang, C. Gao, F. Wang, Y. Ding, M. Yang, Crosslinking of β-cyclodextrin and combining with ammonium polyphosphate for flame-retardant polypropylene, Applied Polymer Sciences 2020 48320
[156] A. Arbenz, L. Averous Chemical modification of tannins to elaborate aromatic biobased macromolecular architectures Green. Chem., 17 (2015)
[157] L.D.H. Pedro, M. Juliette, L. Jalel, C.E.B. Fatima Tannins extraction: a key point for their valorization and cleaner production J. Clean. Prod., 206 (2019)
[158] A. Duval, G. Couture, S. Caillol, L. Avérous Biobased and aromatic reversible thermoset networks from condensed tannins via the diels-alder reaction ACS Sustain. Chem. Eng., 5 (2017)
[159] X. Wang, G. Yang, H. Guo, Tannic acid as biobased flame retardants: A review Journal of Analytical and Applied Pyrolysis 174, 2023, 106111.
[160] Y. Liu, A. Zhang, Y. Cheng, M. Li, Y. Cui, Z. Li, Recent advances in biomass phytic acid flame retardants Polymer Testing 124, 2023, 108100.
[161] E. Abraham, B. Deepa, L.A. Pothan, M. John, S.S. Narine, S. Thomas, et al.
Physicomechanical properties of nanocomposites based on cellulose nanofibre and natural rubber latex Cellulose, 20 (1) (2013), 417-427
[162] L. Liu, Y. Pan, Z. Wang, Y. Hou, Z. Gui, Y. Hu Layer-by-Layer assembly of hypophosphorous acid-modified chitosan based coating for flame-retardant polyester–cotton blends Ind. Eng. Chem. Res., 56 (34) (2017), pp. 9429-9436
[163] G. Schinazi, J.R. Moraes d'Almeida, J.K. Pokorski, D.A. Schiraldi Bio-based flame retardation of acrylonitrile–butadiene–styrene ACS.Appl. Polym.Mater, 3 (1) (2020), 372-388
[164] Z. Zheng, C. Liao, Y. Xia, Y. Liu, B. Dai, A. Li Co-microencapsulation of biomass-based char source and melamine polyphosphate and investigation for their synergistic action in flame-retarding polypropylene Polym. Test., 90 (2020), Article 106741

ABSTRACT:

This manuscript summarizes my researches conducted at the Materials and Processing Unit (UMET UMR 8207) in Villeneuve d'Ascq. The first chapter focuses on improving the flame retardant properties of foams during the manufacturing process. This work uses rigid polyurethane and polyisocyanurate foams as raw materials. It highlights the difficulties encountered in finding new effective flame retardants for foams when they are introduced into the polymer during the manufacturing process. Different foam formulations were characterized using various analytical tools in order to fully understand the mechanism of action of each flame retardant. The following chapter focuses on flame-retardant coatings for polymer foams. In the case of surface coatings, different cases are studied, including open-cell and closed-cell foams and hydrophilic and hydrophobic surfaces. Thin sol-gel coatings for open-cell foams and thick paints and varnishes for closed-cell foams were studied. It should be noted that when the surface is hydrophobic, it is necessary to pre-treat the surface to be coated in order to improve the adhesion of the coating. Finally, the last section deals with the use of inherently flame-retardant foams, which aims at avoiding the toxicity and safety issues associated with the use of flame retardants. In this context, the flame-retardant and mechanical properties of phenolic foams have been studied.

RESUME :

Ce mémoire résume l'ensemble de mes recherches menées à l'Unité Matériaux et Transformation (UMET UMR 8207), à Villeneuve d'Ascq. Le premier chapitre porte sur l'amélioration des propriétés retardatrices de flammes des mousses pendant le procédé de fabrication. Il s'agit d'un travail utilisant comme matières premières des mousses rigides de polyuréthane et de polyisocyanurate. Ce travail met en évidence les difficultés rencontrées pour trouver de nouveaux retardateurs de flamme efficaces pour les mousses lorsqu'ils sont introduits dans le polymère pendant le processus de fabrication. Différentes formulations de mousse ont été caractérisées à l'aide de divers outils analytiques afin de comprendre pleinement le mécanisme d'action de chaque retardateur de flamme. Le chapitre suivant porte sur les revêtements retardateurs de flammes pour mousses à matrice polymère. Dans le cas des revêtements de surface, différents cas sont étudiés, les mousses à cellules ouvertes et à cellules fermées et les surfaces hydrophiles et hydrophobes. Des revêtements sol-gel minces pour les mousses à cellules ouvertes et des peintures et vernis épais pour les mousses à cellules fermées ont été étudiés. Il est a noté que lorsque la surface est hydrophobe, il est nécessaire de pré traiter la surface à revêtir pour améliorer l'adhésion du revêtement. Enfin, la dernière partie traite de l'utilisation de mousses intrinsèquement ignifuges qui font partie des recherches les plus récentes visant à éviter les problèmes de toxicité et de sécurité liés à l'utilisation de retardateurs de flamme. Dans ce cadre, les propriétés retardatrices de flammes et mécaniques des mousses phénoliques ont été étudiées.